universität wien

DISSERTATION

Titel der Dissertation

Meiotic DNA repair in *Arabidopsis thaliana*
Characterisation of the *Arabidopsis thaliana* homologues
of *MND1* and *COM1*

angestrebter akademischer Grad

Doktorin der Naturwissenschaften

Verfasserin / Verfasser:	Tanja Siwiec
Matrikel-Nummer:	9505209
Dissertationsgebiet Atxrcc3 :	Genetik und Mikrobiologie
Betreuer:	Dr. Dieter Schweizer und Dr. Peter Schlögelhofer

Wien, im April 2009

1. Table of contents

2. Summary

Meiosis is a specialized nuclear division characteristic for sexually reproducing eukaryotes. Each diploid progenitor generates four genetically different haploid cells proceeding through two successive nuclear divisions that follow a single round of genome replication. This process relies on meiotic homologous recombination (HR) that establishes a physical connection between pairs of homologs and allows the correct alignment of bivalents. Moreover, genetic diversity is generated by the exchange of DNA sequences between maternal and paternal chromosomes.

Homologous recombination is initiated by programmed DNA double strand breaks (DSBs) catalyzed by Spo11, a homologue of the archaebacterial topoisomerase subunit Top6A. In *Saccharomyces cerevisiae*, Mre11, Rad50, Xrs2 and Com1/Sae2 are essential to process these DSBs. *Arabidopsis thaliana Atcom1-1* mutants are sterile, accumulating *At*SPO11-1 during meiotic prophase and failing to form *At*RAD51 foci, indicative for un-processed DSBs. Furthermore, DNA fragmentation seen in *Atcom1-1* mutants is suppressed in the absence of *AtSPO11-1*, pointing to a defect in DSB repair. In accordance with data in other organisms, we found that *At*COM1 interacts with *At*NBS1, a protein which is involved in the early steps of DNA repair.

After processing of DSBs, a single stranded DNA molecule recognizes and invades the homologous sequence. Many proteins are involved in this crucial step of homology search. Among others Mnd1 has been identified as one of the key players in the strand invasion process. The *Arabidopsis* homologue, *AtMND1*, is essential for male and female meiosis. Furthermore, other proteins involved in meiotic recombination can be found in *Arabidopsis thaliana*, for instance the RecA related proteins DMC1, RAD51 and XRCC3. Few is known about the interplay between these proteins during meiosis. *At*MND1 promotes the strand invasion process together with AHP2, the *Arabidopsis* protein closely related to budding yeasts Hop2. In the absence of *At*MND1, severe chromosome fragmentation is observed, depending on the presence of *At*SPO11-1. Moreover *At*RAD51 as well as *At*DMC1 foci, have been observed to accumulate on cytological preparations of meiotic cells. They demonstrate that DNA breaks remain un-repaired. Furthermore, immunolocalization studies provide insight into the functional differences of *At*RAD51 and *At*XRCC3 during meiosis, by first demonstrating that *At*XRCC3 is dispensable for *At*DMC1 nucleoproteinfilament formation in an *Atmnd1* mutant background, and second that *At*XRCC3 is indispensable for efficient loading of *At*RAD51.

3. Zusammenfassung

Meiose ist eine spezielle Form der Zellteilung die den diploiden Chromosomensatz auf einen haploiden reduziert. Zwei Kernteilungen folgen einer prämeiotischen DNA Replikation, so dass schließlich vier haploide Tochterzellen vorliegen. Während in der ersten meiotischen Teilung die Trennung der homologen Chromosomen erfolgt, werden in der zweiten meiotischen Teilung die Schwesterchromatiden getrennt.

In der Meiose kommt es zum reziproken Austausch genetischer Information, ein Prozess der homologe Rekombination genannt wird. Spo11, ein verwandtes Protein der archeabakteriellen Topoisomeraseuntereinheit Top6A, leitet die HR durch die kontrollierte Einfügung von Doppelstrangbrüchen ein. In der Bäckerhefe *Saccharomyces cerevisiae* sind die Proteine Mre11, Rad50, Xrs2 und Com1/Sae2 essentiell um diese Doppelstrangbrüche zu prozessieren und in weitere Folge, deren Reparatur zu ermöglichen. Die *Arabidopsis thaliana Atcom1-1* Mutante ist steril. Darüber hinaus reichert sich *At*SPO11-1 während der meiotischen Prophase I an. Das Fehlen von *At*RAD51 in der *Atcom1-1* Mutante deutet auf nicht reparierte Doppelstrangbrüche hin. Die für *Atcom1-1* typische DNA Fragmentierung kann durch Mutation von *At*SPO11-1 unterdrückt werden. In dieser Studie konnten wir interessanterweise eine Interaktion von *At*COM1 mit *At*NBS1, einem Protein der DNA Reparaturmaschinerie, nachweisen. Nach erfolgter Prozessierung der Doppelstrangbrüche dient die einzelsträngige DNA (ssDNA) als Sonde zum Auffinden des homologen Partnerchromosoms. Für diesen entscheidenden Schritt der DNA Homologiesuche sind mehrere Proteine nötig. Unter anderem wurde Mnd1 als eines für den Strangaustausch essentielles Protein identifiziert. Das homologe Protein in *Arabidopsis*, *At*MND1, ist, gemeinsam mit AHP2, dem Homologen von Hop2 der Hefe, wichtig für die Meiose. Weitere Proteine, wie die RecA Homologen DMC1, RAD51 und XRCC3 sind essentiell für den korrekten Austausch des genetischen Materials. Über das Zusammenspiel dieser Proteine ist bis jetzt wenig bekannt. Das Fehlen von *At*MND1 verursacht schwere DNA Fragmentierung. Eine Akkumulierung von *At*RAD51, wie auch von *At*DMC1 kann in der *Atmnd1* Mutante beobachtet werden. Dies ist auf nicht reparierte DSB zurückzuführen. Immunolokalisationsstudien zeigen die funktionellen Unterschiede von *At*RAD51 and *At*XRCC3 während der Meiose auf. *At*XRCC3 ist für die Nukleoproteinfilamentbildung des *At*DMC1 Proteins in einer *Atmnd1* Mutante entbehrlich, während *At*XRCC3 unverzichtbar für eine effiziente Anlagerung von *At*RAD51 an die prozessierten ssDNA Enden ist.

4. General introduction

Meiosis is fundamental for genetic diversity of sexually reproducing organisms. It was described for the first time by the German biologist Oscar Hertwig (1849-1922) in sea urchin eggs in 1876. The existence of chromosomes was described in 1883, by the Belgian zoologist Edouard Van Beneden (1846-1910), in *Ascaris* worm oocytes. In 1890 the German biologist August Weismann (1834-1914) noted that two cell divisions were necessary to transform one diploid cell into four haploid cells if the number of chromosomes had to be maintained and hence the significance of meiosis for reproduction and inheritance was recognized. Further insight into the basics of genetics was provided in 1911 by the American geneticist Thomas Hunt Morgan (1866-1945), who observed recombination in *Drosophila melanogaster* meiosis.

During meiosis one round of DNA replication is followed by two rounds of nuclear cell divisions. As a consequence a diploid cell gives rise to four haploid cells. Homologous recombination (HR) ensures the stability of the organisms karyotype in this context. Therefore, it is expected that it is tightly controlled. Mutations in genes involved in HR have in most cases dramatic effects on the eukaryotic organism. Many HR genes were first identified due to their hypersensitivity to DNA damaging agents which induce DNA lesions and by their inability to give rise to viable meiotic products. In mammals, respective mutations concerning genes for homologous recombination are very often lethal, especially if they are homozygous knockouts. In yeast, these mutations result in an arrest during meiotic prophase I or nonviable spores. In *Arabidopsis thaliana*, mutated genes, which are involved in meiosis, give nevertheless rise to fully viable plants. This and many other aspects, like small genome size, short life cycle and also the simple breeding system, make *A. thaliana* the organism of choice when it comes to analyzing both the control and the evolution of meiotic recombination.

4.1. How to repair a meiotic double-stranded break?

Lesions affecting both strands of the DNA double helix (DNA double strand breaks) are can lead to cell death. DSBs can be a result of exogenous or endogenous genotoxic agents as well as cellular processes like repair of DNA lesions or DNA replication. But DSBs are not only disadvantageous for the cells, they are also a pre-requisite for the exchange between maternal and paternal genetic information during meiosis and are therefore mechanistic requirement for genetic diversity.

Two classes of mechanisms may be employed to repair DSBs: homologous recombination (HR), by using homologous DNA sequence as repair template and non-homologous recombination (NHR), which rejoins the two ends of the break (Bleuyard et al., 2006).

There are two different pathways described for NHR in plants: non-homologous end joining (NHEJ) and micro-homology-mediated end-joining (Bleuyard et al., 2006). The main pathway of non-homologous recombination is NHEJ (Figure 1) and was first described in mammalian cells (Bleuyard et al., 2006). In some cases NHEJ can result in the loss of few nucleotides and hence in loss of genomic integrity.

It is believed that the cell cycle stage plays a crucial role for the decision between HR or NHEJ. The homologous template for HR is only present in the S and G2 phase of the cell cycle, whereas NHEJ is thought to be the prevailing pathway during G1 and M phase. NHEJ requires a tightly regulated interplay of a subset of enzymes. In mammalian cells this process is depends on the Ku70/80 heterodimer complex, which binds to both ends of the DNA lesion and is thought to act as a scaffold for the subsequent assembly of additional NHEJ key enzymes (Weterings and Chen, 2008; Weterings et al., 2009).

The recognition and the juxtaposition of broken DNA ends is promoted by the DNA-dependent protein kinase catalytic subunit (DNA-PK_{CS}) together with the KU heterodimer (Jones et al., 2001; Walker et al., 2001). Crystallography studies have revealed that the human KU complex has an open ring shaped structure which is composed of one Ku70 and one Ku80 protein (Walker et al., 2001). The central regions of Ku70 and Ku80 are responsible for the heterodimerization of the complex (Cary et al., 1998; Walker et al., 2001). The structure of the KU complex enables it to migrate to the side of DSBs within seconds after the onset of the damage (Mari et al., 2006). Biochemical studies have shown that the KU complex has the ability to bind to hairpins, blunt ends and 3' and 5' overhangs, as well as to double strand DNA molecules carrying a single strand gap (Smith and Jackson, 1999). These data suggest the involvement of the KU complex in the recognition and protection of DSB ends. By the interaction with the KU/DNA complex the DNA-PK_{CS} is recruited to the double strand break. The 460kDa serine/threonine kinase DNA-PK_{CS} belongs to the PI3 kinase family and is able to phosphorylate five of the six proteins identified in the NHEJ pathway: Ku70, Ku80, Artemis, Xrcc4 and DNA-PK_{CS} itself. However, the *in vivo* significance of DNA-PK_{CS} mediated phosphorylation of Xrcc4 and Ku70/80 has not been conclusively

demonstrated (Douglas et al., 2005). The interaction between KU and DNA-PK_{CS} is thought to be mediated by the Ku80 carboxy- terminus (Gell and Jackson, 1999; Singleton et al., 1999). Furthermore, biochemical studies have shown that DNA molecules can be held together by DNA-PK_{CS} (DeFazio et al., 2002). All together these data lead to the assumption that two KU dimers and two DNA-PK_{CS} can form a synaptic complex which juxtaposes two DNA termini.

The most recently identified component of the NHEJ pathway is Artemis. This enzyme was initially recognized as an essential factor in V(D)J recombination, by playing a role in opening the hairpin structures at coding ends (Ma et al., 2002). The Artemis protein by itself only displays a 5'-3' exonuclease activity. The association of Artemis and DNA-PK_{CS} is most likely responsible for the recruitment of Artemis to the synaptic repair complex.

For processing of DNA termini during repair of radiation-induced DSBs both, the DNA-PKCS-independent exonuclease activity and the DNA-PK_{CS}-dependent endonuclease activity of Artemis, can be relevant. It is therefore unclear whether the association of Artemis with DNA-PK_{CS} is only necessary for the physical attachment of Artemis to the repair complex or that it is also essential to expand the nucleolytic potential of the Artemis enzyme. After exposure of cells to ionizing radiation, Artemis is (hyper)phosphorylated by both the ATM and DNA-PK_{CS} kinases (Dahm, 2007).

The final step of NHEJ, the ligation of broken DNA ends, is carried out by the XRCC4/DNA ligase IV heterodimer. The catalytic domain of the 100 kDa, ATP utilizing ligase IV protein is located in the amino-terminal region (Tomkinson et al., 2006). Interestingly, however, the interaction between ligase IV and XRCC4 is not thought to be mediated by the BRCT motifs of ligase IV themselves, but by the sequence that lays in between the two BRCT domains, encompassing amino-acids 755 to 782 (Critchlow et al., 1997; Grawunder et al., 1998). BRCT motifs usually consist of 90−100 amino acids and are found in many eukaryotic proteins, either as an isolated domain or in tandem repeats of two or more BRCT units (Huyton et al., 2000). Although most BRCT proteins are involved in the cellular response to genotoxic stress, a common biochemical function for this motif has not been identified. The crystal structure of XRCC4 reveals that this protein has a globular amino-terminal head and a long carboxyterminal stalk (Junop et al., 2000), which mediates the interaction between XRCC4 and ligase IV (Sibanda et al., 2001). In view of this structure, it is likely that the amino-terminal heads of the XRCC4 molecules mediate an interaction with the DNA

helix, while the ligase IV enzyme repairs the DSB (Modesti et al., 2003; Sibanda et al., 2001).

Several studies have demonstrated interactions between the ligase IV/XRCC4 complex and the Ku70/80 heterodimer, suggesting that the ligase IV/XRCC4 complex is attracted to the synaptic repair complex by the DNA-Ku scaffold in a manner similar to the recruitment of DNA-PK_{CS} and several additional processing enzymes (Costantini et al., 2007; Nick McElhinny et al., 2000).

Homologues of most of these NHEJ proteins have been identified in *A. thaliana.* The characterization of mutant plants has clearly demonstrated roles for AtKU70, AtKU80 and AtLIG4 proteins in NHEJ. Even so, mutant plants do not show growth defects or decreased viability, inactivation of the *AtKU70*, *AtKU80*, or *AtLIG4* genes confers hypersensitivity to DSB-inducing reagents (Friesner and Britt, 2003; Gallego et al., 2003; Tamura et al., 2002; van Attikum et al., 2003; West et al., 2002) and the absence of theAtKU80 protein strongly reduces the efficiency of NHEJ in an *in vivo* plasmid-based end-joining assay (Gallego et al., 2003). *At*XRCC4 was found by yeast two-hybrid and co-immunoprecipitation experiments to interact with the *At*LIG4 protein (Tamura et al., 2002; West et al., 2000; West et al., 2002). Finally, the genome of *A. thaliana* encodes a putative orthologue of Artemis (*AtSNM3*) (Molinier et al., 2004), but the identification and characterization of mutant plants has not been reported to date.

Another mechanism to repair double strand DNA breaks is the single strand annealing (SSA) pathway (Figure 1), which is maybe initiated when a DSB is made between two repeated sequences oriented in the same direction. SSA is always associated with deletions and therefore with the potential risk of oncogenic chromosomal aberrations. SSA is well characterized in yeast since it was found that the HO endonuclease could stimulate deletion events between *ura3* sequences *in vivo* (Haber and Leung, 1996; Ivanov et al., 1996; Sugawara et al., 2000). Recently, SSA has also been identified as a significant pathway leading to translocations frequently inflicted in human cancers (Weinstock et al., 2006). Moreover it was shown that SSA can serve as a sort of back-up mechanism for NHEJ (Mansour et al., 2008). Also the loss of Ku80 promotes SSA (Mansour et al., 2008), because the KU protein 'hides' DNA ends, protects them from degradation (Liang and Jasin, 1996; Mimori and Hardin, 1986; Walker et al., 2001) and hence prevents repair by recombination. In addition in humans, KU may compete with Rad52, which is a key player in SSA, for DNA binding. Biochemically it has been shown that Rad52 mediates ligation of blunt and cohesive ends similar to KU (Van

Dyck et al., 1999). The absence of KU might significantly facilitate access of Rad52 to double-stranded DNA ends, in particular, as these become prone to nucleolytic attack. In yeast, a single-stranded overhang of only 8–10 bp is sufficient to initiate a Rad52-mediated recombination process by SSA (Ristic et al., 2003).

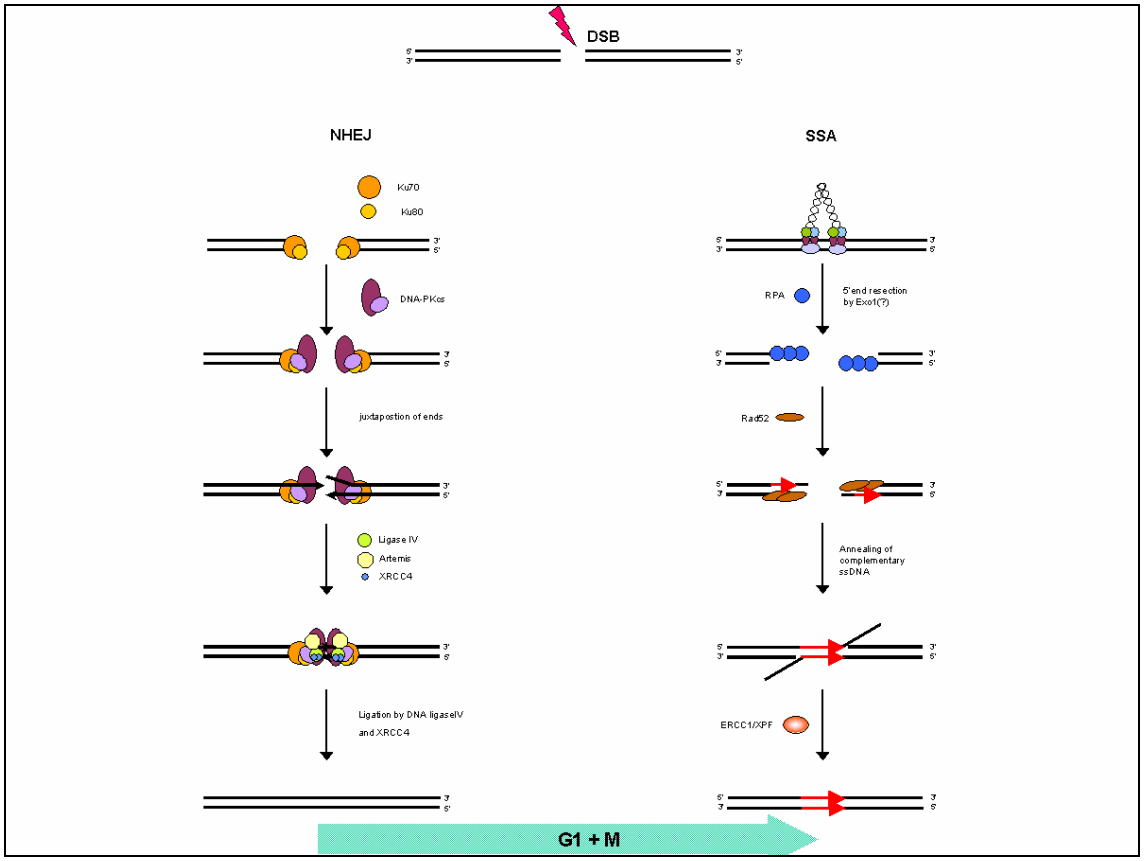

Figure 1: Non-homologous end joining and single strand annealing repair pathways. For detailed explanation see text. Modified from Nature Reviews/Microbiology (2005).

Another way to repair a double strand break is homologous recombination (Figure 2). There have been several sub-pathways identified, namely double strand break repair (DSBR), synthesis dependent strand annealing (SDSA) and break induced replication (BIR). The latter is also known as recombination-dependent replication or break copy duplication. It is RAD52-dependent and RAD51-independent and can be studied in mitotically growing cells. During all three processes broken DNA ends are degraded in 5' to 3' direction and give rise to 3' single-stranded DNA ends (Symington, 2002), which serve as a template to initiate pairing and strand invasion.

In the course of BIR (Figure 2), a processive replication fork is established after strand invasion and DNA synthesis proceeds to the end of the chromosome. In eukaryotes, BIR is thought to elongate telomeres when telomerase is absent or when telomeres are uncapped (McEachern and Haber, 2006). In contrast to SDSA, which only needs leading strand DNA synthesis, the break induced replication mechanism requires

leading as well as lagging DNA synthesis (Lydeard et al., 2007; Wang et al., 2004). Physical monitoring has revealed a significant delay in the initiation of DNA synthesis from the invading 3' end during BIR compared to SDSA or DSBR and therefore might be the reason for the low level (<2%) of BIR even if homology on both sides of the DSB is present (Malkova et al., 2005).

Synthesis dependent strand annealing (Figure 2) is an important mechanism of non-crossover (NCO) recombination in mitosis as well as in meiosis, although models for SDSA giving rise to crossover (CO) products have been suggested (Allers and Lichten, 2001; Paques and Haber, 1999). During SDSA, repair of a DSB is achieved by invasion of an overhanging 3' end into the intact donor chromatid. The joint formed by the invasion may be subject to mismatch repair, leading to shortening of the invading end. Following this opportunity for mismatch excision, repair synthesis can extend the invading end past the site of the DSB. Once the end is extended, disruption of the joint occurs. The extended end can then anneal with its partner. The product of annealing is then converted into an intact duplex by repair synthesis and ligation. SDSA models were first designed to explain a lack of crossovers, but they received experimental support by various observations that could best be explained by such a mechanism (Paques et al., 1998; Silberman and Kupiec, 1994).

Versions of the SDSA model were proposed to explain properties of mating-type conversion in budding yeast that did not fit well to the Holliday junction (HJ) intermediate model, including the fact that mating-type conversion is not associated with crossover (McGill et al., 1989; Nasmyth, 1982; Strathern et al., 1988; Strathern et al., 1982). So far, only one result argues for the association of SDSA with crossover in *S. cerevisiae*. The fact that DSB repair induces frequent rearrangements in tandem repeats, and that nearly always in the recipient molecule (Paques et al., 1998). This accounts for non-crossover DSB repair events (where the donor and recipient molecules are clearly identifiable), which are the vast majority of the gene conversion events. However, some crossover-associated rearrangements can be explained by the reinvasion of one end during the copying of the template-containing repeats. Most of the time, the conversion event could be accomplished by an annealing with the second end of the DSB. However, if the second end also paired with the template, it might sometimes stabilize the displaced strand. DNA synthesis on both strands could then become semiconservative, and Holliday junctions could arise and be cut, as predicted by

Szostak et al. (Szostak et al., 1983). Thus, SDSA may sometimes be associated with crossover.

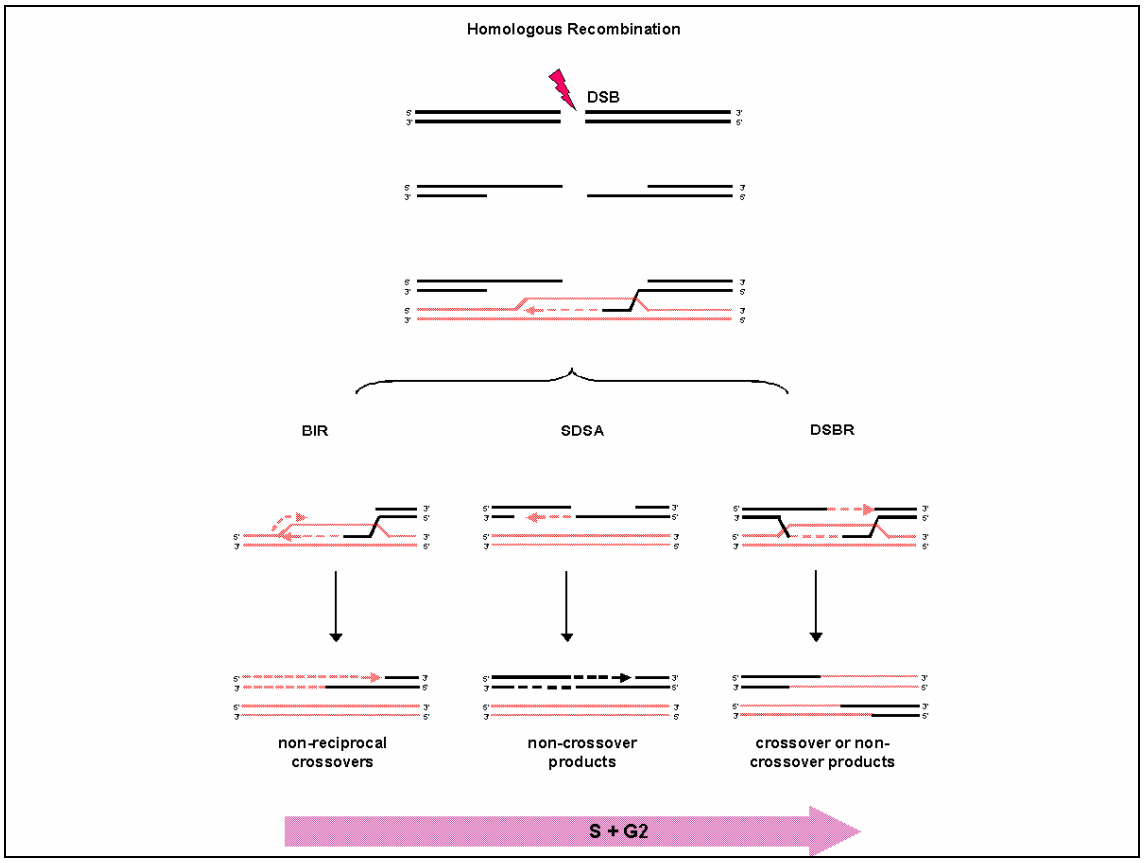

Figure 2: Break induced replication, synthesis-dependent strand annealing and double strand break repair. Models for the repair of DSBs: All three mechanisms initiate with the invasion of the 3' end. After priming DNA synthesis, the second end is captured and a double Holliday junction intermediate is formed (DSBR). Resolution can occur in either plane at both junctions to generate crossover or non-crossover products. In the SDSA model, the nascent strand is displaced, pairs with the other 3' single-stranded tail and DNA synthesis completes repair. Extensive replication primed from the invading 3' end (BIR) occurs when the other end of the DSB is absent or is heterologous. 3' ends are indicated by arrowheads, newly synthesized DNA is represented by dashed lines. Modified from Llorente et al.(Llorente et al., 2008)

The last important pathway for DSB repair is double-stranded break repair (Figure 2). By the canonical DSBR model, the other end of the break interacts with the displaced strand from the donor duplex (D-loop) to prime DNA synthesis and seal the break (Szostak et al., 1983). The resulting double HJ intermediate can be resolved to generate crossover or non-crossover products. If the heteroduplex DNA formed during single-strand pairing contains a mismatch, repair of the mismatch can result in gene conversion.

During meiosis, initiation of homologous recombination starts with the programmed induction of DSBs made by the conserved Spo11 protein. Spo11 shares homology with the catalytic subunit (Malik et al., 2007) of the archeal bacteria type II topoisomerase

(Bergerat et al., 1997). Only a selected number of Spo11 catalyzed DSBs proceed to form crossovers (Basile et al.). These ensure subsequent normal chromosome segregation. For instance, in male mice 200 to 400 DSBs are made per cell but only around 23 result in COs (Turner, 2007).

As DSBs are formed, Spo11 becomes covalently attached by a phosphodiester link between its catalytic tyrosine, Y135, to the DNA 5'terminus. Before break site resection can occur, Spo11 is removed from DNA by a ssDNA nick next to the DSB. In budding yeast, the release of Spo11 protein, attached to a few nucleotides, is mediated by Rad50, Mre11 and Com1/Sae2 (Keeney, 2001; Prieler et al., 2005; Smith and Nicolas, 1998). The nucleolytic resection by a so far unknown 5'-3' exonuclease, give rise to single-stranded 3'-OH ends, which are believed to serve as probes for finding the homologous partner chromosome and subsequent formation of recombinase filaments (Hunter and Kleckner, 2001; Neale and Keeney, 2006; Paques and Haber, 1999). Two proteins play a major role in establishing the presynaptic filament and finding the homologous chromosome- the RecA homologues Rad51 and Dmc1. Rad51 works in mitotic DSB repair as well as in meiotic HR, whereas Dmc1 in only active during meiosis. Genetic and biochemical studies of *S. cerevisiae rad51* mutants revealed significant homology with those RecA residues that are critical for its recombinase function, including DNA binding and ATP hydrolysis (Aboussekhra et al., 1992; Basile et al., 1992b). Rad51 exists as a homo-oligomer in solution, being heptameric and hexametric (Bianco et al., 1998; Shin et al., 2003). In the presence of ATP *S. cerevisiae* Rad51 protein can assemble onto ssDNA or dsDNA to form a right-handed helical polymer (Ogawa et al., 1993; Sung and Robberson, 1995).

The meiosis specific recombinase Dmc1 was isolated by Bishop et al. (Bishop et al., 1992) in a screen for meiosis specific cDNA species. Dmc1 exists as an octamer in solution (Passy et al., 1999) and biochemical studies have provided evidence that it forms right-handed, helical filaments on ssDNA in an ATP-dependent manner as well as catalyzes homologous DNA pairing and strand exchange reaction (Bugreev et al., 2005; Sauvageau et al., 2005; Sehorn et al., 2004). Thus, Dmc1 possesses the same functional attributes that have been documented for Rad51 and RecA. For stabilization of the presynaptic filament another protein complex appears onto the scene- the Mnd1-Hop2 complex. *S. cerevisiae* and *A. thaliana* Mnd1 and Hop2 proteins were co-immunoprecipitated, indicating that they exist as a complex (Tsubouchi and Roeder, 2003; Vignard et al., 2007b). Moreover they build a stable, heterodimeric complex,

when they are coexpressed in *E.coli* (Chen et al., 2004; Enomoto et al., 2006; Pezza et al., 2006). The yeast and human Mnd1-Hop2 complex strongly stimulates the recombinase activity of Dmc1 (Chen et al., 2004; Enomoto et al., 2006; Petukhova et al., 2005), whereas the mouse and human Mnd1-Hop2 complex is just active towards Rad51 in this regard (Enomoto et al., 2006; Petukhova et al., 2005).

After a successful homology search, presynaptic filament stabilization, strand invasion into the homologous sequence and synaptic complex formation, a D-loop intermediate is formed (Figure 3). Two crossed strands or a Holliday junction is formed, the latter gets then resolved and give rise to CO or NCO products.

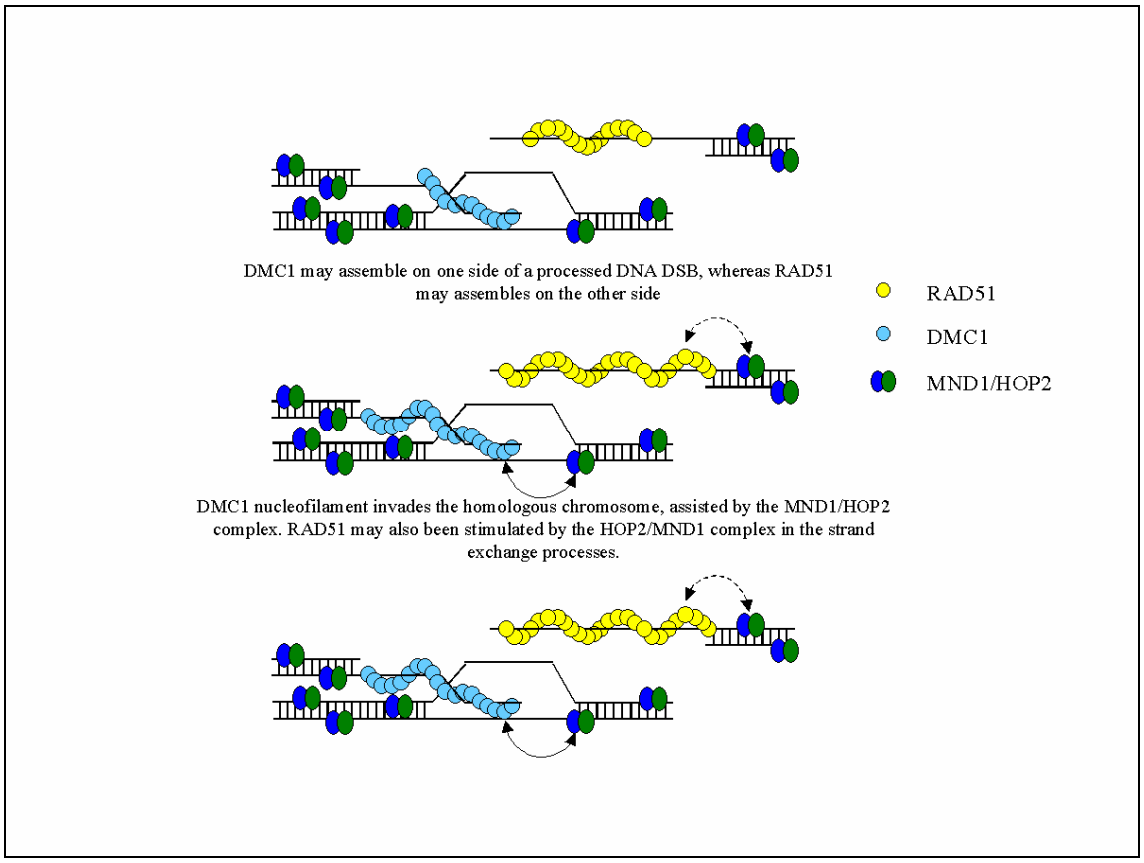

Figure 3: Model of the strand invasion step of meiotic recombination. Mnd1-Hop2 acts on the recombinase activity of Rad51 and Dmc1. The complex stabilizes the presynaptic filament and then cooperates with the presynaptic filament to capture dsDNA (Chen et al., 2004; Chi et al., 2007). Taken from Vignard, Siwiec et al. (2007).

4.2. Introduction to meiosis with special emphasis on plant proteins

Meiosis has two division phases, meiosis I and meiosis II, during which homologous chromosomes and sisterchromatids became separated, respectively (Figure 4A). The products are four haploid gametes. During this process not only the up-and downregulation of various proteins plays a major role, also the changing chromosome-structure is absolutely important to assure the correct progression through meiosis. In contrast to sisterchromatids, which are held together by sisterchromatide-cohesins, homologous chromosomes have no physical connection per se. The breakup of the cohesin complex is the prerequisite for the proper segregation of chromosomes during meiosis. In budding and fission yeast the cohesin complex is comprised of four major subunits: a heterodimeric pair of structural maintenance of chromosomes (SMC) subunits (SMC1/SMC3) and at least two non-SMC subunits, Scc1/Rad21 and Scc3/Psc3 (Ishiguro and Watanabe, 2007). The release of the cohesion complex is catalyzed by a specific endopeptidase, the seperase. Cohesion gets resolved first along the arms of the chromosomes during anaphase I and finally at the centromeres at anaphase II, ensuring the segregation of the sisterchromatids. Centromeric cohesion is protected by the shugoshin protein (Watanabe and Kitajima, 2005). In *Arabidopsis* a meiosis specific Rad21 subunit (Rec8), Syn1/Dif1 has been identified (Bai et al., 1999; Bhatt et al., 1999). Also a homologue of SCC3 could be found and characterized in *Arabidopsis* (Chelysheva et al., 2005). Furthermore the meiotic and mitotic function of the seperase homologue could be shown (Liu and Makaroff, 2006) and two shugoshin homologues were found, but couldn't be characterized so far (Mercier and Grelon, 2008). However during prophase I physical linkage between homologous chromosomes is established through the formation of the synaptonemale complex (SC). The synaptonemal complex is a tripartite structure consisting of two parallel lateral regions and a central element (Figure 4). In *Arabidopsis* only few components of the SC has been described. The central element of the SC is encoded by two partially redundant genes ZYP*a* and ZYP*b* (Higgins et al., 2005). Furthermore ASY1 (Armstrong et al., 2002; Caryl et al., 2000), which is the yeast Hop1 homologue as well as the cohesions REC8 and SCC3 has been found to date (Cai et al., 2003; Chelysheva et al., 2005). The links are cytological visible as a structure called chiasmata. These interconnections are crucial to ensure first the reciprocal exchange of genetic information, and second the proper alignment of homologous chromosomes on the metaphase plate, followed by the correct segregation of homologous chromosomes to opposite poles during anaphase I.

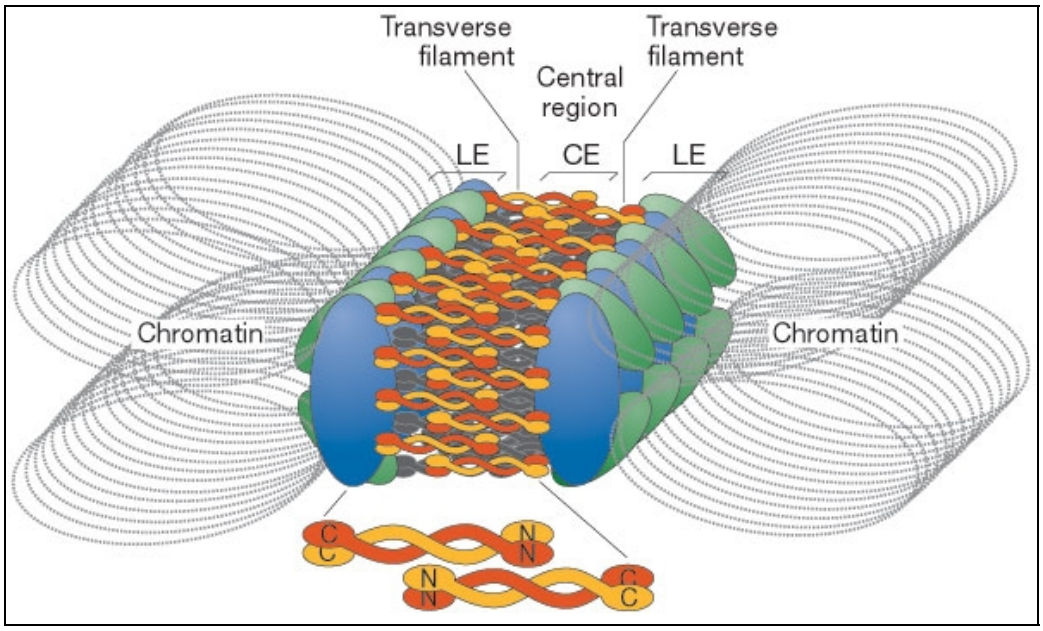

Figure 4: Model of the synaptonemal complex structure. The synaptonemal complex (SC) is a tripartite structure formed by a lateral element (LE), central element (CE) and transverse filaments. The LE comprises cohesins (Rec8, SMC1 and SMC3) as well as the HORMA-domain proteins Hop1/Asy1. The transverse filaments are formed by the proteins Zip1/ZYP1. (Adapted from Page & Hawley (2004) Annual Review of Cell and Developmental Biology 20 ©2004 by Annual Reviews www.annualreviews.org).

Cytologically one of the first meiotic markers detectable to date in *A. thaliana* is REC8, which is loaded onto the chromosomes. It is involved in axis formation and loading of the protein to chromosomes is SPO11-1 independent (Chelysheva et al., 2005). The first stage of meiosis which can be seen by chromosome preparation is the leptotene stage, when chromosomes start to condense and axes begin to form. By meiotic spreading technique pre-leptotene stages are very difficult to identify, because chromatin appears only diffuse, which can be easily mistaken with a cell in G2 stage. Nuclei in leptotene stage are round-shaped and sometimes a chromosome- and organelle-free space corresponding to the nucleolus is visible. Leptotene chromosomes appear as thin, thread like structures, which are evenly dispersed and in some cells brightly stained dots associated with the chromosomes, the chromocentres, are seen. These chromocentres are presumed to be large heterochromatin blocks. In well-spread nuclei up to 14 densely staining chromosome blocks are visible, corresponding to the 10 pericentromeric heterochromatin regions and four nucleolus-organizing regions (NORs) (Ross et al., 1996) (Figure 5A).

With the help of immunostaining technique some of the early recombination proteins can be visualized. *At*SPO11-1 associates on chromatin already in an early leptotene stage (Sanchez-Moran et al., 2007), as well as *At*MRE11-3 (unpublished data) and *At*COM1-1 (Uanschou et al., 2007). At late leptotene/early zygotene, when the

recruitment of recombination proteins, such as *At*RAD51 (this thesis) and *At*DMC1 (Vignard et al., 2007b) reach a peak, pairing of homologous chromosomes begins. Late leptotene and zygotene nuclei show clustering of chromosomes to one side of the cell and point-shaped organelles around the chromatin (Figure 5B). Chromosomes are still very decondensed, when they begin to synapse.

At pachytene stage around 10 *At*RAD51 foci (Rene Ladurner diploma thesis) and 9-10 *At*MLH3 foci become visible in *A.thaliana* (Jackson et al., 2006). *At*MLH3 as well as *At*MLH1, the Arabidopsis homologues of the prokaryotic MutL mismatch repair gene, is required for normal levels of meiotic crossovers. Pachytene chromosomes appear as thick, short and heavily stained chromosome threads, when homologous chromosomes are fully synapsed (Figure 5C).

In diplotene, the late prophase I stage, homologues become separated except at chiasmata through the disassembly of the SC. Chromosomes appear again as thin thread-like structures but they seem to be "fuzzy" and more diffuse than chromosomes in zygotene stage. In addition cytoplasmatic organelles are evenly distributed and can be found around the chromatin. (Figure 5D). Progressive condensation of the chromosomes leads to a sort of culminated structure in late diplotene. From this stage on chromosomes are highly condensed structures, which are intensely stained by DAPI.

In diakinesis, bivalents (pairs of homologues) became visible as very condensed, short structures with prominent pericentromeric heterochromatin blocks. In well spread nuclei ring-shaped bivalents, which have chiasmata on both arms, and rod-shaped bivalents, which have chiasmata on only one arm can be seen (Figure 5E).

At metaphase I the five bivalents are fully condensed and are co-oriented on the spindle with homologous centromeres pointing to opposite poles (Figure 5F). Homologous chromosomes, consisting of two chromatids each, separate at anaphase I, as cohesins are removed from the arms of the chromosomes and chiasmata disassemble (Figure 5G). In telophase I a distinct band of cytoplasmatic organelles is formed between the daughter nuclei and persists until the second meiotic division. Telophase I chromosomes do not show movement and begin to de-condense again (Figure 5H).

At dyad stage (or prophase II), two round-shaped nuclei, each containing five partially de-condensed chromosomes are visible. Cytoplasmatic organelles are forming a dense band between the two nuclei (Figure 5I). At metaphase II the nuclear membrane and the nucleolus break down, chromosomes are highly condensed and the second division spindle appears. On opposite sides of the metaphase band five chromosomes, consisting

of two sister chromatids can be seen, which are held together at pericentromeric adhesion sites (Figure 5J). At anaphase II sisterchromatids become separated and migrate to the spindle poles. As a result late anaphase II cell contain four groups, each containing five chromatids (Figure 5K). At telophase II sister-chromatids stop to migrate and begin to de-condense (Figure 5L) to give rise to the tetrade stage (Figure 5M). Then the four haploid microspores develop into mature pollen grains.

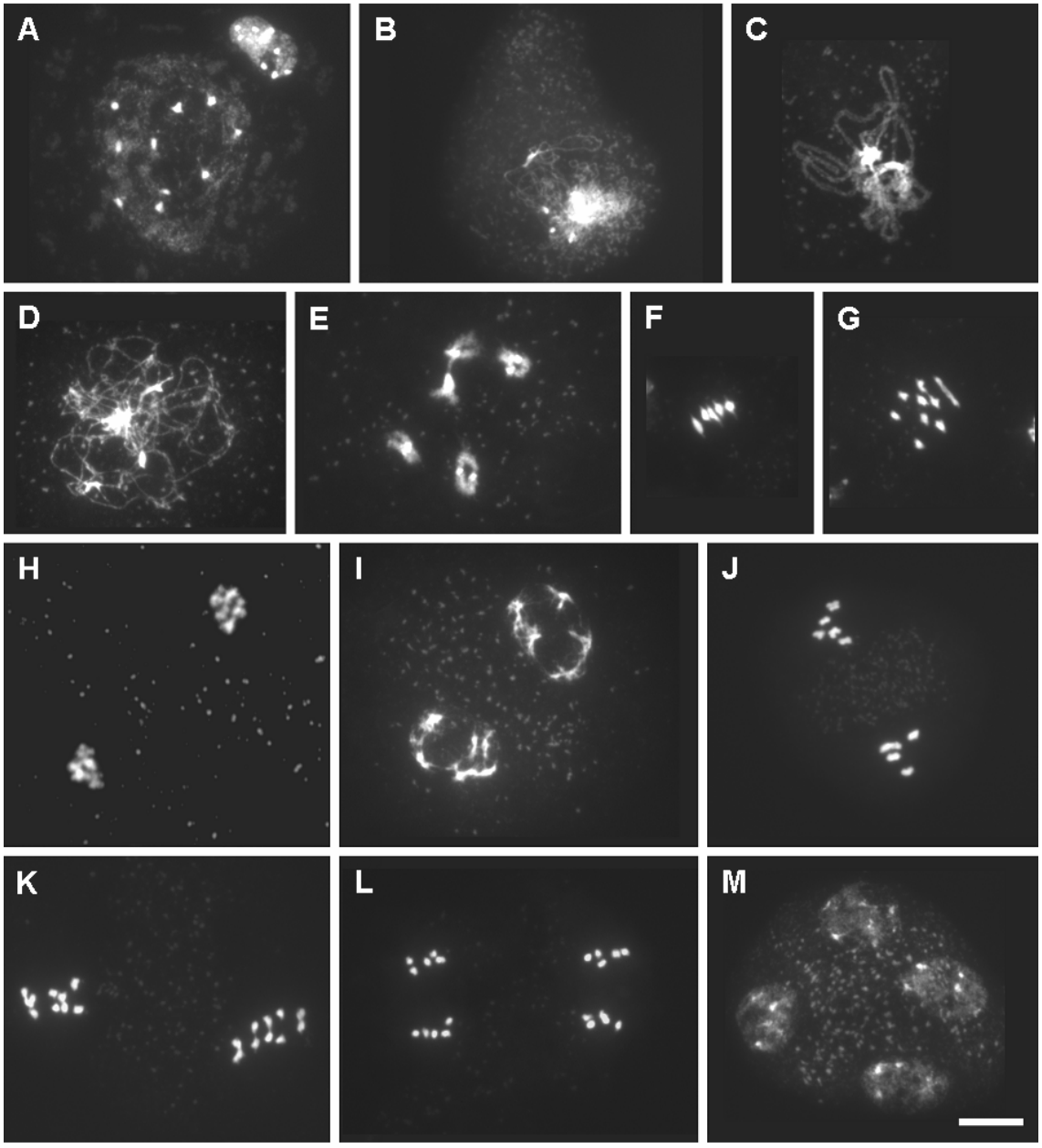

Figure 5: Male meiosis in *A. thaliana.* (A) leptotene stage, (B) zygotene, (C) pachytene, (D) diplotene, (E) diakinesis, (F) metaphase I, (G) anaphase I, (H) telophase I, (I) dyade stage, (J) metaphase II, (K) anaphase II, (L) telophase II, (M) tetrade stage. Chromosomes are stained with DAPI, Size bar 10µm.

5. Introduction *At*MND1

5.1. The Mnd1/Hop2 complex

MND1 (meiotic nuclear division 1) was first identified in a screen for genes expressed early during meiosis in *S. cerevisiae* (Rabitsch et al., 2001). Genes were initially examined cytologically for defects in chromosome segregation and spore formation. Extensive synapsis occurred in *mnd1Δ* mutants, but nuclei containing 16 fully synapsed bivalents were rarely found. Rabitsch et al. concluded that the *mnd1Δ* mutants may be defective in late phase of recombination, synapsis, and/or SC disassembly. Almost contemporaneously DeRisi et al. isolated *MND1* in a functional genomics approach designed to identify genes required for meiotic recombination. *Mnd1* mutants arrest before the first meiotic division with a phenotype comparable to *dmc1* mutants. Physical and genetic analysis showed that these cells initiated recombination, but did not form heteroduplex DNA or double Holliday junctions, suggesting that *MND1* is involved in strand invasion (Gerton and DeRisi, 2002). *Mnd1* mutants arrest in prophase I due to DNA-damage checkpoint activation dependent on Mec1 with DSBs whose 5' strands undergo massive degradation. Furthermore, through deletion of Red1 or Hop1, which are axial element proteins, nuclear division and spore formation in *mnd1Δ* mutants can be restored to wild-type levels. The *red1* mutation may allow Mnd1-independent repair from the sister template (Figure 6). These results are best explained by assuming that the axis components Red1 and Hop1 prevent repair from the sister chromatid in the *mnd1Δ* mutant, similar to Red1's effect on *dmc1Δ* mutants (Zierhut et al., 2004).

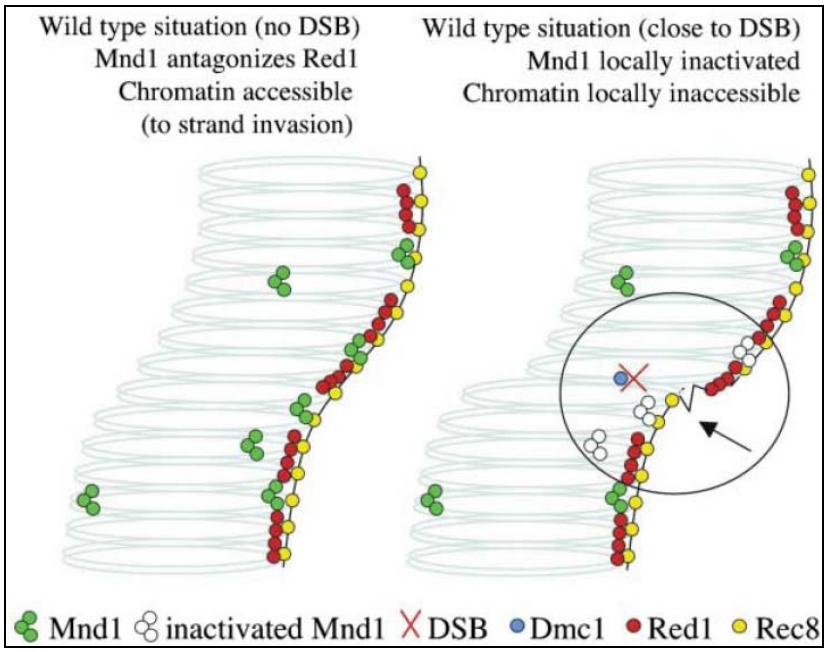

Figure 6: Local inhibition model for IH bias, taken from Zierhut et al. 2004.The right chromatid shows DSBs loaded with DMC1 protein and the chromosome is available for Dmc1-dependent repair. Inhibition of Mnd1 on both chromatids close to a DSB would exclude the sister from serving as a repair template.

Overexpression of Rad54, which is involved in the intersister- (IS) repair pathway, partially restores the sporulation of *dmc1Δ* mutants, probably by channelling the repair pathway to repair via the sister chromatid. The overexpression of Rad54 in the *dmc1Δ* and *mnd1Δ* single mutant as well as in the *dmc1Δ mnd1Δ* double mutant showed that the restoration of spore formation is only possible in the absence Dmc1 in a *mnd1Δ* mutant background. This leads to the conclusion that Dmc1 bias the repair to the homologue chromosome only in the presence of Mnd1, whereas Mnd1 alone may not interfere with a successful Rad54-mediated IS-repair (Zierhut et al., 2004). The phenotype of *mnd1Δ* mutants in *S. cerevisiae* is similar to the one found in *hop2* mutants of yeast. The *hop2-1* mutant was isolated in a screen for mutants defective in meiotic gene conversion (Leu et al., 1998). Furthermore Mnd1 was found to be a multicopy suppressor of a *hop2-ts* mutant, which produces spores at 23°C but fails to sporulate at 33°C. The multicopy of *MND1* does not suppress the null mutant of *hop2*, showing that overexpression can not bypass the requirement of Hop2 (Tsubouchi and Roeder, 2002). The ability to suppress the *hop2-ts* allele by Mnd1 overproduction suggests that Hop2 and Mnd1 act in the same pathway. If so, then a *hop2 mnd1Δ* double mutant should display a defect similar to the one of the single mutants. If *mnd1Δ* and *hop2* affect pairing thorough different mechanisms, there should be additive effects visible in the double mutants. To address this question homologous pairing was assayed by FISH. And it was shown that the

double mutant behaves similarly to the two single mutants, indicating that *HOP2* and *MND1* are in the same epistasis group with respect to pairing (Tsubouchi and Roeder, 2002). Interestingly, Mnd1 and Hop2 also act together *in vivo* as shown with a GFP tagged version of Mnd1 in spread meiotic nuclei. Not only that they show similar staining pattern and a significant overlap, the localization of Mnd1 onto chromosomes requires Hop2 and vice versa (Tsubouchi and Roeder, 2002). Furthermore Mnd1 and Hop2 co-immunoprecipitate in meiotic cell extract, arguing for the possibility that Mnd1 and Hop2 act as a heterocomplex in the strand invasion process (Enomoto et al., 2006; Pezza et al., 2006; Pezza et al., 2007; Tsubouchi and Roeder, 2002).

Analyses of Hop2 in organisms other than budding yeast, such as fission yeast, mouse and *Arabidopsis* have underlined its importance for the regular processing of DSBs and synapsis between homologues (Nabeshima et al., 2001; Petukhova et al., 2003; Schommer et al., 2003). Genetic studies in yeast suggested a role for the Hop2 protein in homologous pairing and recombination. Although the yeast *hop2* mutant is unique in the way that defective homologous pairing is combined with synapsis between non-homologous chromosomes (Leu et al., 1998; Tsubouchi and Roeder, 2002). In *Hop2* knockout mice meiosis arrests prior to pachytene stage with chromosomes whose axial element formation is complete but, as in yeast, synapsis in *Hop2*$^{-/-}$ spermatocytes takes place mostly between nonhomologous chromosomes (Petukhova et al., 2003). Since numerous Rad51 and Dmc1 foci form and stay along the chromosomes, the removal of Spo11 and resection of DSB ends seems unaffected. Furthermore Hop2 acts upstream of Dmc1 and Rad51 first shown in epistastis analysis in mouse (Petukhova et al., 2003). And second Hop2 localizes to chromatin before Rad51 and Dmc1 and even in the absence of DSBs (Tsubouchi and Roeder, 2002). Hop2 localization to chromatin loops and not to chromosome cores is important, because most of the DSBs occur in the chromatin loops (Blat et al., 2002). Hop2 might localize to the chromatin regions that will eventually be susceptible to the action of Spo11, thus ensuring that Hop2 will be in the vicinity of the ssDNA exposed on the resected ends. And finally, biochemical data indicate that mouse Hop2 can be involved in single strand invasion, the initial step in heteroduplex formation during homologous recombination (Chen et al., 2004).

In *S. cerevisiae*, the Mnd1-Hop2 complex assists in a Dmc1 pathway during homologous recombination as it can promote Dmc1 strand assimilation activity *in vitro* (Chen et al., 2004). The absence of Mnd1 or Hop2 leads to the accumulation of both Dmc1 and Rad51 on processed DNA ends, but various studies have suggested that the

Mnd1-Hop2 complex is active only in a Dmc1-dependent pathway (Leu et al., 1998; Tsubouchi and Roeder, 2002; Zierhut et al., 2004). Genetic interactions between *DMC1* and *HOP2*/*MND1* appear conserved in evolution. For example, nematodes, fruit flies and *Neurospora crassa* do not possess *DMC1*, *MND1* or *HOP2* orthologues (Gerton and Hawley, 2005).

However, human and mouse TBPIP proteins have been identified as mammalian orthologues of Hop2 (Ijichi et al., 2000; Tanaka et al., 1997). In a competitive DNA-binding experiment it was shown that hTBPIP/Hop2-hMnd1 binds preferentially to dsDNA. This DNA-binding property is the same as the one of the yeast Hop2-Mnd1 complex (Chen et al., 2004). The mouse TBPIP/Hop2-hMnd1 complex binds to ssDNA as well as to dsDNA without any preferences (Petukhova et al., 2005). This suggests that the DNA-binding activity of the human and the mouse TBPIP/Hop2-hMnd1 complex may differ from each other. Human TBPIP/Hop2-hMnd1 stimulates homologous pairing promoted by hDmc1, which was shown in a D-loop formation assay. In this assay, hDmc1 formed D-loops within 5 min, and the D-loops were dissociated by the subsequent strand exchange promoted by hDmc1. hTBPIP/Hop2-hMnd1 itself did not promote D-loop formation, but significantly stimulated the Dmc1-mediated D-loop formation Interestingly, hTBPIP/Hop2-hMnd1 significantly enhanced the D-loop yield, but it did not inhibit the D-loop dissociation (Enomoto et al., 2006). This observation suggests that the hTBPIP/Hop2-hMnd1 complex may stimulate strand exchange and homologous pairing.

Furthermore, hTBPIP/Hop2-hMnd1 does not enhance the DNA-dependent ATP hydrolyzing abilities of hDmc1 and hRad51. Moreover hTBPIP/Hop2-hMnd1 preferentially binds to a three-stranded DNA branch, that mimics an intermediate for strand exchange than Y-form DNA or dsDNA (Enomoto et al., 2006).

In mouse, mDmc1 and mHop2 coimmunoprecipitate with mMnd1 from mouse testis and purified mMnd1/mHop2 enhances the strand invasion activity of mDmc1 35-fold *in vitro* (Petukhova et al., 2005). In contrast, purified yeast Mnd1/Hop2 stimulates the strand invasion activity of yeast Dmc1 only threefold *in vitro* (Chen et al., 2004). Furthermore, there are at least two results in yeast that are inconsistent with a direct, stable interaction between Mnd1/Hop2 and Dmc1 (Chen et al., 2004). Genetic and biochemical data regarding the function of Mnd1/Hop2 with Rad51 is even less clear. In one study, purified mMnd1/mHop2 stimulated strand invasion by mRad51 10-fold *in vitro* (Petukhova et al., 2005), in another study, mHop2 had no effect on human Rad51

in vitro (Enomoto et al., 2004). The physical interaction of the mMnd1/mHop2 complex with mRad51 is weaker than with mDmc1 (Petukhova et al., 2005).

In fission yeast the strength of interaction between spHop2 and spMnd1 is similar to spRad51 homodimerization. Truncation analysis revealed that the C-terminus of spHop2 interacts with the C-terminus of spMnd1. Interestingly, spHop2 and spMnd1 interact with themselves, suggesting the possibility that they can form homo- as well as hetero-complexes *in vivo*. The spHop2-spMnd1 complex shows strand exchange activity which is increased 5-fold when spDmc1 is present. This result reveals that stimulation by spHop2-spMnd1 is specific for spDmc1, as the effect is not observed with spRad51. Only a pull down assay shows an interaction of Mnd1 and Hop2 with both spDmc1 and spRad51. Moreover spHop2-spMnd1 complex can simulate spDmc1 D-loop formation activity 8-fold when magnesium is added and 17-fold in a calcium containing buffer (Ploquin et al., 2007).In *S. cerevisiae*, the phenotype of the *hop2* and *mnd1Δ* mutants is very similar to that of *dmc1* and different from that of *rad51* (Chen et al., 2004; Gerton and DeRisi, 2002). Second, the meiotic defects of *mnd1* or *hop2* can be bypassed by overexpressing *RAD51*, as reported for *dmc1* (Tsubouchi and Roeder, 2003). A physical interaction between Rad51 and Mnd1/Hop2 has not been demonstrated in budding yeast. The fact that mammalian Mnd1-Hop2 complexes can interact with Dmc1 but also with Rad51, stimulating the activities of both proteins, suggests that the function of the Mnd1-Hop2 complex has evolved from yeasts to mammals (Enomoto et al., 2006; Petukhova et al., 2005).

Recently, it has been found that the heterodimer Mnd1/Hop2 aided by Dmc1 enhances the alignment of homologues sequences (Pezza et al., 2007). Furthermore, it was shown that Mnd1/Hop2 is able to increase the stability of pre-formed Dmc1-ssDNA nucleoprotein filament and moreover, play also a role prior to duplex DNA capture (Pezza et al., 2007). Chi et al (Chi et al., 2007) showed that the DNA-binding capability of the heterodimeric complex Mnd1/Hop2 is mainly dependent on Hop2. The ability of Mnd1/Hop2 to interact with hRad51, depends on both subunits of the complex, but Mnd1 plays the more prominent role (Chi et al., 2007). In addition Mnd1/Hop2 enhances the stability of the pre-synaptic hRad51 filament and engages duplex DNA capture (Chi et al., 2007).

5.2. RecA-related proteins and their relationship with Mnd1-Hop2

At the beginning of homologous recombination, an ssDNA tail derived from a DSB site invades the homologous dsDNA. This initial strand-invasion step is called homologous pairing. Just after homologous pairing, homologous pairing is expanded by strand exchange. These two homologous-pairing and strand-exchange steps may play distinct roles. Homologous pairing mediates the initial contact in a short tract, and may be important for finding homologous sequences between chromosomes (Enomoto et al., 2006). Only short homologous sequences are required for homologous pairing. In fact, bacterial RecA promotes homologous pairing with short oligonucleotides (Hsieh et al., 1992; Rao et al., 1993).

The enzymes that mediate pairing during HR are called recombinases, and the reaction mediated by these enzymes is termed "homologous DNA pairing" and "strand exchange". Two recombinases, Rad51 and Dmc1, exist in eukaryotes. Rad51 is involved in both mitotic and meiotic recombination, whereas Dmc1 is involved only in meiosis and seems to have a specific role in recombination between homologs (Paques and Haber, 1999).

The two RecA homologs play unique, different roles during meiotic DSB repair, but they also cooperate to achieve efficient meiotic recombination, presumably by asymmetric assembly at either end of the DSB (Shinohara and Shinohara, 2004). Once assembled, the presynaptic filament captures a duplex DNA molecule and searches for homology in the latter. From studies done with RecA (Bianco et al., 1998), it is expected that the homology search process occurs by random collisions between the presynaptic filament and the duplex molecule.

In *S. cerevisiae*, the inactivation of the *RAD51* gene results in a decrease of both mitotic and meiotic HR, as well as hypersensitivity to several DNA damaging reagent (Dudas and Chovanec, 2004; Symington, 2002). Cells accumulate DSBs and show defects in SC formation and homologous pairing. (Dudas and Chovanec, 2004; Richardson et al., 2004; Symington, 2002). Rad51 is well conserved among eukaryotes and orthologues of Rad51 have been identified in many species. As an example, human Rad51 shares 67% of sequence identity with *S. cerevisiae* Rad51 (Shinohara et al., 1993; Yoshimura et al., 1993). Rad51 protein is , as mentioned before, able to promote strand exchange reactions between homologous single- and double-stranded DNA molecules (Sung et al., 2003). Orthologues of Rad51 have been identified in several plants, including *A .thaliana*, maize and the moss *Physcomitrella patens* (Doutriaux et al., 1998; Franklin et

al., 1999; Markmann-Mulisch et al., 2007). While the *Arabidopsis* genome codes for a single Rad51 orthologue, *AtRAD51*, the genomes of both, maize and *Physcomitrella*, code for two closely related Rad51 orthologues. *Atrad51* mutants show *Atspo11-1* depended chromosome fragmentation and are completely male and female sterile. In contrast to *A. thaliana*, where *Atrad51* mutants are viable (Li et al., 2004), *rad51* mutant mice die early in embryonic development and *rad51* cell lines cannot proliferate *in vitro* (Lim and Hasty, 1996; Tsuzuki et al., 1996). Furthermore, inactivation of RAD51 in *D. melanogaster* and *C. elegans* leads to lethality, a phenotype more comparable to the *RAD51* knockout in mouse (Lim and Hasty, 1996; Takanami et al., 1998; Tsuzuki et al., 1996).

Another, but meiosis specific, RecA homologue is the Dmc1 protein. In *S. cerevisiae* a physical interaction between Rad51 and Dmc1 has been found *in vivo* (Bishop, 1994). Furthermore a co-localization has been shown on spreads of meiotic chromosomes (Bishop, 1994). The inactivation of Dmc1 reduces the meiotic HR efficiency as shown by a *rad51 dmc1* double mutant which exhibits a significant reduction in the frequency of meiotic recombination than the single mutants alone (Dresser et al., 1997; Shinohara et al., 1997). Dmc1 is required for the inter-homolog bias in yeast (Schwacha and Kleckner, 1997) and therefore for the use of the homologous chromosome to repair meiotic DSBs. Also in vertebrates an orthologue of Dmc1 has been identified (Habu et al., 1996). *Dmc1* mutant mice are viable, but the mutation in the *DMC1* gene still leads to a sterility defect, which results in an absence of gametes (Yoshida et al., 1998). Meiosis arrests in meiotic prophase and chromosomes show a defect in assembly of the synaptonemal complex (Pittman et al., 1998). In the genome of plants orthologues Dmc1 has been found. Dmc1 has been identified in *Arabidopsis* (*AtDMC1*) as well as in *Lily* (Lim15) (Doutriaux et al., 1998; Klimyuk and Jones, 1997; Kobayashi et al., 1994). In *Arabidopsis*, even so the expression of *At*DMC1 seems to be meiosis specific, it also has been shown that *At*DMC1 is expressed in mitotically active suspension culture in a cell cycle dependent manner like *At*RAD51 (Doutriaux et al., 1998). But in contrast to *AtRAD51*, *AtDMC1* is not up-regulated after ionizing radiation (Doutriaux et al., 1998). Immunolocalization studies from *Lily* show that Lim15 associates in foci and co-localizes with Rad51 on meiotic chromosomes (Anderson et al., 1997; Terasawa et al., 1995). Yeast interaction experiments have shown that *At*RAD51 and *At*DMC1 interact, supporting the idea that these two proteins work together in meiotic HR events (Dray et al., 2006). Interestingly, the absence of *At*DMC1 possibly leads to repair of DSBs via

the sister chromatid by *At*RAD51, whereas the *At*rad51 mutation shows severe chromosome fragmentation in *A. thaliana* (Couteau et al., 1999; Li et al., 2004). This suggests a role for *At*DMC1 to bias meiotic DSB repair to the homolog chromosome, in contrast to *At*RAD51 which seems to bias repair in an inter-sister chromatid dependent pathway.

Additional RecA-related proteins are found in eukaryotes. Rad55 and Rad57 seem to be specific to yeast, whereas vertebrates have five Rad51 paralogues: RAD51B, RAD51C, RAD51D, XRCC2 and XRCC3.

Rad55 and Rad57 are involved in mitotic as well as in meiotic homologous recombination (Krogh and Symington, 2004; Richardson et al., 2004; Symington, 2002). Rad55 and Rad57 do not possess any strand exchange activity, but it was shown that the heterodimer, which interacts with Rad51 through the Rad55 subunit (Sung et al., 2003), can stimulates Rad51 activity (Sung, 1997), suggesting a role in the assembly of the Rad51-DNA nucleoprotein filament.

RecA homologue Xrcc3 is thought to be involved in late holliday junction resolution in vertebrate cells, as well as in mitotic recombination, DNA repair and chromosome stability (Brenneman et al., 2002; Liu et al., 2007; Symington and Holloman, 2004). Also in *A. thaliana* an orthologue of Xrcc3 has been found (Bleuyard and White, 2004). Mutant plants are mildly sensitive to DSBs inducing agents, highly sensitive to DNA cross-linking agents and show chromosomal fragmentation in meiosis. Interestingly, in contrast to *Atrad51* mutants plants, where chromosome fragmentation is dependent on *At*SPO11-1, in *Atxrcc3-Atspo11-1* mutant plants, chromosome fragmentation and chromosomal bridges are visible in meiosis II, which implies unresolved sister chromatid events (Bleuyard et al., 2004).

In higher eukaryotes three stable complexes involving Rad51 paralogues have been identified (see Table1). One contains RAD51B, RAD51C, RAD51D, and XRCC2, and the other one RAD51C and XRCC3 (Masson et al., 2001; Wiese et al., 2002). *Arabidopsis* homologues of the RAD51B, RAD51C and XRCC2 have been identified (Bleuyard et al., 2005). A third complex consists of RAD51 and XRCC3 (Schild et al., 2000). Recently, a hypomorphic mutation of the RAD51C gene has been generated in mice, that affects male and female meiosis (Kuznetsov et al., 2007). So far it seems that, in *A. thaliana* only RAD51C plays a role in meiosis and transcription is induced upon gamma radiation (Abe et al., 2005). In addition, AtRAD51C is important for both normal homolog pairing and/or juxtaposition and synapsis (Li et al., 2005). In contrast,

Atrad51B and *Atxrcc2* mutants are fertile and do not have detectable developmental defects (Bleuyard et al., 2005). Therefore, *AtRAD51B*, *AtRAD51C*, and *AtXRCC2* most likely only, play a role in DNA repair during the mitotic cell cycle. Furthermore, *AtRAD51C* is required for meiotic prophase I and cannot be substituted by *RAD51* or other *RAD51* paralogues.

In recent years, efforts have focused on clarifying meiotic mechanisms in *Arabidopsis thaliana*. The apparent absence of strict meiotic checkpoints and the greater viability of several meiotic *Arabidopsis* mutants than of their counterparts in mammals have made the use of powerful genetic approaches possible.

Two Spo11 homologues are essential for meiotic recombination: *AtSPO11-1* and *AtSPO11-2* (Grelon et al., 2001; Stacey et al., 2006). Furthermore, homologues of Rad51 and Dmc1 have been identified, and characterization of the corresponding mutants has revealed important differences in their role during meiosis. *Atrad51* mutants fail to repair meiotic DSB, as shown by extensive *AtSPO11-1*-dependent chromosome fragmentation during meiosis (Liu et al., 2004). In contrast, the chromosomes remain intact in *Atdmc1* mutants, do not form bivalents and segregate as univalents during meiosis (Couteau et al., 1999). The formation of intact univalents in *Atdmc1* is dependent on *AtRAD51* and it is thought that the DSB formed in *Atdmc1* mutants are repaired via the sister chromatid (Siaud et al., 2004a). Disruption of *AHP2* (the *Arabidopsis* Hop2 homolog) or *At*MND1 leads to meiotic defects similar to those observed in *Atrad51* with chromosome fragmentation indicating the failure to repair DSB (Kerzendorfer et al., 2006a; Schommer et al., 2003). *At*MND1 function seems to be required after recombinase assembly because, as in yeast, *At*RAD51 foci are seen in *Atmnd1* mutants (Kerzendorfer et al., 2006a).

In addition to *AtRAD51* and *AtDMC1*, the five *RAD51* paralogues identified in vertebrates are also present in the *Arabidopsis* genome (Bleuyard et al., 2005). *AtRAD51B*, *AtRAD51C*, *AtXRCC2* and *AtXRCC3* are required for DNA repair, but only the products of *AtRAD51C* and *AtXRCC3* are involved in meiosis (Bleuyard and White, 2004; Li et al., 2005). Phenotypic analyses of *Atrad51c* and *Atxrcc3* mutants have shown that, as in *Atrad51*, *Atmnd1* and in *ahp2* mutants, chromosome fragmentation occurs without prior chromosome synapsis. All the proteins cited above are required for correct DSB repair, chromosome pairing and synapsis. However, little is known about their functional relationship and their genetic and physical interactions in *Arabidopsis*.

Two-hybrid assays have shown that *At*MND1 interacts with AHP2 and that *At*XRCC3 interacts with *At*RAD51 and *At*RAD51C (Kerzendorfer et al., 2006a; Osakabe et al., 2002).

6. Results *AtMND1*

6.1. Initial characterisation of the *AtMND1* gene

The initial characterization of *AtMND1* was performed by Claudia Kerzendorfer (Kerzendorfer et al., 2006b).

Expression analysis by RT-PCR revealed a ubiquitous expression within the plant body, with highest expression levels in cell suspension and seedlings. To investigate the *AtMND1* gene function in *Arabidopsis*, we searched for mutants in the Salk Institute Genomic Analysis Laboratory T-DNA collection (Alonso et al., 2003). An insertion mutant line (SALK_110052), carrying a T-DNA insertion within the 7th intron of the *AtMND1* gene, was found and the corresponding allele was named *Atmnd1*.

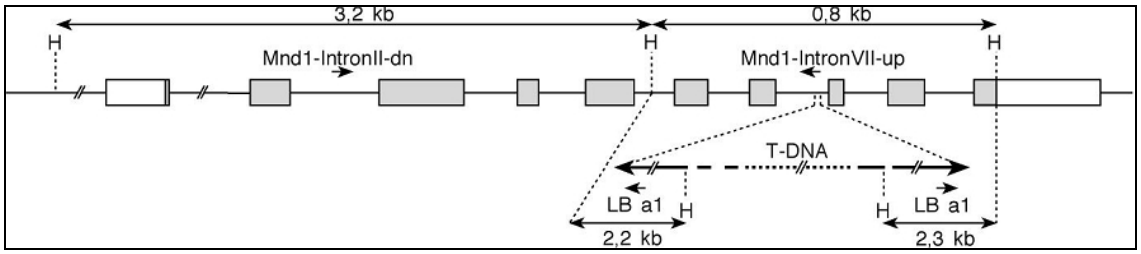

Figure 7: Overview of the AtMND1 gene locus and the Atmnd1 mutant allele. Grey boxes represent exons, white indicate 5' and 3' UTRs. The position of the T-DNA insertion with its borders is denoted as a triangle. Primers and Hind III restriction sites are marked. Expected fragments after Hind III digestion are depicted as double-arrows. (taken from Kerzendorfer et.al.; 2006)

6.2. Morphological characterisation of *Atmnd1*

We observed a sterility phenotype in the progeny of self-fertilized heterozygous *Atmnd1* plants that co-segregates with the homozygous mutant genotype. Whereas wild-type plants develop long siliques with an seed average of 32 seeds/siliques (counted siliques: n=657, seed count has been performed by Claudia Kerzendorfer), homozygous *Atmnd1* mutants develop short siliques that produce only 0.033 seeds/silique (n=4930). Morphologically, plants heterozygous for the *Atmnd1* mutation were indistinguishable from wild-type plants and self-fertilisation produced homozygous mutants in the expected 3:1 ratio. Homozygous plants show no vegetative growth defect and germination is not delayed. Only the flowering time of homozygous *Atmnd1* mutant plants is longer than for wild-type, a phenotype which is often observed in sterile plants. Mitotically dividing cells of *Atmnd1* mutant plants behave normally, indicating that plants show no defect in vegetative growth (Figure 8) (Kerzendorfer et al., 2006).

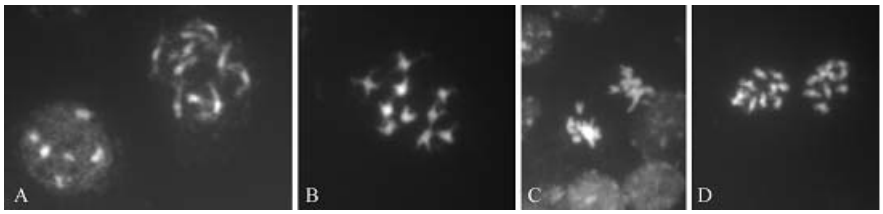

Figure 8: DAPI stained mitotic cell of *Atmnd1*.(A) and (B) mitotic nuclei in G phase, (C) mitotic anaphase, (D) mitotic telophase. Chromosomes stained with DAPI. (experiment done by A. Pedrosa-Harand)

Heterozygous *Atmnd1* plants were transformed with a T-DNA, containing the genomic copy of the *AtMND1* gene and its putative promoter region, to confirm that the sterility phenotype of the *Atmnd1* mutant is caused by aforementioned mutation. All offspring plants (n = 108) of 4 individual transformants, which were heterozygous or homozygous for the *Atmnd1* allele and contained the complementing T-DNA were fertile, indicating a complete reversion of the sterility phenotype by a genomic copy of *AtMND1* (Figure 9).

Figure 9: *Atmnd1* mutant plants develop short siliques and no regular pollen grains. (A) *Atmnd1* plants look like wild-type plants, except that they have shorter and empty siliques. The left panel shows a stem with full-grown siliques of a wild-type plant (wt). The middle panel shows the stem of an *Atmnd1* plant of the same age, which failed to develop siliques (*Atmnd1*). The right panel displays an *Atmnd1* homozygous mutant plant, transformed with a wild-type copy of the genomic *AtMND1* region showing restored fertility. (taken from Kerzendorfer et al.,2006; experiment done by Tanja Siwiec and Svetlana Akimcheva)

6.2. Male and female meiosis are severely disrupted in *Atmnd1* mutants

To further investigate the defects of the *Atmnd1* mutant plants, we looked at the viability of pollen grains, the products of male meiosis. The viability of pollen grains can be easily visualized by Alexander staining (Alexander, 1969). Red staining of the cytoplasm corresponds to mature, viable pollen and green staining is indicative of aborted pollen grains. As shown in Figure 10 wild-type anthers contain red stained pollen grains whereas *Atmnd1* mutant plants are almost completely devoid of viable pollen, recognizable by the green counter staining of the pollen wall. The aborted pollen grains are generally smaller and variable in size (Kerzendorfer et al., 2006b).

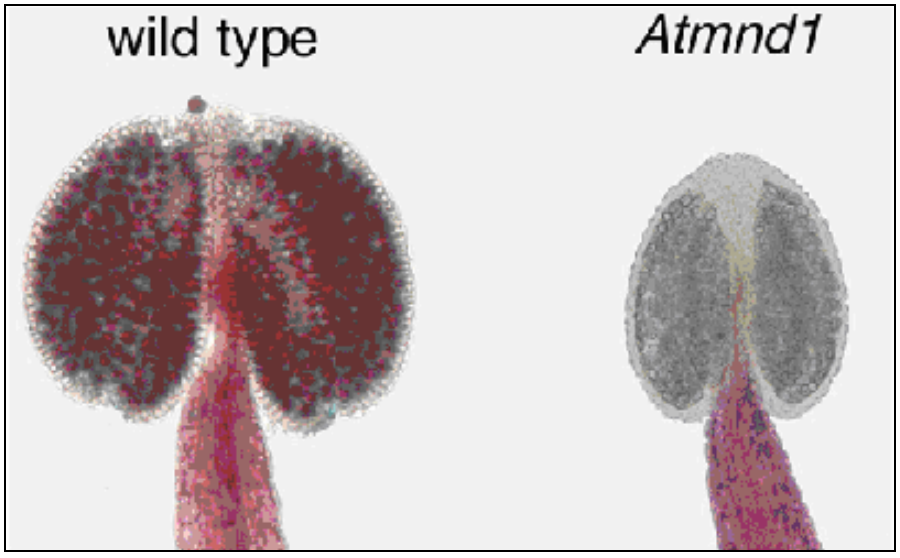

Figure 10: Anthers of wild-type (left panel) and *Atmnd1* (right panel) plants stained according to Alexander (1969). The purple stained cytoplasm indicates viable pollen grains. *Atmnd1* plants did not develop regular pollen grains. (taken from Kerzendorfer et al.,2006; experiment done by Tanja Siwiec)

Applying a chromosome spreading technique we analyzed the behaviour of male meiotic chromosomes in wild-type as well as in *Atmnd1* mutant plants (Figure 11). In wild-type meiocytes leptotene chromosomes appear as thin thread like structures, with ten to fourteen visible chromocentres (Figure 11A). In zygotene stage homologous chromosomes begin to synapse, and the chromatin clusters at one side of the cell, with some chromatin loops visible (Figure 11B). At pachytene stage (Figure 11C) homologous chromosomes are fully synapsed along their entire length, and the SC disappears in diplotene stage (Figure 11D). This results in five strongly condensed bivalents in diakinesis, which align at the metaphase plate in metaphase I (Figure 11E). In anaphase I (Figure 11F) homologous chromosomes begin to separate and migrate to opposite poles of the cell. At the end of meiosis II, when sisterchromatide cohesion

breaks down at the centromeres and chromatids get separated four sets of five chromosomes each (Figure 11J) are visible.

In *Atmnd1* meiocytes the earliest stage of prophase I looks similar to wild-type (compare Figure 11L to 11A). However, later on zygotene-like stage failed to develop (compare Figure 11M to 11B) and correct pairing of homologous chromosomes in a pachytene-like stage was completely missing (compare Figure 11N to 11C). Subsequently, chromosomes condensed further and altered chromosome structures during early diakinesis-like stage and diakinesis-like stage was observed. Instead of five aligned bivalents an entangled mass of chromosomes can be seen in metaphase I-like stage (compare Figure 11O to 11E). When chromosomes began to migrate, at anaphase I-like stage (Figure 11P), chromosome fragmentation was observable and sometimes chromatin links were sometimes present. During the second meiotic division, chromosome fragmentation was visible at the metaphase-II-like stage (Figure 11S) and became more pronounced at the late anaphase-II-like stage (Figure 11T).

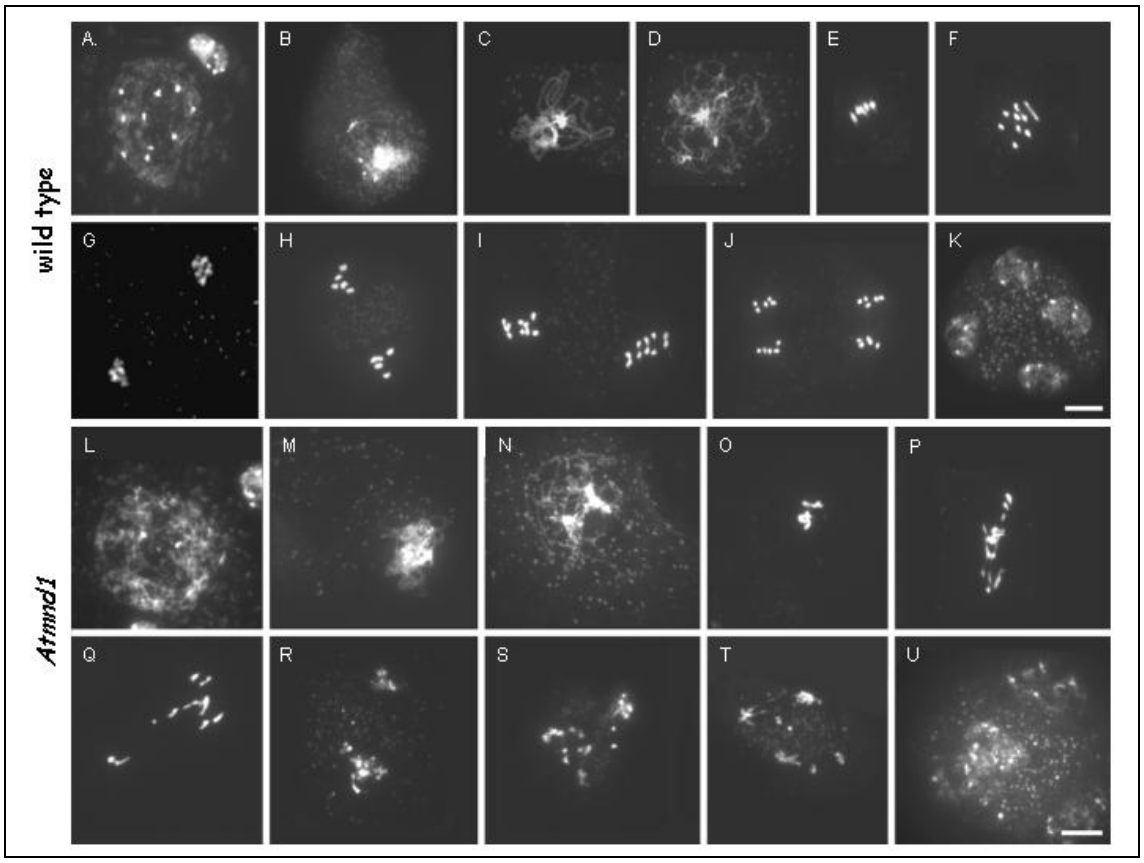

Figure 11: Male meiosis is severely disrupted in *Atmnd1* mutants. Meiosis in wild-type *A. thaliana*: (A) leptotene, (B) zygotene, (C) pachytene, (D) diplotene, (E) metaphase I, (F) anaphase I, (G) telophase I, (H) metaphase II, (I) anaphase II, (J) telophase II, (K) tetrade stage.. Disrupted male meiosis in the *Atmnd1* mutant: (L) leptotene, indistinguishable from the wild-type. (M) Zygotene-like stage. (N) Pachytene-like stage. The mutant failed to go through typical zygotene and pachytene stages, displaying no pairing and synapsis of chromosomes. (O) metaphase I-like stage, (P)and (Q) Progression through anaphase I with stretched chromatin and limited chromosome fragmentation. (R) telophase I-like stage, (S) Metaphase II-like stage with chromosome fragments. (T) Late-anaphase-II-like stage with severe chromosome fragmentation, (U) polyade stage. Chromosomes were stained with DAPI. Scale bar, 10 µm. (taken from Kerzendorfer et al.,2006; experiment done by Tanja Siwiec)

As male and female meiosis are sometimes differently affected in *Arabidopsis* (Mercier et al., 2001), we analyzed gametophyte development and female meiosis in *Atmnd1* mutants. We found that 2.4% of fully grown ovules in *Atmnd1–/–* mutants contained apparently normal embryo sacs, 2.8% contained an embryo sac blocked during mitotic divisions and 94.8% contained a degenerated or a single nucleus embryo sac (n = 611) (experiment was performed by Julien Vignard, supplementary Figure S1A-F). We pollinated *Atmnd1–/–* mutants with wild-type pollen and found 2.2% seed formation (1.08 seeds/silique, n = 25) when compared with the wild-type (50 seeds/silique). Only 0.68 seeds/silique were viable, leading to an overall fertility of 1.4%. This indicates that female meiosis is less affected than male meiosis (experiment was performed by Julien Vignard).

The cytological defects of observed chromosomes were similar to those seen in male meiosis (Fig. 12). Typical pachytene stages were not observed (compare Fig. 12D to 12A). An entangled chromosome mass instead of five bivalents was formed at metaphase I-like stages (compare Fig. 12E to 12B) and chromosome fragmentation was seen at anaphase I-like stages (compare Fig. 12F to 12C) (Kerzendorfer et al.;2006).

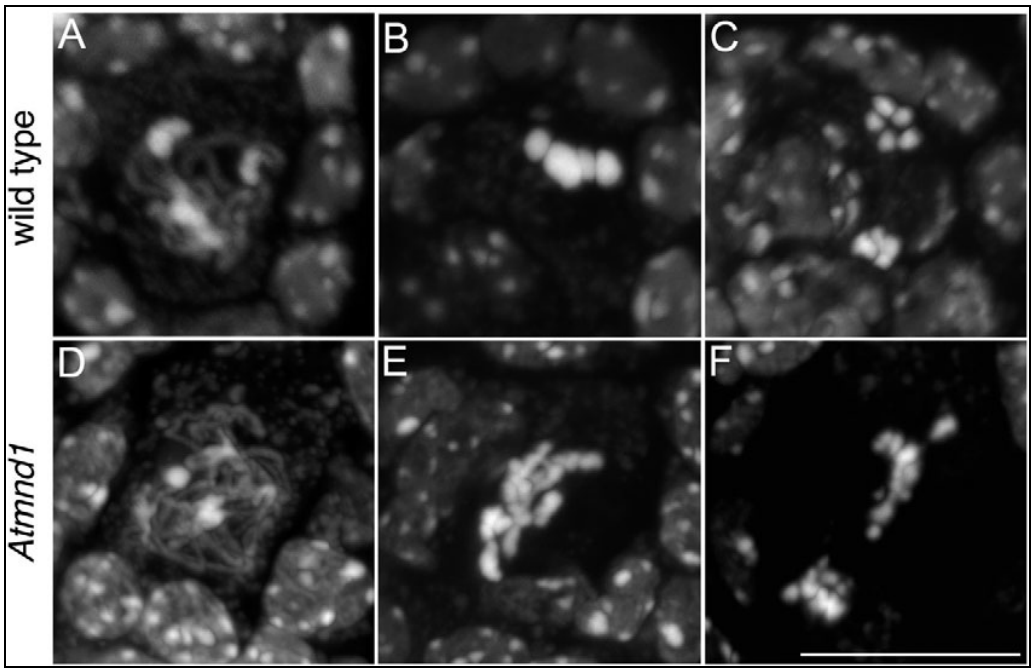

Figure 12: Female meiosis is disrupted in *Atmnd1* mutants. Female meiosis in wild-type *A. thaliana*: (A) pachytene, (B) metaphase I, (C) anaphase I. Disrupted female meiosis in the *Atmnd1* mutant: (D) failed zygotene/pachytene, (E) metaphase-I-like stage with entangled chromosomes, (F) anaphase-I-like stage. Images show DAPI staining of the chromosomes. Scale bar, 10 µm. (taken from Kerzendorfer et al.,2006; experiment done by Julien Vignard)

6.3. Defective pairing and non-disjunction of chromosomes in *Atmnd1* mutants

To understand the fact that we did not see pachytene stage in *Atmnd1* mutant plants we took advantage of fluorescence *in situ* hybridization to analyze the pairing behaviour of chromosomes. In *Arabidopsis* the centromer regions of chromosomes remain unpaired and unassociated during leptotene. They eventually associate pairwise during zygotene. Telomeres, by contrast, show a persistent association with the nucleolus throughout meiotic interphase. During leptotene the paired telomeres lose their association with the nucleolus and become widely dispersed. As the chromosomes start to synapse during zygotene, the telomeres reveal a loose clustering, which may represent a degenerate bouquet configuration and seems to be a nucleolus-associated telomere clustering (Armstrong et al., 2001). In zygotene, FISH signals corresponding to regions adjacent to telomeres, were paired or are in close proximity to each other (Figure 13A, red signal corresponds to a sub-telomeric region of chromosome 2), whereas centromeric

chromosomal regions show pairing or not, depending on the progression of zygotene (Figure 13A, green signal corresponds to an interstitial region of chromosome 1). In pachytene, chromosome pairing was completed and only one signal can be seen for each FISH probe (Figure 13B). Homologous chromosomes separated during anaphase I and therefore, a pair of FISH signals, corresponding to the two sister-chromatids, were frequently seen on each homologue (Figure 13C).

In *Atmnd1* mutants, no pairing of homologues was observed. In zygotene, the sub-telomeric regions were sometimes paired or in close proximity to each other (red signal, Figure 13D), but pairing was never detected at both loci analyzed as the nuclei progressed through meiotic prophase (pachytene-like stage shown in Figure 13E). At the anaphase-I-like stage (Figure 13F), chromosome fragmentation and chromosome bridges were visible and the FISH signals indicate that homologous chromosomes 1 and 2 do not segregate accurately.

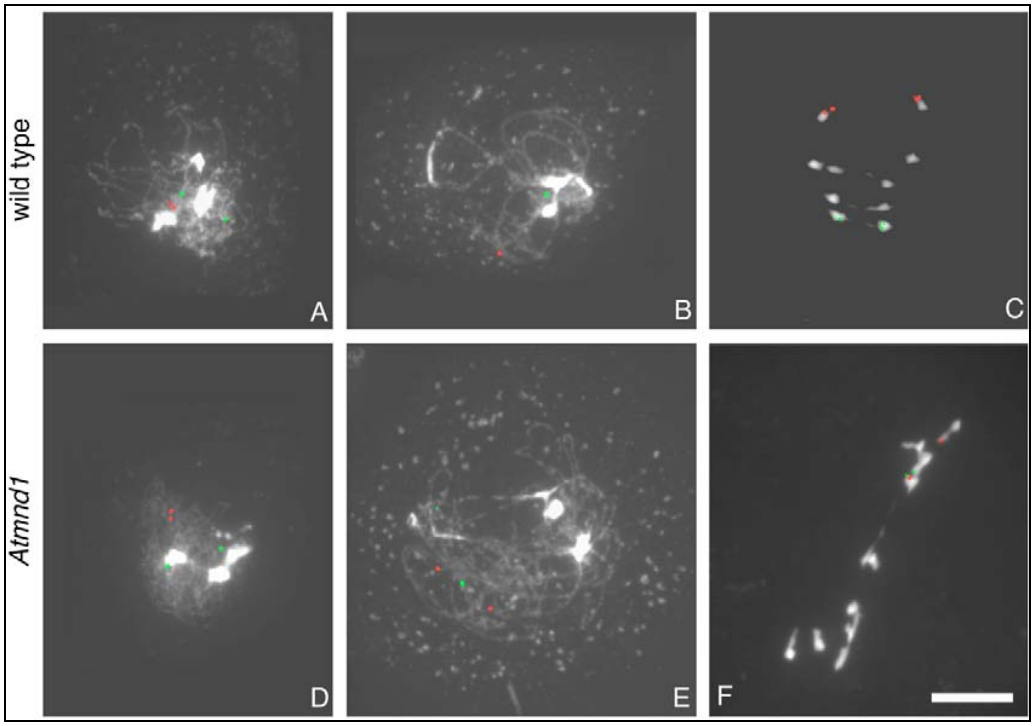

Figure 13: FISH analysis of *Atmnd1* mutants reveals defects in pairing and chromosome disjunction. Preparations of wild-type (A-C) and *Atmnd1* (D-F) meiocytes were hybridised with FISH probes directed against an interstitial region of chromosome 1 (BAC F1N21, green) and a sub-telomeric region of chromosome 2 (BAC F11L15, red). (A,D) Zygotene stage, shows consistent association of sub-telomeric regions in wild-type and occasional association in *Atmnd1* cells. (B) Wild-type pachytene/diplotene transition with paired FISH probes. (E) *Atmnd1* pachytene-like stage with unpaired FISH signals. (C,F) Anaphase I with a regular distribution of chromosomes and FISH signals in wild-type meiocytes, as opposed to the irregular chromosome disjunction and DNA fragmentation in *Atmnd1* cells. Chromosomes are stained with DAPI. Scale bar, 10 µm. (taken from Kerzendorfer et al.,2006; experiment done by Tanja Siwiec)

6.4. Chromosome fragmentation seen in *Atmnd1* mutants depends on SPO11-1

The observed chromosome fragmentation could be due to un-repaired breaks, leading to unpaired homologues chromosomes and therefore recognition of the homologous is impossible. To test the possibility that formation of DSBs was abolished in the *Atmnd1* mutant we investigate in the analysis of the mutant phenotype if the responsible endonuclease SPO11 is absent. Therefore we generated *Atmnd1/Atspo11-1-1* double mutants. Although *A. thaliana* possesses three *SPO11* homologues, only *SPO11-1* and *SPO11-2* have a function during meiosis (Grelon et al., 2001; Hartung et al., 2007; Stacey et al., 2006). We compared at meiotic progression in *Atspo11-1-1* mutants compared to the double mutant *Atspo11-1-1/Atmnd1*. Leptotene and zygotene stages of both mutants (Figure 14A and 14G) were comparable with wild-type meiocytes. However in a pachytene-like stage (Figure 14B and 14H) only unsynapsed chromosomes were observed. During diakinesis (Figure 14C and 14I), chromosomes condensed and ten univalents were visible, that sometimes show linkage between few univalents, corresponding to the residual chiasmata frequency in *Atspo11-1-1* mutants (Grelon et al., 2001). In anaphase I-like stage (Figure 14D and 14J) we observed unequal distribution of chromosomes and randomly distributed chromosomes aligned in metaphase II–like stage (Figure 14E and 14K) to give rise to polyades (Figure 14F and 14L). The *Atspo11-1-1/Atmnd* double mutant displayed the same meiotic defect as the *Atspo11-1-1* mutant, indicating that the function of *AtSPO11* is epistatic to *AtMND1* and the absence of fragments in the double mutant is therefore based on no DSBs.

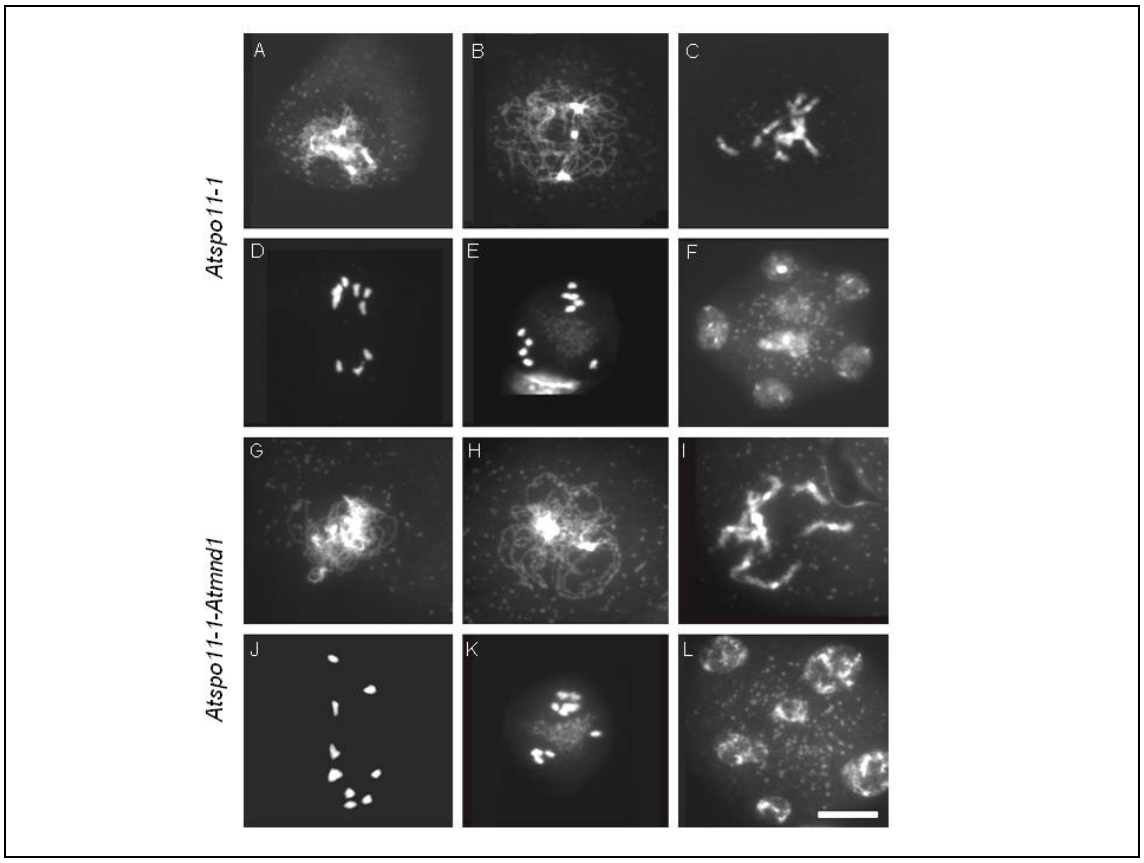

Figure 14: Chromosome entanglement and fragmentation observed in *Atmnd1* mutants depends on SPO11-1. Comparison of meiotic progression in the *spo11-1* mutant (A-F) and in the *Atmnd1 spo11- 1* double mutant (G-L). (A,G) Zygotene-like stage. No typical pachytene cells were detected, and only unsynapsed chromosomes were observed in the pachytene-like stage (B,H). In diakinesis (C,I), ten condensed univalents are visible. (D,J) Anaphase I. (E,K) Metaphase II. (F,L) Polyads. Chromosomes are stained with DAPI. Scale bar, 10 µm. (taken from Kerzendorfer et al.,2006; experiment done by Tanja Siwiec)

6.5. Axial element formation, sister chromatid cohesion and initiation of recombination appears normal in *Atmnd1* mutants

To further analyze the pairing defect of *Atmnd1* mutants we investigated in the behaviour of structural components of the synaptonemal complex. ASY1 is a meiosis-specific protein intimately associated with the chromosome axes during prophase I (Armstrong et al., 2002). *At*SCC3, a member of the cohesion complex, can be detected in meiotic nuclei as early as interphase, and it appears to the chromosome axis from early leptotene to anaphase I. *At*SCC3 is necessary to maintain centromere cohesion at anaphase I and for the monopolar orientation of the kinetochores during the first meiotic division (Chelysheva et al., 2005).

Both proteins behaved similarly in *Atmnd1* mutants compared to wild-type plants during the leptotene stage (data not shown) indicating that axial elements were formed normally in time and that sister-chromatid cohesion proteins are present in *Atmnd1*

mutants. In *Atmnd1* mutants, chromosome axes, visualised with antibodies against ASY1 and *At*SCC3, respectively, were not incorporated into SC structure. As a consequence we could not identify a pachytene stage in *Atmnd1* mutants as we did in the wild-type (Fig. 15).

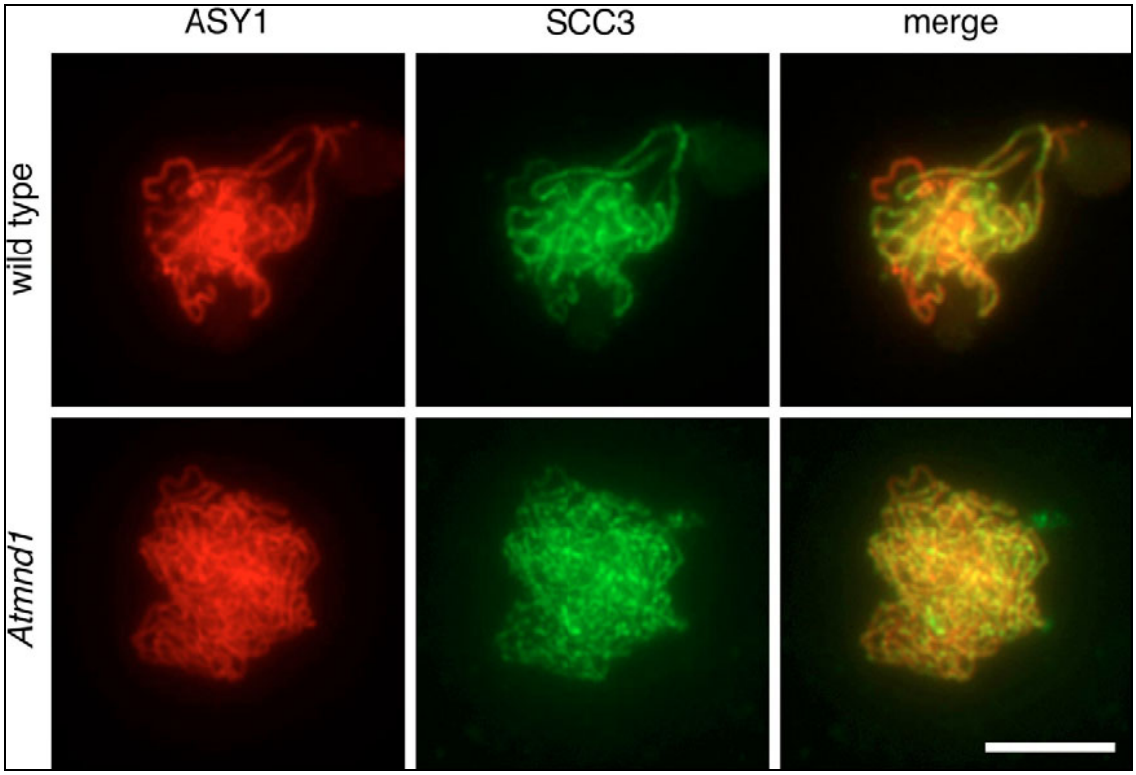

Figure 15: Immunolocalization of ASY1 and SCC3 in *Atmnd1* mutant plants. In *Atmnd1* mutants (lower panels), loading of the SCC3 cohesin protein (green) and of the axial-element associated ASY1 protein (red) is similar to that in wild-type plants (upper panels). However, no synapsis was observed in *Atmnd1* in contrast to wild-type cells. Scale bar, 10 µm. (taken from Kerzendorfer et al.,2006; experiment done by Sue Armstrong).

The chromosome fragmentation defect observed during meiosis in *Atmnd1*, as suggested before by the analysis of the *Atspo11-1-1/Atmnd1* double mutant, may be a result of unprocessed DSBs in prophase I.

We investigated the behaviour of *At*RAD51, a key protein involved in mediating strand invasion during DSB repair, since we expected that if there is no homologous chromosome for repair available, *At*RAD51 protein will accumulate. We visualized the *At*RAD51 protein on chromosome spreads and observed numerous *At*RAD51 foci at leptotene (Figure 16A), most likely corresponding to sites at which recombination had been initiated. Also during zygotene stage (Figure 16B) *At*RAD51 foci were visible. The *Atmnd1* leptotene and zygotene stages were indistinguishable from wild-type cells, with respect to *At*RAD51 focus formation (Figure 16C, D), indicating that DSBs are initiated at the correct time and at a normal level. See below for further analysis how

*At*RAD51 foci behave during later stages of meiosis. It is possible that foci accumulate to an bigger extend in mutant nuclei than in wild-type due to hyper-resected DNA ends.

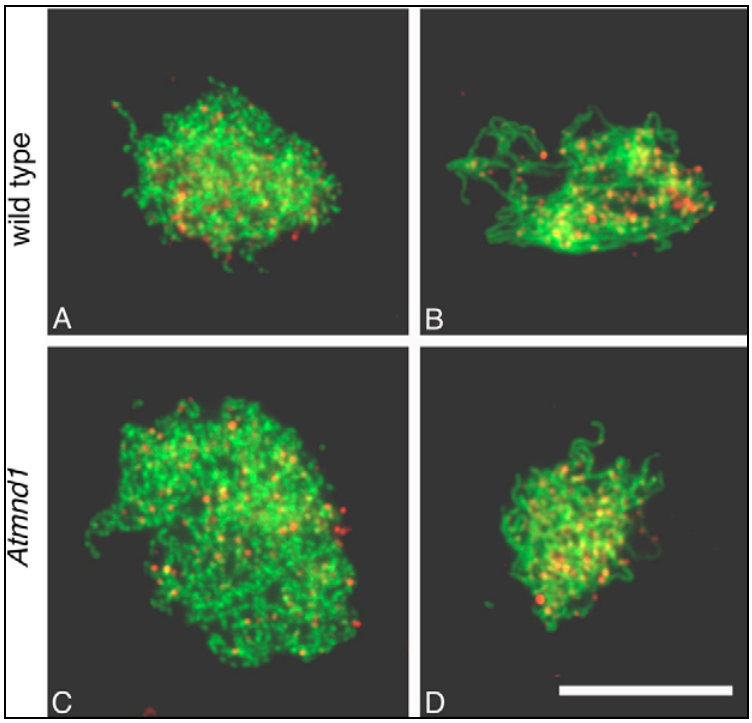

Figure 16: *At*Rad51 foci are formed normally in *Atmnd1* mutants. Comparison of *At*RAD51 focus formation in wild-type (A,B) and *Atmnd1* mutant (C,D) plants. *At*RAD51 foci (red) were observed in leptotene (A,C) of wild-type and of *Atmnd1* mutants cells and in zygotene (B) and failed zygotene stages (D) of wild-type and *Atmnd1* mutant cells, respectively. The abundance of *At*RAD51 foci was similar in wild-type and *Atmnd1* mutant meiocytes. Immunolocalization of ASY1 is represented in green. Scale bar, 10 µm. (taken from Kerzendorfer et al.,2006; experiment done by Tanja Siwiec and A. Pedrosa-Harand)

6.6. *At*MND1 is localized to chromatin during prophase I

To understand the role of *At*MND1 during meiotic progression we investigated the distribution of the *At*MND1 protein during meiosis by immunolocalization in wild-type meiotic cells, using a polyclonal antibody against *At*MND1 (Vignard et al., 2007a). ASY1 was used as a marker for meiotic progression.

The specificity of the *At*MND1 antibody was demonstrated by both western blot analysis (Figure 17) (experiment done by Tanja Siwiec) and immunolocalization studies (Figure 18) (experiment done by Julien Vignard) by comparing wild-type and *Atmnd1* mutant plants. The signals observed in wild-type plant material disappeared in both western blot and cytology experiments when the serum was pre-incubated with the recombinant *At*MND1 protein, confirming the specificity of the serum (Figure 17 and 18D).

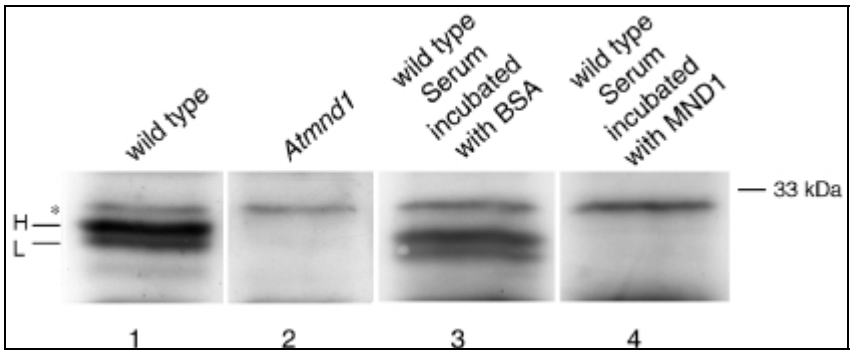

Figure 17: Protein analysis of the anti-*At*MND1 antibody. The *At*MND1 antibody yields two specific bands when applied to blotted protein extracts from wild-type buds, designated ''H'' and ''L,'' for *At*MND1 species with ''higher'' (29.8 kDa) and ''lower'' (29 kDa) molecular mass (Lane 1). These bands were not detected in the *Atmnd1* mutant (Lane 2). Furthermore, no such bands were detected when the serum was depleted of the specific AtMND1 antibody by pre-incubation of the serum with recombinant *At*MND1 protein (Lane 4). The *At*MND1 antibody was not depleted by incubation of the serum with BSA (Lane 3). The asterisk designates a non-specific band. (taken from Vignard et al.,2007; experiment done by Tanja Siwiec)

Meiotic chromosomes from wild-type plants were strongly stained with anti-*At*MND1 antibody (Figure 18A–C). *At*MND1 was first detected at early leptotene, when ASY1 filaments had not yet completely formed along the chromosomal axes (Figure 18A). *At*MND1 was also detected in the nucleolus (Data not shown). Several data suggest that the nucleolus may function as a reservoir of proteins, including proteins involved in DNA repair and meiosis (Boisvert et al., 2007). A pool of *At*MND1 protein may thus be stored in the nucleolus. As meiosis progressed and the ASY1 signal extended all along the chromosome, *At*MND1 was detected along the entire length of the chromosome, in both unsynapsed and synapsed chromosome regions (Figure 18B and C). The *At*MND1 labeling was more prominent than the one for ASY1, for which the signal was detected exclusively along the axis of the chromosomes. Thus, in clear contrast to ASY1, *At*MND1 was localized to both chromosome axes and loop regions (Figure 18B,C). Regions of lower and higher intensity of *At*MND1 signal were detected. The signal higher-intensity regions resembled foci. Based on this result we can say that *At*MND1 is present on the chromosome from an early phase of meiotic prophase on maybe even in premeiotic S-phase. From the mechanistically point of view it seems therefore possible that *At*MND1 can be immediately at the side of strand invasion when needed.

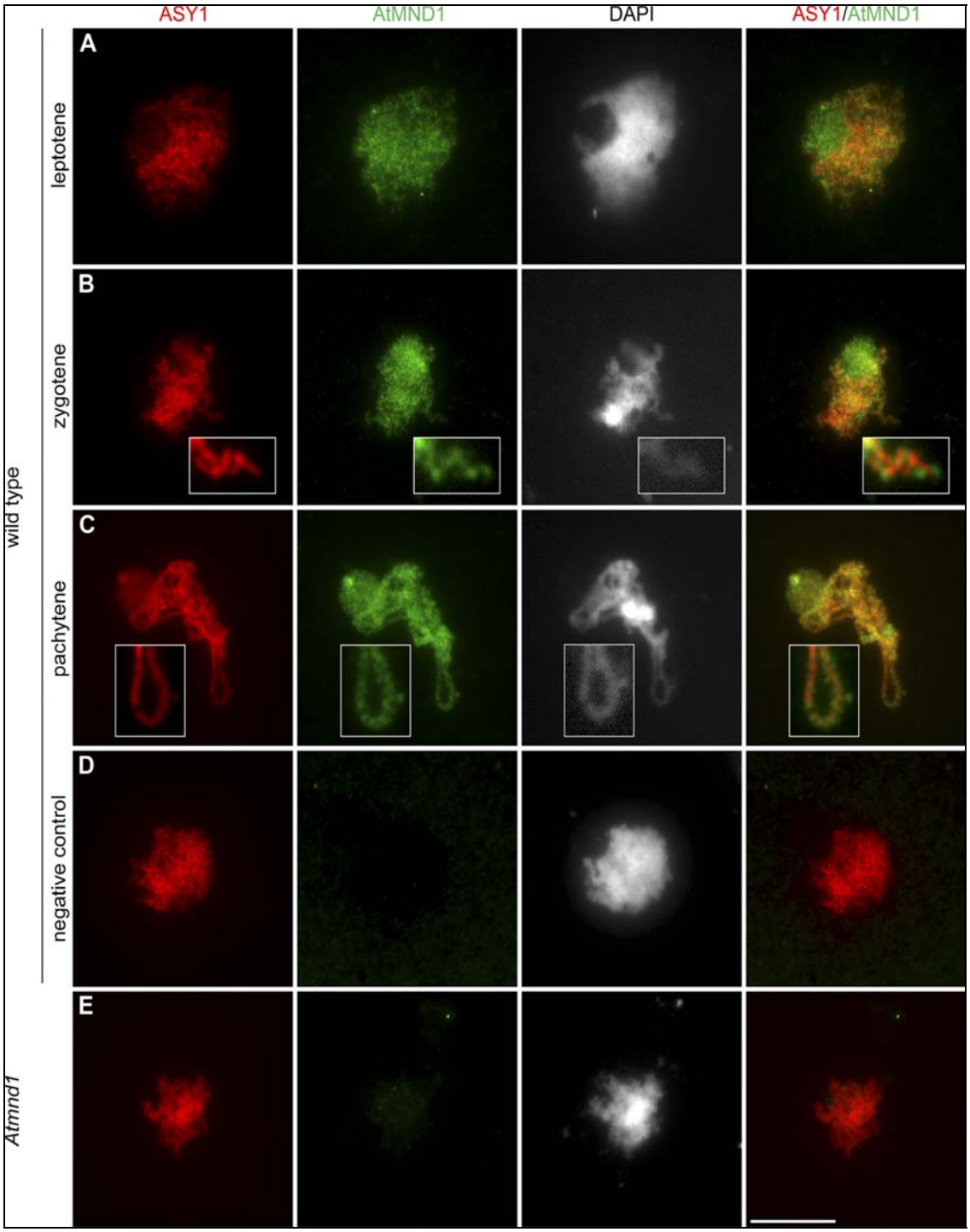

Figure 18: Immunolocalization of the *At*MND1 protein. Male meiocytes of the wild-type (A–D) and the *Atmnd1* mutant (E). Chromosomes are stained with the ASY1 antibody (red), the *At*MND1 antibody (green), and DAPI (gray). The *At*MND1 antibody strongly labels the chromosomes and nucleolus in the wild-type (B), whereas no signal is detected in *Atmnd1* mutants (E). The signal disappears also in wild-type when the serum was pre-incubated with the recombinant *At*MND1 protein (D). Scale bar, 10 µm. (taken from Vignard et al.,2007; experiment done by Julien Vignard).

6.7. The distribution of *At*MND1 depends on AHP2, but not on the initiation of recombination or establishment of cohesion

To analyze the mutual dependencies of the *At*MND1 protein we observed the distribution of *At*MND1 in several mutants. We investigated *At*MND1 loading in mutants with disrupted meiotic recombination initiation (*Atspo11–1*), DSB processing (*Atmre11-3*), strand invasion (*ahp2*), homology search (*Atrad51*, *Atxrcc3*, and *Atdmc1*), and SC formation (*asy1*) (experiment done by Julien Vignard). The distribution of *At*MND1 was not affected in these six mutants (Fig. 19A and S2), showing that the localization of *At*MND1 is independent of the abovementioned processes.

We also investigated the distribution of *At*MND1 in *Atscc3* and *Atrec8* mutants, to determine whether cohesins were required for *At*MND1 loading on chromosomes. We observed no aberration of *At*MND1 distribution in these mutants (Fig. 19B and S2F). These results indicate that *At*MND1 is present on meiotic chromosomes during meiosis, even in the absence of recombination, axis formation, or cohesion. This finding was confirmed by the normal *At*MND1 distribution in *swi1* mutants (Figure S2G), in which meiotic recombination, the establishment of cohesion, and the formation of axial elements are defective.

In addition we investigated whether *At*MND1 distribution depended on AHP2, the Arabidopsis homolog of Hop2, referring to the fact that Mnd1 is found in a heterodimeric complex with Hop2 in yeast as well as mammals. *At*MND1 was not detected on meiotic chromosomes of *ahp2* mutants (Figure 19C), demonstrating the crucial role of AHP2 in controlling *At*MND1. Western blot experiments showed that *At*MND1 protein is absent in *ahp2* mutant plants (Figure 20). A possible interdependency of this two proteins has to be elucidated by visualization of the loading of AHP2 in different mutant background, especially *Atmnd1*.

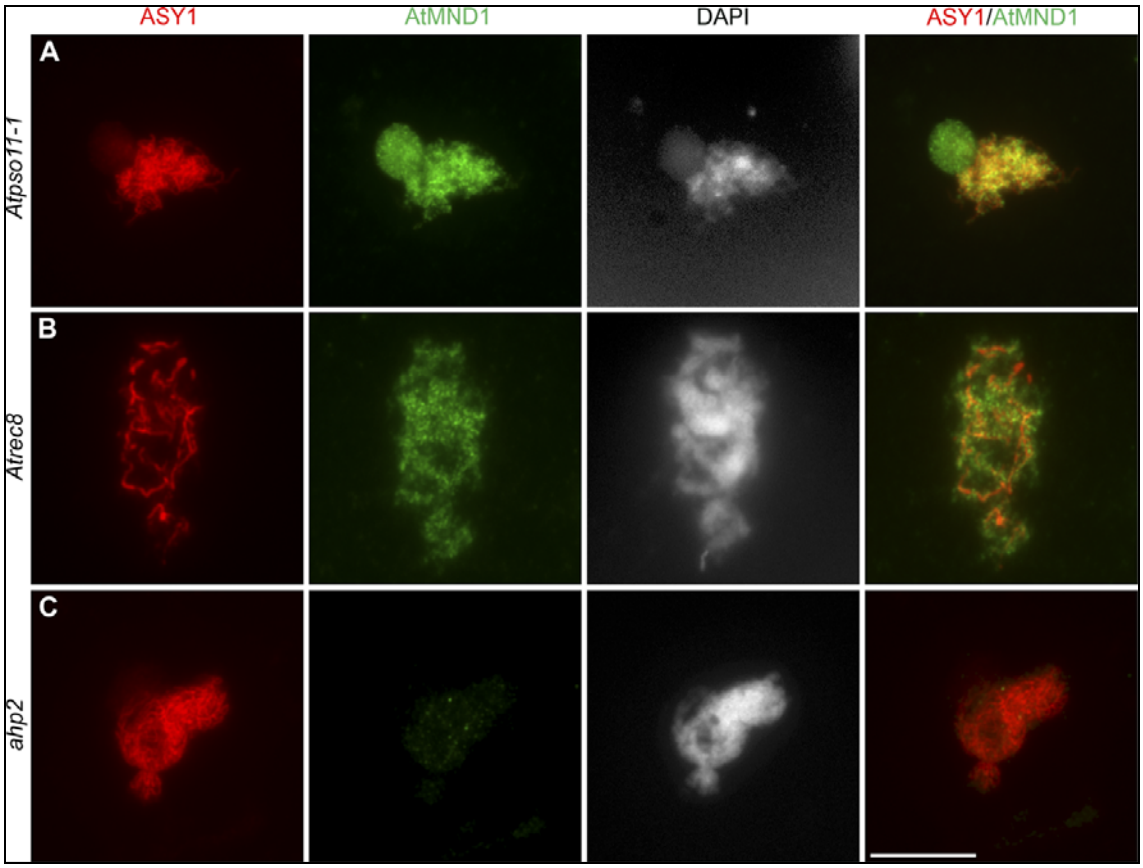

Figure 19: The distribution of *At*MND1 depends on AHP2, but not on AtSPO11–1 or AtREC8. Male meiocytes of *Atspo11–1* (A), *Atrec8* (B), and *ahp2* (C) mutants. Chromosomes are stained with the ASY1 antibody (red), the *At*MND1 antibody (green), and DAPI (gray). Magnified images of individual chromosome axes are shown within white rectangles. No *At*MND1 signal is detected in *ahp2* meiocytes, whereas the distribution of *At*MND1 appears to be normal in *Atspo11–1* and *Atrec8*. Scale bar, 10 µm. (taken from Vignard et al.,2007; experiment done by Julien Vignard).

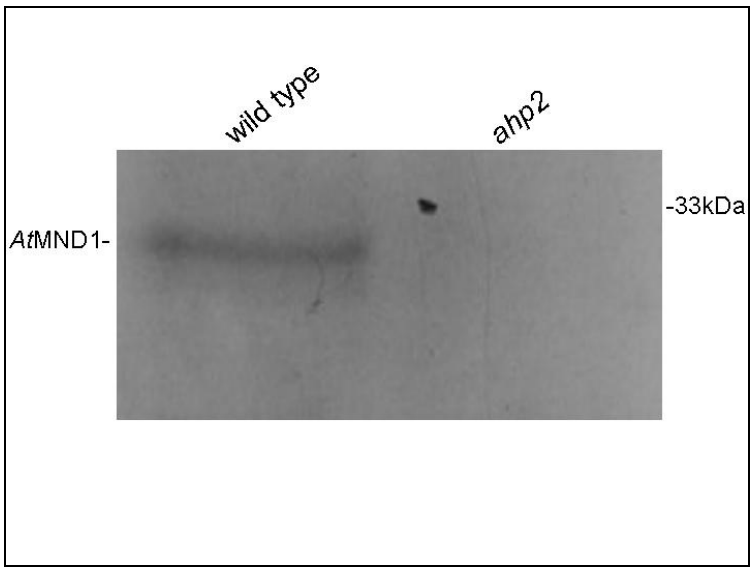

Figure 20: Western Blot with the *At*MND1 antibody. Lane 1 wild-type plants with a specific band around 30 kDa, in lane 2 of *ahp2* mutant plants this specific band is completely absent.

6.8. Interconnection of *At*MND1 with the early recombination protein *At*MRE11

The MRX complex, which is composed of Mre11, Rad50 and Nbs1. plays a central role in processing of DSBs and DNA checkpoint activity (Connelly and Leach, 2002; D'Amours and Jackson, 2002). It has been shown that the Mre11 protein possesses double-strand and single-strand nuclease activities, which suggests a role in resection of DSB. However the 3'-5' nuclease activity of Mre11 stands in contrast to the 5'-3' resection needed for processing Spo11 induced DSBs, which leading to the assumption that a different protein is responsible for either changing the direction of nuclease activity of Mre11 or being responsible for the resection itself.

For *Arabidopsis* there are three T-DNA insertion lines of MRE11 available, *Atmre11-1*, *Atmre11-2* and *Atmre11-3*. *Atmre11-1* mutant plants are dwarf, sterile and show many developmental defects (Bundock and Hooykaas, 2002), *Atmre11-2* mutant plants are normal and fertile (Bundock and Hooykaas, 2002) and *Atmre11-3* mutant plants are sterile show severe defects in the repair of DSBs, documented by chromosome fragmentation, as well as defects in vegetative growth (Puizina et al., 2004). For our cytological analysis for the epistatic relations of *AtMND1*, the *Atmre11-3* mutant was chosen and crossed to *Atmnd1* mutant plants.

In the *Atmre11-3* mutant background leptotene stage was comparable to in wild-type (Figure 21A). First defects in the repair of meiotic DSBs can be seen in zygotene-like stage (Figure 21B), where broken DNA threads were visible even in DAPI stained chromosomes, giving the chromosomes a kind of "fluffy" appearance. A real pachytene, characterized by fully paired homologous chromosomes was never seen. Instead a pachytene-like stage (Figure 21C) with apparently un-repaired breaks can be observed. Metaphase I-like stage (Figure 21D) was characterized by an entangled mass of chromosomes which showed severe chromosome fragmentation from anaphase I-like stage (Figure 21E) until late stages of meiosis II (Figure 21F). At the end of meiosis polyades (Figure 21G) can be detected which often contain intensively stained amount of chromatin (n=13).

Interestingly, the analysis of the *Atmre11-3/Atmnd1* double mutant revealed different results. Although early stages of meiosis (Figure 21H-21N) seemed to look similar as in the single mutants, there was an obvious difference in later stages of meiosis. From metaphase II-like (Figure 21P) stage to telophase II-like (Figure 21Q) stage the grade of condensation of chromatin was altered in 95% of observed meiocytes (n=19). Chromosomes seemed to be more condensed than in the *Atmre11-3* single mutant.

Furthermore 26% of observed meiocytes show chromatin bridges in stages of meiosis II. Instead of the extremely de-condensed structures seen in the *Atmre11-3* single mutant in meiosis II, compact strongly fluoresced DAPI stained bodies are visible.

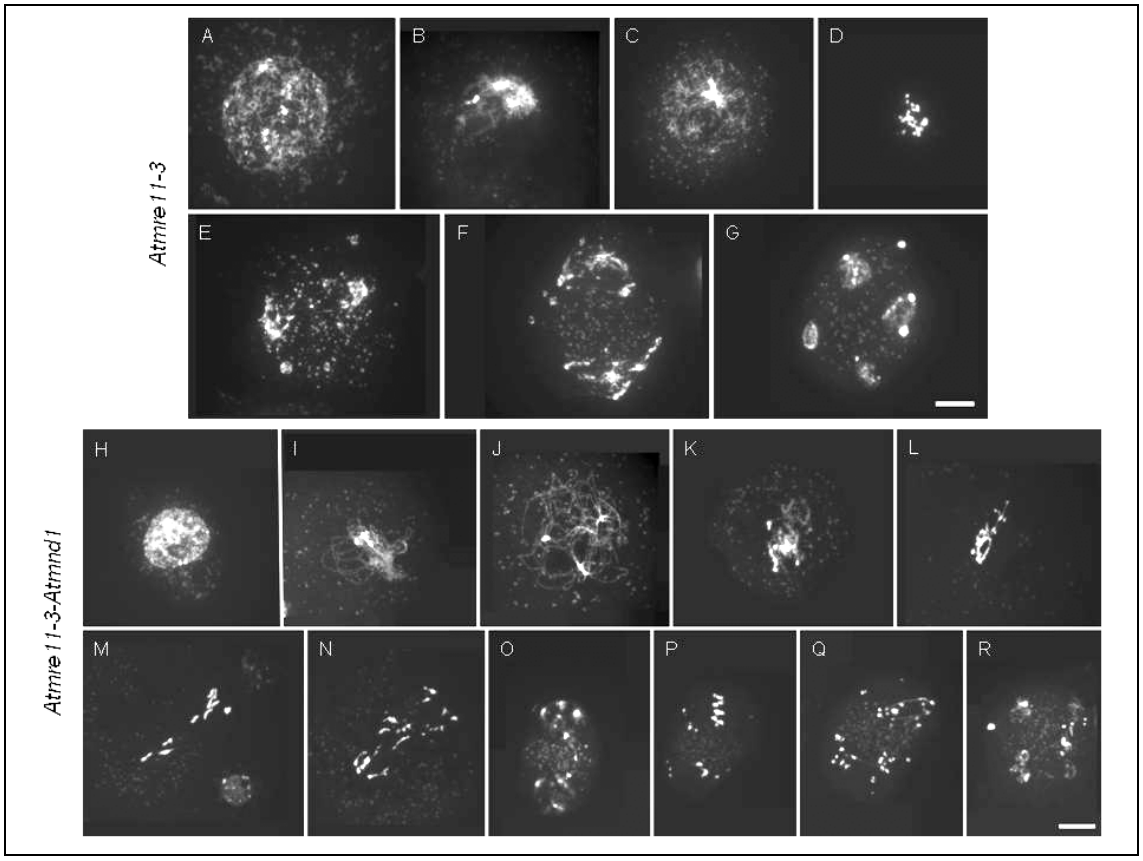

Figure 21: Chromosome decondensation and fragmentation observed in *Atmre11* and the *Atmre11/Atmnd1* double mutant. Meiotic progression in the *Atmre11* (A-G) and the *Atmre11/Atmnd1* mutant and in the *Atmnd1* (H-R). /A,H) Leptotene-like stage, (B,I) Zygotene-like stage. No typical pachytene cells were observed, and only unsynapsed chromosomes were seen in the pachytene-like stage (C,J). In late diakinesis-like stage (K), entangled chromosomes threads were visible in the double mutant, whereas this stage was never seen in the *Atmre11* single mutant. (D,L) Metaphase I-like, (E,M,N) Anaphase I-like, (O) Dyade-like stage, (P) Metaphase II-like stage. (F,Q) Anaphase II-like stage (G,R) Polyades. Chromosomes are stained with DAPI. Scale bar, 10 µm.

6.9. Epistatic relation of *AtMND1* with proteins of the meiotic repair machinery

To analyze the epistatic relation of *AtMND1* with essential proteins of the homologous recombination pathway, we investigated the analysis of the behaviour of chromosomes in the absence in the *Atmnd1/asy1* double mutant. ASY1 is a protein required for synapsis and cross over formation in *Arabidopsis*. Axis morphogenesis is independent of ASY1, but axis structure may be compromised in *asy1* mutants (Sanchez-Moran et al., 2007). Moreover in *asy1* mutants DSBs are made and are repaired via the sister as template, via an *At*RAD51 dependent pathway. This suggests that ASY1 ensures proper chromosome structure and bias the repair to the homologous chromosome. In its

absence this bias seems to be abrogated and repair via the sisterchromatide and not the homologous chromosome is taking place. However, because the chromosome structure plays an important role to assure meiotic progression, the absence of ASY1 may have severe consequences for proper timing as well as progression of repair of meiotic DSBs..

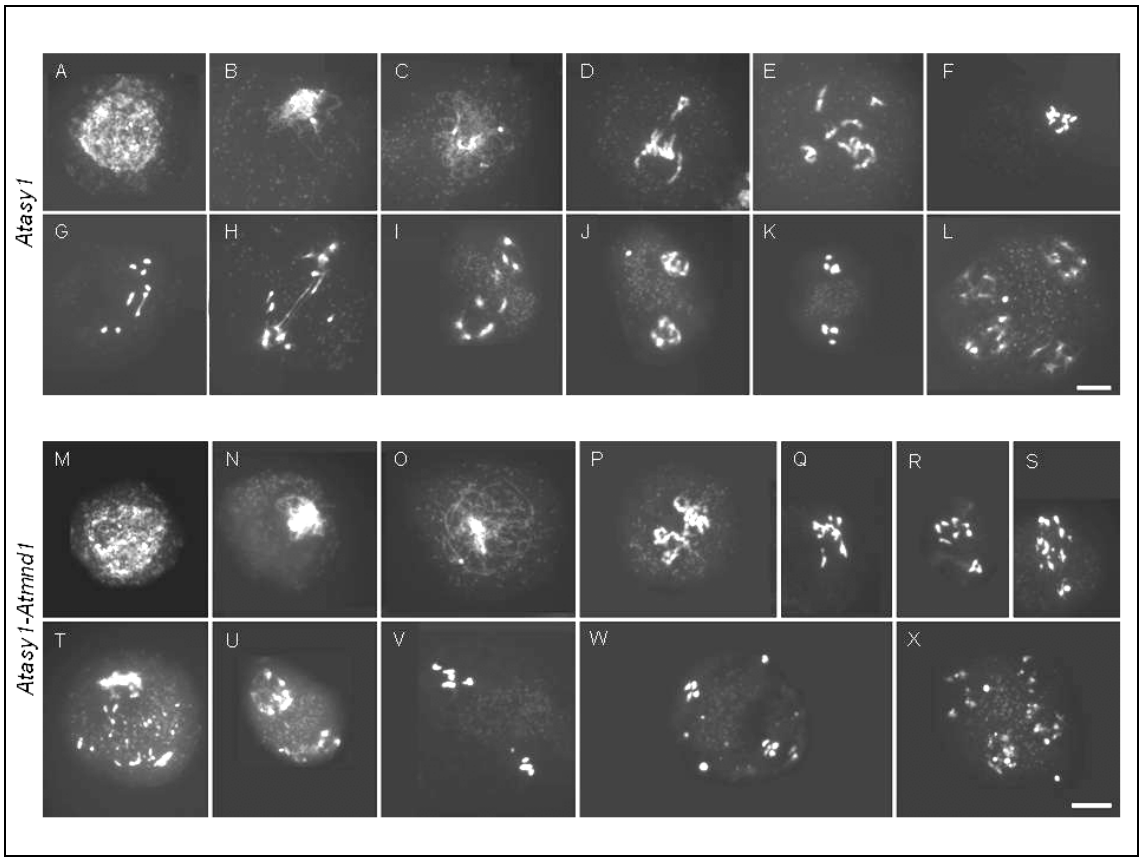

Figure 22: Male meiosis of *asy1* and *asy1 Atmnd1*double mutant. Male meiocytes of *asy1* (A-L) and male meiocytes of *asy1-Atmnd1* mutant (M-X). Leptotene-like stage (A,C), zygotene-like stage (B,N), pachytene-like stage (C,O), late diakinesis-like stage (D,P), univalents of *asy1* mutant (E), metaphase I-like stage (F,Q), anaphase I-like stage (G,H,I,R), anaphase I-like stage of *asy1-Atmnd1* with fragmentation (S), telophase I-like stage (J,U), telophase I-like stage of *asy1-Atmnd1* with fragmentation (T), metaphase II-like stage (K,V,W) and polyades (L,X). Scale bar, 10 µm

Cytological analysis of DAPI stained chromosomes of *asy1* mutant plants showed that early stages of meiotic prophase I were comparable to like wild-type. The first obvious defects were visible in a diakinesis-like stage (Figure 22D and 22E), where 10 univalents instead of 5 bivalents were seen. In some cases also few bivalents (mean bivalent frequency 1.57 per cell) could be seen which corresponds to a residual chiasmata frequency in *asy1* mutants of 1.63 per cell (Ross et al., 1997). During metaphase I–like stage (Figure 22M) chromosomes condensed further and in anaphase I-like stage (Figure 22G) chromosomes were unequally distributed to opposite poles of

the cell. In 25% (n=47) of anaphase I-like and telophase I-like meiocytes (Figure 22H-22J) chromatin bridges were visible (unpublished data Tanja Siwiec). This is presumably caused by ectopic synapsis of chromosomes maybe through another component of the SC. At the end of meiosis II polyades (Figure 22P) could be detected, which correspond to the previous unequal distribution of chromosomes.

In the *Atmnd/asy1* double mutant early stages of meiotic prophase progressed like in single mutants (Figure 22M-22O) until zygotene-like stage (Figure 22N). A typical pachytene stage was absent in the double mutant and in a diakinesis-like stage thick treats, more or less separated from each other could be seen (Figure 22P). No univalents like in *asy1* mutant were detectable, Furthermore in 15% of meiocytes from anaphase I-like stage (Figure 22R-22U) to anaphase II-like stage (Figure 22V and 22W) (n=27) chromatin bridges were detectable. Whereas in the *Atmnd1* mutant meiocytes from metaphase I-like stage on showed 100% fragmentation, the *Atmnd1/asy1* double mutant showed 85% of meiocytes in anaphase I-like stage till telophase II-like stage (n=27) with fragmentation. The observed fragmentation was not as severe as in *Atmnd1*, but it seems that if the axis component ASY1 and *At*MND1 are missing the bias to repair DSBs via the sister chromatid is abolished and furthermore that in the additional absence of *At*MND1 the repair via the sister chromatid through *At*RAD51 cannot take place effectively. This explanation suggests a role for *At*MND1 or the *At*MND1-AHP2 complex in positively regulating the activity of *At*RAD51.

6.10. Interdependence between *AtMND1, AtDMC1, AtRAD51,* and *AtXRCC3*

We investigated the reciprocal dependencies between *AtMND1* and RecA-related proteins in Arabidopsis, by studying the epistatic relationships between *AtMND1*, *AtRAD51*, *AtDMC1*, and *AtXRCC3*, and by analysing the phenotypes of the corresponding double and triple mutants.

In wild-type, homologous chromosomes synapse along their entire length at pachytene (Figure 23A). At this stage, a fully extended SC can be visualized by immunolocalization of the *At*ZYP1 protein, which forms the transverse filament of the SC, and furthermore immunolocalization of ASY1, to label the chromosome axes (Figure 24A). *Atrad51* and *Atmnd1* mutants, which display similar meiotic phenotypes, show absence of a normal pachytene stage. This stage is replaced by a "failed pachytene" stage with unsynapsed chromosomes (Figure 23B and 23C). In *Atdmc1* mutants, the chromosomes also fail to synapse (Figure 23D). In the *Atxrcc3* mutant,

synapsis has been reported (Bleuyard and White, 2004); however, we exclusively observed failed pachytene stages (n = 125) and never synapsed chromosomes in this mutant (Figure 23E). To clarify the question if an SC could be formed in the before mentioned RecA mutants, we did immunolocalizing studies of *At*ZYP1 in *Atdmc1*, *Atxrcc3*, *Atmnd1*, and *Atrad51* mutants. The *Atdmc1* mutant has been shown to be defective in *At*ZYP1 localization (Figure 24B). *At*ZYP1 is observed only as numerous foci on chromosome axes, a minority of which elongate to form short filaments. A similar staining pattern was observed in this study for *At*ZYP1 in *Atxrcc3*, *Atmnd1*, and *Atrad51* mutants (Figure 24C–24E), demonstrating that synapsis is impaired in all these mutants. This result is consistent with DAPI staining and clarifies that there is no synapsis in *Atxrcc3* mutants. A similar type of *At*ZYP1 loading was also seen when both recombinases, *At*RAD51 and *At*DMC1, were disrupted in the same genetic background (Figure 24F).

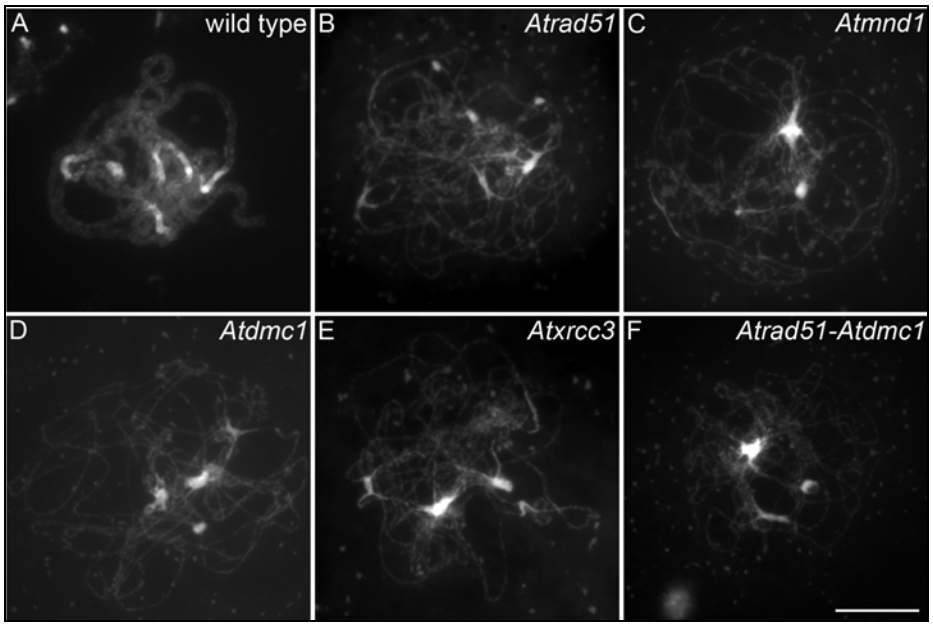

Figure 23: Synapsis in wild-type and various meiotic mutants. Chromosomes stained with DAPI. Scale bar 10µm. (Taken from Vignard et al.,2007; experiment done by Tanja Siwiec and Julien Vignard).

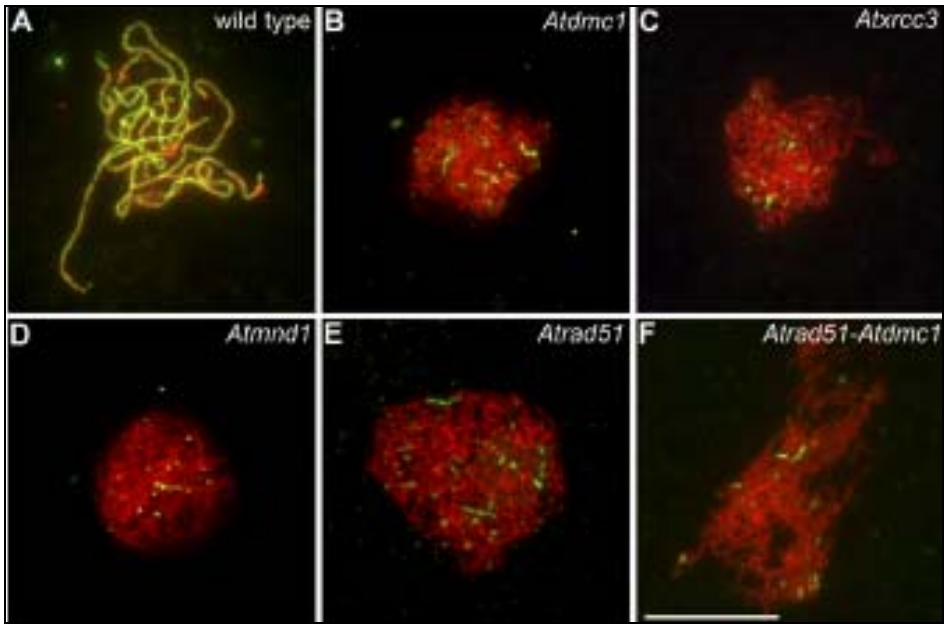

Figure 24: Synapsis is impaired in *Atdmc1*, *Atxrcc3*, *Atmnd1*, *Atrad51*, and *Atrad51/Atdmc1* mutants. Male meiocytes stained with the ASY1 antibody (red) and the *At*ZYP1 antibody (green). During wild-type pachytene stages *At*ZYP1 extends along the entire length of the axes (A). In *Atdmc1* (B), *Atxrcc3* (C), *Atmnd1* (D), *Atrad51* (E), and *Atrad51/Atdmc1* (F) mutants, *At*ZYP1 staining is restricted to a few foci and a few short stretches. Scale bar, 10 μm. (taken from Vignard et al.,2007; experiment done by Julien Vignard).

During metaphase I in wild-type, five bivalents were aligned, allowing homologous chromosomes to segregate properly at anaphase I (Figure 27A and 27B). In contrast, chromosomes of *Atmnd1*, *Atrad51* and *Atxrcc3* showed an entangled mass of chromosomes which are sometimes interconnected by chromatin links (Bleuyard and White, 2004; Kerzendorfer et al., 2006b; Li et al., 2004) (Figures 27C and 25). When chromosomes began to separate at anaphase I they give rise to extensive chromosomal fragmentation (Figures 27D and 25). The generated double mutants showed identical phenotypes compared to the single mutant (Figure 25). In all of the double mutants no pachytene stage can be observed, instead unsynapsed chromosomes can be seen. As meiosis progresses, chromosomes get fragmented and severe chromosome fragmentation can be seen from anaphase I-like stage on.

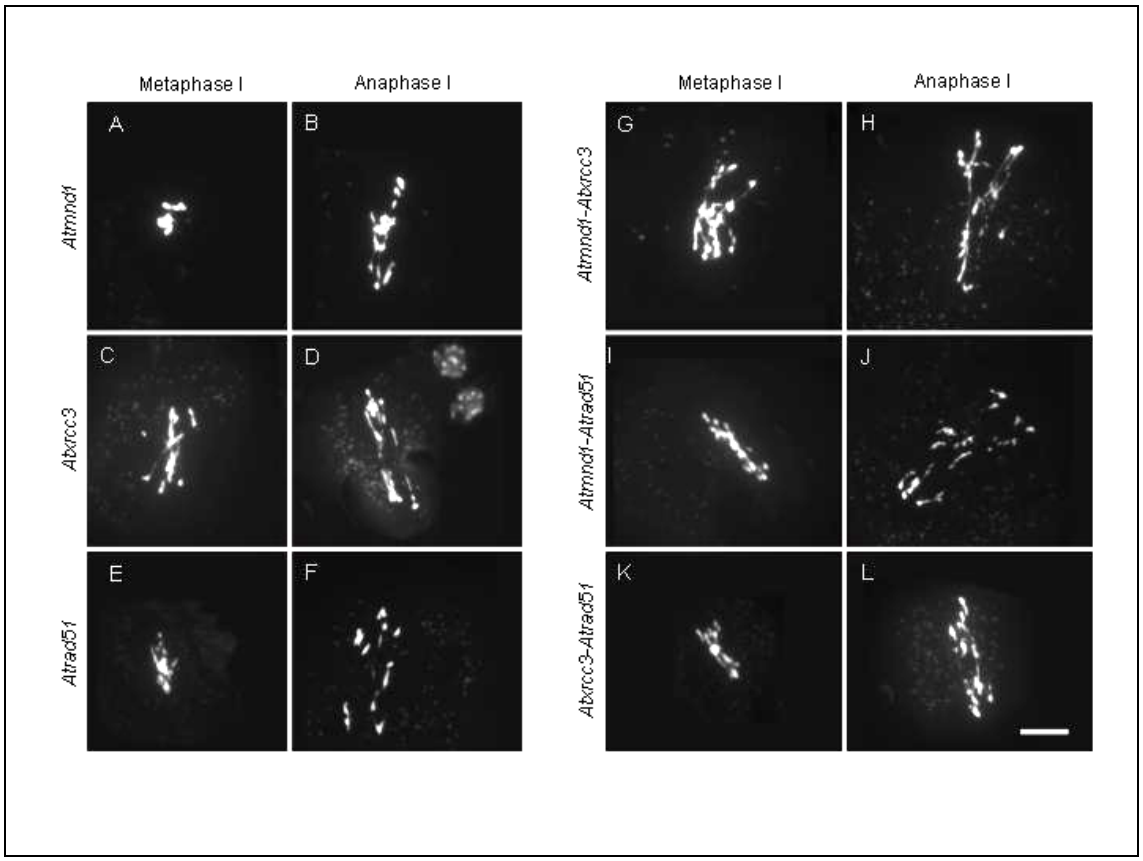

Figure 25: Metaphase I and anaphase I-like stages of various meiotic mutants. Fragmentation can be observed in the single mutants *Atmnd1* (A, B), *Atxrcc3* (C, D) and *Atrad51* (E, F) as well as in the respective double mutants *Atmnd1/Atxrcc3* (G, H), *Atmnd1/Atrad51* (I, J) and *Atxrcc3/Atrad51* (K, L). Scale bar, 10µm. (Experiment performed by Tanja Siwiec).

Interestingly, the *Atdmc1* mutant displayed a different phenotype at the end of prophase I compared to the above mentioned mutants. Chromosomes in the *Atdmc1* background did not form bivalents as in wild type or show chromosome fragmentation as the other RecA homologue mutants. Instead the chromosomes of the *Atdmc1* mutant formed ten univalents, visible in diakinesis-like stage resulting in chromosome non-disjunction in anaphase I-like stage. (Couteau et al., 1999) (Figure 27E). Taking advantage of this difference we investigated the meiotic behaviour of *Atmnd1*, *Atrad51*, and *Atxrcc3* mutants in the *Atdmc1* background to decipher epistatic relationships between these factors.

The metaphase–anaphase I-like stages of the double mutants *Atrad51/Atdmc1* and *Atxrcc3*/*Atdmc1* mutants show entanglement of chromosomes followed by chromosome fragmentation which resemble those of the *Atrad51* and *Atxrcc3* single mutants (Figure 27F and 27G). Therefore, AtRAD51 and AtXRCC3 are epistatic to AtDMC1. In contrast, the *Atmnd1*/*Atdmc1* double mutant shows intermediate meiotic defects

between those of the two single mutants. Sometimes meiocytes show ten apparently intact univalents (42%, n = 220) during metaphase-anaphase I-like stage (Figure 27H) showing meiocytes with fewer chromatid links and fewer chromosome fragmentation than the *Atmnd1* mutant (Figure 27I).

During the second meiotic division, when sister chromatids separate, fragmentation and chromatid links are obvious (Figure 27J) in the *Atmnd1/Atdmc1* double mutant. Indeed, a larger proportion of meiocytes (98%, n = 57) presented fragmented chromosomes during the second division than during the first. Seed counts as well as Alexander staining of the *Atmnd1-Atdmc1* double mutants showed that seed formation rates were similar to those for the *Atmnd1* single mutant, and significantly lower than those for the *Atdmc1* single mutant (Figure 26). It seems that in the *Atmnd1/Atdmc1* double mutant to some extend repair via the sister occurs, but cannot be completed. Conclusively, compared to the *Atmnd1* single mutant, meiosis I appears to be more unaffected, but during meiosis II, when sisters chromatids get separated, chromosome fragmentation due to incomplete repair of meiotic DSBs is visible. Meiotic chromosomes in the triple mutant *Atrad5/Atdmc1/Atmnd1* and *Atdmc1/Atmnd1/Atxrcc3* were similar to that of the *Atmnd1*, *Atrad51*, and *Atxrcc3* single mutants (Figure 27K and 27L). Thus, the depletion of *At*RAD51 or *At*XRCC3 in the *Atmnd1/Atdmc1* background results in a reversion of the defect resembling the *Atmnd1*, *Atrad51*, or *Atxrcc3* single-mutant defect. In conclusion, the disruption of *At*MND1, *At*RAD51, or *At*XRCC3 leads to the same meiotic phenotype, characterized by chromosome fragmentation. The formation of intact univalents during prophase I in *Atdmc1* mutants is not affected by the *Atmnd1* mutation, but absolutely requires *At*RAD51 or *At*XRCC3. We deduce that *At*RAD51 and *At*XRCC3 are epistatic to *At*DMC1, and to *At*MND1, in an *Atdmc1* mutant background.

A

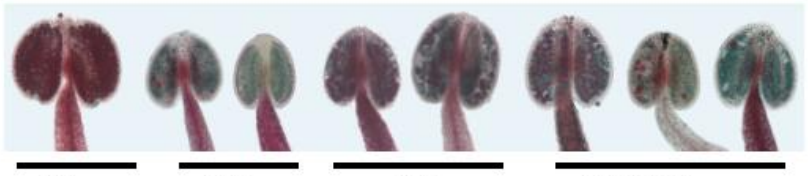

B

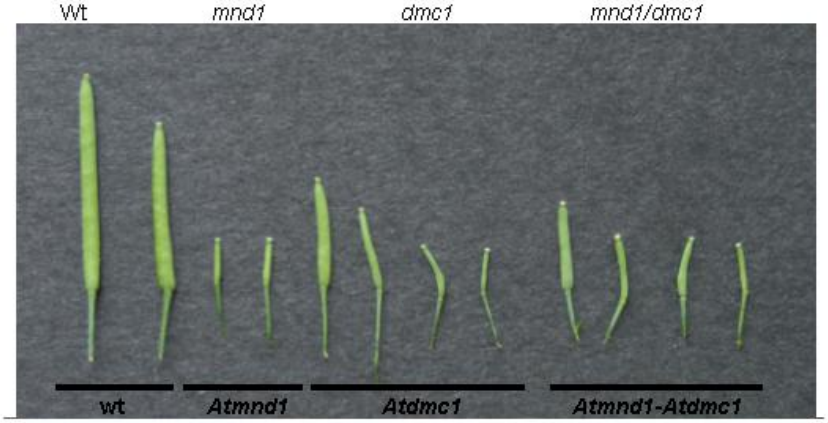

C

	wt	*Atmnd1*	*Atdmc1*	*Atmnd1-Atdmc1*
Seeds/silique	32	0.03	1.29	0.17
siliques	657	2947	1829	1096
Individual plants	9	63	69	29

Figure 26: Alexander staining, silique length and seed count of wild-type, *Atmnd1*, *Atdmc1* and *Atmnd1/Atdmc1* double mutant. (A) Visualization of viable pollen grains via Alexander staining. Red staining is indicative for viable pollen, green staining for non-viable pollen, respectively. (B) Variation of the silique length corresponding to the number of seeds per silique. (C) Seed count of wild-type, *Atmnd1*, *Atdmc1* and *Atmnd1/Atdmc1* double mutant.

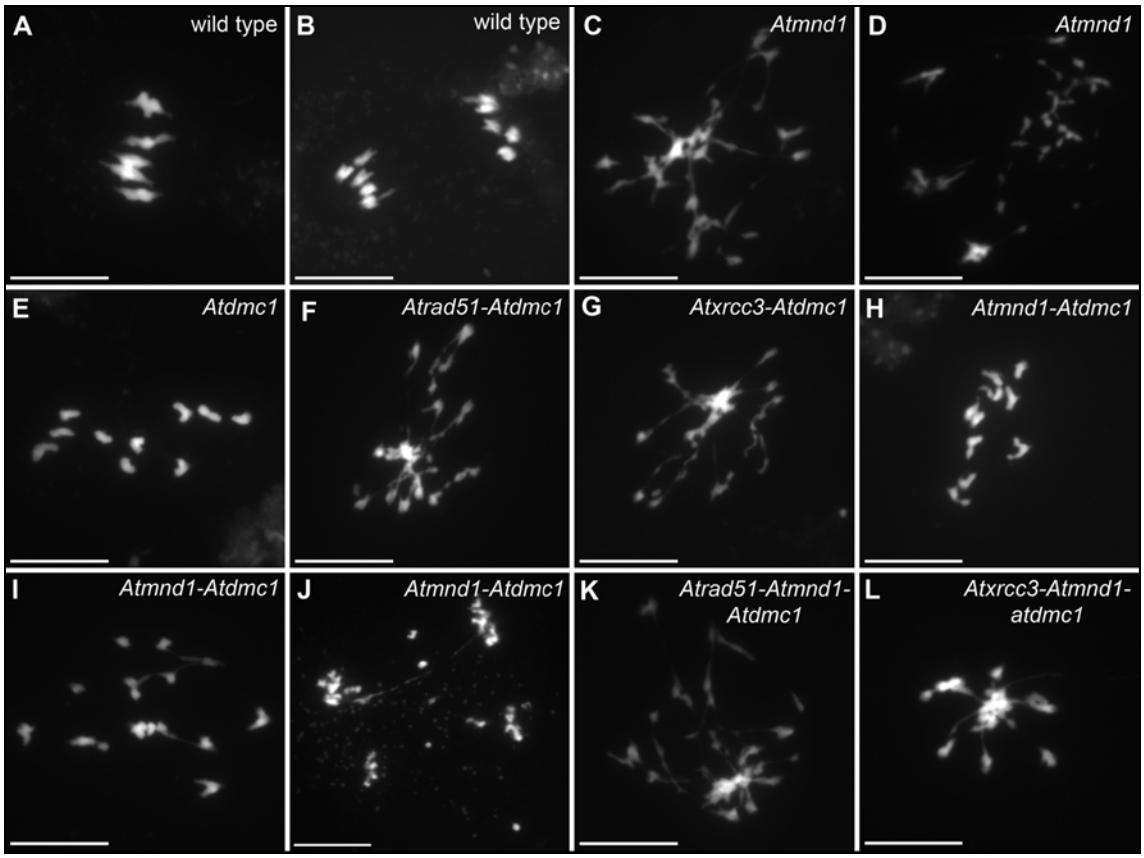

Figure 27: Epistatic relationships between *At*MND1, *At*RAD51, *At*XRCC3, and *At*DMC1. In wild-type, five bivalents are aligned at metaphase I (A), and the homologous chromosomes segregate at anaphase I (B). In *Atmnd1* (C), as in *Atrad51* and *Atxrcc3* (Figure 25), an entangled mass of chromosomes is observed at metaphase I, with chromatid connections between multiple chromosomes. Segregation at anaphase I leads to chromosome fragmentation (D). In *Atdmc1*, ten univalents are visible at metaphase I (E). Typical *Atrad51* or *Atxrcc3* single mutant metaphase I defects are seen in *Atrad51/Atdmc1* (F) and *Atxrcc3/Atdmc1* (G) double mutants, respectively. Metaphase I defects in *Atmnd1/Atdmc1* mutants are intermediate between those of the single mutants: some meiocytes have ten univalents (H), whereas the others display chromatin links and fragmentation (I). In most *Atmnd1/Atdmc1* anaphase II chromatid connections and fragmentation were observed (J). The mutation of either *AtRAD51* (K) or *AtXRCC3* (L) in the *Atmnd1/Atdmc1* mutant results in a typical *Atrad51*-like meiosis defect. Scale bar, 10 µm. (taken from Vignard et al.,2007; experiment done by Julien Vignard and Tanja Siwiec).

6.11. The accumulation of *At*DMC1 foci in *Atmnd1* depends on *At*RAD51 but not on *At*XRCC3

To get further insights into the epistatic correlation of the RecA homologs, *AtDMC1*, *AtRAD51* and *AtXRCC3,* in *A. thaliana*, we investigated in the distribution and the number of *At*DMC1 foci in wild-type, *Atmnd1*, *Atrad51*, *Atxrcc3* and the respective double mutants. The distribution of *At*DMC1 varies substantially in the above mentioned mutants (Figure 28).

We analyzed the number of *At*DMC1 foci on wild-type chromosomes during meiotic progression and obtained results similar to those reported by Chelysheva et al. (2007), with the number of *At*DMC1 foci reaching a maximum during zygotene (Figure 28A). The mean number of *At*DMC1 foci in the wild-type was 234±89 (n=28). We counted

*At*DMC1 foci in *Atmnd1* cells during the failed pachytene stage replacing the wild-type zygotene-pachytene stages (Figure 28B). We observed a mean of 342±103 (n=22) foci, a number significantly higher than that for the wild-type ($p<10^{-4}$; custom hypothesis tested with a contrast using the GLM procedure of SAS 8.1; SAS Institute). Thus, *At*DMC1 foci accumulate in the *Atmnd1* mutant, indicating a failure in the meiotic strand invasion process. The mean number of 50±11 (n=21) foci in the *Atrad51* mutant and 56±13 (n=17) foci in the *Atxrcc3* mutant showed no significant difference between these two mutants (p=0.81) (Figure 28C and 28D). We therefore concluded that *At*RAD51 and *At*XRCC3 are required for an efficient loading of the *At*DMC1 protein.

Following the previous results we analyzed the number of *At*DMC1 foci in *Atrad51/Atmnd1* and *Atmnd1/Atxrcc3* double mutants (Figure 28G). In the *Atrad51/Atmnd1* double mutant we observed far fewer AtDMC1 foci than in the *Atmnd1* single mutant (Figure 28E), with a mean foci number of 87±16 (n = 17), this is significantly lower than that seen in the *Atmnd1* single mutant ($p<10^{-4}$) or in wild-type ($p<10^{-4}$). We therefore concluded that the accumulation of *At*DMC1 foci in *Atmnd1* mutant depends on *At*RAD51. Interestingly, the mean number of *At*DMC1 foci in the *Atmnd1/Atxrcc3* double mutant (Figure 28F, 217±76; n=35) is only slightly lower than that for the *Atmnd1* single mutant ($p<10^{-4}$). Thus, *At*DMC1 foci formation is not dependent on *At*XRCC3 in an *Atmnd1* mutant background and we conclude that *At*RAD51 and *At*XRCC3 play different roles during meiosis (all data taken from Vignard et al, 2007, analysis performed by Julien Vignard and Raphael Mercier). See discussion for further interpretation of results.

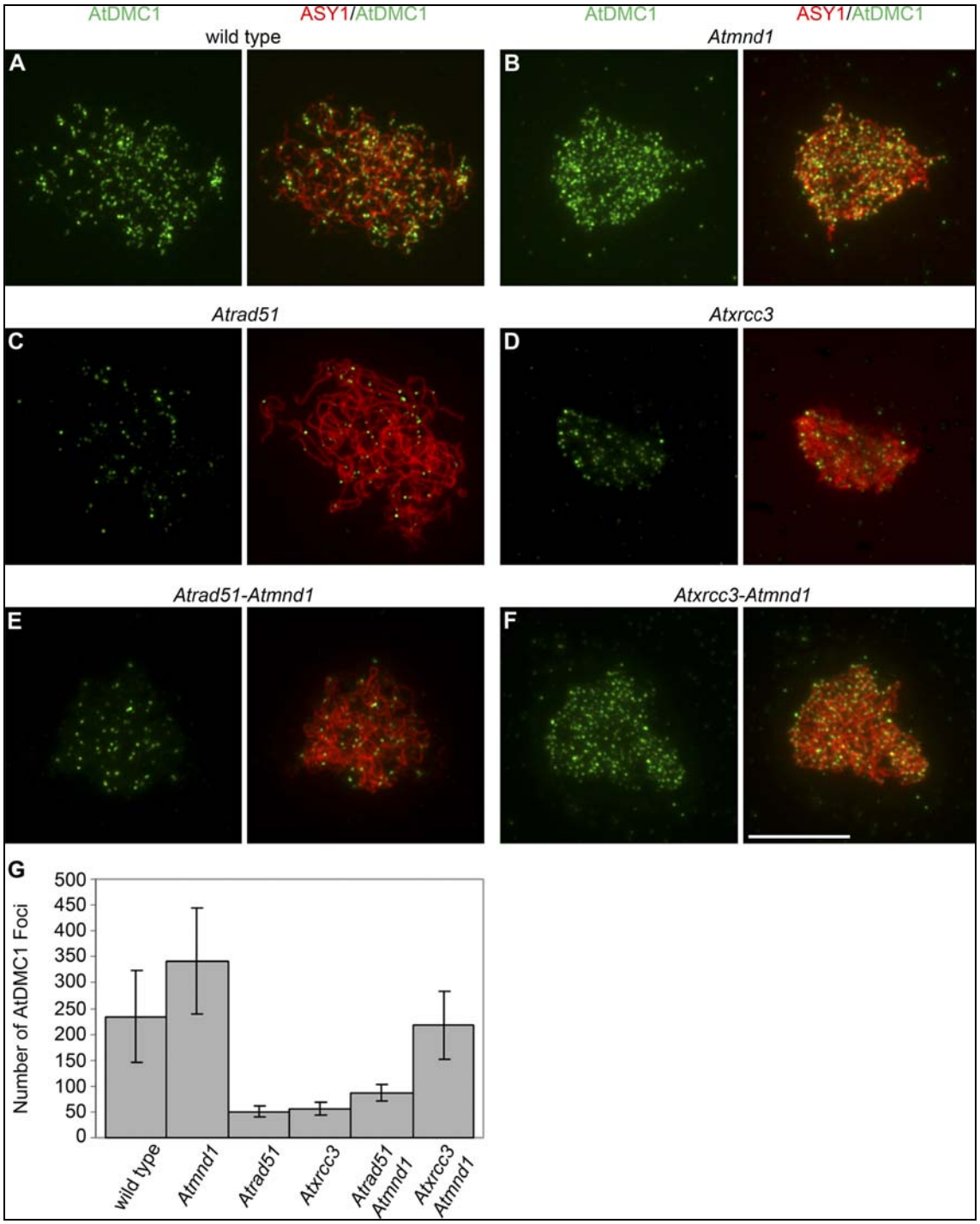

Figure 28: Efficient *At*DMC1 loading requires the presence of *At*RAD51, but not of *At*XRCC3, in the *Atmnd1* mutant background. Distribution of *At*DMC1 foci in male meiocytes of the wild-type (A), *Atmnd1* (B), *Atrad51* (C), *Atxrcc3* (D), *Atrad51/Atmnd1* (E), and *Atxrcc3/Atmnd1* (F) mutants. Chromosomes have been stained with the ASY1 antibody (red) and the *At*DMC1 antibody (green). The *At*DMC1-only (left) and the *At*DMC1–ASY1 merge (right) images are shown. *At*DMC1 foci are localized on the chromosome axes, as revealed by the ASY1 signal. The mean number of *At*DMC1 foci for the wild-type and all mutants is presented in the histogram (G). Scale bar, 10 µm. (Taken from Vignard et al.,2007; experiment performed by Julien Vignard and Luidmilla Chelycheva).

6.12. *At*XRCC3 is important for an efficient loading of the *At*RAD51 protein

For clarifying the issue of reciprocal interdependency of the RecA homologs and *At*MND1 we investigated in distribution and loading of the RecA homolog *At*RAD51 in various mutant background (Figure 29). We analyzed the number of *At*RAD51 foci on wild-type chromosomes and observed maximum foci number during leptotene, with a mean number of 176±32 (n=21). In *Atmnd1* mutant cells we observed a mean number 130±37 (n=26) during leptotene-like stage, a number which is lower than in wild-type and corresponds to the inefficient loading of *At*RAD51 and therefore to un-repaired DSBs in *Atmnd1* mutants or a faster turnover of *At*RAD51. More Data have to be analysed to get a statistical significance. The mean number of 95±23 (n=21) in the *Atdmc1* mutant showed that loading of *At*RAD51 is possible. According to data from yeast and looking at the phenotype of the *Atdmc1* mutant it seems possible that the repair via the sister in the *Atdmc1* mutant is faster than the repair via the homologous chromosome like in wild type, represented by the lower *At*RAD51 foci number in *Atdmc1* compared to wild type. More Data have to be analysed to get a statistical significance. The mean number of 9±6 (n=7) *At*RAD51 foci in *Atxrcc3* mutant revealed that *At*XRCC3 is not only a stabilizing factor for the DMC1 nucleoprotein filament, moreover it is also an essential factor for the RAD51 protein filament formation. In contrast, *At*MND1 as well at *At*DMC1 seem to be dispensable for efficient loading of *At*RAD51. But more Data have to be analysed to get a statistical significance. Following the previous results we analyzed the number of *At*RAD51 foci in *Atdmc1/Atmnd, Atmnd1/Atxrcc3*, *Atdmc1/Atxrcc3* as well as in the *Atdmc1/Atmnd1/Atxrcc3* triple mutants. In the *Atdmc1/Atmnd1* double mutant we observed a mean foci number of 63±15 (n=6). This could be due to a inefficient loading of *At*RAD51 or an inefficient repair via the sisterchromatid by *At*RAD51, because the missing of *At*RAD51 support factor *At*MND1. But more Data are needed to get a statistical significance. In the *Atxrcc3/Atmnd1* with a *At*RAD51 mean foci number of 40±27 (n=8) we conclude that the Rad51 filament formation is slower, like the DMC1 filament formation in this double mutant. *At*MND1 might acts destabilizing onto *At*XRCC3, but more analysis is needed to elucidate this prediction. In the *Atdmc1/Atxrcc3* double mutant we observed a mean foci number of 50±12 (n=10). More data are needed to get a statistical significance, but it seems possible that because *At*XRCC3 as a stabilizing factor for *At*RAD51 is missing, repair via the sister is impossible represented by the fragmented phenotype of this double mutant. To get a statistical significance of the triple mutant

Atdmc1/Atmnd1/Atxrcc3 we have to analyse more data. Meanwhile this mutant is represented by a mean *At*RAD51 foci number of (74±20; n=13).

Based on this preliminary data we conclude that, *At*XRCC3 is the essential factor for the loading of *At*RAD51.

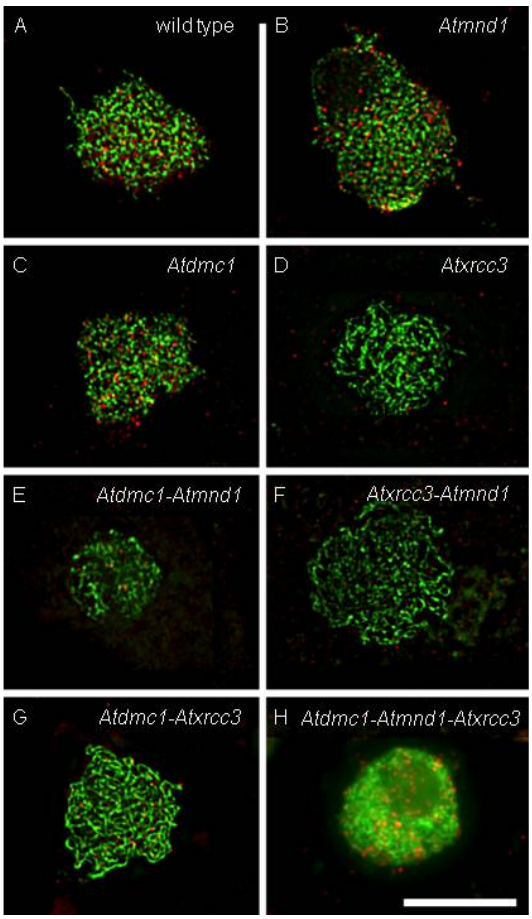

Figure 29: Dependency of loading of *At*RAD51 protein in different meiotic mutant background. Leptotene and zygotene stages of various meiotic mutants. ASY1 is stained in green and *At*RAD51 is stained in red. Explanation see text.

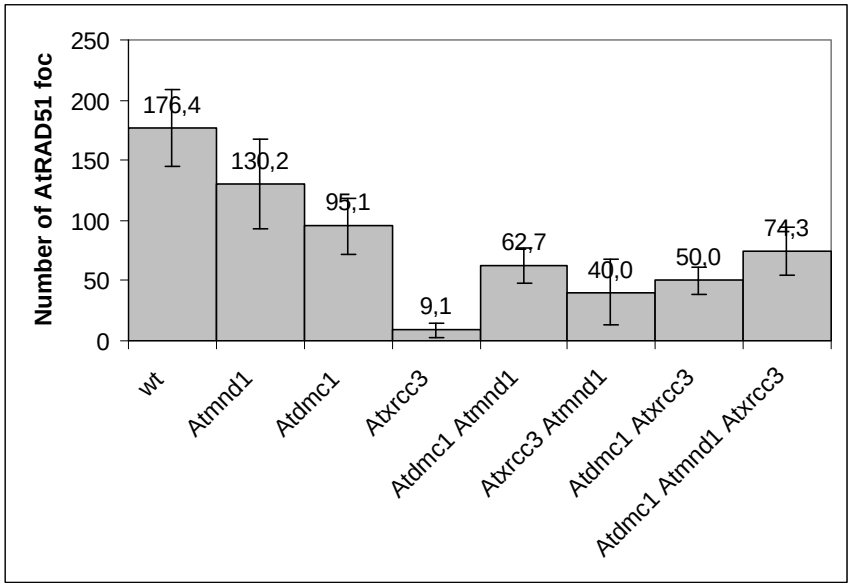

Figure 30: Dependency of loading of AtRAD51 protein in different meiotic mutant background.

6.13. *At*MND1 interacts with AHP2 as well as with *At*MIP1 in a Y2H assay

AHP2 is the *Arabidopsis* homologue of Hop2 (Schommer et al., 2003), a yeast protein that interacts with Mnd1. We used a Y2H assay to test for a potential interaction between *At*MND1 and AHP2. For this, we cloned the *AtMND1* cDNA into a yeast expression vector in-frame with a GAL4 DNA binding domain, and the AHP2 cDNA in-frame with a GAL4 activator domain, and vice versa. Plasmids encoding DNA binding domain and activator-domain fusion proteins were transformed into yeast strain YM706 (*MATα* ga14-542 ura3-52 his3-200 ade2-101 lys2-801 tql-901 tyrl-501) and PJ69-4A (*MATa* trpl-901 leu2-3,112 ura3-52 *his3-200* ga14A ga18OA LYSZ::GALl-HIS3 GAL2-ADE2 metZ::GAL7-lacZ), respectively and mated. Control experiments were performed, by transforming YM706 and PJ69-4A with combinations of fusion-protein-containing vectors and empty vectors (Figure 32).

The *At*MND1-interacting protein 1 (MIP1, At1g32530) was found by Claudia Kerzendorfer in a Y2H screen searching for novel interaction partners of *At*MND1 (thesis Claudia Kerzendorfer). *At*MIP1 has a conserved "structural-maintenance-of-chromosomes" (SMC) domain, typical for ATPases involved in chromosome segregation (Jessberger, 2002) and a C-terminal RING finger domain, implicated in protein-protein interactions and is a E3 ligase (Figure 31). The *At*MND1 interaction screen identified an *At*MIP1 fragment of the C-terminal region (498-589) as being sufficient for *At*MND1 binding. This region of *At*MIP was also interacting with AHP2,

but not with the GAL4 DNA binding domain alone (Figure 32). These results suggest an interaction of *At*MIP1 with the AHP2-*At*MND1 complex in *Arabidopsis thaliana.*

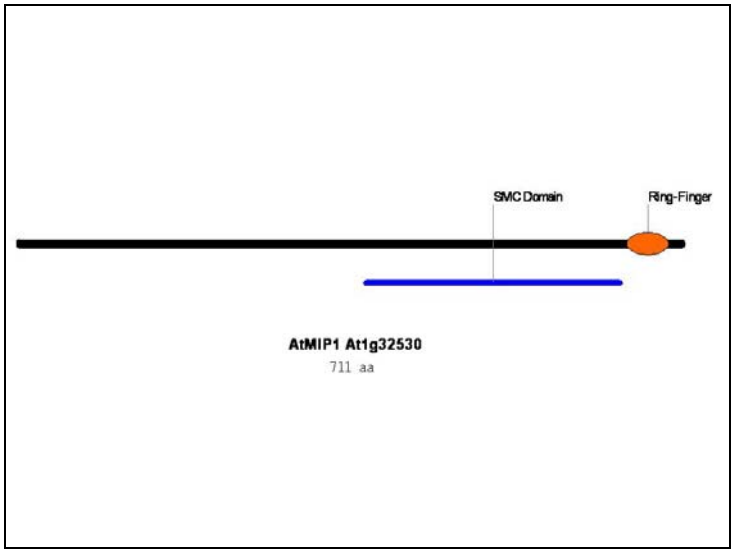

Figure 31: Structure of *At*MIP1 taken from NCBI.

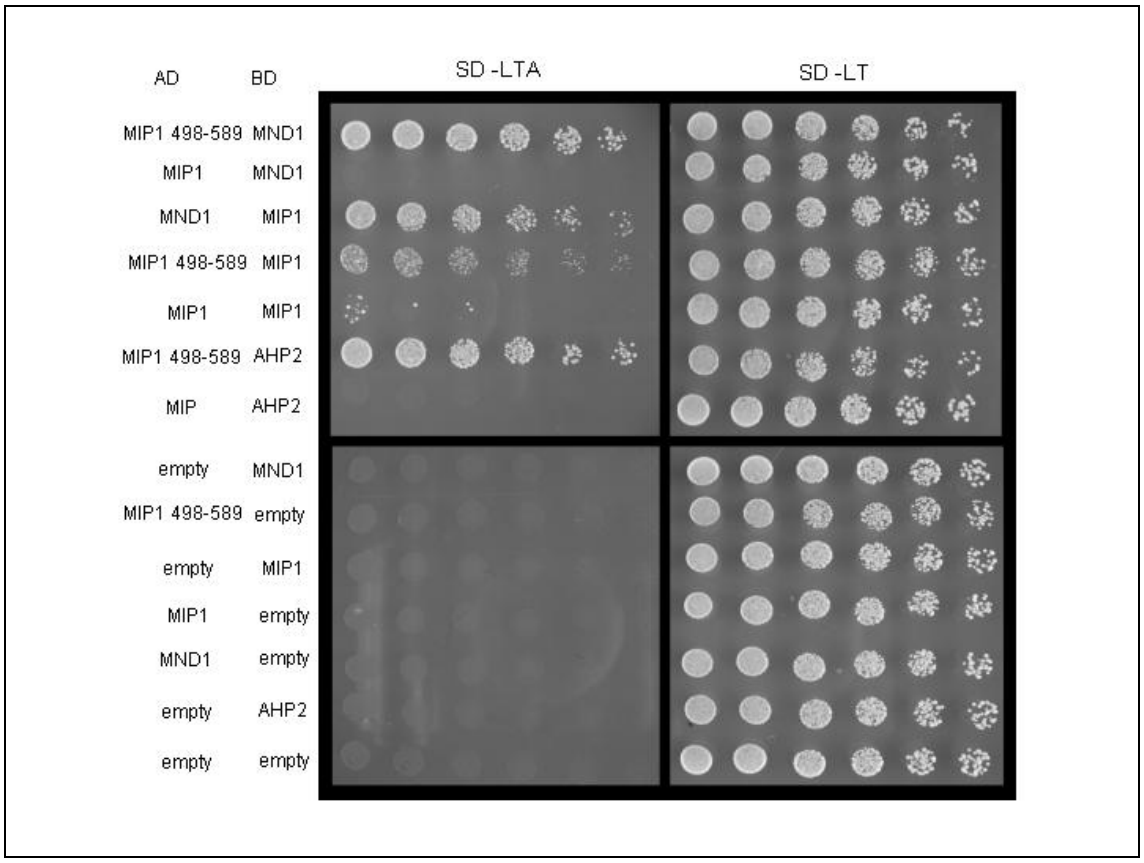

Figure 32: Interactions between MIP1, AHP2 and *At*MND1. Yeast two hybrid analysis showing interaction between MIP, *At*MND1 and AHP2. Yeasts grown in liquid culture were plated in a series of 5-fold dilutions onto drop out plates selecting for the activation and DNA binding domain plasmids (SD-L-T) or selecting for plasmids and activation of the ADE reporter gene (SD-L-T-A).

Furthermore, we wanted to test if we could confirm the interaction of *At*MND1 with *At*MIP1 with *in vitro* translated proteins. Therefore, we co-*in vitro* translated *At*MND1 fused to an HA-tag or MYC-tag and *At*MIP1 (full length) fused to a HA-tag or MYC-tag in the presence of radiolabled S^{35}-methionine (Figure 33). We demonstrated binding of *At*MND1-MYC and *At*MIP1-HA when we co-immunoprecipitated with the MYC-tag (Figure 33, Lane 1). Unfortunately, we were not able to confirm this result when we co-immunoprecipitated the same *in vitro* translated plasmids with the HA-tag (Figure 33, Lane 2). When we tested the protein interactions with *At*MND1-HA and *At*MIP1-MYC we were not able to get any reliable interaction, neither when we co-immunoprecipitated with the MYC-tag nor with the HA-tag (Figure 33, Lane 3 and 4). The control experiments (Figure 33, Lane 5 to 12) revealed that we cannot demonstrate specificity of the immunoprecipitations Figure 33 Lane 5, 7, 9, 10, 12).

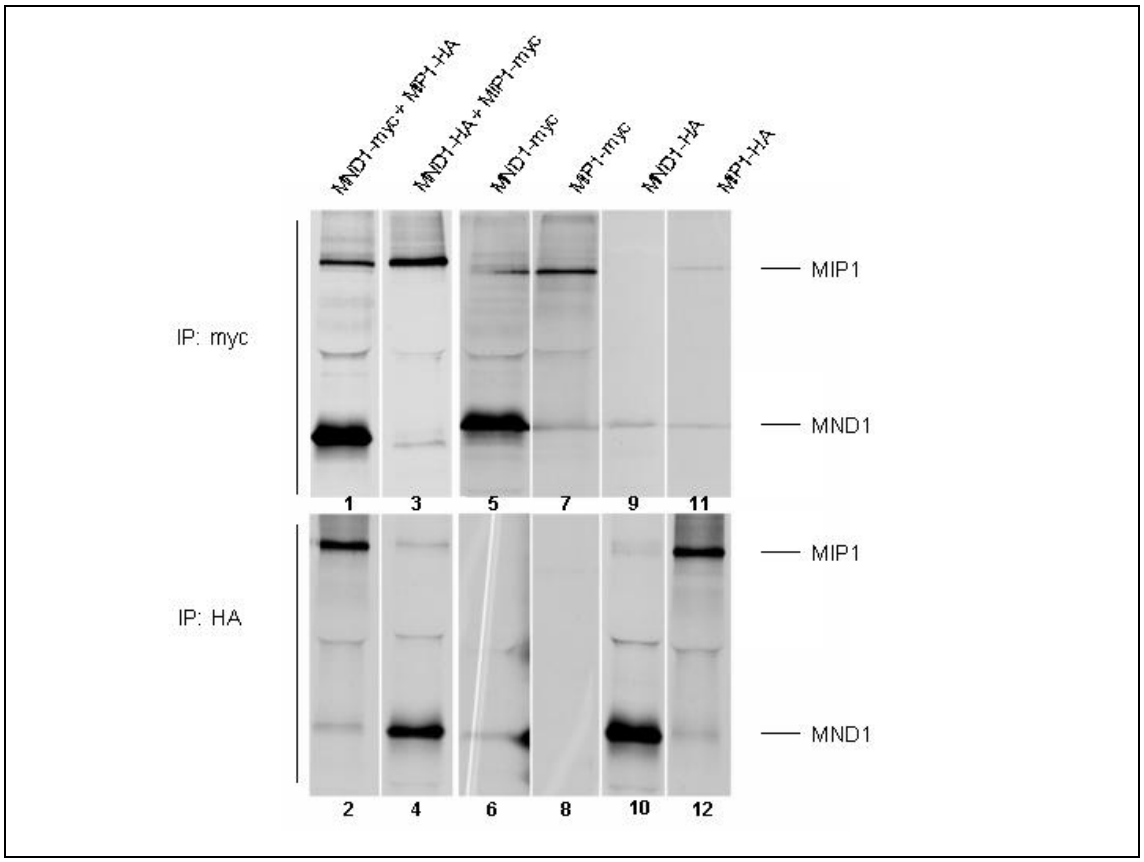

Figure 33: *In vitro* translated protein interactions. *In vitro* coupled transcription/translation of *At*MND1and *At*MIP1 was performed either alone or in the indicated combinations, in the presence of radioactively labeled L-methionine. Samples were split and incubated with one of the antibodies, directed against the c-myc or the HA epitope tag. The protein bands corresponding to *At*MND1and *At*MIP1 are indicated. The first two lanes correspond to coimmunoprecipitation experiments, the following four lanes correspond to controls, demonstrating the specificity of the immunoprecipitations (Experiment done by Tanja Siwiec).

6.14. *At*MND1 and AHP2 interact with *At*RAD51 and *At*DMC1

We addressed the issue of direct interaction between the RecA-related proteins, *At*RAD51 and *At*DMC1, and *At*MND1/AHP2 by carrying out *in vitro* protein interaction studies with proteins produced by *in vitro* transcription and translation. We demonstrated binding of *At*MND1 and AHP2 (Figure 34, lane1), this interaction was also observed in a yeast two-hybrid system study (Kerzendorfer et al.;2006). *At*MND1 also interacted with itself, but the co-immunoprecipitation of an *At*MND1–*At*MND1 complex was only possible with one of the two epitope tags used (Figure 34, lane 2). Interactions of *At*MND1 with itself can also be observed in a yeast two-hybrid assay (unpublished data). Both *At*MND1 and AHP2 interacted with *At*DMC1 (Figure 34, lanes 3 and 4). In addition, both AHP2 and *At*MND1 interacted with *At*RAD51 (Figure 34, lanes 5 and 6). While the AHP2-*At*RAD51 interaction was detected with only one of the two epitope tags used (Figure 34, lane 5), the interaction of *At*MND1 with *At*RAD51 was detected with both epitope tags (Figure 34, lane 6).

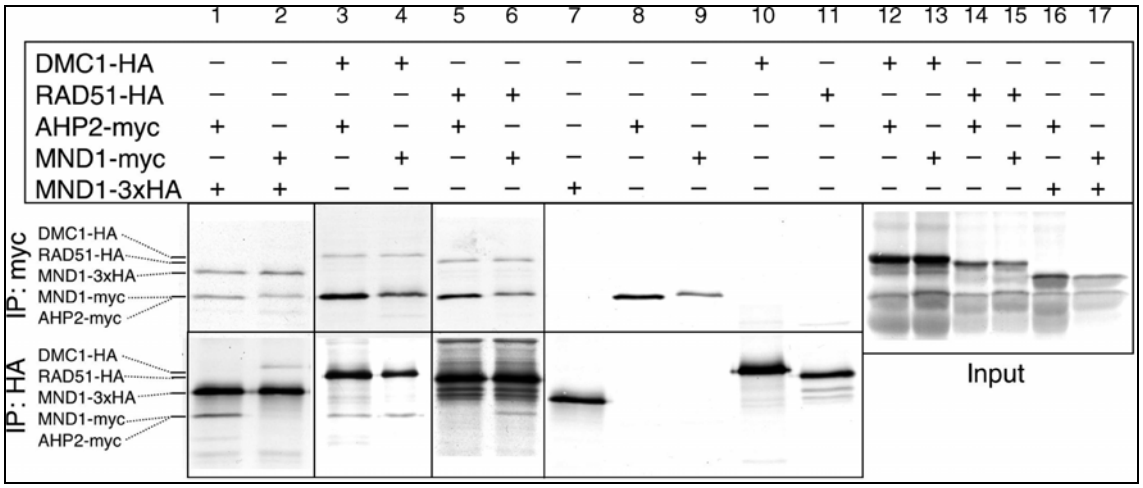

Figure 34: *At*MND1 and AHP2 interact with *At*DMC1 and *At*RAD51. *In vitro* coupled transcription/translation of *At*MND1, AHP2, *At*RAD51, and *At*DMC1 was performed either alone or in the indicated combinations, in the presence of radioactively labelled L-methionine. Samples were split and incubated with one of the antibodies, directed against the c-myc or the HA epitope tag. The protein bands corresponding to *At*MND1, AHP2, *At*RAD51 and *At*DMC1 are indicated. The first six lanes correspond to co-immunoprecipitation experiments, the following five lanes correspond to controls, demonstrating the specificity of the immunoprecipitations, and the last six lanes correspond to the co-translated protein samples before immunoprecipitation. (Taken from Vignard et al.,2007; experiment done by Tanja Siwiec).

6.15. Does MND1 have a role in somatic DNA repair?

Somatic expression of *MND1* has been observed in humans (Zierhut et al., 2004) and in *A. thaliana* but not in yeast. Data from publicly accessible microarray databases (http://www.genevestigator.ethz.ch) show that *AtMND1* expression is upregulated

approximately fivefold in response to genotoxic stress (*AHP2* is upregulated eightfold under the same conditions). These expression data point to a potential role of Mnd1 in somatic cells, presumably in DNA repair; this hypothesis has not been tested yet in mammals, as there is no mutant available.

However, we investigated this issue in wild-type and *Atmnd1* mutant plants exposing them to different genotoxic treatments. Mutant plants were germinated on plates containing different concentrations of hydroxyurea (HU). HU depletes the pool of dNTPs by inhibiting ribonucleotide reductase (RNR) (Krakoff et al., 1968), leading to a replication block and subsequent DNA DSBs. The length of developing roots of a heterozygous population of *Atmnd1* plants was monitored and compared (Culligan et al., 2004). We could not detect any influence of the *Atmnd1* mutation on root growth on media plates with HU (Figure 35). In addition, we germinated seedlings on media plates and exposed them to different doses of gamma-radiation to induce DSBs (Garcia et al., 2003). Exposure to gamma-radiation interfered with development to a similar extent in mutant and wild-type plants (Figure 35).

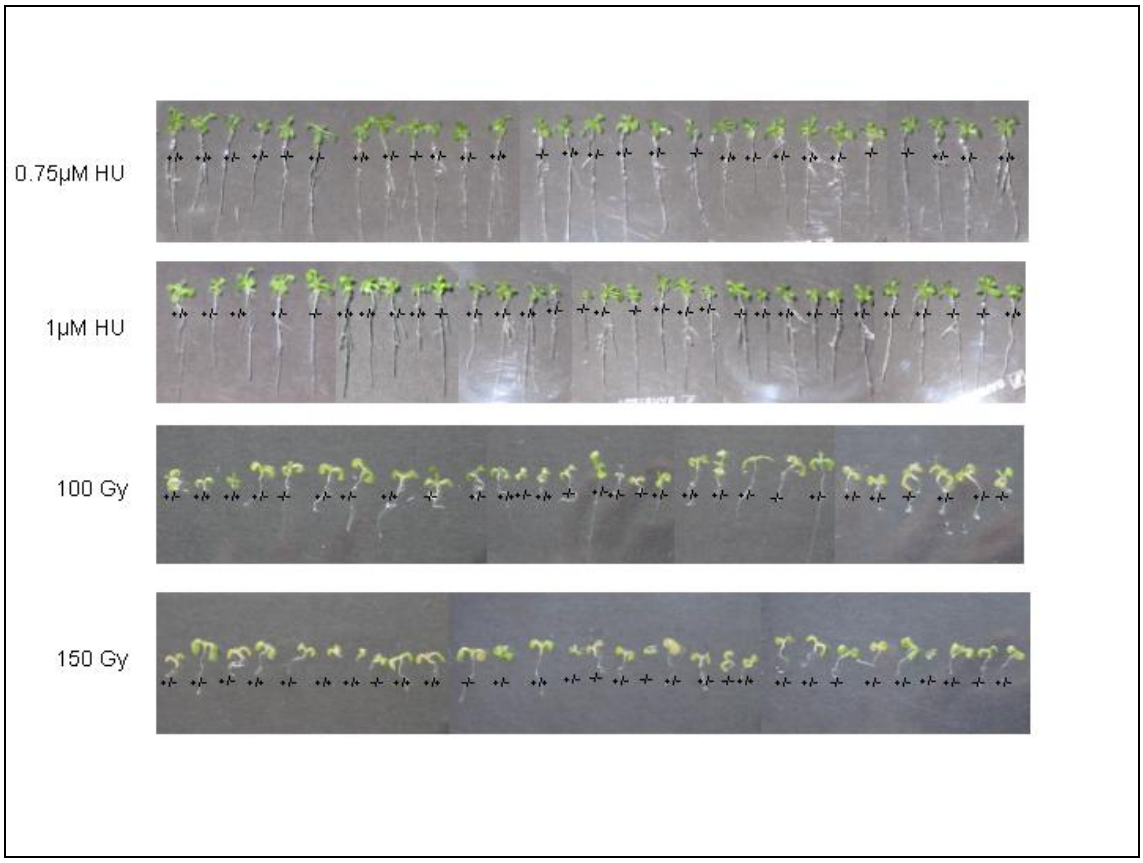

Figure 35: Heterozygous *Atmnd1* population grown on media plates and exposed to different concentrations of HU or different doses of gamma radiation. No difference in root development could be observed within the heterozygous *Atmnd1* population.

Furthermore the heterozygous *Atmnd1* population was grown on plates containing mitomycin C (MMC). MMC causes interstrand cross links, which lead to DSB formation. Plants (n=54) were grown on media containing 40µM MMC for two weeks and showed a Mendelian segregation. Plants were not affected by the genotoxic stress, producing true leaves and showing no growth defects (Figure 36).

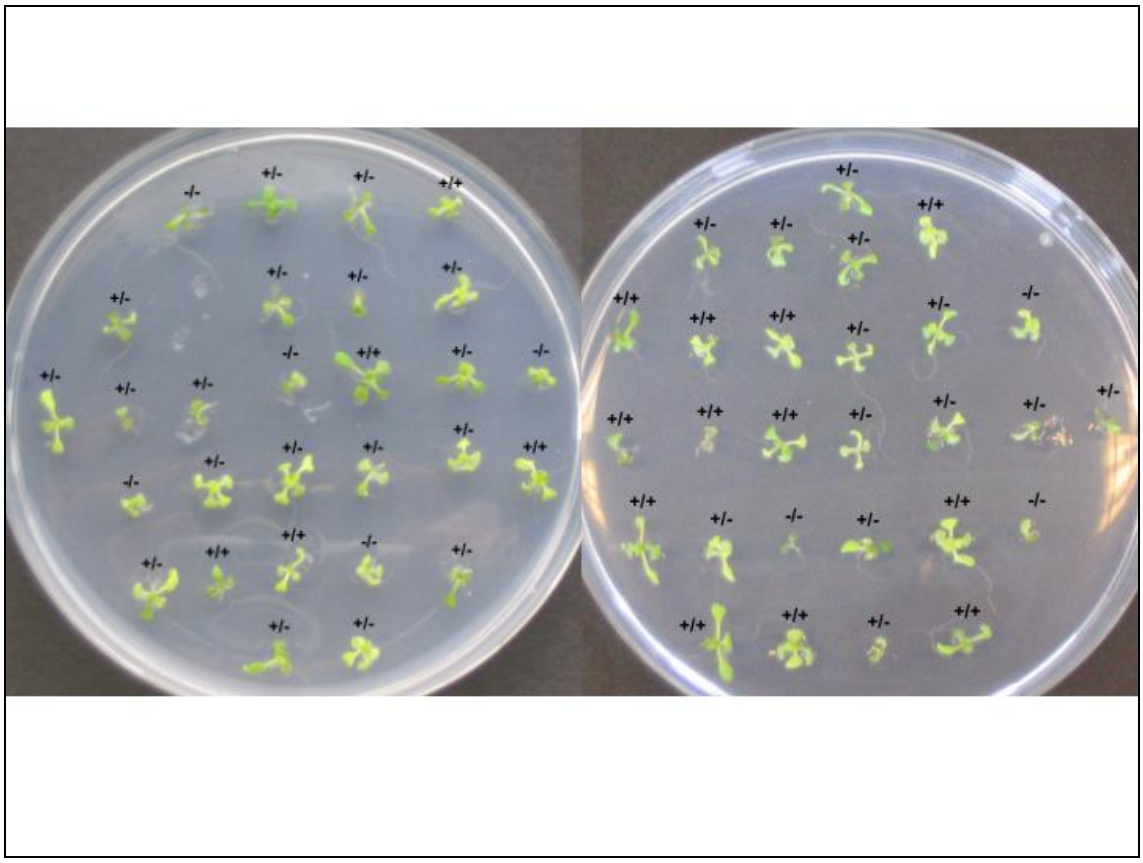

Figure 36: Heterozygous population of *Atmnd1* plants are not sensitive to mitomycin C.

Furthermore, *Atmnd1* mutant plants had no growth defect when grown under normal conditions, contrary to the DNA-repair-deficient mutants *mre11* (Bundock and Hooykaas, 2002). Therefore, we concluded that *AtMND1* has no essential role in somatic DNA repair, at least under the conditions tested.

6.16. Over-expression of *At*MND1 is lethal for plants

We constructed various over-expression-lines, containing the cDNA of *AtMND1* and fused to different tags, to get more insight into the localization of *At*MND1 and co-localization of *At*MND1 with other proteins (Figure 37).

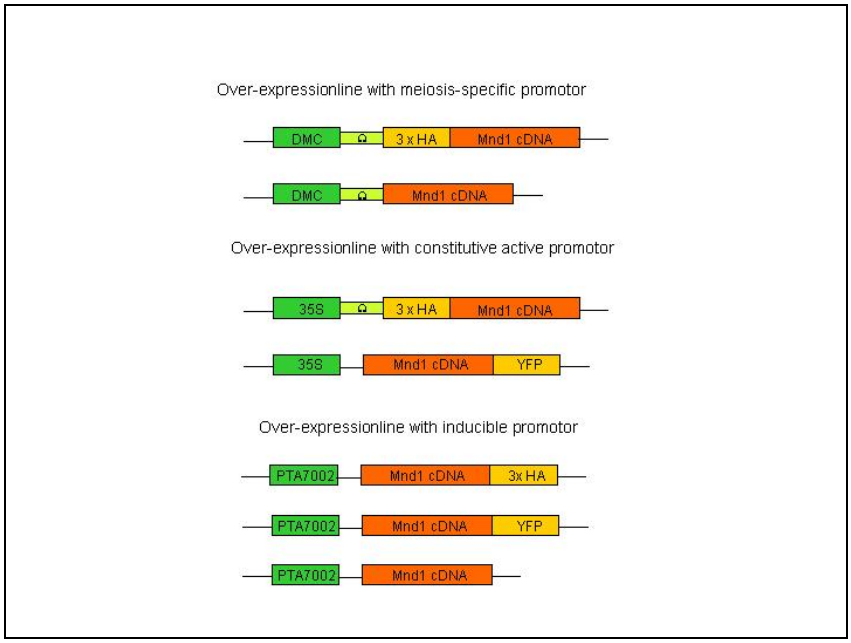

Figure 37: Over-expression-lines with different promotors and *At*Mnd1 cDNA fused to HA- or YFP-tag. Constructs without a tag were designed to avoid a possible interference of the tag with the function of the construct.

The *AtMND1* cDNA and a three times HA tag were introduced into a plant binary vector, containing the *AtDMC1* promoter (Siaud et al., 2004b). Successful complementation, after plant transformation, of the *Atmnd1* sterility phenotype would demonstrate that the fusion protein is functional. Subsequently, an *Atmnd1* plant expressing the AtMnd1/HA fusion can be used to analyse the localisation of the AtMND1 protein during meiosis in wild-type and different mutant backgrounds. Furthermore, this fusion protein could be used in co-localisation experiments with other proteins.

It had to be taken into consideration however, that the tag might disturb the expression of *AtMND1*, therefore also constructs without the YFP or HA-tag were made. If expression from the *AtDMC1* promoter is not strong enough, the CaMV 35S promoter could be used instead. Recently, the 35S CaMV promoter has been successfully used to express meiotic genes in complementation studies (Li et al., 2004).

Moreover, we also generated a plasmid containing a dexamethasone inducible promoter PTA7002. If the *At*Mnd1-HA fusion protein does not complement the phenotype, even

though the protein is expressed, the HA protein tag could be placed at the C-terminal end. However, the use of a fusion protein in the way outlined above could have many disadvantages like first the fusion protein has to be crossed into the desired mutant backgrounds, second the promoter used might have the wrong temporal activation pattern (*AtDMC1* promoter) or third the promoter used might be too strong (35CaMV promoter) and thereby distort the stoichiometry of protein complexes involved. Heterozygous *Atmnd1* plants transformed by floral dip transformation with the construct containing the *AtDMC1* promoter were selected on selective media. Of the five selected T0 plants only one contained the transgene. Further selection has to be made with plants of T1 generation. Heterozygous *Atmnd1* plants transformed with the construct containing the CaMV 35S and the HA-tag, were selected. Three T1 plants were heterozygous for the *AtMND1* mutation, one plant was homozygous for the mutation but showed no complementation. Heterozygous *Atmnd1* plants transformed with the CaMV 35S promotor construct with the YFP-tag, were selected and all plants of the T1 generation were silenced. Heterozygous *Atmnd1* plants transformed with the construct containing the inducible promoter and the HA-tag, were selected and all plants of the T1 generation were silenced. Plants transformed with the same construct but instead of the HA-tag having the YFP-tag were selected and all but one line were silenced in T1 generation (Figure 38). Interestingly, this one line dies upon induction, leading to the assumption that *AtMND1* is inducible by special genotoxic treatment and furthermore that the overexpression of *AtMND1* is lethal.

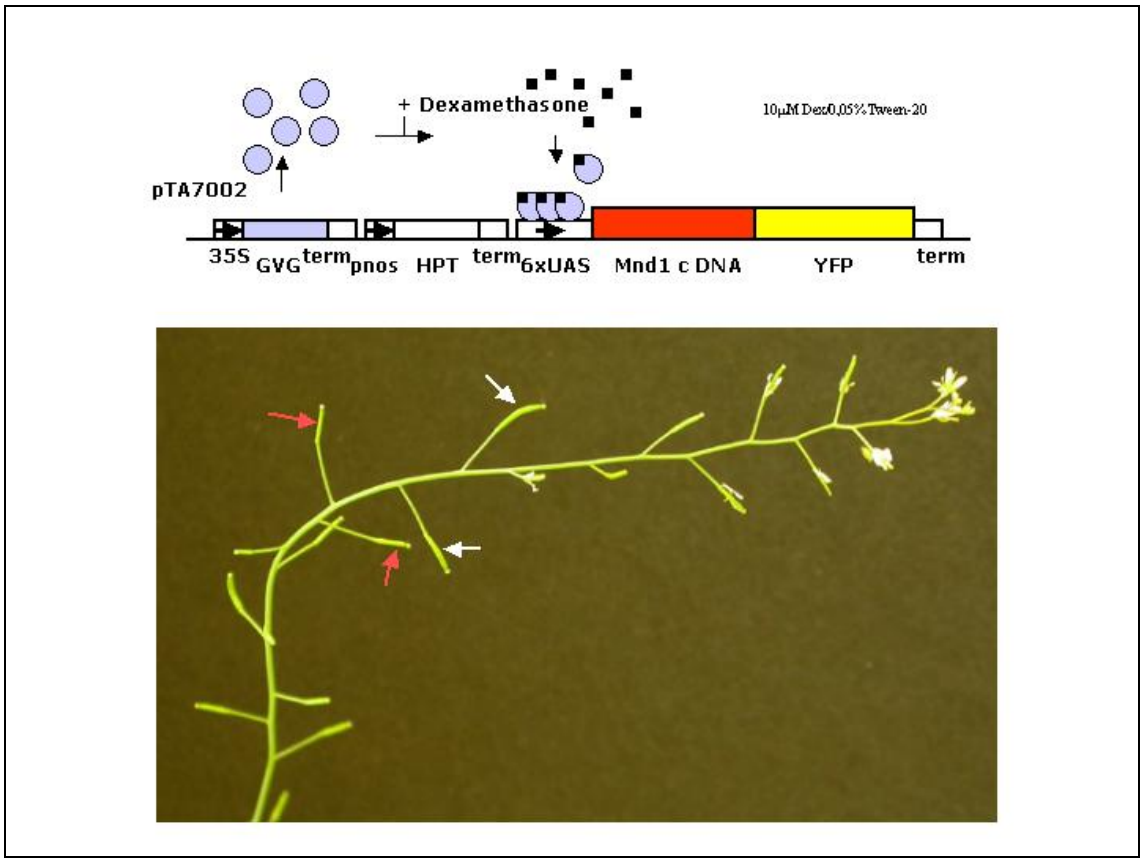

Figure 38: Partial complementation of the *Atmnd1* sterile phenotype. Heterozygous *Atmnd1* plants were transformed with an dexamethasone inducible promoter fused to the AtMND1 cDNA and a YFP tag. After induction of the promotor by spraying 10µM Dexamethasone solution upon the inflorescences, all plants died. Red arrows point to siliques without seeds, white arrows point to siliques with seeds.

7. Discussion-*AtMND1*

During the last years effort has been made to get deeper insight into the sophisticated processes of meiosis. Meiosis has been extensively studied in budding yeast because of its easy handling in genetic and biochemical assays. It is important to expand the wide research field of meiosis to higher eukaryotic organism, like *Arabidopsis thaliana*. Short life time cycle, easy cultivation and small genome size make this plant an attractive model organism for molecular biology.

Topic of this PhD thesis is the *Arabidopsis thaliana* homologue *AtMND1*. It is characterized and analyzed. *At*MND1 is an important meiotic protein to ensure the proper reciprocal exchange of genetic information between homologous chromosomes. Studies in *S. cerevisiae* showed that inactivation of Mnd1 inhibit homologous recombination. In *Arabidopsis thaliana*, the *AtMND1* gene is comprised of ten exons and the ORF is 693bp in length. T-DNA insertion of *AtMND1* is located within the seventh introns (Kerzendorfer et al., 2006b). The mutation leads to fully viable, but sterile plants. Siliques are short and almost completely devoid of seeds (0.033 seeds/silique), the flowering time of plant homozygous for the mutation is prolonged, as often seen in plants with meiotic mutations. The sterility phenotype of the homozygous plants can be reversed by introducing a genomic copy of the *AtMND1* gene thorough transformation with *Agrobacterium tumefaciens* carrying T-DNA plasmid with the *AtMND1* gene and its putative promoter region. This confirms that the observed phenotype is caused by the *Atmnd1* mutation.

7.1. *At*MND1 is essential for male and female meiosis

The *Atmnd1* mutation leads to strong male and female sterility, confirmed by cytological analysis of male and female meiosis. During male meiosis severe chromosome fragmentation is visible in metaphase I-like stage which give rise to chromatin connection in anaphase I-like stage and results in completely unequally dispersed chromatin at the end of meiosis II. Also female meiosis is strongly affected as seen by chromosome fragmentation in the mega spore mother cells compared to fully intact chromosomes in wild type. The observation of chromosomal rearrangements are often detected in mutation harboring meiotic genes (Bleuyard and White, 2004; Li et al., 2004; Puizina et al., 2004; Schommer et al., 2003).

7.2. Chromosome breaks in *Atmnd1* remain un-repaired

The observed meiotic aberrations obviously depend on the SPO11 protein, because in mutants were both proteins, *At*SPO11-1 as well as *At*MND1, are missing, genetic defects resemble the ones seen in the *Atspo11-1* single mutant. Furthermore, the presence of *At*RAD51 foci in the *Atmnd1* mutant demonstrates the existence of chromatin breaks, a prerequisite for synapsis in *Arabidopsis*. Also in mouse Hop2 (Petukhova et al., 2003) mutants as well as in budding yeast *mnd1* and *hop2* mutants (Gerton and DeRisi, 2002; Tsubouchi and Roeder, 2002; Zierhut et al., 2004) a normal induction of RAD51 foci could be detected. The majority of DSBs in *Atmnd1* mutants remain un-repaired, leading to chromosome fragmentation. This defect is comparable to yeast *mnd1* mutants, in which hyper-resected DSBs accumulate (Gerton and DeRisi, 2002; Tsubouchi and Roeder, 2002).

7.3. Pairing and synapsis of meiotic chromosomes depends on *At*MND1

In *Arabidopsis*, synapsis is the prerequisite for the correct reciprocal exchange of maternal and paternal genetic material, ensured by cross over. Synapsis in *Atmnd1* mutant plants is severely disrupted shown by a failed pachytene stage, where in wild type homologous chromosomes are fully synapsed. Although the axial component protein ASY1 (Armstrong et al., 2002; Caryl et al., 2000) as well as the cohesin complex protein SCC3 (Chelysheva et al., 2005), are loaded onto meiotic chromosomes during early prophase I in *Atmnd1*, synapsis cannot be fully established in *Atmnd1* mutants. Furthermore, a defect in pairing has been detected by FISH using probes against regions on chromosome I and II. Only telomere pairing seems to be unaffected in early stages of meiotic prophase I. But as meiosis progresses the pairing of centromeric regions is completely absent even in early stages of meiosis. Yeast *mnd1* (Zierhut et al., 2004) and mouse *hop2* (Petukhova et al., 2003) mutants were defective in SC formation. Limited synapsis can be seen, but most of it is non-homologous (Leu et al., 1998). Subsequently, it seems that plants, mammals and yeast have a common synapsis control pathway, which depends on the Mnd1-Hop2 complex. As mentioned before this complex is not conserved in all eukaryotes, as *C. elegans* (Dernburg et al., 1998) and *D. melanogaster* (McKim et al., 2002), where DSB formation is not required for intact SC formation, lack the Mnd1-Hop2 protein complex as well as the Dmc1 protein (Gerton and Hawley, 2005).

7.4. Synapsis is similarly impaired in *Atmnd1*, *Atrad51*, *Atdmc1*, and *Atxrcc3*

Also other *Arabidopsis* mutants display an asynaptic phenotype like *Atmnd1*. Also *Atrad51* (Li et al., 2004), *Atdmc1* (Couteau et al., 1999) and *Atxrcc3* (this thesis, (Vignard et al., 2007a) show a lack of a typical pachytene stage and an incomplete SC. This assumption in based on the immunolocalization studies with the *At*ZYP1 antibody applied to the *Atrad51*, *Atdmc1*, and *Atxrcc3* mutant plants. *At*ZYP1 is visible as few foci and short linear stretches. We therefore conclude that these genes are needed for DSB repair as well as for normal SC formation.

Furthermore, cytological analysis of *Atmnd1*, *Atrad51*, and *Atxrcc3* male meiocytes showed that all three mutants display the same meiotic defect in meiosis I. These mutants display an entangled mass of chromatin during metaphase I resulting in chromosome fragmentation in anaphase I. Through depletion of the DSB responsible meiotic nuclease *At*SPO11-1 this fragmentation phenotype can be suppressed in all three mutants (Bleuyard et al., 2004; Kerzendorfer et al., 2006b). The observation of the corresponding double mutants with *Atspo11-1* revealed the same results, suggesting that these three mutants are epistatic to *Atspo11-1*. Moreover, all three mutants show chromatin links between multiple chromosomes at metaphase I, possibly pointing to a previous interaction between non-homologous chromosomes, which can be seen in genes involved in the NHEJ pathway (Siaud et al., 2004b). However, the generation of double mutants between *Atku80* (Tamura et al., 2002) and *Atmnd1* and *AtligIV* (West et al., 2000) and *Atmnd1* (*AtKU80* as well as *AtLIGIV* are known to be key player in the NHEJ pathway), respectively, did not reduce the chromatin links seen in the *Atmnd1* single mutant (Julien Vignard and Tanja Siwiec, unpublished data) and therefore suggesting that the observed chromatin linkages are not generated by the NHEJ pathway.

7.5. *At*RAD51 and *At*XRCC3 cooperate in sister chromatid–mediated DSB repair in the *Atdmc1* mutant

In the *Atdmc1* mutant DSBs appear normally, but are repaired via the sister giving rise to ten univalents in metaphase I. This process is thought to be mediated by *At*RAD51 (Couteau et al., 1999; Siaud et al., 2004b) based on the results that if *At*RAD51 is mutated fragmentation is detected in *Atdmc1* mutants (Siaud et al., 2004b) or in the *Atdmc1/Atrad51* double mutant shown in this thesis. These results point to a role of *At*DMC1 in the inter-homolog bias, and therefore preventing DSB repair between the

sisterchromatids. Interestingly, *At*RAD51 seems to initiate the search for the homologous chromosome regardless of the target (sister chromatid or the chromatids of the homologous chromosome). This is supported by data in mammals and yeast during mitotic recombination (Dudas and Chovanec, 2004) and the preference of Rad51 for inter-sister homologous recombination in somatic cells (Johnson and Jasin, 2001; Kadyk and Hartwell, 1992). It should be noted that, efficient Rad51-dependent inter-sister recombination in the absence of Dmc1 occurs only in *Arabidopsis*, but not in yeast (Schwacha and Kleckner, 1997).

The meiotic defects, like chromosome fragmentation, seen in the *Atrad51* as well as in *Atxrcc3* mutants are different than the one seen in *Atdmc1* mutant. Furthermore, it has been shown that the meiotic defects of *Atdmc1-Atxrcc3* and *Atdmc1-Atrad51* double mutants are the same as the ones observed for *Atxrcc3* and *Atrad51* single mutants. This demonstrates that both *At*RAD51 and *At*XRCC3 are required for the sister chromatid mediated DSB repair in the *Atdmc1* mutant. Moreover, these results lead to the assumption that *AtRAD51* and *AtXRCC3* act at the same step of meiotic recombination during strand invasion and that their functions are not redundant. These results are supported by data from human Xrcc3 which interacts with Rad51 (Liu et al., 1998). Additionally it has been shown that Xrcc3 forms a complex with Rad51C, and that this complex may contain Rad51 (Liu et al., 2002; Masson et al., 2001; Wiese et al., 2002). In *Arabidopsis* it has been shown by yeast-two hybrid analysis that *At*XRCC3 interacts with *At*RAD51 (Osakabe et al., 2002). These results indicate that the *At*RAD51 and *At*XRCC3 proteins cooperate in the same recombination step during meiosis.

7.6. *At*MND1 interacts with *At*RAD51

Interestingly, the *Atmnd1-Atdmc1* double mutant showed an intermediate meiotic defect between those of the single mutants. We assume that this intermediate phenotype is dependent on *At*RAD51 and *At*XRCC3. In the *Atdmc1* mutant the efficient repair of DSBs via the sisterchromatide might not only require *At*RAD51 and *At*XRCC3, but also *At*MND1. We therefore analyzed a putative physical interaction between *At*MND1 and *At*RAD51 by *in vitro* immunoprecipitation assays. In mammals it has been demonstrated that the Mnd1–Hop2 complex stimulates the strand exchange activity of Dmc1 or Rad51 (Enomoto et al., 2006; Petukhova et al., 2005). We showed that both *At*MND1 and AHP2 interact with *At*RAD51 and *At*DMC1 *in vitro*. However, we

assume that in the presence of *At*DMC1, *At*MND1 may not interact with *At*RAD51 *in vivo* due to the higher affinity of the *At*MND1–AHP2 complex for *At*DMC1.

7.7. *At*DMC1 foci formation depends on *At*RAD51 and *At*XRCC3 and their number increases in *Atmnd1* mutants

In *hop2* knockout mice Dmc1 as well as Rad51 foci are formed and accumulate during meiotic progression (Petukhova et al., 2003). Also in *S. cerevisiae mnd1* and *hop2* Dmc1 and Rad51 foci formation is observed, but to a larger amount than in wild-type (Leu et al., 1998; Tsubouchi and Roeder, 2002; Zierhut et al., 2004). It seems that in these mutants DSB formation is not impaired and the process of strand invasion is disturbed.

Here, we show that in *Arabidopsis Atmnd1* mutants *At*DMC1 foci are formed. Foci accumulate in this mutant to a larger number than in wild-type, suggesting that un-repaired and hyper-resected DNA end remain after DSB formation or that more breaks are made in the absence of *At*MND1. We also cannot exclude the possibility that in *Atmnd1* mutant more DSB are formed than in wild-type. It seems that, as in yeast and mammals, the absence if *At*MND1 leads to un-repaired DSBs and possibly a delay in *At*DMC1 nucleoprotein filament turn-over.

7.8. *At*XRCC3 is dispensable for *At*DMC1 loading in an *Atmnd1* mutant background, whereas *At*RAD51 is not

Interestingly, *Atrad51* and *Atxrcc3* mutants show far fewer AtDMC1 foci than wild-type or *Atmnd1*. This points to the fact that *At*RAD51 as well as *At*XRCC3 are needed for *At*DMC1 foci formation. Also in S. cerevisiae it has been shown that Rad51 is required for normal formation and distribution of Dmc1 (Bishop, 1994; Shinohara and Shinohara, 2004). About the potential requirement of Xrcc3 for the correct distribution of Dmc1 only less is known. It seems possible, that in *Arabidopsis Atxrcc3* mutants and *Atrad51* mutants fewer *At*DMC1 foci are formed, or their turnover rate is faster than in wild-type due to an unstable *At*DMC1 nucleoprotein filament structure based on the absence of the recombinase *At*RAD51 and *At*XRCC3.

*At*RAD51 and *At*DMC1 proteins are loaded onto DSBs to form nucleoprotein filaments, which are the prerequisite for the strand invasion process and subsequently the homologous bias. The *At*MND1-AHP2 complex may support for an efficient homology search, through a possible role in promoting the nucleoprotein filament formation by

interacting with *At*DMC1 or *At*RAD51, respectively. If *At*MND1 is absent, this process is disturbed, resulting in an higher *At*DMC1 foci count. During our investigations we found out that *At*RAD51 and *At*XRCC3 play different roles during meiotic progression in an *Atmnd1* mutant background. Based on our results it seems, that *At*XRCC3 might be needed for stabilization of *At*DMC1 nucleoprotein filament. If *At*XRCC3 is depleted, the nucleoprotein filament is rapidly disassembled or unable to be formed at all and resulting therefore in an lower *At*DMC1 foci count. Consistent with this proposal, in the *Atmnd1/Atxrcc3* double mutants the number of *At*DMC1 foci is reduced compared to the one in the *Atmnd1* single mutant but higher than in the *Atxrcc3* single mutant. This result points to the conclusion that *At*XRCC3 is dispensable for *At*DMC1 foci formation in an *Atmnd1* mutant background, whereas *At*RAD51 is not (Figure 39).

7.9. *At*XRCC3 is important for an efficient loading of the *At*RAD51 protein

In somatic cells from Chinese hamster, chicken, and human no Rad51 foci formation can be observed when Xrcc3 is depleted (Bishop et al., 1998; Takata et al., 2001; Yoshihara et al., 2004). Furthermore, Xrcc3 is recruited to DSB sites earlier and independently of Rad51 in human somatic cells (Forget et al., 2004). Further studies, analyzing the distribution and number of *At*RAD51 foci in various mutant backgrounds during meiosis, were made to decipher this divergence between mammalian somatic recombination and meiosis in *Arabidopsis*. To clarify this issue we show that the *At*RAD51 foci formation is almost completely absent in *Atxrcc3* mutants. In contrast, in the *Atdmc1* as well as in the *Atmnd1* mutant *At*RAD51 foci formation can occur, even if the number of *At*RAD51 is reduced. It seems that *At*XRCC3 is an essential factor for the loading of *At*RAD51. In contrast *At*MND1 as well at *At*DMC1 seem to be dispensable for efficient loading of *At*RAD51. Consistently, also the analysis of the respective double and triple mutants revealed that the number of *At*RAD51 foci is only slightly increased compared to the one in the *Atxrcc3* single mutant. Leading to the conclusion that *At*XRCC3 seems to be not only required to stabilize *At*DMC1-containing nucleoprotein filaments but for the stabilization of the *At*RAD51 filament it is absolutely necessary (Figure 39).

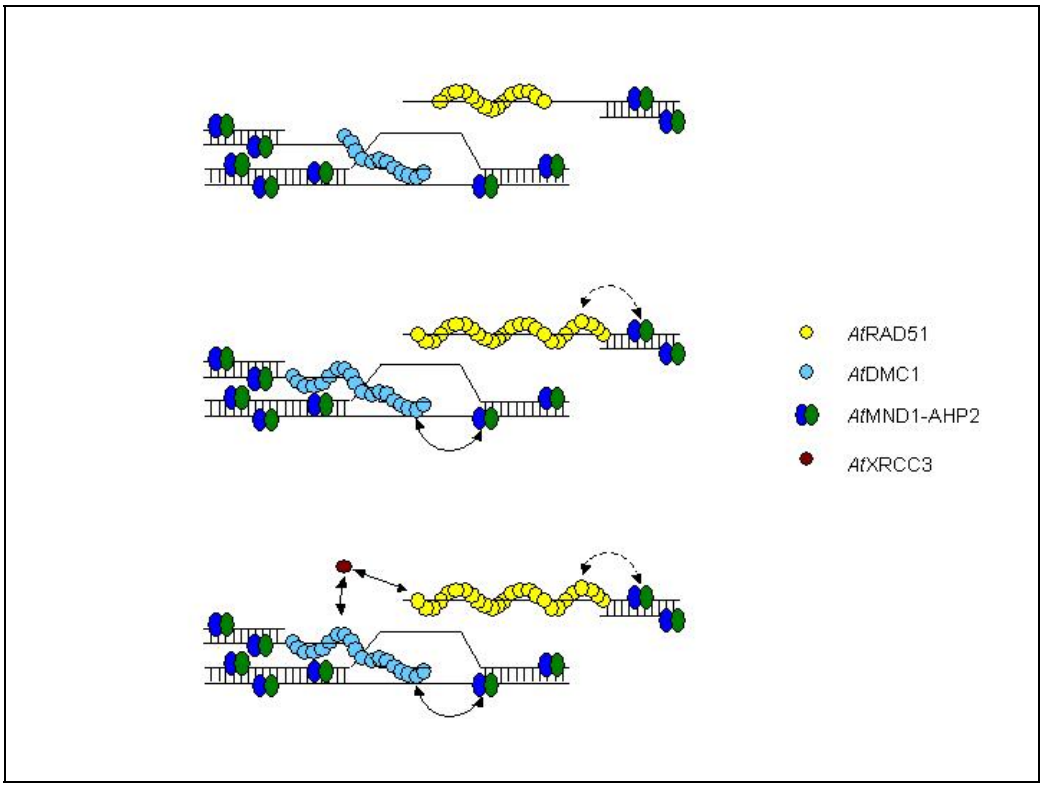

Figure 39: Model of the strand invasion step of meiotic recombination. *At*DMC1 may assemble on one side of a processed DNA DSB, whereas *At*RAD51 may assembles on the other side. *At*DMC1 nucleoprotein filament invades the homologous chromosome, assisted by the *At*MND1-AHP2 complex. *At*RAD51 may also be stimulated by the *At*MND1-AHP2 complex in the strand exchange processes. XRCC3 seems to be needed for stabilization of the *At*DMC1 nucleoprotein filament and the *At*RAD51 nucleoprotein filament, and *At*MND1-AHP2 seems to be a putative promoting factor for the strand invasion process.

7.10. Localization of AtMND1 on chromosomes depends on AHP2

Immunolocalization studies revealed that during prophase I the *At*MND1 protein is evenly distributed on chromosomes. *At*MND1 labels the entire length of chromosomes, with interspersed regions of higher staining intensity Axial element formation, cohesion or meiotic recombination is not necessary for the loading of *At*MND1. Like in yeast (Zierhut et al., 2004), we cannot detect co-localization of *At*MND1 with *At*DMC1. The only factor which is absolutely fundamental for the distribution of AtMND1 is AHP2. In meiocytes of the *ahp2* mutant we are not able to observe staining of the AtMND1 protein by immunocytological analysis as well as the AtMND1 protein was not detectable in *ahp2* mutant plants on western blot. This is consistent with findings in *S. cerevisiae*, where a regular distribution of Mnd1 requires Hop2, but, as in *A. thaliana*, does not rely on cohesion, axial element formation or DSB formation (Tsubouchi and Roeder, 2002; Zierhut et al., 2004). Furthermore, AHP2 and AtMND1 interact in a Y2H assay (Kerzendorfer et al., 2006b) and *in vitro* studies (this thesis). Consistently, Mnd1

and Hop2 are immunoprecipitated in yeast and mammals (Enomoto et al., 2004; Petukhova et al., 2005; Ploquin et al., 2007; Saito et al., 2004). Taken together this result leads to the assumption of a strongly conserved role of the Mnd1-Hop2 complex.

7.11. Experimental Outlook

During meiosis the repair machinery is biased toward inter-homolog (IH) events. In budding yeast, two mechanisms seem at work to ensure IH bias, first suppression of inter-sister (IS) recombination and second active promotion of IH recombination (Paques et al., 1998). Rad51 is needed for both inter-homologue (IH) and inter-sister (IS) repair, while Dmc1 seems to be the important player to mediate IH repair. Interestingly, recent data suggest that purified Dmc1 and Rad51 (from human and budding yeast) are not distinct from each other with respect to their biochemical properties (Bugreev et al., 2005; Ogawa et al., 1993; Sauvageau et al., 2005; Sehorn et al., 2004; Sheridan et al., 2008; Sung and Robberson, 1995). Therefore it has been suggested that a set of distinct accessory proteins, that modulate the activity of Dmc1 or Rad51, are responsible for the observed differences in the meiotic function.

Suppression of IS recombination is mediated in yeast by the activation of the threonine/serine DNA damage check-point-kinase Mek1. Targets of activated Mek1 have not been identified yet. Assembly of the Red1-Hop1-Mek1 protein complex precedes activation of Mek1. For this, Red1 has to be phosphorylated by a Spo11 independent process, and Hop1 has to be phosphorylated in response to Spo11-mediated DSB formation by the Tel1/Mec1 kinases. Red1 and Hop1 are structural components of the meiotic chromosome axes, are a needed for normal levels of DSB induction and for IH repair. The implication of Red1 in IH comes from the observation that in red1 mutants, IH but not IS repair intermediates are reduced (Hollingsworth et al., 1995). Furthermore, in *red1* mutants being additionally deficient in either *dmc1*, *hop2* or *mnd1*, IH repair is further reduced, indicating that Rad51 promotes inter-sister repair in afore mentioned genetic backgrounds. In plants, no homologues for Red1 or Mek1 could be identified so far. The HORMA domain protein ASY1 is conserved among plant species and shares homology with Hop1 from yeast. *Arabidopsis* mutants lacking ASY1 preferentially repair meiotic DSBs via the sister chromatid (Sanchez-Moran et al., 2007). Furthermore, ATM/ATR kinases (the Tel1/Mec1 homologues in higher eukaryotes) are needed for establishing IH bias during meiosis in plants (unpublished results).

The promotion of IH repair in yeast meiosis seems to be actively promoted by the activity of the RecA protein Dmc1 and its partner proteins Hop2 and Mnd1. Analysis in yeast showed that both *mnd1* and *hop2* mutants initiate recombination, but do not form heteroduplex DNA or double Holliday junctions, suggesting that they are involved in strand invasion (Gerton and DeRisi, 2002). These mutants arrest in prophase I due to DNA-damage checkpoint activation. Furthermore, in yeast, Dmc1 directs meiotic repair to the homologue chromosome only in the presence of Mnd1, whereas Mnd1 alone may not interfere with IS-repair (Zierhut et al., 2004).

We are interested how the *At*MND1 and the *At*HOP2/AHP2 proteins are distributed during meiosis. This has already been established for *At*MND1, and we demonstrated that *At*MND1 is deposited at meiotic chromosomes loops and cores and that it is not present in *ahp2* mutants (but in all other meiotic mutants tested, *At*MND1 appears to be located correctly) (Vignard et al., 2007a). We are now interested to compare these data to *At*HOP2 (Peptide *At*HOP2 antibodies are generated and under test now) localisation during meiosis of wild-type plants as well as in various mutant backgrounds: *Atmnd1, Atdmc1*, *Atrad51*, *Atspo11* mutant alleles.

We will also investigate the temporal and spatial distribution of *At*MND1 in the new *Athop2/ahp2* mutant alleles. Three *Athop2* alleles are available so far: *ahp2* described by Schommer et al. (Schommer et al., 2003) in which strong meiotic DNA fragmentation was observed and recently two novel mutant alleles of the *Arabidopsis AHP2/AtHOP2* gene have been isolated (unpublished results), that differ from the already characterized *ahp2* allele (Schommer et al., 2003). The new lines EXI5 and EYU48, showing IS DSB repair. We aim at understanding the epistatic relation of the *ahp2* allele and the two new *Athop2/ahp2* mutant alleles to afore mentioned IH factors. To this end we will generate a battery of double mutants between each of the three available *Athop2/ahp2* and *Atdmc1*, *Atrad51*, *Atmnd1*, *Atxrcc3.*

Furthermore, we want to characterization of new *Athop2/ahp2* mutant alleles. The molecular details of the three available *Athop2/ahp2* mutant alleles will be investigated by Southern blot analysis and T-DNA border sequencing. Each *Athop2* allele will carefully be examined for residual expression, for potentially truncated mRNA versions by quantitative RT-PCR to detect different parts of the mRNA and for potentially truncated residual *At*HOP2/AHP2 protein (using the anti-*At*HOP2 antibodies). From these results, the *Athop2/ahp2* phenotypic differences will be correlated either to a difference in *At*HOP2 protein level or to the production of truncated versions of

*At*HOP2 protein. If the latter case turns out to be the base for the observed IS bias in the new lines EXI5 and EYU48, this information will be important for gaining insights into the function of HOP2 in meiotic recombination.

8. Introduction *AtCOM1*

After induction of programmed meiotic DSBs by the Spo11 protein, the DNA ends undergo 5'-3' nucleolytic processing to give rise to single-stranded DNA, which is the substrate for RecA proteins to initiate homologous recombination. This process is poorly understood in eukaryotes, but several factors have been implicated, including the Mre11 complex (Mre11-Rad50-Xrs2/NBS1) and Com1/Sae2/CtIP/Ctp1. Mutants lacking these proteins are sensitive to DNA-damaging agents and defective in strand resection of DSB ends during mitosis (Baroni et al., 2004; Clerici et al., 2005; McKee and Kleckner, 1997). Thus, Mre11, Rad50, Xrs2, and Sae2/Com1 are implicated in DSB end-processing mechanisms during mitotic cell cycles as well as meiosis.

Mre11, Rad50, and Xrs2 form a protein complex called the MRX complex (D'Amours and Jackson, 2002). Mre11 was originally identified in a screen for genes essential for meiosis in *S. cerevisiae* (Ajimura et al., 1993). The Mre11 protein has endonuclease and 3'-5' single-stranded and double-stranded exonuclease activity *in vitro* (Assenmacher and Hopfner, 2004). Furthermore the nuclease domain contains four conserved N-terminal phosphoesterase motifs (Borde, 2007). Mre11 also contains two DNA-binding domains, one conserved in the centre of the protein and one less conserved in the C-terminus (Usui et al., 1998). The Rad50 protein is a ATPase which contains two heptad repeats, N- and C-terminal Walker A and Walker B motifs carrying the ATPase activity and a central region forming a zinc hook, that facilates the interaction between RAD50 molecules (de Jager et al., 2001; Hopfner et al., 2000). Walker A and Walker B motifs can also interact with two Mre11 monomers, forming a globular domain that is able to interact with DNA (de Jager et al., 2001). ATP as well as Rad50 can stimulate the 3'-5' exonuclease and hairpin-opening activities of Mre11 (Hopfner et al., 2002). Moreover, Mre11 helps to remove Spo11 which is covalently bound to the break site by endonucleolytic cleavage a few bases away from the site of attachment. This leads to the release of a Spo11-oligonucleotide complex (Neale et al., 2005).

Rad50 was recently reported to have adenylate kinase activity, which is required for the efficient tethering of DNA molecules (Bhaskara et al., 2007). Both Mre11 and Rad50 are conserved among eukaryotes.

However, compared to Mre11 and Rad50 the conservation of the Xrs2/NBS1 amino acid sequence is quite low and only limited regions or short sequence motifs are conserved. Xrs2/NBS1 has a N-terminal forkhead-associated (FHA) domain, which is

involved in protein-protein interaction and binds phosphorylated histone H2AX (Kobayashi et al., 2002), a conserved C-terminal region which is involved in interaction with Mre11 (Kobayashi et al., 2004) and phosphorylation sites for the checkpoint kinase Atm. Furthermore, Xrs2/NBS1 proteins enhance the nuclease activity of Mre11 *in vitro* (Paull and Gellert, 1999). In *S. cerevisiae* it was shown that the interaction of Xrs2 with Mre11 is crucial for the translocation of Mre11 to the nucleus and therefore for the function of the Mre11 complex (Tsukamoto et al., 2005).

Yeast's Com1/Sae2 was detected independently in three genetic screens. Two screens were designed to isolate meiotic mutants, defective after the initiation of Spo11-induced DSBs, but before resolution of recombination intermediates (McKee and Kleckner, 1997; Prinz et al., 1997). The phenotypes of the isolated *com1/sae2*-null mutations are similar to those conferred by the previously identified non-null mutations of *RAD50* (*rad50S*) and *MRE11* (*mre11S*) (Alani et al., 1990; Keeney et al., 1997; Nairz and Klein, 1997; Tsubouchi and Ogawa, 1998).

Turnover and resection of DSBs are completely blocked in these mutations. The third screen aimed for the identification of mutants with low fidelity DSB repair during vegetative growth (Rattray et al., 2001). Together with the MRN complex Com1/Sae2 is essential to prevent chromosomal rearrangements, the repair of hairpin-capped DSBs and for the juxtapostioning of DNA ends after DSB formation in mitotic cells (Clerici et al., 2005; Lobachev et al., 2002). This finding may explain the resistance of Com1/Sae2 to genotoxic treatments (Birrell et al., 2002; Deng et al., 2005).

Moreover, it was shown that Com1/Sae2 gets phosphorylated by Mec1 and Tel1 protein kinases (ATR and ATM orthologues in yeast) and that it interferes with the DNA replication and DNA damage checkpoints during mitosis and meiosis (Baroni et al., 2004; Cartagena-Lirola et al., 2006; Clerici et al., 2006). Also the human homologue of Com1/Sae2, CtIP, gets phosphorylated at special serine residues in an ATM-dependent manner in response to gamma radiation. Furthermore phosphorylation of CtIP is important for its interaction with the breast cancer susceptibility gene BRCA1 (Li et al., 2000; Yu et al., 2006). Interestingly, CtIP-/- mice die much earlier in development than mice nullizygous for its known interacting partners, like Brac1 and Rb. (Chen et al., 2005; Fusco et al., 1998; Yu et al., 1998). This fact may indicate that CtIP has an essential function that does not involve its known interacting partners. Interestingly, hemizygous CtIP+/- mice are viable, but their life span is shortened by the development of multiple types of tumors, particularly large lymphomas (Chen et al., 2005). Perhaps

these phenotypes arise because CtIP is required for HR repair of DSBs. This possibility is consistent with studies showing that the homozygous disruption of MRN subunits in mice results in early embryonic lethality (D'Amours and Jackson, 2002). Furthermore, increased tumorigenesis is observed in mice having a hypomorphic mutation of RAD50 or a hemizygous NBS1+/- genotype (Bender et al., 2002; Dumon-Jones et al., 2003). If CtIP is required for HR repair of DSBs, these data suggest a mechanism for regulating DSB repair during the cell cycle in human cells.

By sequence analysis it has been found that the homologues of Com1/Sae2 show a conserved C-terminal domain (Limbo et al., 2007; Penkner et al., 2007; Uanschou et al., 2007). The core of homology is centred around ~70 amino acid which include a CxxC and RHR motif (Figure 40). The CxxC motif is potentially involved in zinc chelation. The N-terminal region of Com1/Sae2 possesses coiled-coil motifs (Figure 38), which are thought to mediate homodimerization (Dubin et al., 2004). In plants, the coiled-coil domain is followed by an amino acid rich PEST sequence, that may promote rapid turnover (Rechsteiner and Rogers, 1996). The C-terminal region is much conserved among eukaryotes, although is has unknown function (Limbo et al., 2007).

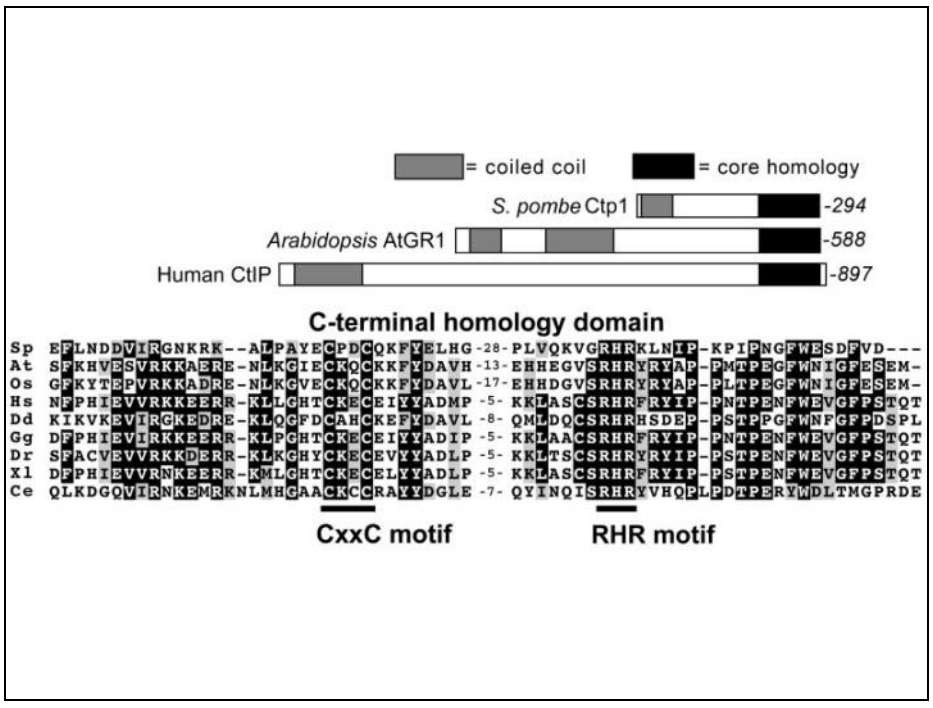

Figure 40: Domain structures of Com1/Sae2. The domain structures of *S. pombe* Ctp1, *A.. thaliana* *At*GR1 which corresponds to *At*COM1 and *H. sapiens* CtIP. Alignments of the C-terminal core homology domains of *S. pombe* Ctp1 (Sp) and its homologs in *A. thaliana*, At (4e-21); *Oryza sativa*, Os (4e-19); *H. sapiens*, Hs (5e-17); *Dictyostelium discoideum*, Dd (9e-15); *Gallus gallus*, Gg (1e-17); *Danio rerio*, Dr (6e-16); *Xenopus laevis,* Xl (3e-16); and *Caenorhabditis elegans*, Ce (6e-10). The PSI-BLAST Expect values are shown in parentheses. Taken from Limbo et al., 2007.

8.1. Identification of *Com1/Sae2* homologue in *A. thaliana*

The homologue of yeast *Com1/Sae2* in *A. thaliana* was found by a PSI-BLAST and reciprocal proteome BLAST search (with low-complexity filtering, E-value cut-off 0.001, (Altschul et al., 1997)) by Uanschou et al. (2007).

The reciprocal PSI-BLAST searches (against the NCBI non-redundant database (nr), version 12/2006; low-complexity filtered, inclusion cut-off 0.001) (Altschul et al., 1997; Marchler-Bauer et al., 2002) yield a coherent set of related sequences in a wide variety of eukaryotes including the *Arabidopsis* NP_850683 (At3g52115) and the metazoan CtIP protein (*Homo sapiens* CtIP, (Fusco et al., 1998), shown in Figure 38 aligned by their common C-terminal homology). The *Arabidopsis* and the *human* proteins share 54% identity and 45% similarity in their conserved C-termini. Arabidopsis At3g52115 is upregulated after ionising irradiation and was called *At*GR1 (*A. thaliana* gamma response gene 1, (Deveaux et al., 2000). The ATM kinase is required (Garcia et al., 2003) for transcriptional induction of *At*GR1. Because of the homology to *Com1/Sae2* *At*GR1 was suggested to be called *At*COM1 (Uanschou et al., 2007).

8.2. *Atcom1* mutant plants are sterile

Homozygous plants for the *Atcom1* mutant alleles (*Atcom1-1*, *Atcom1-2*) germinate and develop indistinguishable from wild type plants. Rosette leaves are of normal size, shape and number, and bolting is not delayed. Inflorescences look normal, but the siliques of *Atcom1* mutant plants are completely devoid of seeds (Figure 41A). This observed phenotypes can be completely reversed by introduction of a genomic wild-type copy of the gene (Figure 41A) (Uanschou et al., 2007). To further characterise the fertility defect, male gametophyte development was monitored. *Atcom1-1* mutant plants anthers do not contain viable pollen (Figure 41A) (Uanschou et al., 2007). This conclusion is supported by the fact that *Atcom1-1* plants (n=8 buds) could not fertilise wild type pistils. (Experiment done by Clemens Uanschou).

Figure 41: Phenotypes of the *Atcom1-1* mutant. (A) *Atcom1-1* mutants look like wild-type plants, but do not develop mature siliques. The left panel shows a stem with mature siliques of a wild-type (wt) plant. The middle panel shows the stem of an *Atcom1-1* mutant plant of the same age, which failed to develop mature siliques. The right panel shows an *Atcom1-1* mutant plant containing a fertility restoring genomic copy of *At*COM1. Inlays: anthers of wild-type (wt) and *Atcom1-1* plants stained as described (Alexander, 1969). The purple-stained cytoplasm indicates viable pollen grains; green indicates empty pollen. Regular-sized and viable purple pollen is absent in *Atcom1-1* anthers. (Taken from Uanschou et al.,2007, experiment performed by Clemens Uanschou).

9. Results *AtCOM1*

9.1. Male and female meiosis is severely disrupted in *Atcom1-1* mutant plants

Female gametogenesis was severely impaired in *Atcom1-1* mutant plants. In wild-type plants three out of four haploid spores degenerate immediately after meiosis. The one remaining spore is called functional megaspore mother cell. The megaspore mother cell undergoes three mitotic divisions to give rise to an eight cell stage embryosac. It consists of three antipodal cells, two synergids, one egg cell and two haploid nuclei, which fuse to become the central cell (Figure 42A). In *Atcom1*-1 mutant gametophytes only degenerated nuclei could be observed (Figure 42A). Moreover, already meiosis of the megaspore mother cell is disrupted. Whereas in wild-type ovules two sets of five chromosomes each could be seen in a telophase I stage (Figure 42B), *Atcom1-1* mutants showed fragmented chromosomes and chromatin bridges in telophase I-like stage (Figure 42B).

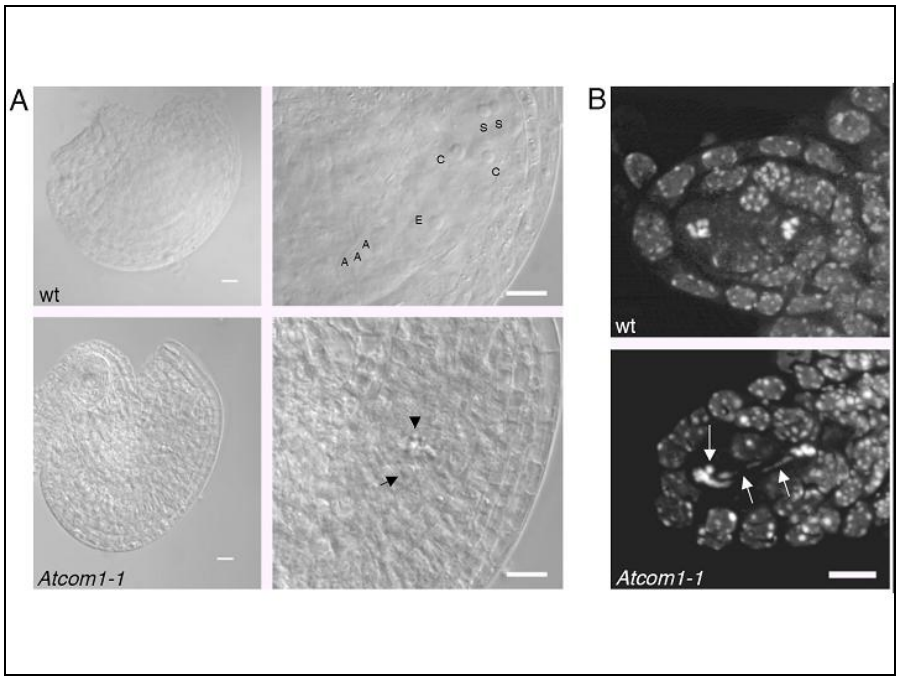

Figure 42: *Atcom1-1* plants produce degenerated embryos. (A) The wild-type (wt) ovule contains an eight cell-stage embryo sac with two synergid cells (S), the egg cell (E), two cells that will give rise to the central cell (C) and three antipodal cells (A). An *Atcom1-1* ovule of the same age contains a degenerated embryo sac with only one cell (arrow) and some irregular structures (arrow head). Scale bar, 10µm. (B) Meiosis in megaspore mother cells of *Atcom1-1* mutant plants is severely disrupted. Shown are confocal microscopy images of telophase I stages of wild-type (wt) and *Atcom1-1*. Arrows indicate DNA bridges and fragments observed in *Atcom1-1* mutants. Chromosomes were stained with propidium iodide. Scale bar, 5µm. (Taken from Uanschou et al.,2007; experiment done by Tanja Siwiec)

Male meiosis showed almost the same defects as observed during female meiosis. Cytological analysis by chromosome spreading technique and FISH failed to detect any synapsed homologous chromosome in the *Atcom1-1* mutant plant. To identify homologous chromosomes an interstitial FISH probe for chromosome I and a subtelomeric FISH probe for chromosome II were used.

In contrast, to wild-type zygotene and pachytene (Figure 43B, C) no close pairing of homologue chromosomes was observed in zygotene-like stage (Figure 43M, N) in the mutant nuclei. This leads to the assumption that *Atcom1-1* mutant is unable to form a stable interaction between homologue chromosomes.

Emerging from condensation during diakinesis (Figure 43E) five bivalents could be seen in metaphase I stage in wild-type. From diakinesis-like (Figure 43O) to metaphase I-like stage (Figure 43P) in *Atcom1-1* mutants chromosomes were always connected and entangled. In anaphase I DNA fragments, typically telomeric fragments are left behind at the metaphase plate in *Atcom1-1* plants (Figure 43Q–S), suggesting that meiotic DSBs remain un-repaired in the mutant. Furthermore, DNA bridges connecting two centromeres (Figure 43R), which segregate to different poles were seen. FISH analysis using a probe directed to the 180 bp repeat region of centromeres showed that some of the bridges observed in *Atcom1-1* mutants consist of centromeric DNA, indicating that bridges could either originate from separation of sister chromatids, persisting DNA catenation or from a non-homologous repair mechanism. DNA fragments and bridges were never observed in wild-type cells during anaphase or telophase I (Figure 43G, H).

In addition to fragmentation, massive chromosome missegregation might be caused by the often asymmetric distribution of nuclear material in the first meiotic division in *Atcom1-1* cells. At anaphase II figures a high incidence of fragmentation and missegregation, usually culminating in the formation of more than four, poorly condensed, unequal masses of chromatin at telophase II (Figure 43U). We conclude that the sterility of *Atcom1-1* mutants is caused by aberrant meiosis and defective repair of meiotic DSBs.

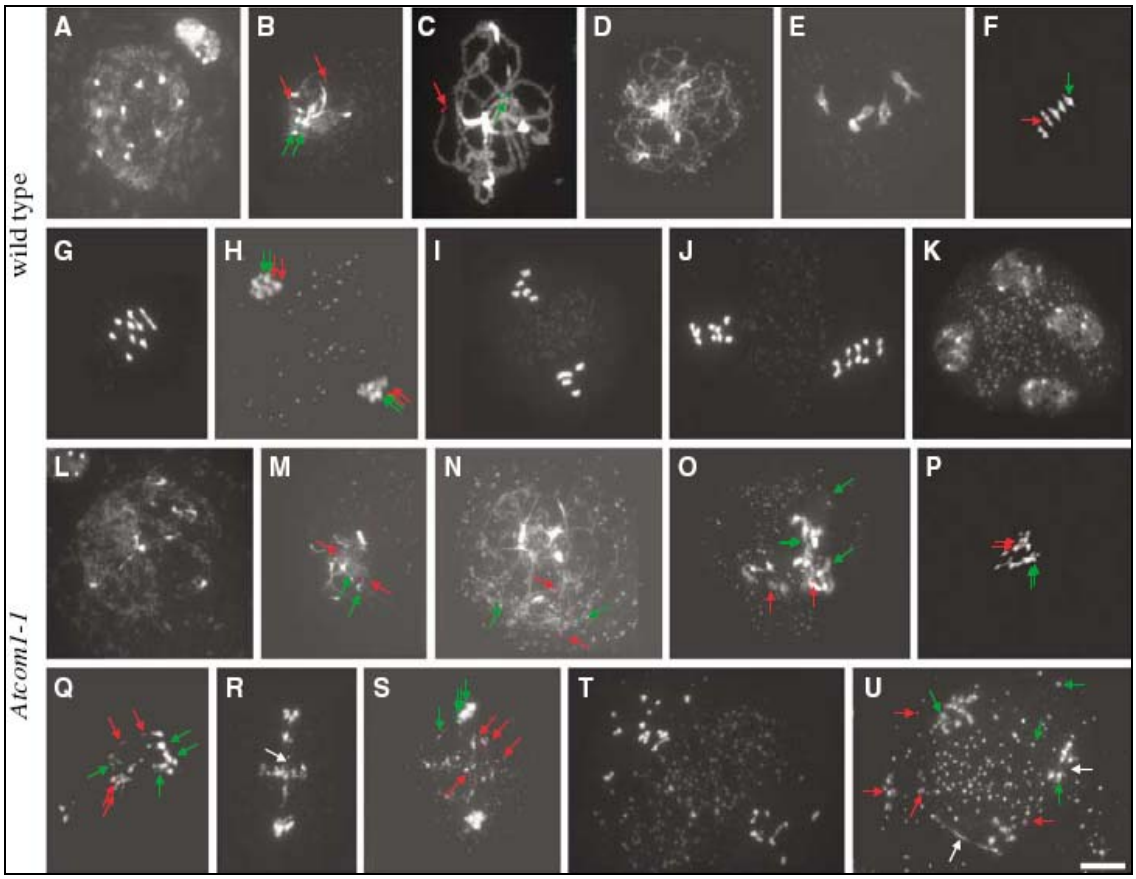

Figure 43: Male meiosis in wild-type (A–K) and Atcom1-1 mutant (L–U) plants. Wild-type: (A) leptotene; (B) zygotene; (C) pachytene; (D) diplotene; (E) diakinesis; (F) metaphase I; (G) anaphase I; (H) prophase II; (I) metaphase II; (J) anaphase II; (K) telophase II. Meiosis is severely disrupted in the *Atcom1-1* mutant plants: (L) leptotene; (M) zygotene-like stage; (N) pachytene-like stage, without normal chromosome pairing; (O) diakinesis-like stage; (P) metaphase I-like stage with entangled chromosomes; (Q, R) progression of anaphase I with fragmentation of chromosomes; (S) prophase II-like stage; (T) anaphase II-like stage; (U) telophase II-like stage. Green and red arrows highlight FISH signals corresponding to an arm region of chromosome I (BAC F1N21, green) and a subtelomeric region of chromosome II (BAC F11L15, red), respectively (panels B, C, H, M–Q, S and U). White arrows indicate chromosome bridges seen during *Atcom1-1* meiosis (R, U). Meiotic progression in pollen mother cells was followed after chromosomes were stained with DAPI. Scale bar 10µm. (Taken from Uanschou et al.,2007; wild type analysis performed by Tanja Siwiec, *Atcom1-1* analysis was performed by Andrea Pedrosa-Harand.)

9.2. Chromosome fragmentation observed in *Atcom1-1* mutants depends on SPO11-1 but not on the RecA-related DMC1 protein

Based on the assumption that the observed chromosome fragments as well as the chromatin bridges were caused by the inability of *Atcom1-1* mutant to repair meiotic DSBs, the *Atspo11-1-1/Atcom1-1* double mutant was analysed. Moreover, one has to state that the *Atspo11-1-1* mutation does not completely eliminate DSBs, either due to residual activity or due to its paralogs AtSPO11-2 (Stacey et al., 2006) or due to DSBs from the premeiotic S-phase. As we generated the homozygous *Atcom1-1/Atspo11-1-1*

double mutant, DNA fragmentation was suppressed in most cells (Figure 44), demonstrating that the inability to repair meiotic DSBs is responsible for *Atcom1-1* chromosome aberrations.

Cells repair meiotic DSBs by using the homologue rather than the sister chromatid as a template, a phenomenon called interhomologue bias (Zickler and Kleckner, 1998, 1999). We, therefore, asked whether relaxing interhomologue bias might permit repair in *Atcom1-1* meiocytes. DMC1, a meiosis-specific RecA recombinase, is specifically required for interhomologue interactions (Schwacha and Kleckner, 1997) and *Atdmc1* mutants are thought to repair all DSBs by using the sister chromatid as a template (Couteau et al., 1999). However, chromosome fragmentation persists in the *Atcom1-1/Atdmc1* double mutant meiosis (Figure 44), suggesting that *Atcom1-1* affects both intersister and interhomologue recombination alike. This result is expected, if *At*COM1 is not specific to the interhomologue repair pathway, but obligatory for meiotic repair as Com1/Sae2 is in yeast.

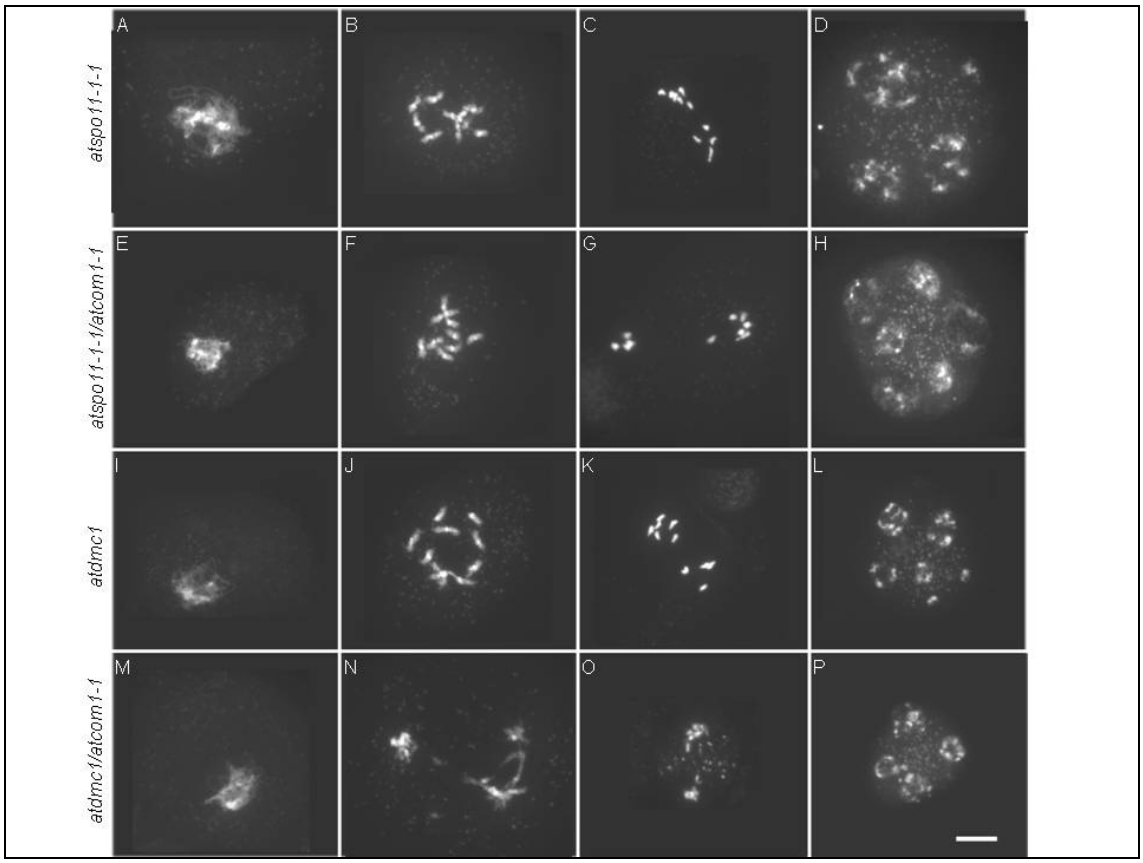

Figure 44: *At*COM1 acts downstream of *At*SPO11-1 and upstream of *At*DMC1. Comparison of meiotic progression in the *Atspo11-1-1* mutant (upper panel) and in the *Atcom1-1/Atspo11-1-1* double mutant (second panel from top). In both, zygotene-like stages(A, E) are followed by progressive condensation and formation of univalents (B, F), which subsequently segregate at random (C, G), forming polyads at the end of meiosis II (D, H). Comparison of meiotic progression in the *Atdmc1 mutant* (third panel from top) and in the *Atcom1-1/Atdmc1* double mutant (lowest panel). Whereas *Atdmc1* mutants form univalents (J), which segregate at random (K) to give rise to polyads at the end of meiosis II (L), the *Atcom1-1/Atdmc1* double mutant resembles *Atcom1-1*, displaying fragmented chromosomes (N). Chromosomes are stained with DAPI. Scale bar: 10 µm. (Taken from Uanschou et al.,2007;analysis of the *Atcom1-1/Atdmc1* double mutant was performed by Clemens Uanschou, analysis of *Atdmc1*, *Atspo11-1-1* and *Atspo11-1-1/Atcom1-1* was done by Tanja Siwiec).

9.3. *At*COM1 is essential for regular turnover of *At*SPO11-1 and normal processing of DSBs

For the processing of DSBs 3'single stranded ends are coated by the recombinase *At*RAD51 for subsequent strand invasion and D-loop formation (Li et al., 2004; Shinohara and Shinohara, 2004). We wanted to know if the observed fragmentation in the *Atcom1-1* mutant was due to failed loading of *At*RAD51 and therefore persistent DSBs. Filament formation was cytologically observed by indirect immunofluorescence staining with anti-*At*RAD51 antibody on wild-type and mutant meiocytes (Figure 45A). While in wild-type a high number of foci appeared transiently in prophase I nuclei, only very few foci, comparable to those found in *Atspo11-1-1* (Figure 45B) and *Atmre11-3* (Figure 45D) are seen in *Atcom1-1* (Figure 45C) cells. One interpretation of this result could be that meiotic DSBs were reduced or absent. We therefore performed immunolocalization analysis for γH2AX (done by Sanchez- Moran), a phospho form of a histone H2A variant representing a specific, local and fast response to DSBs (Fernandez-Capetillo et al., 2004; Friesner et al., 2005) (Figure 46). This control confirmed the presence of high levels of DSBs in *Atcom1-1* cells (Figure 46B), similar to the staining observed in early stages in wild-type meiocytes (Figure 46A). Thus, we inferred that *Atcom1-1* mutants generate DSBs, but did not form *At*RAD51 filaments.

A critical early step in repair is the removal of Spo11, which is covalently attached to some nucleotides (at least in yeast), a step known to depend on Rad50 (Alani et al., 1990), Mre11 (Nairz and Klein, 1997; Tsubouchi and Ogawa, 1998) and Com1/Sae2 (McKee and Kleckner, 1997; Prinz et al., 1997) in *S. cerevisiae*. In such a situation, Spo11 foci were shown to accumulate in mutant nuclei by visualising an epitope-tagged Spo11 (Prieler et al., 2005). We tried to address this question in *A. thaliana* using an *At*SPO11-1-specific antibody (Sanchez-Moran et al., 2007). While *At*SPO11-1 was virtually undetectable in meiocytes of wild-type cells (99.7% of prophase I cells show no *At*SPO11-1 foci, n=440; Figure 47A), the same antibody detected *At*SPO11-1 in 98% of *Atcom1-1* meiocytes (n=50; Figure 47B), some of which showed striking *At*SPO11-1 hyper-accumulation (30/50 cell showed very intensive staining, 19/50 showed staining with lower intensity). Interestingly, we found a similar hyper-accumulation of *At*SPO11-1 in meiocytes of *Atmre11-3* and *Atrad50* mutants (Figure 47C and D). We summarise that the available evidence places the defect of *Atcom1-1* upstream of *At*RAD51 filament formation and that it suggests a problem with *At*SPO11-1 removal.

Thus, our study suggests that yeast Com1/Sae2 and *Arabidopsis At*COM1 are required for equivalent mechanisms during meiotic DSB repair.

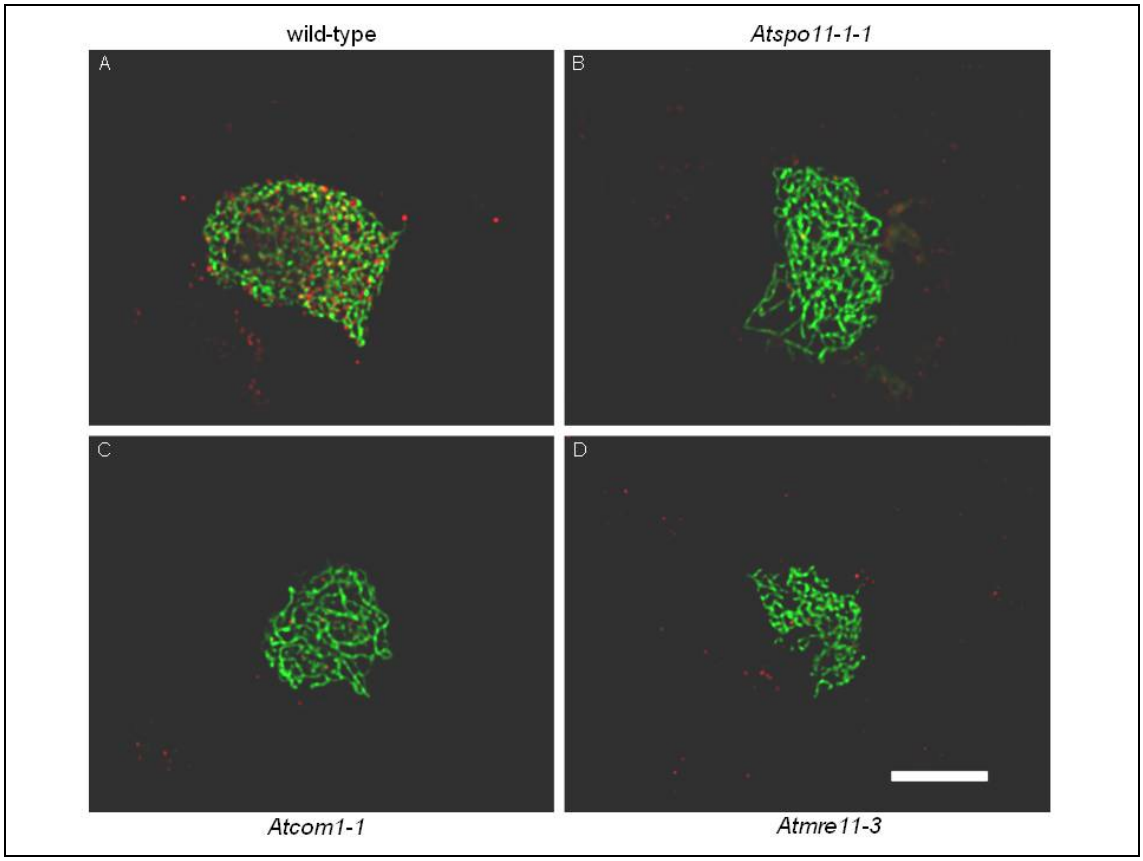

Figure 45: *Atcom1-1* cells fail to form *At*RAD51 foci, but accumulate *At*SPO11-1. *Atcom1-1* cells fail to form *At*RAD51 foci. Immunofluorescent staining of spreads of meiotic cells with antibodies directed against the axial element protein ASY1 (green) and against *At*RAD51 (red). Whereas in wild-type (A) numerous *At*RAD51 foci are observed in zygotene, representing loci of meiotic DNA repair and recombination, only very few foci are seen in *Atspo11-1-1* (B), *Atcom1-1* (C) and *Atmre11-3* (D) mutants. Scale bar: 5 µm. (Taken from Uanschou et al.,2007; experiment done by Tanja Siwiec).

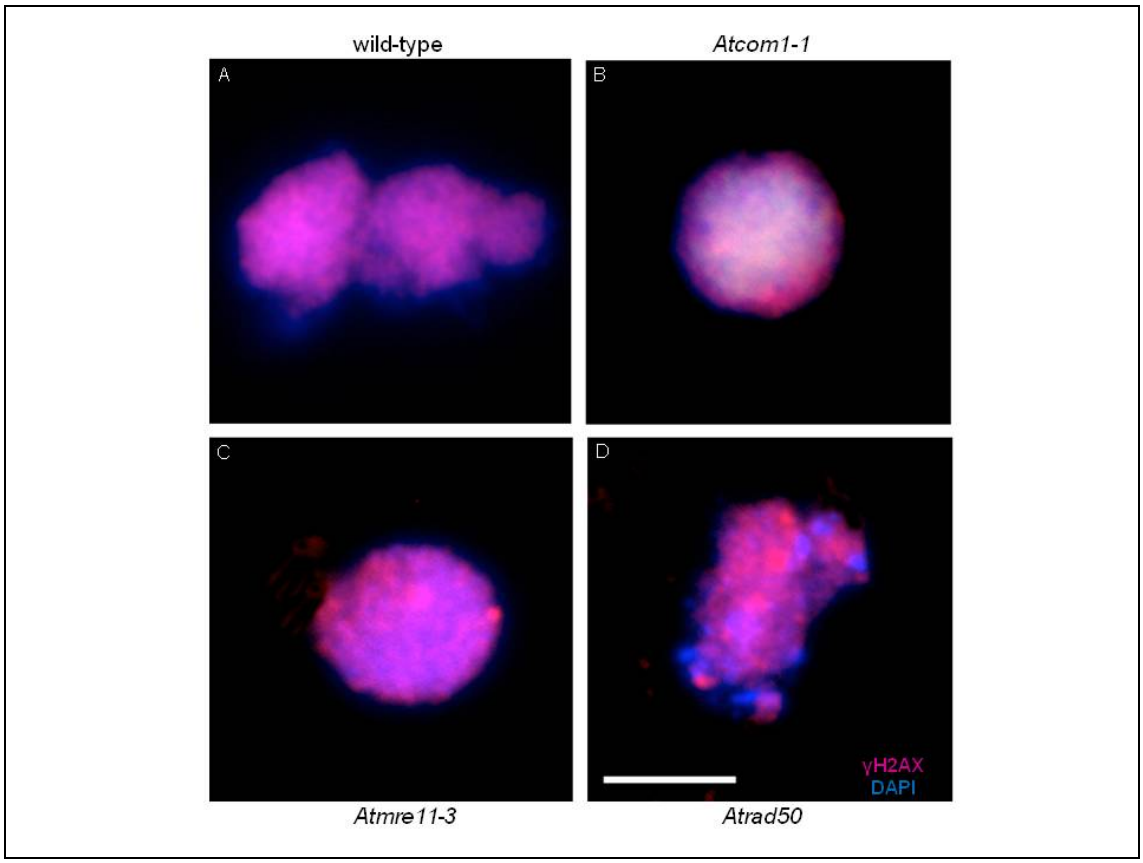

Figure 46: DSBs are generated in *Atcom1-1, Atmre11-3* and *Atrad50* meiocytes, as in wild-type cells indicated by immunofluorescent staining with an antibody directed against γH2AX. Numerous diffuse γH2AX foci (red) accumulated at early stages of prophase I. DNA was counterstained with DAPI (blue). Scale bar 10μm. (Taken from Uanschou et al.,2007; experiment performed by E. Sanchez-Moran.).

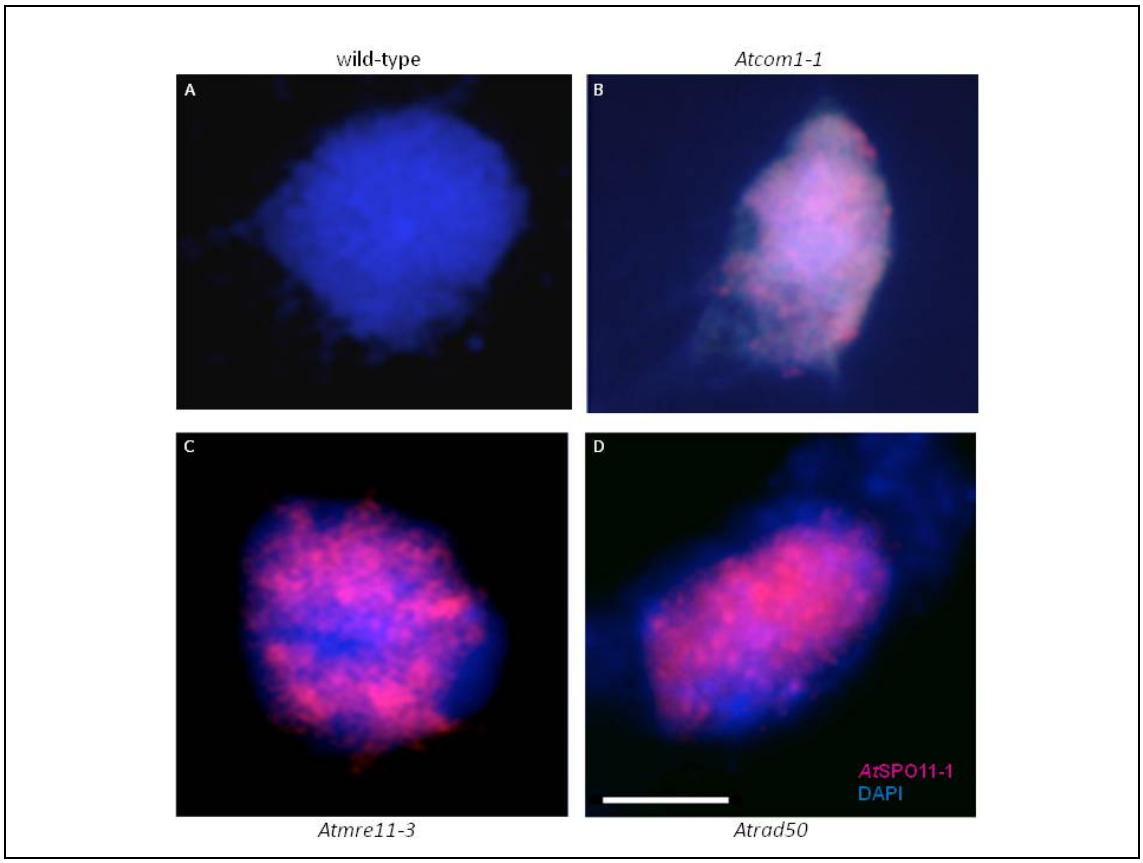

Figure 47: *At*SPO11-1 is enriched in prophase I of *Atcom1-1*(B), *Atmre11-3*(C) and *Atrad50* (D) mutant meiosis, demonstrating that in the latter two mutants DSB processing is similarly impaired as in *Atcom1-1*. Images represent immunofluorescent staining of spreads of cells in prophase I stages of mutant meiocytes with an antibody directed against AtSPO11-1 (red). DNA was counterstained with DAPI (blue) Scale bar: 10 µm. (Taken from Uanschou et al.,2007; experiment performed by E. Sanchez-Moran.)

9.4. *At*COM1 localizes to chromatin during prophase I

To understand the role *At*COM1 has during the meiotic progression we investigated the distribution of the *At*COM1 protein during meiosis by immunolocalization studies in wild-type meiocytes, using a e antibody against *At*COM1. Antibody generation is outlined elsewhere (Uanschou et al., 2007). ASY1 was used as a marker for meiotic progression. The specificity of the *At*COM1 antibody was demonstrated by comparing wild-type and *Atcom1-1* mutant plants in immunolocalization experiments (Figure 48).

*At*COM1 was first detected in early leptotene stage as numerous distinct foci along the entire length of the chromosome in synapsed and unsynapsed chromosome regions (figure 48A). As meiosis progressed and the ASY1 signal was observed as long stretches corresponding to the axial elements, the number of *At*COM1 foci decreased. This suggests that, as DSBs become repaired *At*COM1 is not longer attached to the chromatin. The signal observed in wild type plants was absent in *Atcom1-1* mutants plants confirming the specificity of the antibody.

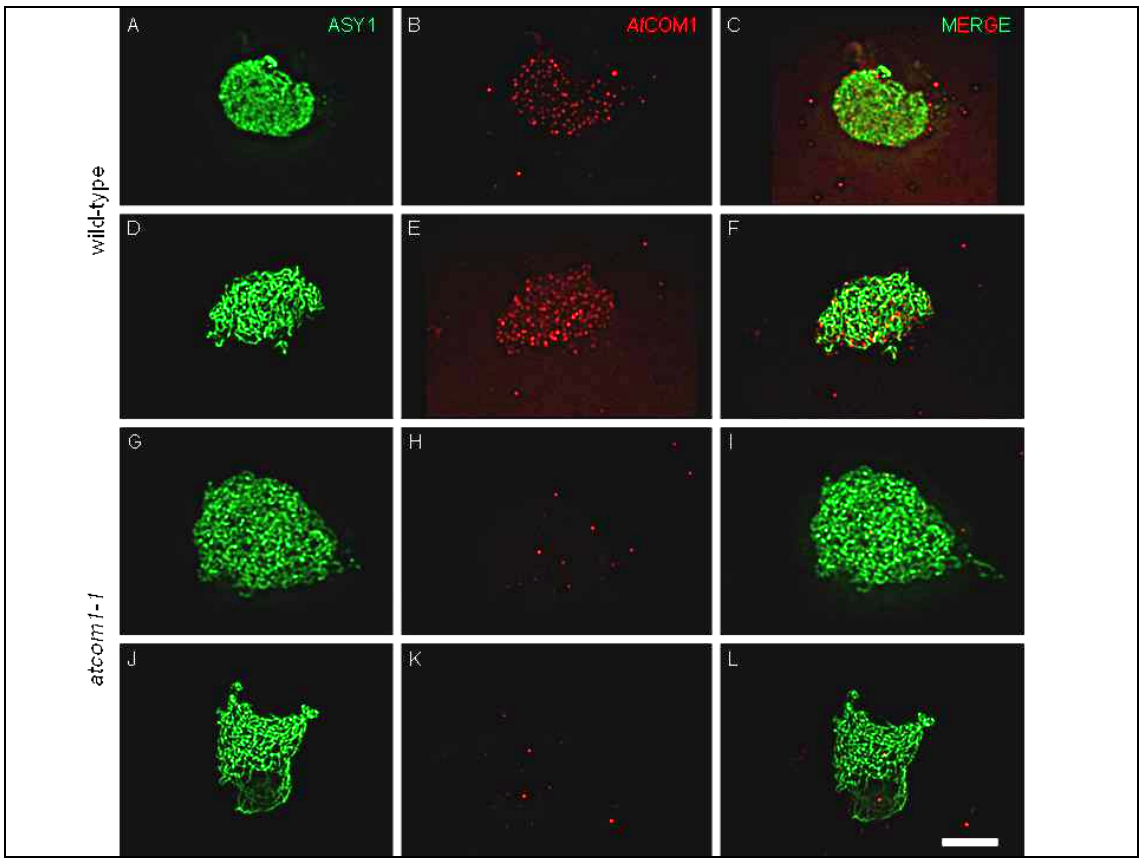

Figure 48: Localization of *At*COM1 in wild-type meiocytes (A-F) and *Atcom1-1* mutant (G-H). (A-C) and (G-I) represent leptotene stage, where in wild-type *At*COM1 foci formation can be observed, which is missing in the atcom1-1 mutant. (D-F) and (J-L) represent zygotene stage. Scale bar 5µm. (Experiment done by Tanja Siwiec)

9.5. The distribution of *At*COM1 depends on the initiation of recombination as well as on the MRN complex

To get insight in the mutual dependencies of *At*COM1 we analyzed the distribution of *At*COM1 in several meiotic mutants. We investigated *At*COM1 loading in mutants with disrupted meiotic recombination (*Atspo11-1-2*), DSB processing (*Atmre11-3*, *Atrad50*) and nucleoprotein filament formation (*Atrad51*). *At*COM1 was absent in the *Atspo1-1-2* mutant as well as in *Atmre11-3* and *Atrad50* mutant (Figure49). These results indicate that DSB formations as well as the processing of the DSB are required for the loading of *At*COM1 protein. Only in the *Atrad51* mutant, as expected, no aberration of *At*COM1 localization was observed compared to wild-type nuclei (Figure49).

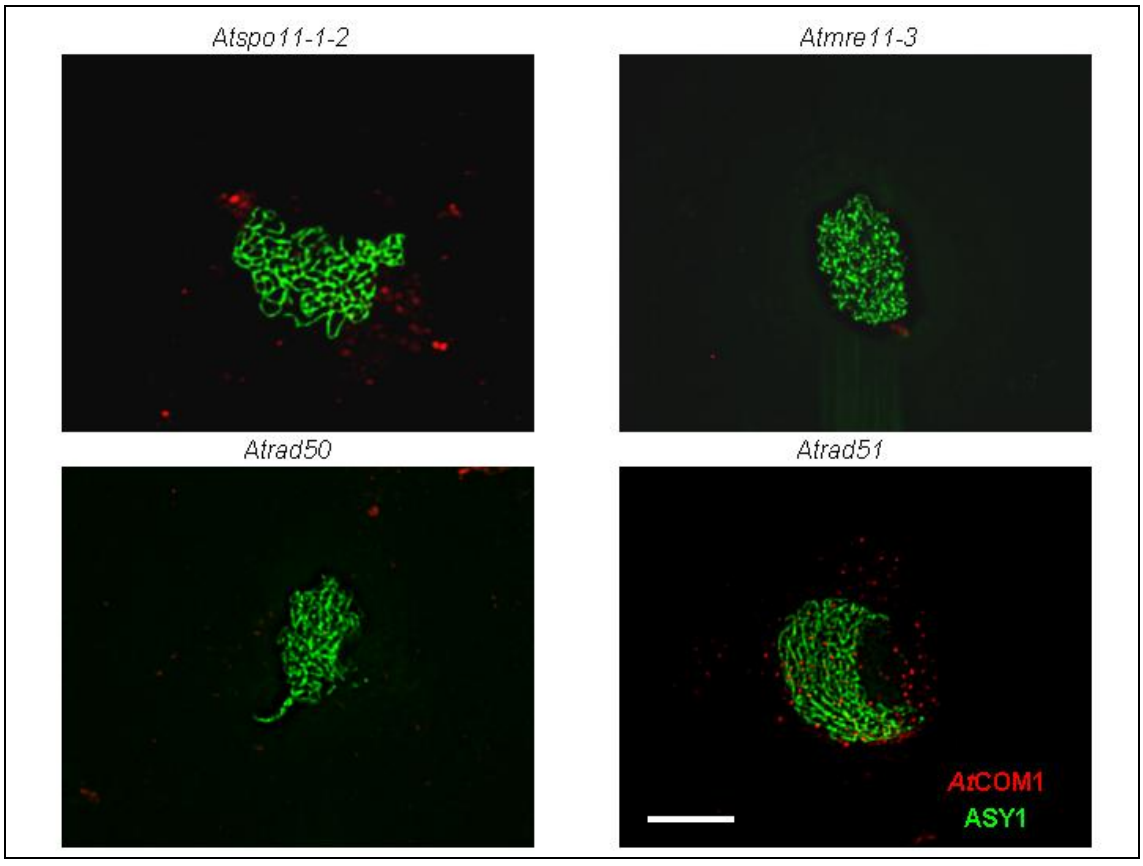

Figure 49: AtCOM1 is absent on meiotic chromosomes of *Atspo11-1-2*, *Atmre11-3* and *Atrad50* mutants. In the *Atrad51* mutant AtCOM1 localization is indistinguishable from wild type nuclei.

9.6. *AtCOM1* and its putative interaction partners

To find putative interaction partners of *At*COM1 we performed an direct yeast two hybrid assay. We used yeast two hybrid plasmids with or without HA- and myc-tag, respectively. Furthermore we cloned the different cDNAs into vectors with activation domain or binding domain. The plasmids encoding DNA binding domain and activator domain fusion proteins were transformed into yeast strain YM706 and PJ69-4A, respectively and afterwards mated. Control experiments were performed by transforming YM706 and PJ69-4A with combinations of fusion protein containing vectors and empty vectors. The used cDNAs were *AtMRE11* (kindly provided by Christopher West), *AtRAD50*, *AtNBS1* (kindly provided by Christopher West), *AtBRCA1*, *AtCOM1*, *AtBRCA2IV* (kindly provided by Marie-Pascal Doutriaux) and *AtBRCA2V* (kindly provided by Marie-Pascal Doutriaux).

After transformation of the two different yeast strains, putative interaction partners in different combinations were mated for 24 hours on full media, and afterwards plated on selective media, lacking the amino acids leucine, histidin and tryptophane and containing 2mM 3-amino-triazol. Reliable interactions could be found between *At*NBS1 and *At*MRE11, as well as between *At*RAD50 and *At*MRE11, also a homodimerization of *At*MRE11 was observable (Figure 50). The mentioned interactions have been previously reported for fission yeast proteins (Limbo et al., 2007). Furthermore an interaction between *At*MRE11 and *At*BRCA2V could be detected. The *Arabidopsis* orthologues of Brca2, a protein whose mutations are involved in breast cancer in humans, were previously shown to be essential at meiosis (Dray et al., 2006). There are two isoforms of Brca2 *At*BRCA2IV and *At*BRCA2V which were shown to be able to interact with *At*DMC1 as well as with *At*RAD51 in vitro (Dray et al., 2006). Moreover, we observed also an interaction of *At*NBS1 with *At*BRCA1 and *At*BRCA2IV, respectively. *At*BRCA2IV was found to interact with *At*BRCA1 and *At*BRCA2V, whereas also a homodimerization of *At*BRCA2V could be detected. Most interestingly and aim of the experiment we found homodimerization of *At*COM1, which was previously reported for fission yeast Ctp1 (Limbo et al., 2007) and also for human CtIP (Dubin et al., 2004). For the first time we demonstrated an interaction of *At*COM1 with *At*NBS1 and stunningly a reliable interaction of *At*COM1 with *At*BRAC2IV and *At*BRCA2V. The interaction of *At*COM1 with *At*BRAC2IV and *At*BRCA2V could be also confirmed on more selective media lacking the amino acids leucine, tryptophane

and adenine. From these results we conclude that *At*COM1 might interact with the MRN complex, through interaction with *At*NBS1. Furthermore the nature of the interaction of *At*COM1 with the two isoforms of *At*BRCA2 has to be elucidated through immunolocalization studies with the *At*COM1 antibody in corresponding mutant background or by yeast two hybrid interaction studies with truncated forms of either *At*COM1 or *At*BRCA2IV and *At*BRCA2V.

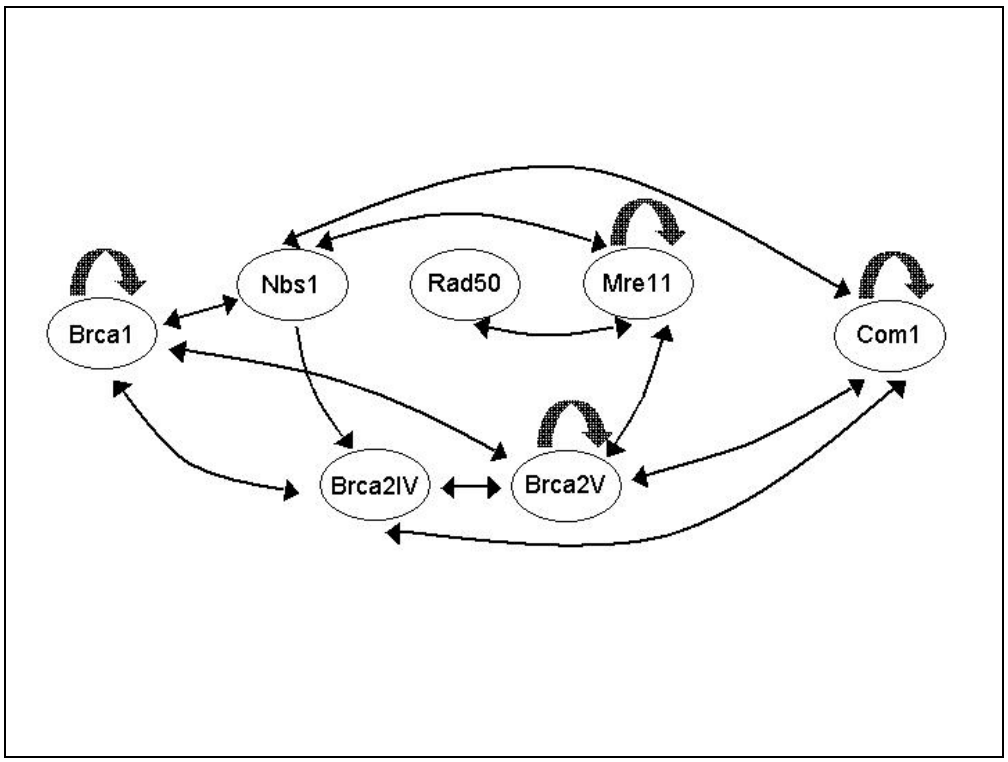

Figure 50: Interaction of AtCOM1 with various proteins of the meiotic repair machinery. Small arrows represent interaction of the respective protein, thick arrows represent self-interactions. For explanation see text.

10. Discussion *AtCOM1*

The mechanistic role of Com1/Sae2 (Prinz et al., 1997) still has to be elucidated. Nevertheless, recently it has been shown, that Com1/Sae2 is needed for the removal of Spo11 from DNA during meiosis in *S. cerevisiae* as well as in *S. pombe*. In budding yeast Spo11p remains covalently attached to unresected DNA ends in *com1/sae2* mutants (Neale et al., 2005; Prieler et al., 2005). During vegetative growth Com1p/Sae2p also plays a role. *com1Δ/sae2Δ* mutants are slightly sensitive to MMS, hydroxyurea and ionizing radiation (Clerici et al., 2005; Lisby et al., 2004; Usui et al., 2001). In fission yeast it has been shown that the sensitivity of *ctp1Δ* to MMS (Hartsuiker et al., 2009b) and ionizing radiation (Limbo et al., 2007) is identical to that of MRN null mutants. Furthermore it has been shown that *ctp1Δ* is as defective in $Rec12^{Spo11}$ removal as *rad32*^{mre11}*-D65N* mutant (Hartsuiker et al., 2009a), a mutant which is deficient for nuclease activity and proficient for MRN complex formation (Krogh et al., 2005). All these observations are consistent with a role of Com1/Sae2/CtIP/Ctp1 in the processing of DSBs during meiosis.

In *S. cerevisiae*, Com1p/Sae2p might be nonessential during mitosis because of redundant functions such as that of the exonuclease ExoI, which assists in the resection of DSBs independently of the MRN complex (Llorente and Symington, 2004; Nakada et al., 2004). While the somatic roles of Com1/Sae2 in yeast are not well defined, the importance of the mammalian Com1/Sae2 homolog, CtIP (a.k.a. RBBP8) for genomic integrity was demonstrated by heterozygous $CtIP^{+/-}$ mice, which suffer from a higher incidence of tumors than wild-type mice (Chen et al., 2005).

Arabidopsis Atcom1-1 mutants show no sensitivity to ionizing radiation they are only sensitive to MMC, which leads to a strong inhibition of seedling growth (Uanschou et al., 2007). Conclusively, *At*COM1 seems to be needed for the repair of interstrand DNA cross links, which are the main effect of MMC. Furthermore, it was shown transcription of *AtCOM1* is strictly dependent on ATM, a conserved protein kinase known to mediate signalling of DNA lesions (Garcia et al., 2003; Shiloh, 1998).

Parts of the efforts in the lab are the characterization of a Com1/Sae2 homologue *AtCOM1* in a higher eukaryotic organism, *Arabidopsis thaliana*. We showed that both female as well as male meiosis is affected in *Atcom1-1* mutant plants. This defects lead to sterility, which is confirmed by the fact that *Atcom1-1* mutants do not form any viable microspores or macrospores, as seen in the analysis of gametogenesis. Analysis

of DAPI-stained chromosomes reveals that in both female and male meiosis severe fragmentation of chromosome occurs sometimes leading to chromatin bridges. Furthermore, no pairing of homologues chromosomes, visualized by DAPI and FISH, is seen in *Atcom1*-1 mutants. Chromosome fragmentation and failed pairing indicate that meiotic DSBs are produced, but processes like strand invasion and heteroduplex formation are impaired in *Atcom1-1* mutants. Epistasis analysis clearly shows that the DNA fragmentation observed in *Atcom1-1* mutant plants depends on the activity of the *At*SPO11-1 protein. This result places Atcom1 downstream of Atspo11-1. In contrast, *Atcom1-1 Atdmc1* double mutants show severe chromosome fragmentation and, therefore, resemble the *Atcom1-1* mutant rather than the *Atdmc1* mutant. This result places AtCOM1 upstream of the RecA-related DMC1 protein.

It has been shown that in yeast Com1/Sae2 is needed for the removal of Spo11, which is covalently bound to the 5'end phosphate of the DNA at the DSB, during meiosis (Neale et al., 2005). This reaction cannot occur if Com1/Sae2 is not present and meiotic progression is therefore blocked. In *Arabidopsis* we show that in *Atcom1-1* mutant plants *At*SPO11-1 protein accumulate during meiotic prophase I. While in wild-type meiocytes almost no *At*SPO11-1 protein can be detected, it seems that in the *Atcom1-1* mutant *At*SPO11-1 remains attached to the DNA and can be visualized through immunolocalization studies. Further experiments are needed to resolve the question if the second Spo11 protein *At*SPO11-2 behaves similar to *At*SPO11-1 in an *Atcom1-1* mutant background. Furthermore, we showed that the recA homologue and strand invasion mediator *At*RAD51 cannot be detected in *Atcom1-1* nuclei. In wild-type meiotic chromosomes *At*RAD51 forms numerous foci from leptotene to pachytene, but they are completely absent in the *Atcom1-1* mutant. This suggests that through the remaining attachment of *At*SPO11-1 onto DSB and subsequentially blocked resection of the DNA ends *At*RAD51 is unable to load onto chromosomes.

While the yeast two hybrid analysis did not detect interactions between *At*COM1 and *At*BRCA1, the importance of ubiquitination of human CtIP in a BRCA1/BARD1 dependent manner is undisputable (Yu et al., 2006). Following DNA damage CtIP associates with BRCA1/BARD1, Rad50, Mre11 and Nbs1 (Greenberg et al., 2006). Moreover, heterozygous *CtIP+/-* mice are prone to develop tumours and homozygous *CtIP-/-* knockout mice die during embryonic development (Chen et al., 2005). Consistently with these data it seems that CtIP is involved in DSB repair similar to Com1/Sae2. Furthermore, Com1/Sae2 and CtIP are phosphorylated by the ATM/Tel1

kinase in response to DNA damage (Baroni et al., 2004; Foray et al., 2003), they play a role in sensing DNA damage checkpoints (Clerici et al., 2006; Yu and Chen, 2004) and cooperate with Mre11 as well as with Rad50 (Greenberg et al., 2006; Lisby et al., 2004; Lobachev et al., 2002). Thus, CtIP and possibly *At*COM1 may have acquired accessory functions in addition to those conserved with yeast Com1/Sae2, where for example BRCA1 is not part of the DNA repair machinery.

Previous data implicates that fission yeast Ctp1 functions together with the MRN complex (Limbo et al., 2007) and may be an important factor in processing hairpin capped DNA ends and DNA ends blocked by covalently bound proteins. Interestingly, in mammals a hypomorphic mutation of *MRE11* compromises embryo viability (Theunissen et al., 2003), deletion of *RAD50* is embryonic-lethal (Luo et al., 1999) just as deletion of *CtIP* (Chen et al., 2005). But all three genes are not essential in yeast and in plants. This is consistent with evolutionary conservation of a potential regulatory role of Com1/Sae2 for the MRN complex. The phenotype of *Atcom1-1* provides information which links yeast Com1/Sae2 and mammalian CtIP. Based on the detailed knowledge on Com1/Sae2, CtIP is required for genome stability as a tumour suppressor and for fertility through meiotic DNA repair because in yeast Com1/Sae2 together with Mre11 processes hairpins. Com1/Sae2 and CtIP have been studied separately, but the knowledge of their relationship should strongly stimulate both hitherto separated fields.

10.1. Experimental Outlook

To get further insight into the epistatic correlation of *At*COM1 with the MRN complex in *Arabidopsis thaliana* we would like to investigate in the distribution of *At*RAD50 as well as *At*MRE11 in wild type, *Atcom1-1*, *Atrad50*, *Atmre11-3* and the respective double mutants. Peptide antibodies for this purpose have already been generated and are under test.

Furthermore, efforts have been made to purify the proteins AtMRE11, AtRAD50, AtNBS1 and AtCOM1 to analyze the process of 5'-3' nucleolytic degradation to generate single-stranded DNA after DSB formation in the higher eukaryotic organism, *Arabidopsis thaliana*.

11. Materials and Methods

11.1. Media

11.1.1 Bacterial media

LB: 10g/l tryptone, 5g/l yeast extract, 5g/l NaCl, pH7.0 (calibrated with 2N NaOH), 15g/l agar

E. coli bacteria were selected on media containing 50 mg/l ampicillin or 30mg/l kanamycin. *Agrobacteria tumefaciens* GV3101 were selected on medium containing 50mg/l gentamycin and 50mg/l kanamycin (stock concentration for all antibiotics was 50mg/ml, dissolved in dH_2O and stored at -20°C).

11.1.2. Yeast Media

YPD: 10g/l yeast extract, 20g/l peptone, 20g/l glucose, 20g/l agar

YPAD: YPD supplemented with 40mg/l adenine sulphate

2xYPAD: 20g/l yeast extract, 40g/l peptone, 20g/l glucose, 40mg/l adenine sulphate

0.5x YPAD: 5g/l yeast extract, 10g/l peptone, 20g/l glucose, 40mg/l adenine sulphate

Synthetic dextrose minimal medium (SD): Yeast nitrogen base without amino acids (without ammoniumsulfate) 1.7g/l, ammoniumsulfate 5g/l, glucose 20g/l, adjust pH to 5.8 with 2N NaOH, add 100ml 10x dropout mix after autoclaving.

Freezing medium: 25% glycerol in YPAD

10x dropout: Amino acids were weighed in, filled up to 1l with dH_2O and autoclaved

L-Isoleucine	300mg
L-Valine	1500mg
L-Adenine hemisulphate salt	600mg
L-Arginine HCL	200mg
L-Histidine HCL monohydrate	200mg
L-Leucine	1000mg
L-Lysine	300mg
L-Methionine	200mg
L-Phenylalanine	500mg
L-Threonine	2000mg
L-Tryptophane	200mg
L-Tyrsosine	300mg
L-Uracil	200mg

Amino acid stocks

	Stock concentration (g/100ml)	Volume of stock for 1 litre of medium (ml)	Final concentration in medium (mg/l)	Volume of stock to spread on plate (ml)
Adenine sulphate	0.2	10	20	0.2
Tryptophane	1	2	20	0.1
Histidine HCl	1	2	20	0.1
Leucine	1	10	100	0.1

11.1.3 Plant media

ARA: 4.33 g/l MS salts, 1% sucrose, 0.5 g/l MES, 1x Gamborg's vitamin solution (Sigma), pH5.7 (calibrated with 1M KOH), 6g/l plant agar (Duchefa)

For Hygromycin the concentration in the media was 25mg/l (stock concentration 50mg/ml, stored at -20°C). For Kanamycin the concentration in the media was 25mg/l (stock concentration 50mg/ml, dissolved in dH_2O and stored at -20°C). For Ticarcillin or Amoxycillin (Duchefa), which are used to avoid growth of *Agrobacterium*, the concentration was 250mg/l (stock concentration 250mg/ml, dissolved in dH_2O and stored at -20°C). For selection with Basta, the concentration was 20mg/l (stock concentration 20mg/ml, dissolved in dH_2O and stored at -20°C)

11.2. Cytology

11.2.1. Analysis of meiotic chromosomes

11.2.1.1 Preparation of male meiotic chromosomes

Inflorescences were collected and fixed in 3:1 96% ethanol (Merck) and glacial acetic acid for at least over night. Fixation solution was changed and inflorescences were dissected under a stereomicroscope using a forcep a needle, keeping the largest with buds sized around 0.2-0.7mm. The Material was washed three times with citrate buffer (0.445µl 100mM citric acid, 0.555µl 100mM trisodiumcitrat filled up to 10ml with dH_2O, autoclaved and kept on 4°C) and digested in 0.33% (w/v) cellulose 'Onozuka R-10' (Serva) and 0.33% (w/v) pectolyase (Sigma-Aldrich) for 90 minutes at 37°C in a moist chamber. Then, up to 5 buds were transferred to a slide and suspensed by using a metal rod. Meiocytes were left in 14µl of 60% acetic acid at 45°C for a few seconds; area with cells was labelled using a diamond needle. Labelled area was re-fixed with 3:1 96% ethanol (Merck) and glacial acetic acid. Slides were dried for at least 2 hours, 10µl of 2µg/ml 4',6-Diamidino-2-phenylindol (DAPI) diluted in Vectashield mounting medium (Vector Laboratories) and a coverslip was applied. Photographs were taken on a Zeiss Axioplan microscope (Carl Zeiss) equipped with a mono cool-view CCD camera (Photometrics, Tucson, AZ) and the IPLab spectrum software (IPLab, Fairfax, USA). Digital images were imported into Adobe Photoshop CS version 8 for final processing.

11.2.1.2 Fluorescence in situ hybridisation (FISH)

The BAC clones F1N21 (chromosome 1) and F11L15 (chromosome 2) were obtained from ABRC (Columbus, Ohio), and used as probes. BAC DNA was isolated using the Qiagen Midi Prep kit and labelled by nick translation, following the manufacturer's instructions (Roche Diagnostics), with SpectrumGreen-dUTP (Vysis) and Cy3-dUTP (Amersham Pharmacia Biotech), respectively. Chromosome spreads were prepared according to 5.2.1.1. For the FISH procedure preparations were pre-treated with 100µl RNase A (10mg/ml, Boehringer) for 30 minutes at 37°C and afterwards washed 3 times for 5min in 2xSSC (20xSSC stock: 3M sodium chloride, 0.3M trisodium citrate, pH adjusted 7). Slides were treated with 1:100 dilution of 1mg/ml pepsin (diluted in dH_2O) in 0.01M HCl for 20 minutes at 37°C and then washed 3 times for 5 minutes in 2xSSC. Preparations were fixed for 10 minutes in 3.7% (v/v paraformaldeyde (Sigma-Aldrich) diluted in 1xPBS (10x stock solution: 1.37M NaCl; 27mM KCl; 100mM Na_2HPO_4; 18mM KH_2PO_4) and washed 3 times for 5 minutes in 2xSSC. Dehydration of the material was carried out by putting slides for 3 minutes into 70% (v/v), 3minutes into 96% (v/v) ethanol and then subsequently slides were air dried for at least one hour. Hybridization mix containing 50% (v/v) formamide, 10% (v/v) dextran, 3µl 20xSSC and approximately 20-50ng/µl of each probe were denatured for 10 minutes at 75°C, immediately transferred onto ice for 5min and then applied to the slides. Chromosomes were denatured in hybridization mix for 3 minutes at 73°C in a thermocycler with three cooling steps. Slides were hybridized overnight or up to three days at 37°C in a moist chamber. Following incubation with the probes, slides were washed, with lightshield, two times for 5 minutes in 2xSSC at 42°C, two times for 5 minutes in 0.1xSSC at 42°C, two times 5 minutes in 2xSSC at room temperature. The slides were taken out to cool down in the second step (two times for 5 minutes in 0.1xSSC at 42°C). Then slides were mounted with 10µl of 2µg/ml DAPI and sealed with a coverslip and nailpolish.
Photographs were taken as describes in 11.2.1.1.

11.2.1.3. Immunostaining of male meiotic chromosomes

Inflorescences were collected and placed on a moist filter paper in a Petri dish. Under the stereomicroscope the buds from one inflorescence were dissected using forceps and needles. Buds of the size of 0.2-0.4mm were kept. Using the forcep up to 6 buds were transferred to the slides and incubated with 7µl digestion mix, containing 0.4% (w/v) cytohelicase (Biosepra), 1% (w/v) polyvinylpyrolidone (Sigma-Aldrich), and 1.5%

(w/v) sucrose. By using a metal rod cells were suspensed and left 2-5 minutes in the digestion mix. The presence of meiocytes was checked under the phase contrast microscope. Afterwards, 14µl of 1% (v/v) lipsol, diluted in borate buffer (500mM, pH 9.5) was applied for 3-5 minutes, solutions were mixed and the area with cells was labelled using a diamond needle. Meiocytes were checked for opened callose under the phase contrast microscope. Spreading was stopped by adding 20µl of 4% (w/v) paraformaldeyde pH8 and dried for at least one hour. Preparations were washed one time for 7 minutes in icecold 1xPBS. 10µl of each desired primary antibody was applied on the slide, covered with a little piece of autoclavingbag and incubated overnight at 4°C in a moist chamber. Thereafter parafilm was removed, slides were washed one time for 7 minutes in icecold 1xPBS, subsequently incubated with 20µl of the appropriate secondary antibody diluted in blocking solution (1xPBS/0.1% Triton/3% BSA) and incubated for one hour at 37°C in a moist chamber. Afterwards slides were washed as described above mounted with 10µl of 2µl/ml DAPI, sealed with a coverslip and nailpolish. Photographs were taken on a Zeiss Axioplan microscope (Carl Zeiss) equipped with a mono cool-view CCD camera (Photometrics, Tucson, AZ) and the MetaVue® Imaging System from Molecular Devices (MDS Analytical Technologies). Digital images were deconvolved, projected and finally imported into Adobe Photoshop CS version 8 for final processing.

The primary antibodies were used in following dilutions: anti-ASY1 rabbit (1:500, kindly provided by Chris Franklin), anti-ASY1 rat (1:500; kindly provided by Chris Franklin), anti-*At*RAD51 rat (1:500; kindly provided by Chris Franklin), anti-*At*DMC1 rabbit (1:20; kindly provided by Raphael Mercier), anti-ZYP rat (1:500; kindly provided by Sue Armstrong), anti-*At*SCC3 rabbit (1:1000; kindly provided by Raphael Mercier), anti-*At*MND1 rat (1:200; Vignard et al. 2007) and anti-COM1 guinea pig (1:300; Uanschou et al, 2007).

11.2.1.4. Female gametogenesis

Whole inflorescences were fixed in FPA50 (5ml 37% formaldehyde, 5ml 99% propionic acid, 90ml 50% ethanol) for at least 3 hours at room temperature. Inflorescences can be stored up to 6 month at 4°C. Then pistils were dissected and cleared in a mix of 85% lactic acid and phenol(2:1 v/v) for 30 minutes. Ovules from different sized pistils were then dissected with a needle in a drop of the lactic

acid/phenol solution, mounted in a drop of the same mix, covered by a cover slide and sealed with nailpolish.

11.2.1.5. Preparation of female meiotic chromosomes

Inflorescences were fixed in PFA (5% v/v propionic acid, 10% v/v formaldehyde 37%, Sigma-Aldrich, 70% v/v ethanol 96%, Merck) for at least one hour. Fixed inflorescence can be stored in ethanol 70%, Merck, at 4°C for several months. For preparation inflorescences were rehydrated successive in ethanol 70%, 50%, 30%, 10% and finally in dH_2O each step for 30 minutes. Then pistils from buds sized around 0.8-1mm were dissected with a needle. Afterwards the material was treated with 20µg/ml RNase A (Boehringer) diluted in 1x NTE (5x NTE: 2.5M NaCl, 50mM Tris-Cl pH 8, 5mM EDTA pH 8) for 30 minutes at 37°C. Following RNase A treatment opened pistils are stained with 25µl propidium iodide (Sigma, stock solution 0.1mg/ml dissolved in 0.1M arginine pH 8) and 0.1M arginine pH 12.4 at 4°C for 2 days. After coloration the material was washed two times for one hour in 0.1M arginine pH 8. Then ovules were dissected on a slide using a needle, all tissue around the ovules was removed, 10µl Vectashield and a coverslip was applied. Pictures were taken with a Zeiss Axioplan 2 microscope, including an LSM 510 Laser module.

11.2.2. Alexander staining of anthers

Anthers from mature flowers or buds of 1-2mm size were isolated and put on a slide. Then 5µl Alexander staining solution (10ml 96% ethanol, 1ml 1% malachite green in 96% ethanol, 50ml dH2O, 25ml glycerol, 5g phenol, 5g chloral hydrate, 5ml 1% acid fuchsin in dH2O, 0.5ml 1% Orange G in dH_2O, 2% glacial acetic acid (add just before starting)) was added to the anthers. Vacuum was applied for 30 seconds and the material was covered by a cover slide. Observation is made under a microscope with equipped with a differential interference contrast (DIC). Pollen wall is coloured in green and cytoplasm of viable pollen grains is colored in red purple.

11.3. Microbiology

11.3.1. RbCl method for making competent cells

A single culture of *E.coli* strain XL1 blue respectively DH5α was inoculated in 2.5ml LB media overnight. The overnight culture was subcultered in 250ml LB/$MgSO_4$ [10mM] media and grown to an OD_{590} of 0.4 to 0.6. Cells were collected by centrifugation at 5000rpm for 5 minutes at 4°C. Cells were exclusively kept on ice from this step on. The cell pellet was gently resuspended in 100ml of precooled TFB1 buffer (100mM RbCl; 50 mM$MnCl_2$; 30mM potassium acetate; 10mM $CaCl_2$; 15% (v/v) glycerol; pH 5.8; sterilized by filtration) and incubated on ice for 5 minutes. Cells were again collected by centrifugation at 5000rpm for 5 minutes at 4°C and gently resuspended in 10ml icecold TFB2 buffer (10mM PIPES; 10mM RbCl; 75mM $CaCl_2$; 15% (v/v) glycerol; pH adjusted to 6.8 with KOH; sterilized by filtration). Cells were incubated on ice for 15-60 minutes before making 100µl aliquots and then immediately freezed in liquid nitrogen.

11.3.2. Transformation of *E.coli*

100 µl competent E.coli (E.coli Xl1 blue, E.coli DH5α), prepared by the rubidium chloride method and thawed up from storage at –80°C, were added to 1-3 µg of vector DNA of 10µl of ligation mix, resuspended and placed on ice for 10 minutes. After heat shock of cells by incubating for 2 minutes at 42°C, 1 ml LB-medium was added and the cells were incubated for 60 minutes at 37°C. Cells were subsequently centrifuged at 12000g for 20 seconds, the supernatant was poured off, and the cells were resuspended in the remaining (~100µl) supernatant. Transformed bacteria were plated on LB/ampicillin plates and incubated over night at 37°C.

11.3.3. DNA preparation from *E. coli* I

1.5 ml of an overnight culture of *E. coli* were centrifuged in an Eppendorf tube for 30 seconds at 14 000 rpm. The supernatant was discarded and the cells were suspended in 200µl GTE buffer (25mM Tris-Cl pH 8; 10mM EDTA; 50mM glucose) by mixing rigorously. After adding 200µl of freshly made Alkali-SDS solution (0.2N NaOH; 1% SDS) the tube was gently inverted several times. 200µl acetate solution (3M KoAc; 11.5% (v/v) acetic acid) were added and the tube was inverted again. The sample was centrifuged for 15 minutes at 14000 rpm at room temperature and the supernatant was

mixed with 1 volume of isopropanol. The DNA was precipitated by centrifugation (15 min, 14 000 rpm, RT), washed with 70% ethanol, dried and suspended in 50µl of 1x TE (10mM TrisCl pH8, 1mM EDTA pH8).

11.3.4. DNA preparation from *E. coli* II

3 ml of an overnight culture of *E. coli* was centrifuged for 30 seconds at 14 000 rpm. The supernatant was discarded and the cells were suspended in 250µl re-suspension buffer (50mM Tris-Cl pH 8; 10mM EDTA; 200µg/ml RNaseA) by mixing rigorously. After adding 250µl of freshly made lysis solution (0.2N NaOH; 1% SDS) the tube was gently inverted several times. 300µl acetate solution (3M KAc; 11.5% (v/v) acetic acid) was added and the tube was inverted again. The sample was centrifuged at 14 000 rpm for 15 minutes at room temperature and the supernatant was mixed with 600µl isopropanol. The DNA was precipitated by centrifugation (10 minutes, 14 000 rpm, room temperature), washed with 70% ethanol, dried and suspended in 50µl dH_2O. 30µl 20% (w/v) PEG(6000) / 2.5M NaCl solution was added and incubated on ice for 1 hour. DNA was precipitated by centrifugation (15 minutes, 14 000 rpm, 4°C), washed with 70% EtOH, dried and resuspended in 20µl dH_2O.

11.3.5. Sequencing

Sequencing reaction was taken out by using ABI PRISM BigDye Termintaor v3.1 Cycle Sequencing Kit (Applied Biosystems). Approximately 350ng of vector DNA were used for the sequencing reaction according to the manufactures protocol. The sequencing program comprised 1 cycle of 96°C for 2 minutes and 25 cycles (96°C for 30 seconds, 45°C for 15 seconds and 60°C for 4 minutes). If necessary the DNA was precipitated. DNA sequence was determined at the Institute of Botany, 1030, Vienna.

11.4. Plant work

11.4.1. Growth conditions

All plant lines were *Arabidopsis thaliana*, either ecotype Columbia or Landsberg erecta, respectively. Plants were grown under long day conditions (16 hours light, 8 hours darkness, humidity 60-80%, 21°C, 5800 LUX, light source PHILLIPS TLD 36W and SYLVANA GroLUX 36W).

11.4.2. Seed sterilization

A volume of about 50µl seeds were added to 1ml sterilization solution (5g $Ca(OCl)_2$ in 100ml dH_2O / 0.02% Triton X-100, not older than 14 days, but at least one day). The seeds were agitated to cover all seeds with solution while incubating at room temperature for 20 minutes. After a short centrifugation step the seeds were washed twice with 1ml sterile water and were dried in the sterile hood for at least 24 hours.

11.4.3. Sensitivity assays

To test sensitivity of plants to mitomycin C (MMC, Sigma), seeds were germinated on ARA plates containing 30µM and 40µM MMC, respectively. The development of true leaves was monitored. To test for sensitivity to hydroxurea (HU) (Sigma), seeds were germinated on ARA plates containing 0.5mM, 1mM and 2mM HU and grown vertically to measure root lengths. To test for sensitivity against ionizing radiation, seeds were germinated on ARA medium and 2 and 5days old seedlings were each treated with 100Gy and 150Gy (Co^{60}, 42Gy/min).

11.4.4. PCR-grade DNA preparation from *Arabidopsis thaliana*

1-3 leaves were harvested in an Eppendorf tube and 400µl of extraction buffer (200mM Tris-Cl pH 7.5; 250mM NaCl; 0.5% SDS; 25mM EDTA) was added. The plant material was homogenized using plastic pestles (SIGMA). After centrifugation (5 minutes, 14 000 rpm, RT) the supernatant was mixed with 1 volume of isopropanol and kept at room temperature for 5 to 10 minutes. The DNA was precipitated by centrifugation (5 minutes, 14 000 rpm, RT). The pellet was washed with 70% ethanol, dried, suspended in 25-50µl 1x TE and incubated at 65°C for 10 minutes.

11.4.5. High-quality grade DNA preparation from *Arabidopsis thaliana*

One to two inflorescences were homogenized in 400µl Urea Lysis buffer (0.3M NaCl, 30mM Tris-Cl pH8, 20mM EDTA pH8, 1% (w/v) N-Lauroylsarcosine, 7M Urea) using plastic pestles (SIGMA) and incubated for 10 minutes at 50°C. After mixing with 400µl Phenol:Chloroform:Isoamylalcohol (25:24:1, biomol) the samples were centrifuged (5minutes, 14000rpm, RT). The upper aqueous phase was recovered and mixed with 40µl 3M NaOAc pH5.2 and 400µl isopropanol and incubated 20 minutes at room temperature. DNA was precipitated by centrifugation (10 minutes, 14000rpm, RT). After washing with 70% EtOH the pellet was air-dried and re-suspended in 100µl dH_2O.

11.4.6. Preparation of electrocompetent *Agrobacterium tumefaciens*

5ml of LB/gentamycin (50mg/l) were inoculated with one colony of *Agrobacterium tumefaciens* strain GV3101 and grown overnight at 26°C. 500ml of LB/gentamycin (50mg/l) were inoculated with 400µl of the fresh overnight Agrobacterium culture. Cells were grown at 26°C till OD_{600} reaches 0.5 to 0.7. From this step on cells were kept on ice for the rest of the procedure. Cells were transferred to Sorvall centrifuge buckets (Nalgene) and centrifuged at 3000rpm for 10 minutes at 4°C. The supernatant was removed and cells were re-suspended in 250ml of ice cold dH_2O. Cells were harvested by centrifugation as above, re-suspended in 100ml ice cold 10% (v/v) glycerol and centrifuged. Then cells were re-suspended in 2ml of 10% (v/v) glycerol, 40µl aliquots were made, frozen in liquid nitrogen and stored at –80°C.

11.4.7. Transformation of electrocompetent *Agrobacterium tumefaciens*

Cells were thawed at ice and mixed with 50-200ng plasmid DNA. Cells were transferred to a pre-cooled 1mm electroporation cuvette and electroporation was performed at 400Ω, 25µF and 1,8kV (pulse length of 5-8ms). After addition of 1ml LB medium cells were incubated for one hour at room temperature. 100µl of the cell suspension were spread on a plate containing 50mg/l gentamycin and an appropriate selective antibiotic for the plasmid. Transformed cells were incubated for 2-3 days at room temperature.

11.4.8. Floral dip transformation

3ml LB medium supplemented with 50mg/l Gentamycin and 25mg/l Kanamycin were inoculated with a single colony of *Agrobacterium tumefaciens* (strain GV3101) and

incubated at 28°C overnight under constant shaking. 500ml of LB containing the same antibiotics as before were inoculated with 3ml of overnight culture and again incubated at 28°C overnight under constant shaking. The cells were harvested by centrifugation for 25 minutes at 3000rpm at room temperature. Then cells were washed with 5% sucrose and centrifuged for 10minutes at 3000rpm at room temperature. The supernatant was discarded and cells were re-suspended in 200ml 5% sucrose supplemented with 0.02% Silwet L-77. Inflorescences were dipped into the bacterial suspension for 30 seconds, and left in a box covered with saran foil for 2 days under light before being returned to normal growth conditions.

11.4.9. BASTA selection on soil

Seeds were sown on soil (100-200 per pot) and left at 4°C for two days for pre-germination. After about one week, when the first true leaves had developed, seedlings were sprayed with 150µg/ml BASTA (200g/l Glufosinate-Ammonium; Bayer). Spraying was repeated every two days until most seedlings were dead (three to four times).

11.5. Protein work

11.5.1. Protein extracts from *Arabidopsis thaliana*

Inflorescences were collected in a microtube with cap (Sarstadt) and always kept on ice. 200-400µl of RIPA buffer (150mM NaCl; 1% (v/v) NP-40; 0.5% (w/v) sodium deoxycholat; 0.1% (v/v) SDS; 50mM Tris-Cl pH 8) or HEPES buffer (20mM HEPES; 420mM NaCl; 1.2M $MgCl_2$; 0.2mM EDTA; 25% (v/v) glycerol; 0.1% NP40; 2mM β-mercaptoethanol) and 1/10 volume of 10x protease inhibitor (10x stock solution: 1 tablet Complete PI Mini (Roche) + 10µl pepstatin A [10mg/ml] + 990µl dH_2O) were added. Plant material was homogenized in a multibeadshocker (YASUI KIKAI) for 10minutes (30sec/ 30sec) at 2500rpm at 4°C. Cell debris was collected by centrifugation for 10 minutes at 14000rpm at 4°C and the supernatant was transferred to a new Eppendorf tube. Protein extracts were immediately frozen in liquid nitrogen or an appropriate volume of 5x SDS sample buffer (1ml Tris/HCl pH 6,8, 5ml 10% SDS, 0,5ml 2-ß-Mercaptoethanol, 2ml glycine, 10mM DTT, ddH_2O to final volume of 10ml) was added.

11.5.2. Protein extraction from plant cell culture

1ml of cell suspension culture was re-suspended in 5ml MS medium and centrifuged at 1800rpm for 5 minutes. The supernatant was discarded and the washing step repeated two more times. 400µl of 2x extraction buffer (100mM TrisCl pH 7.5; 20% (v/v) glycerol; 0.2% (v/v) NP-40; 2mM EDTA; 1mM DTT; sterilized by filtration) and 1/10 volume of 10x Complete PI Mini (Roche)+ Pepstatin A was added and homogenized in the multibeadshocker for 10minutes (30sec/ 30sec) at 2500rpm at 4°C. Cell debris was collected by centrifugation for 10 minutes at 14000rpm at 4°C and the supernatant was transferred to a new pre-cooled Eppendorf tube. Protein extracts were mixed 1:1 with 2x Lämmli buffer, heated up for 5 minutes to 95°C; loaded on a poly-acrylamid (PAA) -gel or stored at –20°C.

11.5.3. Protein extraction from yeast

A single yeast colony was inoculated in 3ml YSD media containing the appropriated amino acids for the particular yeast plasmid selection, and grown at 30°C overnight. 1ml was collected by centrifugation at 3000rpm for 5 minutes at room temperature. The pellet was washed with ddH_2O and centrifuged at 3000rpm for 5 minutes at room temperature. 300µl of 20% (w/v) trichloroacetic acid (TCA) and 30µl of acid washed glass beads were added and rigorously mixed for one minute. The supernatant was transferred into a new Eppendorf tube. The remaining glass beads were washed with 5% (w/v) TCA and rigorously mixed for one minute at room temperature. The supernatant was removed and transferred to the Eppendorf tube with the first supernatant. The proteins were collected by centrifugation at 3000rpm for 10 minutes, and the pellet was re-suspended in 2x Lämmli buffer (100mM TrisCl pH 6.8; 4% SDS; 200mM DTT; 20% glycerol; 0.1% bromophenol blue). 1M TrisCl was added until the solution was blue. The sample was heated for 5 minutes to 95°C, centrifuged at 3000rpm for 10 minutes and an aliquot of the supernatant was loaded on a gel.

11.5.4. Western blot

20µl of the protein extract were loaded per lane onto 8%, 10% or 12% PAA -gels and run at 15 mA/gel for 2 hours with 1x electrophoresis buffer (25mM Tris; 192mM glycine; 0.1% (v/v) SDS to a final volume of 1liter with dH_2O). Afterwards, the gels were blotted onto PVDF membranes (Immobilon-P; Millipore) at 400mA for 1 hour with 1x blotting buffer (150ml methanol, 1ml 20% SDS to a final volume of one liter

with dH_2O). The membranes were blocked with 5% low fat milkpowder in TBS/T (Tris-buffered saline, 0,1% Tween) for 1 hour at room temperature. Subsequently, the membrane was incubated with the primary antibody over night at 4°C. After washing 3x with TBS/T for 10 minutes, the incubation with the secondary antibody for 1 hour at room temperature followed and membrane was washed again. The antibodies were detected with an enhanced chemiluminescence kit (Amersham) used according to the manufactures protocol.

The primary antibody was used in the following dilution: anti-MND1 (Vignard et al, 2007) 1:200. The secondary antibody was ECL (TM) Anti-rat IgG, Horseradish Peroxidase (from goat) (GE Healthcare UK Ltd., Little Chalfont Buckinghamshire, England) used 1:10000.

11.5.5. *In vitro* translation

In vitro translations were done using the TNT® Coupled Reticulocyte Lysate System (Promega) respectively the TNT® Coupled Wheat Germ Extract System (Promega) according to the manufactures protocol.

11.5.6. Co-immunoprecipitation

30µl of ProteinG sepharose (Amersham) was washed three times with NET2 buffer (150mM NaCl; 50mM TrisCl pH 7.4; 0.05% (v/v) NP-40) at 500rpm for one minute. ProteinG sepharose was incubated with 200µl of undiluted sera containing the antibody against c-myc (#9E11; antibody provided by IMP) or 10µl of antibody against HA (HA.11 Clone 16B12 Monoclonal Antibody, purified; Covance) at 4°C overnight. ProteinG sepharose with the coupled antibodies was washed again three times with NET2 buffer. Half of the particular *in vitro* translation (see 11.5.5.) was incubated with the c-myc coupled ProteinG sepharose, the other half with the HA-coupled ProteinG sepharose for at least 2 hours at 4°C. After incubation the ProteinG sepharose with antibodies and bound proteins were washed again three times with NET2 buffer at 500rpm for one minute, re-suspended in 10µl 2x Lämmli buffer, boiled for 5 minutes to 95°C and centrifuged for 30 seconds at 14000rpm. 20-30µl of the supernatant was loaded on an appropriate PAA-gel and proteins were separated at 12mA until the loading dye ran out of the gel. The gel was incubated for 30minutes in 20% (v/v) methanol/10% (v/v) acetic acid under gentle agitation, followed by 15 minutes incubation in acetic acid and 15 minutes in 24% (w/v) diphenoloxazol dissolved in

acetic acid. Afterwards the gel was floated with dH_2O, washed three times for 5 minutes with dH_2O, 5 minutes with 3% (v/v) glycerol and vacuum dried for 2hours at 80°C. Gel was then exposed to a Fudji medical X-ray film.

11.6. Yeast work

11.6.1. Lithium acetate method for making competent yeast

A single colony from the yeast strain YM706 (*MAT*α ga14-542 ura3-52 his3-200 ade2-101 lys2-801 tql-901 tyrl-501) or PJ69-4A (*MATa* trpl-901 leu2-3,112 ura3-52 *his3-200* ga14A ga18OA LYSZ::GALl-HIS3 GAL2-ADE2 metZ::GAL7-lacZ), respectively, was inoculated in 5ml YPAD media and grown overnight at 30°C. 3ml of the overnight culture were transferred to 50ml YPAD in a 250ml Erlenmeyer tube and incubated for 3.5 hours at 30°C. The culture was transferred to a 50 ml sterile tube and centrifuged at 2000rpm for 2 minutes at room temperature. The supernatant was discarded and the cells re-suspended in dH_2O and centrifuged as above. The cell pellet was then re-suspended in 1ml LiTE (0.1M Lithium acetate, 10mM TrisCl, 1mM EDTA) and centrifuged for 2 minutes at 2000rpm. Cells were washed again, re-suspended in 1ml LiTE and kept on 4°C until transformation.

11.6.2. Transformation of yeast

2.5µl carrier DNA (salmon sperm 5mg/ml) was heated up for 5 minutes at 95°C, mixed with 3-5µl plasmid DNA and 100µl competent yeast cells. 700µl PEG/LiAc (40% (w/v) Polyethylenglycol 4000, 0.1M Lithium acetate) was added and re-suspended and incubated for 60 minutes at 30°C. Cells were then heat shocked for 15 minutes at 42°C, centrifuged at 2000rpm for 2 minutes at room temperature, supernatant was discarded and cells plated on a YSD plate containing the appropriate amino acids, YSD plates lacking the amino acid leucine were used for the yeast strain YM706 transformed with plasmids containing the GAL4 binding domain and YSD plates lacking the amino acid tryptophane were used for the yeast strain PJ69-4A transformed with plasmids containing the GAL4 activation domain. Plates were incubated for two to four days at 30°C to recover the transformants.

11.6.3 Mating test

Opposite mating type strains YM706 and PJ69-4A with GAL4 binding domain or GAL4 activation domain vectors containing the particular cDNAs were mated overnight at 30°C on YPAD plates. The mating of adequate combinations of these strains allowed selection of Leu^+, Trp^+ diploids in which pairs of vectors with candidate gene fusions were present. Interactions allowed the reconstitution of a functional GAL4 transcription factor which was assessed by plating the diploids on adequate media (-Leu, -Trp, -His with 2mM 3-amino triazol or -Leu, -Trp, -Ade plates) to reveal reporter gene expression.

11.6.4. Plasmid DNA preparation from yeast

A single colony with the particular plasmid was inoculated in 3ml YSD media ,lacking the amino acid leucine for yeast mating type a and lacking the amino acid tryptophan for yeast mating type α, at 30°C over night. 1.5ml of the culture was centrifuged at maximum speed for 20 seconds and the pellet resuspended in 500µl buffer1 (2% (v/v) tritonX-100, 1% (v/v) SDS, 100mM NaCl, 100mM Tris pH7.5, 1mMNa2EDTA). 200µl of acid treated glass beads were added, put on the Vibrax (IKA Vibrax VXR basic) for 10 minutes at 4°C and then heated for 10 minutes to 70°C without shaking. 200µl 5M KAc and 150µl 5M NaCl were added, inverted several times and placed on ice for 20 minutes. Then the suspension was centrifuged at 4°C at maximum speed and the supernatant was transferred to a new Eppendorf tube. 1/3 volume of PEG6000 (30%w/v PEG6000 in dH20, sterile filtered) was added, kept on ice for 10 minutes and centrifuged at room temperature for 10 minutes at maximum speed. The supernatant was discarded, the pellet resuspended in 40µl 1xTE and used for restriction enzyme analysis to confirm the identity of the plasmid.

12. Abbreviations

bp	base pair
CO	cross over
DAPI	4'-6-diamidino-2-phenylindole
DIC	differential interference contrast
DNA	desoxyribonucleic acid
dHJ	double Holliday-junction
DSB	double-strand break
dsDNA	double-stranded DNA
HR	homologous recombination
HU	Hydroxyurea
IH	inter homologue
IS	inter-sister
kb	kilobase
MMC	Mitomycin C
MMS	methyl methanesulfonate
MRN	MRE11-RAD50-NBS1 complex
MRX	Mre11-Rad50-Xrs2 complex
mRNA	messenger RNA
NCO	non-crossover
NHEJ	non-homologous end-joining
PCR	polymerase chain reaction
SDSA	synthesis-dependent strand annealing
SC	synaptonemal complex
SSA	single strand annealing
SSB	single-strand break
ssDNA	single-stranded DNA

13. Supplementary data

13.1. Primer

All primers are listed in 5'-3' orientation

AtMND1: mnd1_pst1_up: ATACCTGCAGCTAAGCTTCATCTTGTACTAGC
mnd1_ecoRI_dn: ATCGAATTCATGTCTAAGAAACGGGGACTTTC
AHP2: AHP2_dn: TGATGCAGCAAAACAAACCT
AHP2_up: TTTTGTCTTCTGGCCTCACC
AtDMC1: atdmc1_a: CCTGCAATGGTCTCATGATGCATAC
atdmc1_c: AGGTACTCTGTCTCTCAATG
atdmc1_d: ACTAATCCTTCGCGTCAGCAATGC
ASY1: asy1_screen_up: TCCTTCAGCTTCTGAGCCATC
asy1_screen_dn: CTCCATTTCGTATTAGCTGTCG
AtXRCC3: xrcc3_o438: ATGCAAAATGGGAAAATTAAGCCG
xrcc3_o439: CTACGCTTGAACCGCACAAATC
xrcc3_447: GGATTTGGTTGAAACTTCTGATGG
xrcc3_o405: TGGTTCACGTAGTGGGCCATCG
AtMRE11-3: MRE_1: CCAATGGATGAGGCCTGAAGTT
MRE_2: CCAATGGGAGTTTGATCTCTGA
AtCOM1-1: Com1down2: TGTTGCAGGTTAAGGGTTTGG
Lbc1: TGGACCGCTTGCTGCAACTCT
Com1UP_NEW: CATTTCGGATTCAAACCCGATGTTC
AtSPO11-1-2: spo11-1-2-MG52: GGATCGGGCCTAAAAGCCAACG
spo11-1-2-MG96: CTTTGAATGCTGATGGATGCATGTAGTAG
digestion with VspI
AtSPO11-2: GABItest1: CCCATTTGGACGTGAATGTAGACAC
Spo11-2_GABI_down: GCTCGTGGAAGATCGTGTGTTC
Spo11-2_GABI_up: CCTGCATAGGAAAGTGGAGATTAGGAC
AtRAD51: pcr_atrad51_1: GGTTCCATCACGGAGTTATATGG
pcr_atrad51_2: AGCCATGATATTCCCACCAATC
AtLIGIV: Lig4_8: GTGATTTGAAACTAGTCTGTG
Lig4_9: CAGCAAACCGATTCAGAGATG

13.2. Vectors

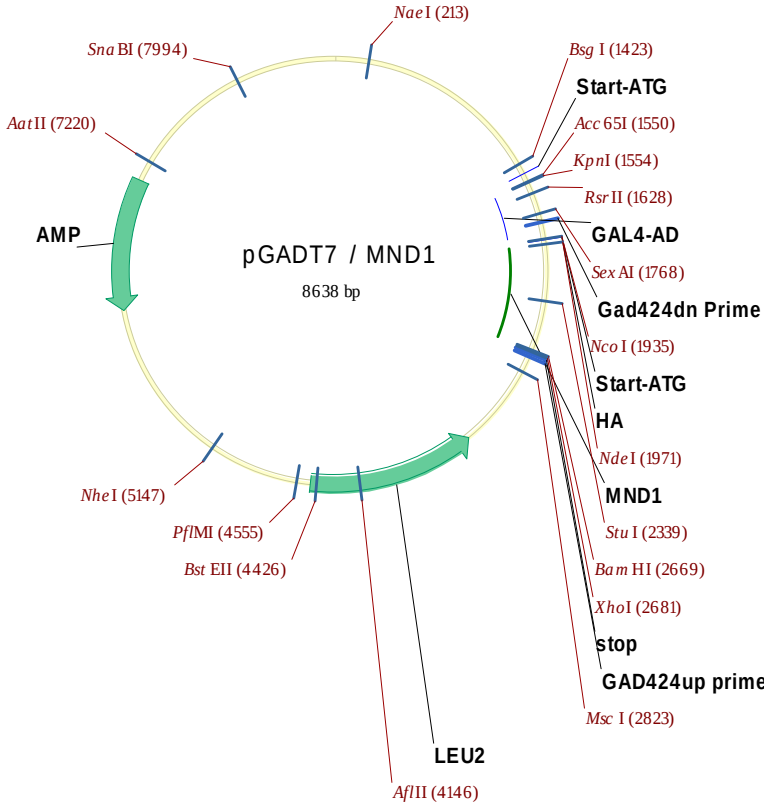
pGADT7 / MND1
8638 bp
NaeI (213)
Bsg I (1423)
Start-ATG
Acc 65I (1550)
KpnI (1554)
RsrII (1628)
GAL4-AD
Sex AI (1768)
Gad424dn Prime
NcoI (1935)
Start-ATG
HA
NdeI (1971)
MND1
Stu I (2339)
Bam HI (2669)
XhoI (2681)
stop
GAD424up prime
Msc I (2823)
LEU2
AflII (4146)
Bst EII (4426)
PflMI (4555)
NheI (5147)
AMP
AatII (7220)
Sna BI (7994)

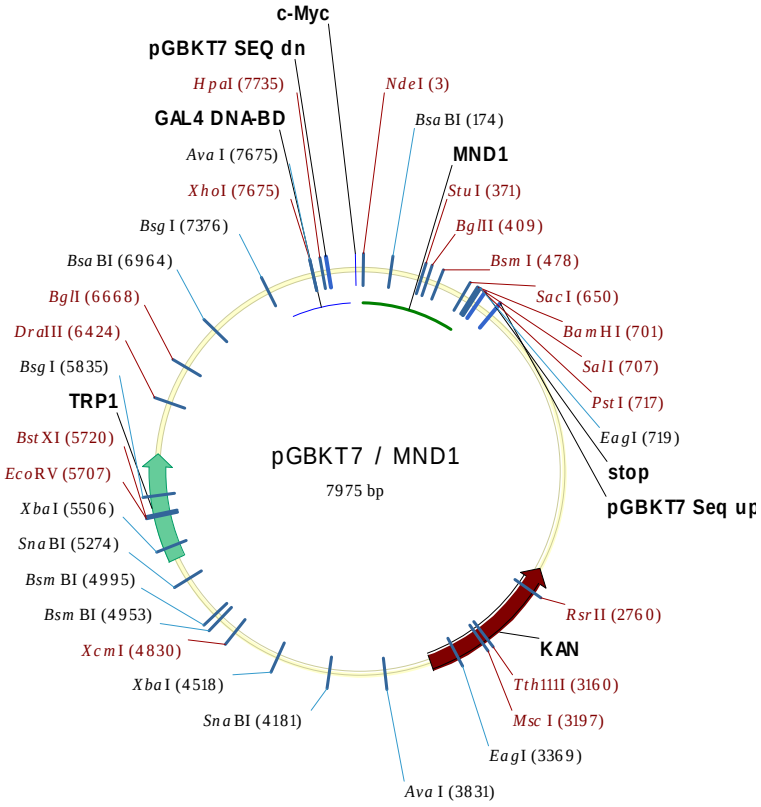
pGBKT7 / MND1
7975 bp
c-Myc
pGBKT7 SEQ dn
HpaI (7735)
NdeI (3)
GAL4 DNA-BD
Bsa BI (174)
Ava I (7675)
MND1
XhoI (7675)
Stu I (371)
Bsg I (7376)
BglII (409)
Bsa BI (6964)
Bsm I (478)
BglI (6668)
Sac I (650)
DraIII (6424)
Bam HI (701)
Bsg I (5835)
Sal I (707)
TRP1
Pst I (717)
Bst XI (5720)
Eag I (719)
EcoRV (5707)
stop
XbaI (5506)
pGBKT7 Seq up
Sna BI (5274)
Bsm BI (4995)
RsrII (2760)
Bsm BI (4953)
KAN
XcmI (4830)
Tth111I (3160)
XbaI (4518)
Msc I (3197)
Sna BI (4181)
Eag I (3369)
Ava I (3831)

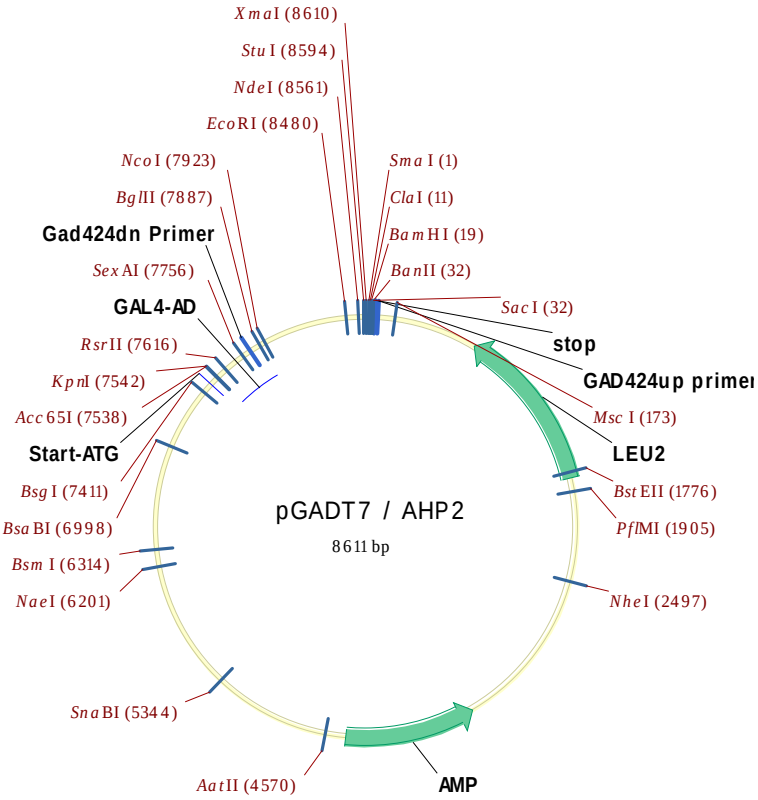
XmaI (8610)
StuI (8594)
NdeI (8561)
EcoRI (8480)
NcoI (7923)
BglII (7887)
Gad424dn Primer
SexAI (7756)
GAL4-AD
RsrII (7616)
KpnI (7542)
Acc65I (7538)
Start-ATG
BsgI (7411)
BsaBI (6998)
BsmI (6314)
NaeI (6201)
SnaBI (5344)
AatII (4570)
AMP
SmaI (1)
ClaI (11)
BamHI (19)
BanII (32)
SacI (32)
stop
GAD424up primer
MscI (173)
LEU2
BstEII (1776)
PflMI (1905)
NheI (2497)
pGADT7 / AHP2
8611 bp

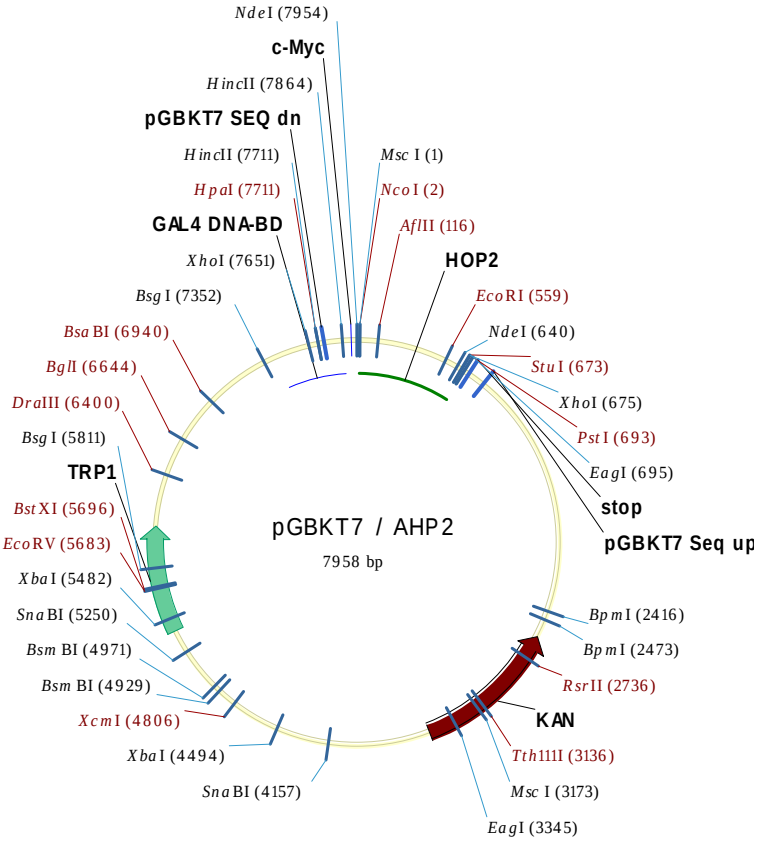
NdeI (7954)
c-Myc
HincII (7864)
pGBKT7 SEQ dn
HincII (7711)
HpaI (7711)
GAL4 DNA-BD
XhoI (7651)
BsgI (7352)
BsaBI (6940)
BglII (6644)
DraIII (6400)
BsgI (5811)
TRP1
BstXI (5696)
EcoRV (5683)
XbaI (5482)
SnaBI (5250)
BsmBI (4971)
BsmBI (4929)
XcmI (4806)
XbaI (4494)
SnaBI (4157)
MscI (1)
NcoI (2)
AflII (116)
HOP2
EcoRI (559)
NdeI (640)
StuI (673)
XhoI (675)
PstI (693)
EagI (695)
stop
pGBKT7 Seq up
BpmI (2416)
BpmI (2473)
RsrII (2736)
KAN
Tth111I (3136)
MscI (3173)
EagI (3345)
pGBKT7 / AHP2
7958 bp

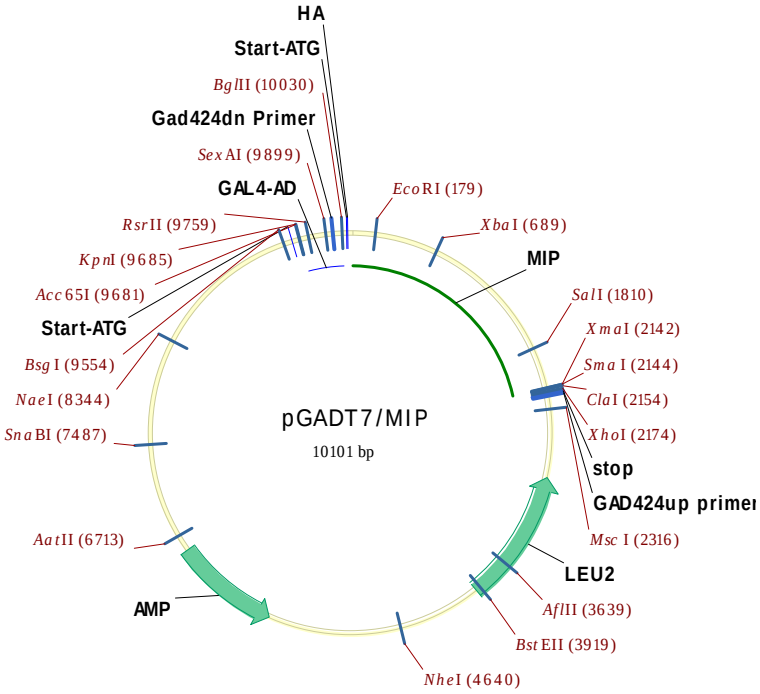
HA
Start-ATG
BglII (10030)
Gad424dn Primer
SexAI (9899)
GAL4-AD
EcoRI (179)
RsrII (9759)
XbaI (689)
KpnI (9685)
MIP
Acc65I (9681)
SalI (1810)
Start-ATG
XmaI (2142)
BsgI (9554)
SmaI (2144)
NaeI (8344)
ClaI (2154)
pGADT7/MIP
SnaBI (7487)
XhoI (2174)
10101 bp
stop
GAD424up primer
AatII (6713)
MscI (2316)
LEU2
AMP
AflII (3639)
BstEII (3919)
NheI (4640)

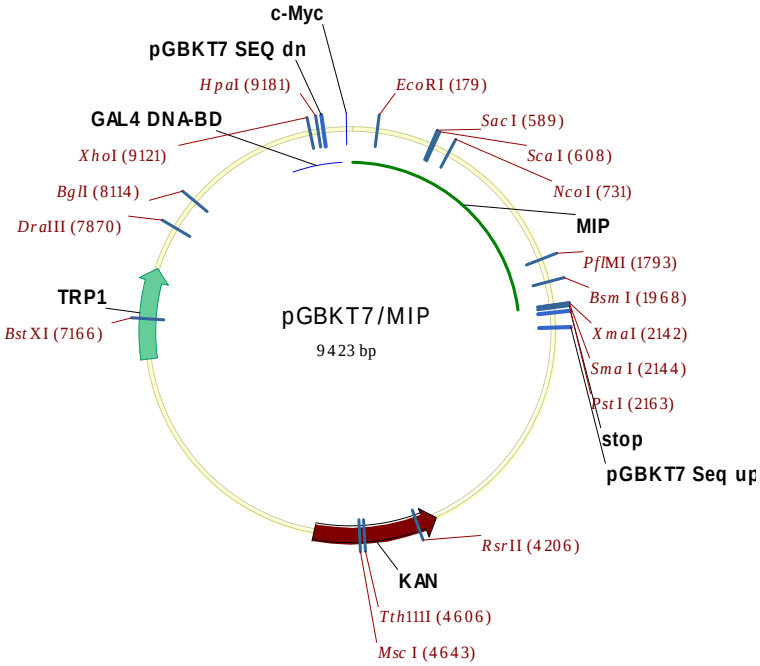
c-Myc
pGBKT7 SEQ dn
HpaI (9181)
EcoRI (179)
GAL4 DNA-BD
SacI (589)
XhoI (9121)
ScaI (608)
NcoI (731)
BglI (8114)
MIP
DraIII (7870)
PflMI (1793)
TRP1
BsmI (1968)
pGBKT7/MIP
BstXI (7166)
XmaI (2142)
9423 bp
SmaI (2144)
PstI (2163)
stop
pGBKT7 Seq up
RsrII (4206)
KAN
Tth111I (4606)
MscI (4643)

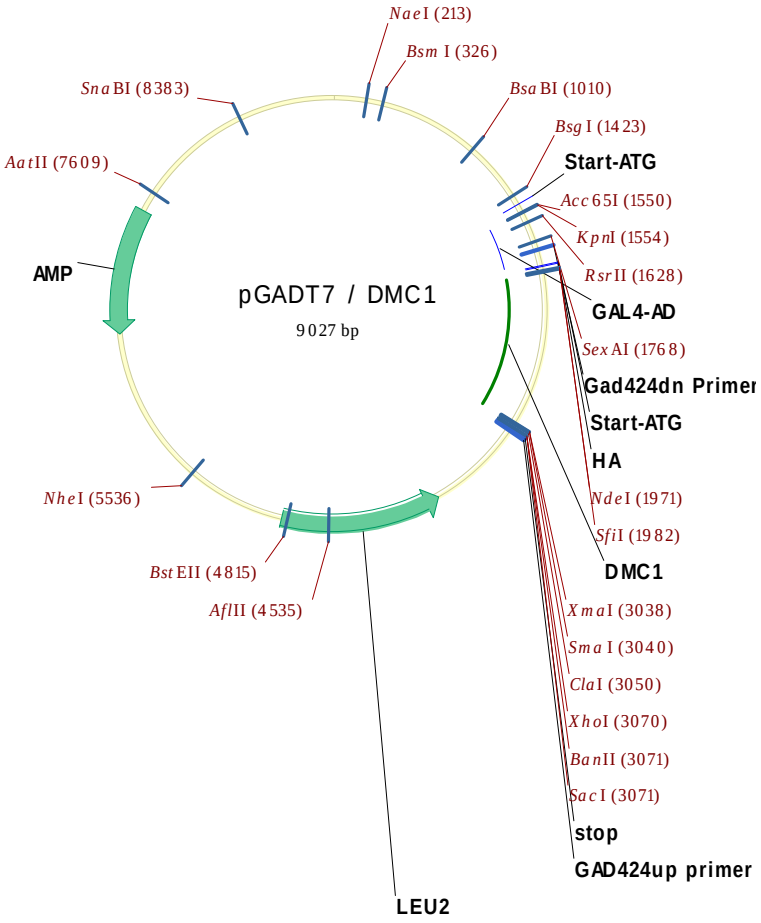
NaeI (213)
BsmI (326)
BsaBI (1010)
BsgI (1423)
Start-ATG
Acc65I (1550)
KpnI (1554)
RsrII (1628)
GAL4-AD
SexAI (1768)
Gad424dn Primer
Start-ATG
HA
NdeI (1971)
SfiI (1982)
DMC1
XmaI (3038)
SmaI (3040)
ClaI (3050)
XhoI (3070)
BanII (3071)
SacI (3071)
stop
GAD424up primer
LEU2
AflII (4535)
BstEII (4815)
NheI (5536)
AMP
AatII (7609)
SnaBI (8383)
pGADT7 / DMC1
9027 bp

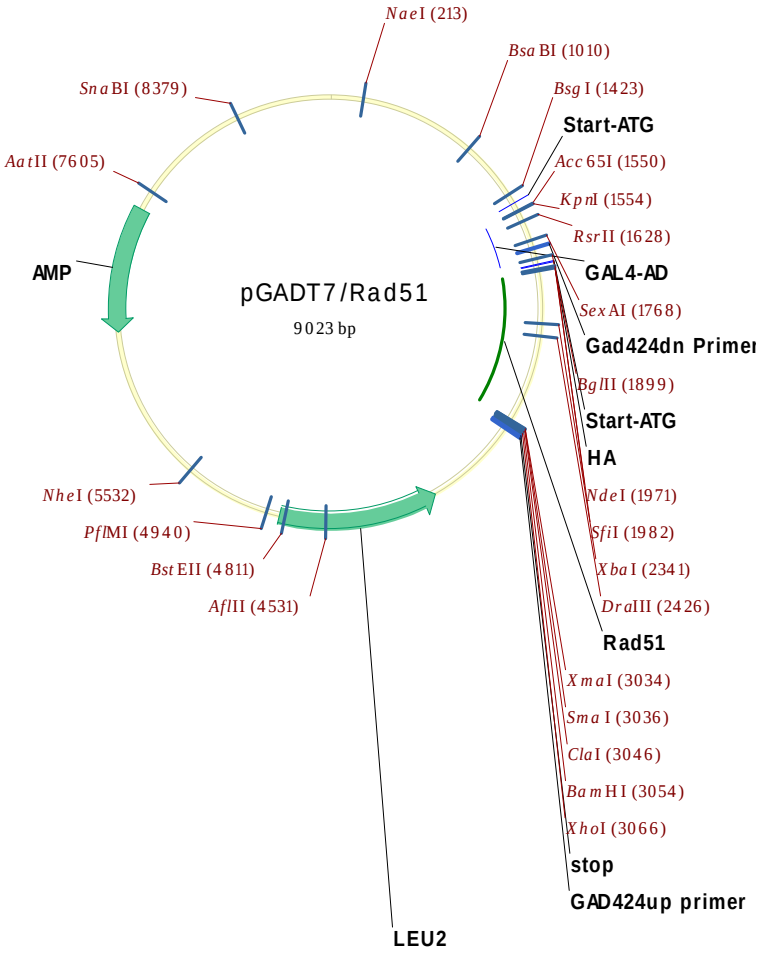
NaeI (213)
BsaBI (1010)
SnaBI (8379)
BsgI (1423)
Start-ATG
AatII (7605)
Acc65I (1550)
KpnI (1554)
RsrII (1628)
AMP
pGADT7/Rad51
9023 bp
GAL4-AD
SexAI (1768)
Gad424dn Primer
BglII (1899)
Start-ATG
HA
NheI (5532)
NdeI (1971)
PflMI (4940)
SfiI (1982)
BstEII (4811)
XbaI (2341)
AflII (4531)
DraIII (2426)
Rad51
XmaI (3034)
SmaI (3036)
ClaI (3046)
BamHI (3054)
XhoI (3066)
stop
GAD424up primer
LEU2

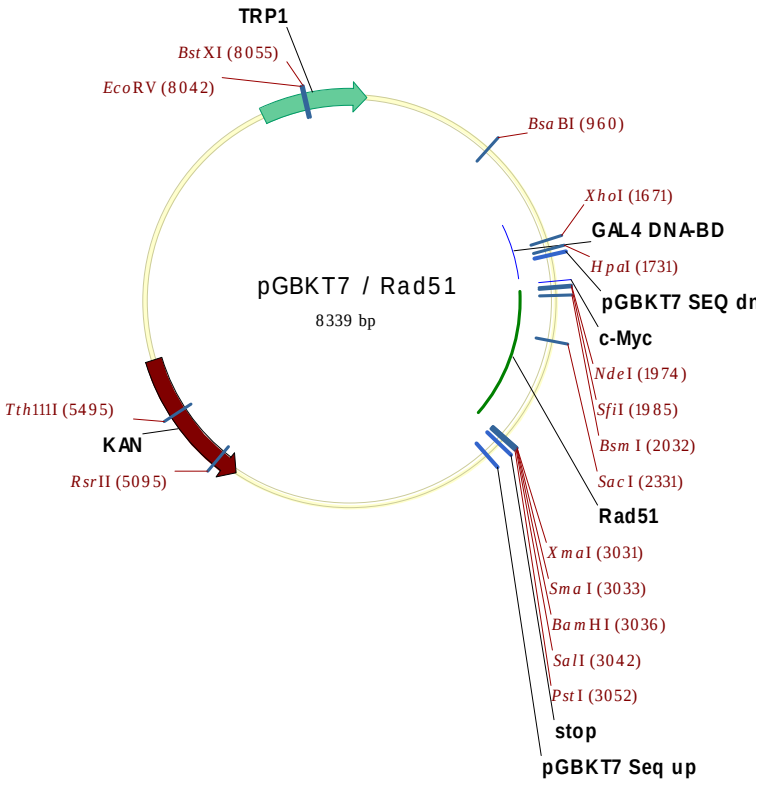
TRP1
BstXI (8055)
EcoRV (8042)
BsaBI (960)
XhoI (1671)
GAL4 DNA-BD
HpaI (1731)
pGBKT7 / Rad51
8339 bp
pGBKT7 SEQ dr
c-Myc
NdeI (1974)
Tth111I (5495)
SfiI (1985)
KAN
BsmI (2032)
RsrII (5095)
SacI (2331)
Rad51
XmaI (3031)
SmaI (3033)
BamHI (3036)
SalI (3042)
PstI (3052)
stop
pGBKT7 Seq up

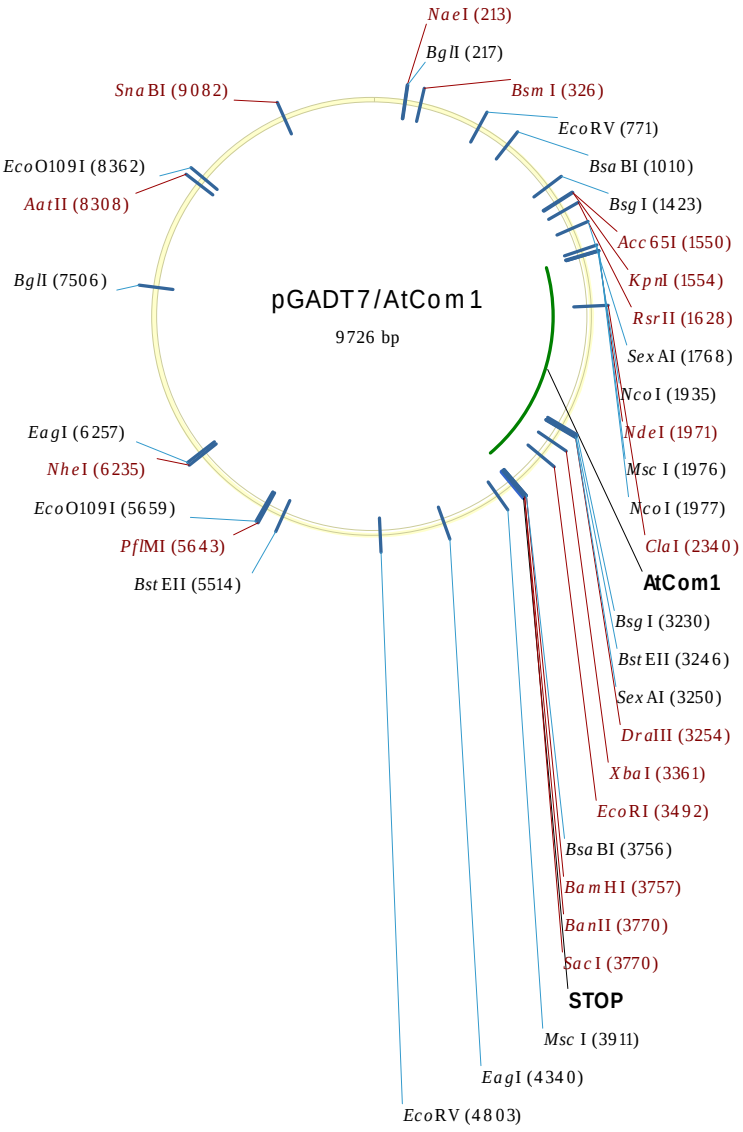
pGADT7/AtCom1
9726 bp
NaeI (213)
BglII (217)
BsmI (326)
EcoRV (771)
BsaBI (1010)
BsgI (1423)
Acc65I (1550)
KpnI (1554)
RsrII (1628)
SexAI (1768)
NcoI (1935)
NdeI (1971)
MscI (1976)
NcoI (1977)
ClaI (2340)
AtCom1
BsgI (3230)
BstEII (3246)
SexAI (3250)
DraIII (3254)
XbaI (3361)
EcoRI (3492)
BsaBI (3756)
BamHI (3757)
BanII (3770)
SacI (3770)
STOP
MscI (3911)
EagI (4340)
EcoRV (4803)
SnaBI (9082)
EcoO109I (8362)
AatII (8308)
BglII (7506)
EagI (6257)
NheI (6235)
EcoO109I (5659)
PflMI (5643)
BstEII (5514)

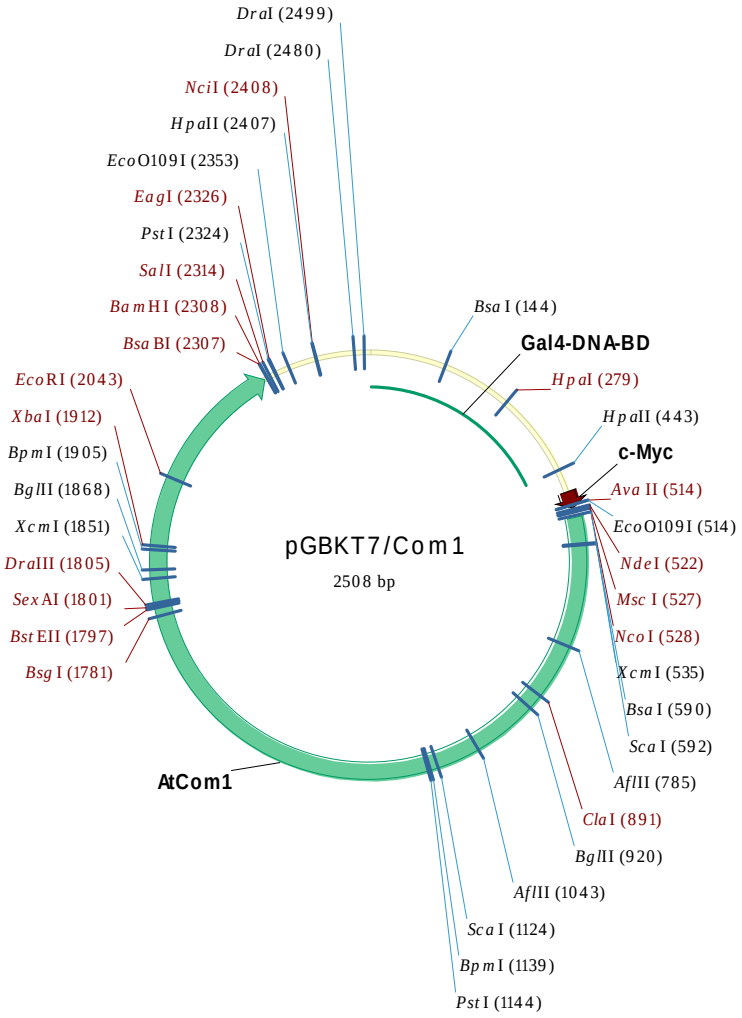
pGBKT7/Com1
2508 bp
AtCom1
Gal4-DNA-BD
c-Myc
DraI (2499)
DraI (2480)
NciI (2408)
HpaII (2407)
EcoO109I (2353)
EagI (2326)
PstI (2324)
SalI (2314)
BamHI (2308)
BsaBI (2307)
EcoRI (2043)
XbaI (1912)
BpmI (1905)
BglII (1868)
XcmI (1851)
DraIII (1805)
SexAI (1801)
BstEII (1797)
BsgI (1781)
BsaI (144)
HpaI (279)
HpaII (443)
AvaII (514)
EcoO109I (514)
NdeI (522)
MscI (527)
NcoI (528)
XcmI (535)
BsaI (590)
ScaI (592)
AflII (785)
ClaI (891)
BglII (920)
AflII (1043)
ScaI (1124)
BpmI (1139)
PstI (1144)

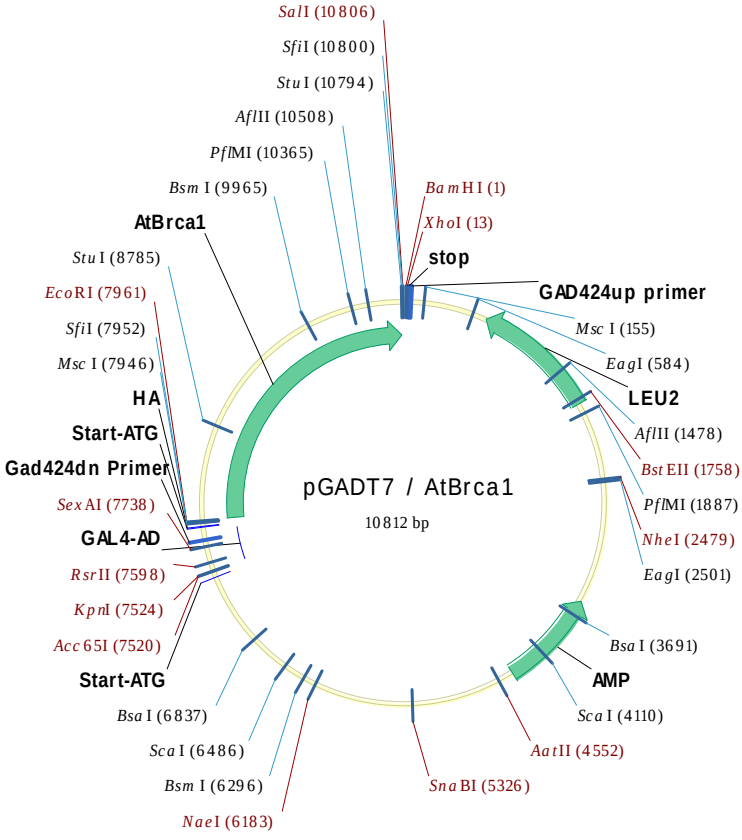
pGADT7 / AtBrca1
10812 bp
AtBrca1
stop
GAD424up primer
LEU2
HA
Start-ATG
Gad424dn Primer
GAL4-AD
Start-ATG
AMP
SalI (10806)
SfiI (10800)
StuI (10794)
AflII (10508)
PflMI (10365)
BsmI (9965)
StuI (8785)
EcoRI (7961)
SfiI (7952)
MscI (7946)
SexAI (7738)
RsrII (7598)
KpnI (7524)
Acc65I (7520)
BsaI (6837)
ScaI (6486)
BsmI (6296)
NaeI (6183)
BamHI (1)
XhoI (13)
MscI (155)
EagI (584)
AflII (1478)
BstEII (1758)
PflMI (1887)
NheI (2479)
EagI (2501)
BsaI (3691)
ScaI (4110)
AatII (4552)
SnaBI (5326)

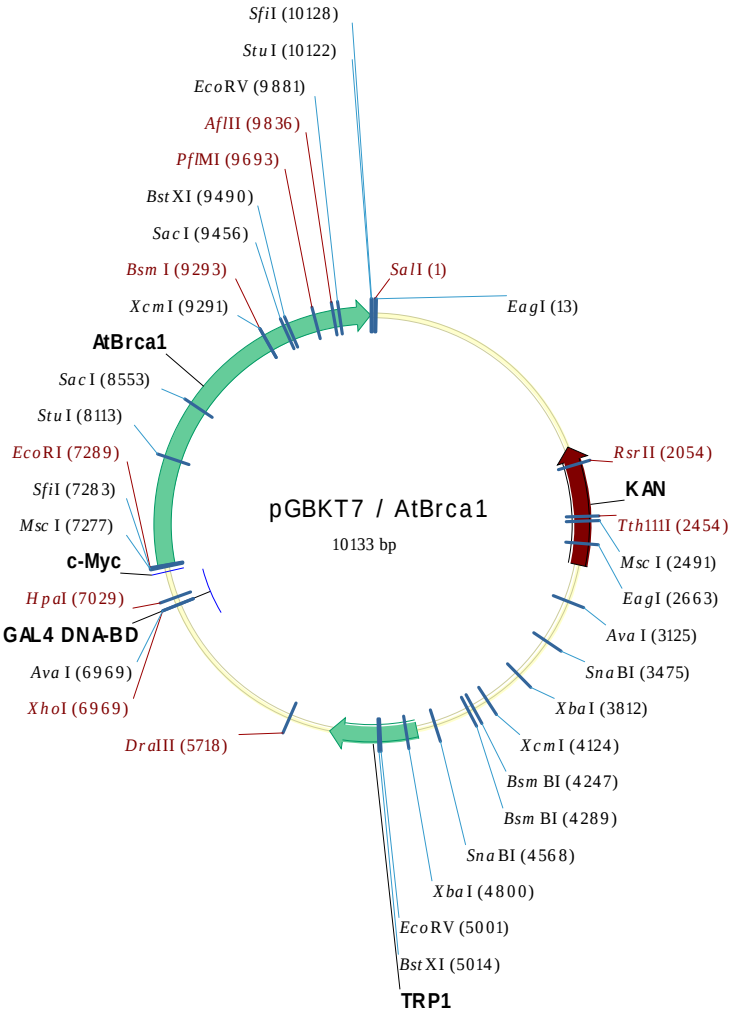
pGBKT7 / AtBrca1
10133 bp
SfiI (10128)
StuI (10122)
EcoRV (9881)
AflII (9836)
PflMI (9693)
BstXI (9490)
SacI (9456)
BsmI (9293)
XcmI (9291)
SalI (1)
EagI (13)
AtBrca1
SacI (8553)
StuI (8113)
EcoRI (7289)
SfiI (7283)
MscI (7277)
c-Myc
HpaI (7029)
GAL4 DNA-BD
AvaI (6969)
XhoI (6969)
DraIII (5718)
RsrII (2054)
KAN
Tth111I (2454)
MscI (2491)
EagI (2663)
AvaI (3125)
SnaBI (3475)
XbaI (3812)
XcmI (4124)
BsmBI (4247)
BsmBI (4289)
SnaBI (4568)
XbaI (4800)
EcoRV (5001)
BstXI (5014)
TRP1

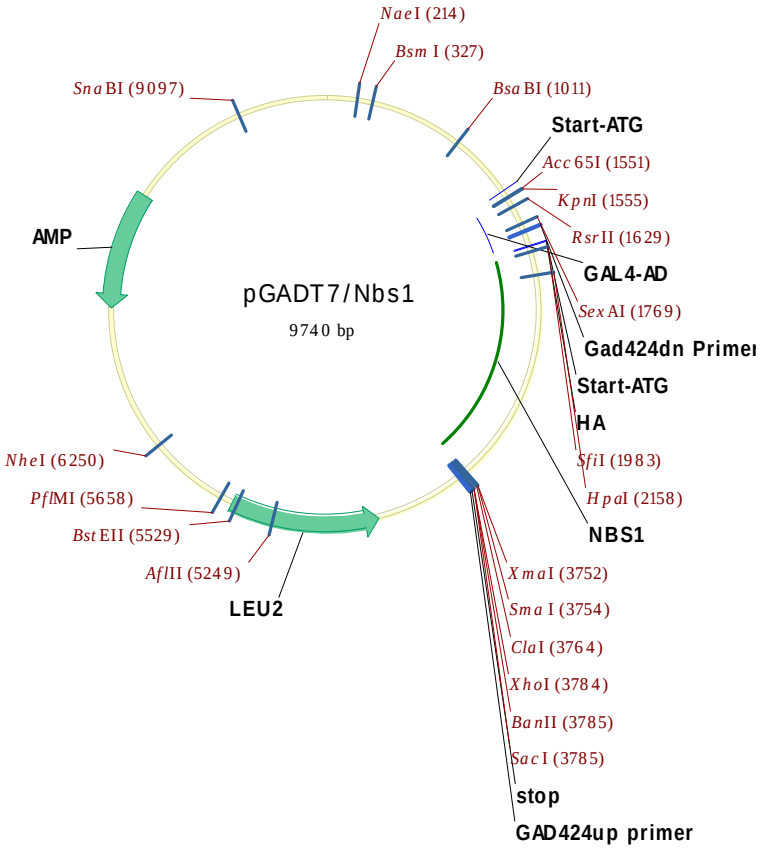
NaeI (214)
BsmI (327)
SnaBI (9097)
BsaBI (1011)
Start-ATG
Acc65I (1551)
KpnI (1555)
RsrII (1629)
AMP
GAL4-AD
pGADT7/Nbs1
9740 bp
SexAI (1769)
Gad424dn Primer
Start-ATG
HA
SfiI (1983)
NheI (6250)
HpaI (2158)
PflMI (5658)
NBS1
BstEII (5529)
AflII (5249)
XmaI (3752)
LEU2
SmaI (3754)
ClaI (3764)
XhoI (3784)
BanII (3785)
SacI (3785)
stop
GAD424up primer

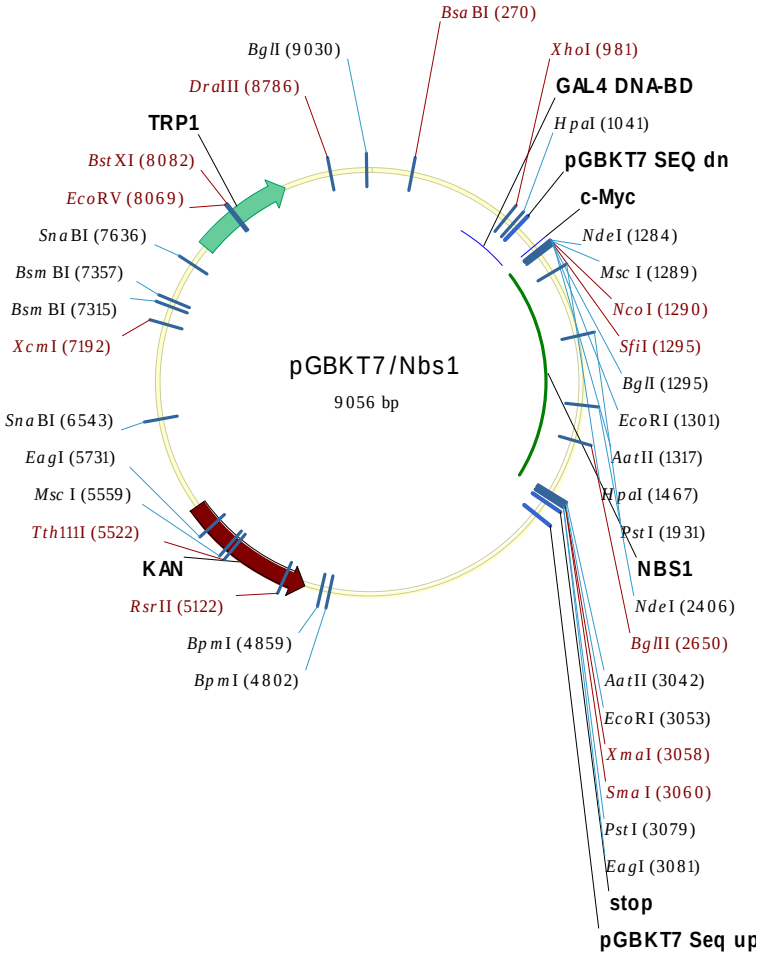
BsaBI (270)
BglI (9030)
XhoI (981)
DraIII (8786)
GAL4 DNA-BD
TRP1
HpaI (1041)
pGBKT7 SEQ dn
BstXI (8082)
c-Myc
EcoRV (8069)
NdeI (1284)
SnaBI (7636)
MscI (1289)
BsmBI (7357)
NcoI (1290)
BsmBI (7315)
SfiI (1295)
XcmI (7192)
pGBKT7/Nbs1
9056 bp
BglI (1295)
EcoRI (1301)
SnaBI (6543)
AatII (1317)
EagI (5731)
HpaI (1467)
MscI (5559)
PstI (1931)
Tth111I (5522)
NBS1
KAN
NdeI (2406)
RsrII (5122)
BglII (2650)
BpmI (4859)
AatII (3042)
BpmI (4802)
EcoRI (3053)
XmaI (3058)
SmaI (3060)
PstI (3079)
EagI (3081)
stop
pGBKT7 Seq up

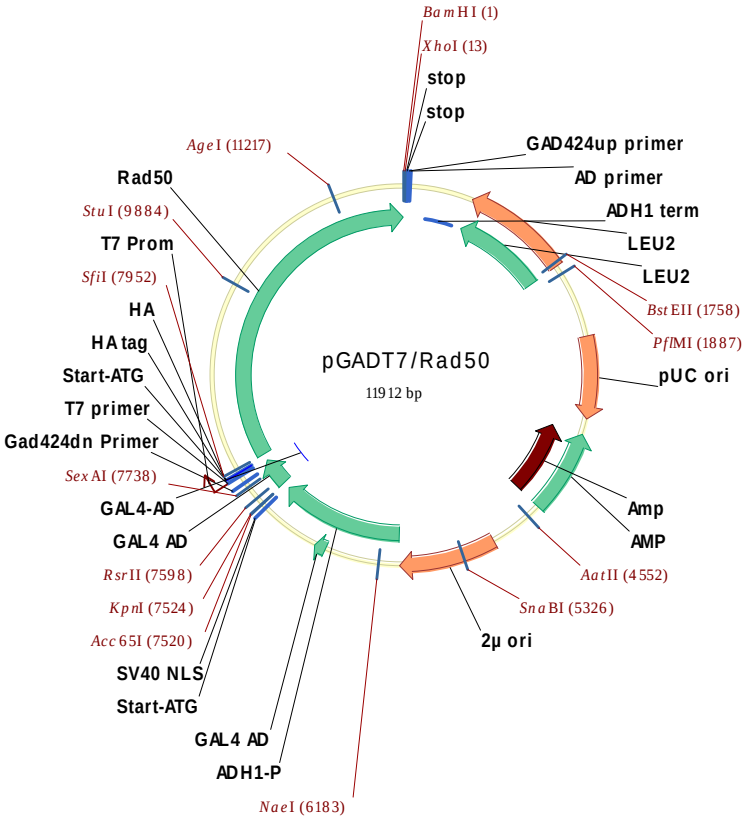
BamHI (1)
XhoI (13)
stop
stop
GAD424up primer
AD primer
ADH1 term
LEU2
LEU2
BstEII (1758)
PflMI (1887)
pUC ori
Amp
AMP
AatII (4552)
SnaBI (5326)
2µ ori
NaeI (6183)
ADH1-P
GAL4 AD
Start-ATG
SV40 NLS
Acc65I (7520)
KpnI (7524)
RsrII (7598)
GAL4 AD
GAL4-AD
SexAI (7738)
Gad424dn Primer
T7 primer
Start-ATG
HA tag
HA
SfiI (7952)
T7 Prom
Stu I (9884)
Rad50
AgeI (11217)
pGADT7/Rad50
11912 bp

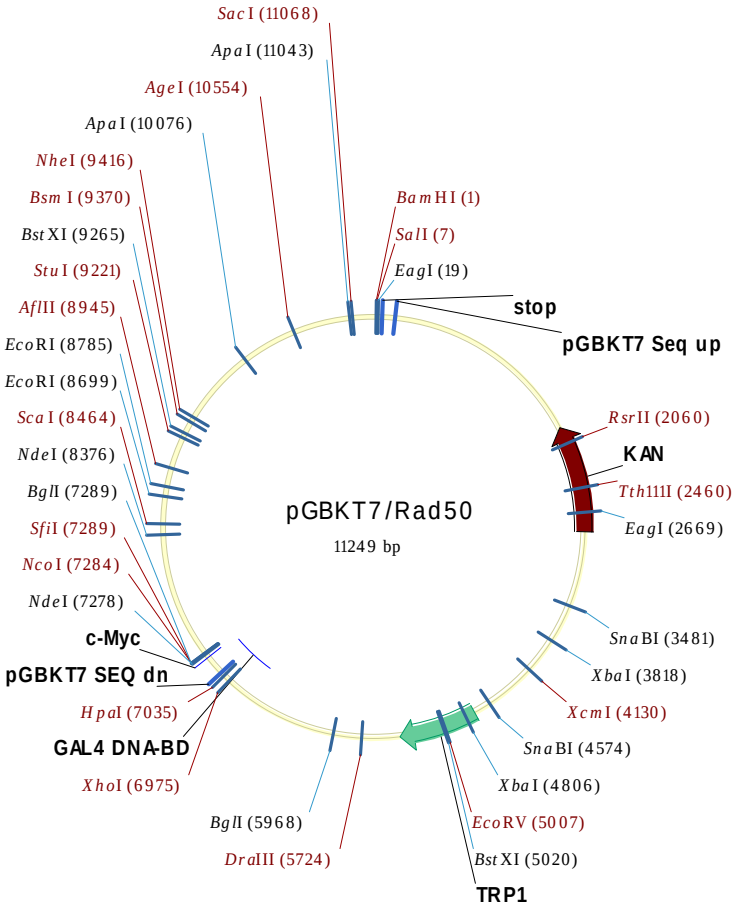
SacI (11068)
ApaI (11043)
AgeI (10554)
ApaI (10076)
NheI (9416)
Bsm I (9370)
BstXI (9265)
Stu I (9221)
AflII (8945)
EcoRI (8785)
EcoRI (8699)
Sca I (8464)
NdeI (8376)
BglII (7289)
SfiI (7289)
NcoI (7284)
NdeI (7278)
c-Myc
pGBKT7 SEQ dn
HpaI (7035)
GAL4 DNA-BD
XhoI (6975)
BglII (5968)
DraIII (5724)
TRP1
BstXI (5020)
EcoRV (5007)
XbaI (4806)
SnaBI (4574)
XcmI (4130)
XbaI (3818)
SnaBI (3481)
EagI (2669)
Tth111I (2460)
KAN
RsrII (2060)
pGBKT7 Seq up
stop
EagI (19)
SalI (7)
BamHI (1)
pGBKT7/Rad50
11249 bp

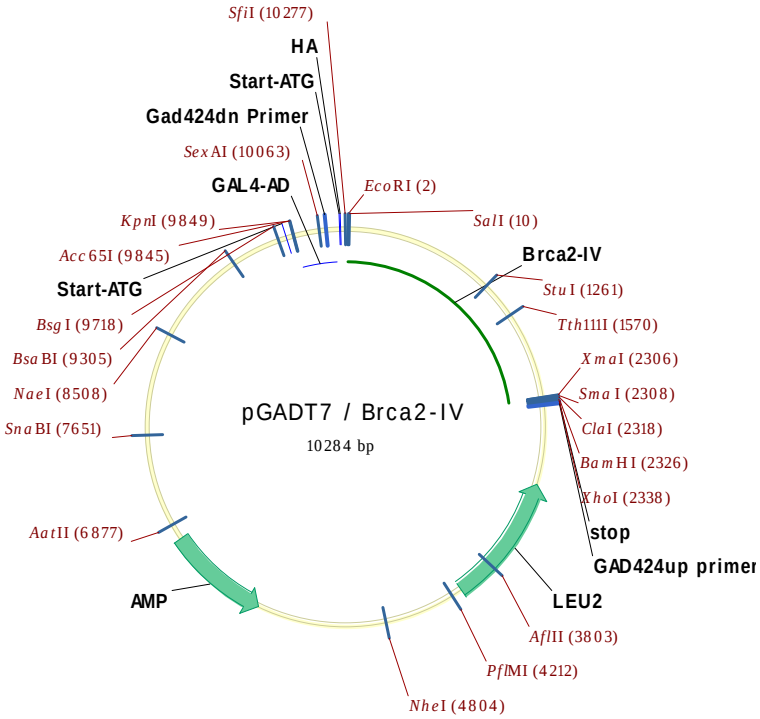
SfiI (10277)
HA
Start-ATG
Gad424dn Primer
SexAI (10063)
GAL4-AD
EcoRI (2)
KpnI (9849)
SalI (10)
Acc65I (9845)
Brca2-IV
Start-ATG
StuI (1261)
Tth111I (1570)
BsgI (9718)
BsaBI (9305)
XmaI (2306)
NaeI (8508)
SmaI (2308)
pGADT7 / Brca2-IV
SnaBI (7651)
10284 bp
ClaI (2318)
BamHI (2326)
XhoI (2338)
AatII (6877)
stop
GAD424up primer
AMP
LEU2
AflII (3803)
PflMI (4212)
NheI (4804)

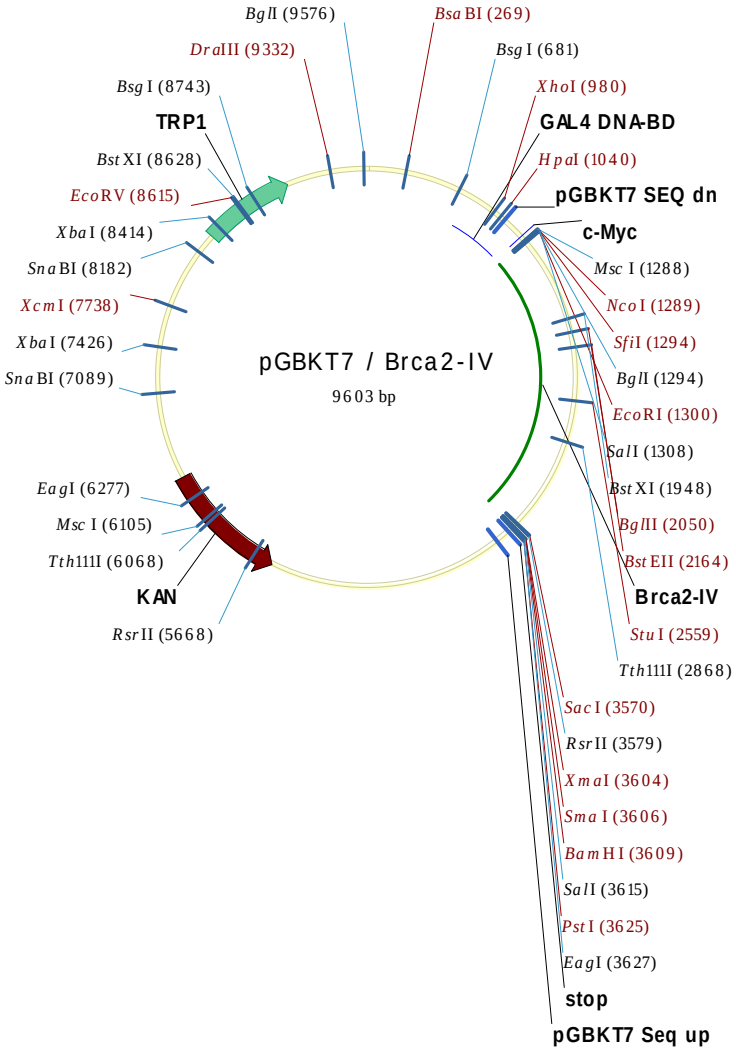
BglI (9576)
BsaBI (269)
DraIII (9332)
BsgI (681)
BsgI (8743)
XhoI (980)
TRP1
GAL4 DNA-BD
BstXI (8628)
HpaI (1040)
EcoRV (8615)
pGBKT7 SEQ dn
XbaI (8414)
c-Myc
SnaBI (8182)
MscI (1288)
XcmI (7738)
NcoI (1289)
XbaI (7426)
SfiI (1294)
pGBKT7 / Brca2-IV
SnaBI (7089)
BglI (1294)
9603 bp
EcoRI (1300)
SalI (1308)
EagI (6277)
BstXI (1948)
MscI (6105)
BglII (2050)
Tth111I (6068)
BstEII (2164)
KAN
Brca2-IV
RsrII (5668)
StuI (2559)
Tth111I (2868)
SacI (3570)
RsrII (3579)
XmaI (3604)
SmaI (3606)
BamHI (3609)
SalI (3615)
PstI (3625)
EagI (3627)
stop
pGBKT7 Seq up

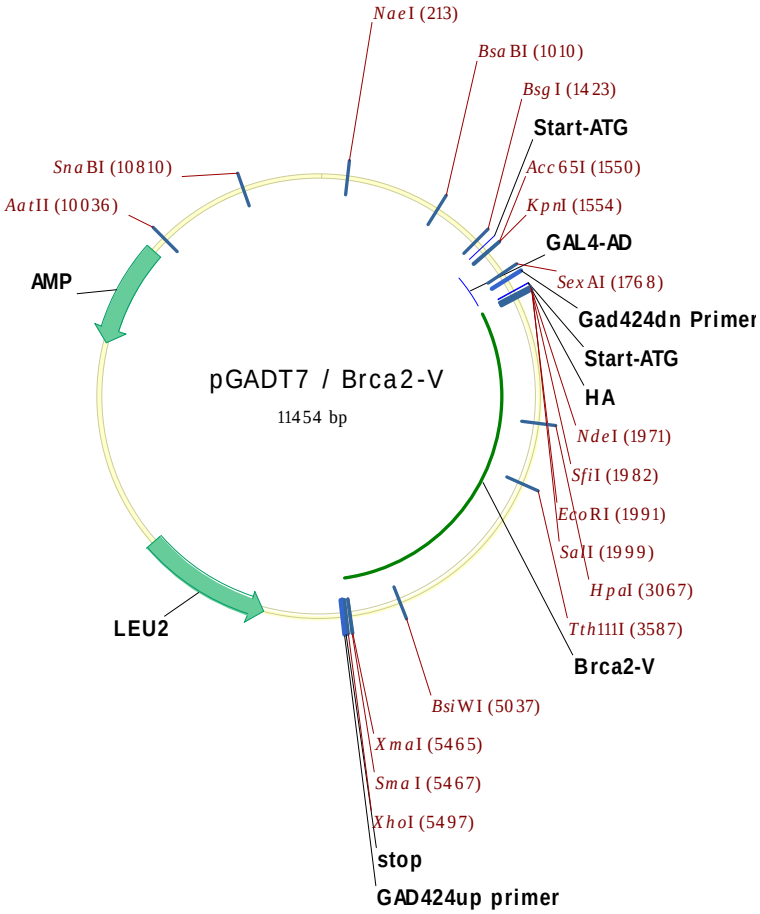
NaeI (213)
BsaBI (1010)
BsgI (1423)
Start-ATG
Acc65I (1550)
KpnI (1554)
GAL4-AD
SexAI (1768)
Gad424dn Primer
Start-ATG
HA
NdeI (1971)
SfiI (1982)
EcoRI (1991)
SalI (1999)
HpaI (3067)
Tth111I (3587)
Brca2-V
BsiWI (5037)
XmaI (5465)
SmaI (5467)
XhoI (5497)
stop
GAD424up primer
SnaBI (10810)
AatII (10036)
AMP
LEU2
pGADT7 / Brca2-V
11454 bp

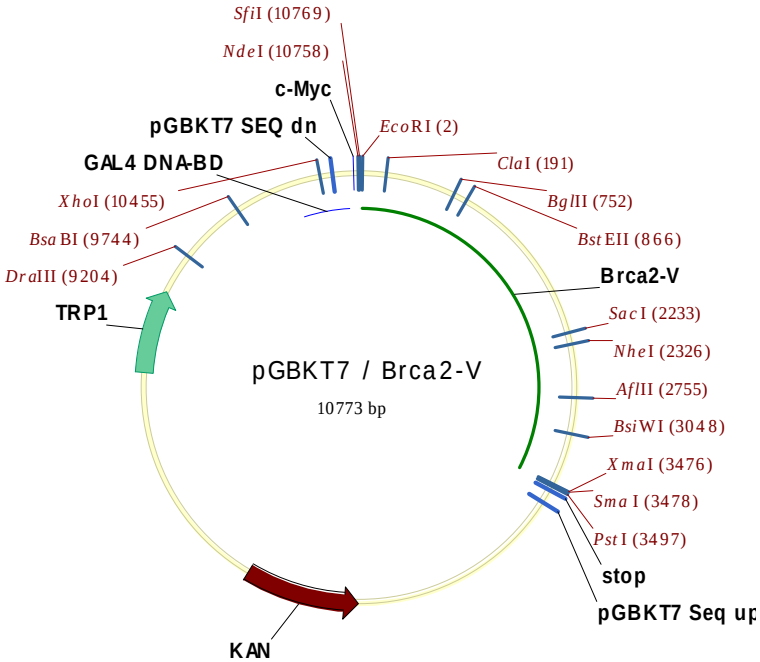
SfiI (10769)
NdeI (10758)
c-Myc
pGBKT7 SEQ dn
EcoRI (2)
ClaI (191)
BglII (752)
BstEII (866)
Brca2-V
SacI (2233)
NheI (2326)
AflII (2755)
BsiWI (3048)
XmaI (3476)
SmaI (3478)
PstI (3497)
stop
pGBKT7 Seq up
GAL4 DNA-BD
XhoI (10455)
BsaBI (9744)
DraIII (9204)
TRP1
KAN
pGBKT7 / Brca2-V
10773 bp

13.3. Cytology

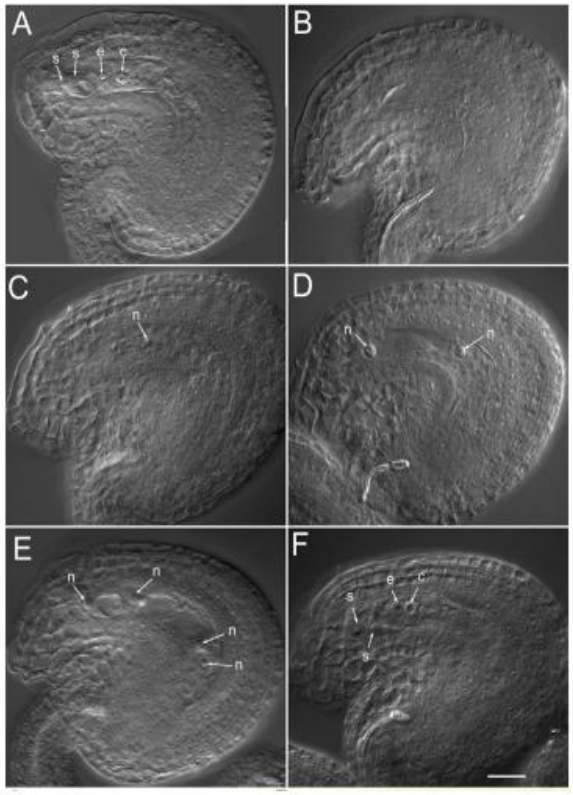

S1: Female and male gametogenesis is disrupted in *Atmnd1* mutants. Mature ovule of wild-type (A) and *Atmnd1* (B to F) were cleared according to Motamator et al. (2000). In *Arabidopsis* ovules three out of the four spores degenerate immediately after meiosis. The one remaining (the functional megaspore) proceeds to three mitotic divisions, giving rise to eight cells. One of them is the egg cell, the central cell arises after fusion of two haploid nuclei, and there are two are synergid cells, whereas the three remaining, the antipodal cells, degenerate before the end of gametophyte development. Thus, in the wild-type, the mature embryo sac (the female gametophyte) contains the egg cell, the central cell and two synergid cells (A). In *Atmnd1* mutants 94.8% of the mature ovules contained an aborted embryo sac (B) or a single cell instead of the embryo sac (C). 2.8% of the embryo sacs were blocked at an intermediate developmental stage after one or two mitotic divisions (D and E). 2.4% of *Atmnd1* mutant ovules were indistinguishable from the wild-type, containing an apparently functional embryo sac (F). e, egg cell; c, central cell; s, synergid cell; n, nucleus.

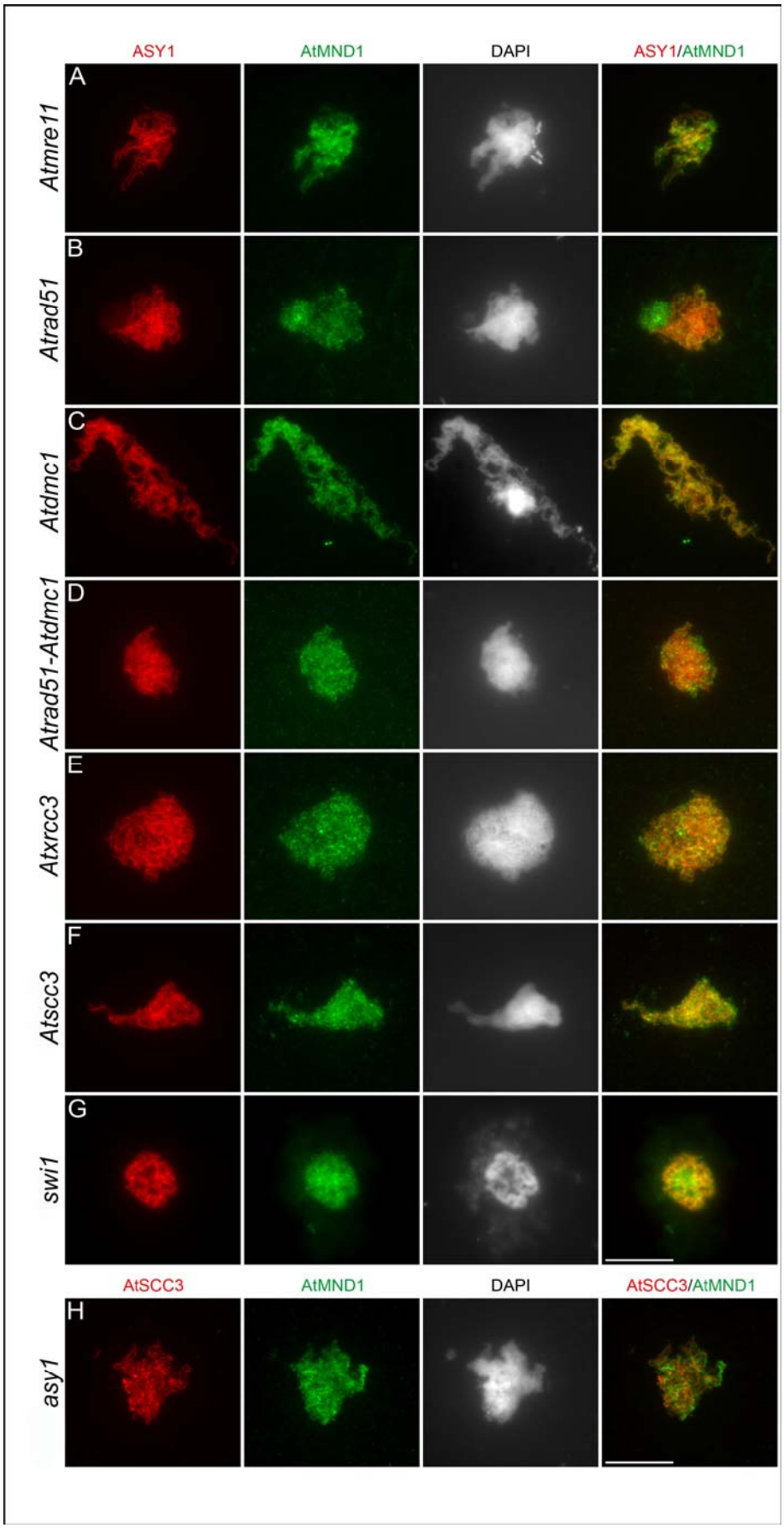

Supplementary figure S2: Immunolocalization of anti-AtMND1 in different meiotic mutants. Scale bar 10µm. Experiment done by Julien Vignard.

14. Acknowledgements

Als erstes möchte ich mich bei meinem Betreuer Peter Schlögelhofer bedanken, der immer ein offenes Ohr für meine wirren Gedanken und meine cytologischen Erkenntnisse hatte. Auch möchte ich mich für seine Unterstützung und sein Verständnis für meinen kleinen Privat-Zoo und den damit verbundenen Problemen bedanken.

Mein Dank geht auch an meine lieben Laborkollegen, mit denen ich vor allem lustige Zeiten durchlebt habe. Tesi, Clemens, Fritz, Müchi, Stefan, Bernd und allen anderen. So ein Arbeitsumfeld kann man sich nur wünschen.

Mein Dank gilt auch Personen, die nichts mit dieser Arbeit direkt zu tun hatten, mich aber bis hierhin begleitet haben. Meinen Eltern und meinem Freund Matthias, der zwar keine Ahnung von Genetik hat, sich aber trotzdem bemühte meine arbeitstechnischen Problemchen zu verstehen ;-).

15. Curriculum vitae

Personal data

Name:	Tanja Siwiec
Date of birth:	August 20, 1977; Vienna, Austria
Nationality:	Austrian
Martial status:	unmarried
Private Address:	Bubergasse 2A/10/7, A-1210 Vienna
E-mail:	tanja.siwiec@univie.ac.at

Education

1983-1987	Primary School, Oswald-Redlich Strasse, 1210 Vienna
1987-1995	Secondary School BG/BRG Franklinstrasse 26, 1210 Vienna
June, 1995	School leaving examination
1995-2009	Study at the University of Vienna
Study:	10/1995-02/1997, study of History of Art 03/1997-10/1997, study of Psychology 10/1997, study of Biology/Genetics
Elective subject:	Study of molecular genetics and pathology
Diploma thesis:	Institute of Cancer Research, Vienna, Tutor Prof. Dr. Wolfgang Mikulits, from March 2003 to May 2004
Title of diploma thesis**:**	**IRES driven translation control in late stage liver tumorigenesis**
December, 2004	final diploma examination
Dissertation:	University of Vienna, Max Perutz Laboratories, Institute of Chromosomebiology; Tutor Prof. Dieter Schweizer and Dr. Peter Schlögelhofer; from April 2005 to April 2009
Title of dissertation:	**Meiotic DNA repair in *Arabidopsis thaliana*: Characterisation of the *Arabidopsis thaliana* homologues of *MND1* and *COM1***

Publications:

1. Dean P, Siwiec T, Waterworth W, Schlogelhofer P, Armstrong S, West C.
A novel ATM dependent X-ray inducible gene is essential for both plant meiosis and gametogenesis. The Plant Journal, Accepted Jan. 2009

2. Uanschou C, Siwiec T, Pedrosa-Harand A, Kerzendorfer C, Sanchez-Moran E, Novatchkova M, Akimcheva S, Woglar A, Klein F, Schlögelhofer P.
A novel plant gene essential for meiosis is related to the human CtIP and the yeast COM1/SAE2 gene. EMBO J. 2007 Dec 12;26(24):5061-70. Epub 2007 Nov 15.

3. Vignard J, Siwiec T, Chelysheva L, Vrielynck N, Gonord F, Armstrong SJ, Schlögelhofer P, Mercier R.
The interplay of RecA-related proteins and the MND1-HOP2 complex during meiosis in *Arabidopsis thaliana*. PLoS Genet. 2007 Oct;3(10):1894-906. Epub 2007 Aug 30.

4. Petz M, Kozina D, Huber H, Siwiec T, Seipelt J, Sommergruber W, Mikulits W.
The leader region of Laminin B1 mRNA confers cap-independent translation. Nucleic Acids Res. 2007;35(8):2473-82. Epub 2007 Mar 29.

5. Kerzendorfer C, Vignard J, Pedrosa-Harand A, Siwiec T, Akimcheva S, Jolivet S, Sablowski R, Armstrong S, Schweizer D, Mercier R, Schlögelhofer P.
The *Arabidopsis thaliana* MND1 homologue plays a key role in meiotic homologous pairing, synapsis and recombination. J Cell Sci. 2006 Jun 15;119(Pt 12):2486-96.

16. References

Abe, K., Osakabe, K., Nakayama, S., Endo, M., Tagiri, A., Todoriki, S., Ichikawa, H., and Toki, S. (2005). Arabidopsis RAD51C gene is important for homologous recombination in meiosis and mitosis. Plant Physiol *139*, 896-908.

Aboussekhra, A., Chanet, R., Adjiri, A., and Fabre, F. (1992). Semidominant suppressors of Srs2 helicase mutations of Saccharomyces cerevisiae map in the RAD51 gene, whose sequence predicts a protein with similarities to procaryotic RecA proteins. Mol Cell Biol *12*, 3224-3234.

Ajimura, M., Leem, S.H., and Ogawa, H. (1993). Identification of new genes required for meiotic recombination in Saccharomyces cerevisiae. Genetics *133*, 51-66.

Alani, E., Padmore, R., and Kleckner, N. (1990). Analysis of wild-type and rad50 mutants of yeast suggests an intimate relationship between meiotic chromosome synapsis and recombination. Cell *61*, 419-436.

Alexander, M.P. (1969). Differential staining of aborted and nonaborted pollen. Stain Technol *44*, 117-122.

Allers, T., and Lichten, M. (2001). Intermediates of yeast meiotic recombination contain heteroduplex DNA. Mol Cell *8*, 225-231.

Alonso, J.M., Stepanova, A.N., Leisse, T.J., Kim, C.J., Chen, H., Shinn, P., Stevenson, D.K., Zimmerman, J., Barajas, P., Cheuk, R.*, et al.* (2003). Genome-wide insertional mutagenesis of Arabidopsis thaliana. Science *301*, 653-657.

Altschul, S.F., Madden, T.L., Schaffer, A.A., Zhang, J., Zhang, Z., Miller, W., and Lipman, D.J. (1997). Gapped BLAST and PSI-BLAST: a new generation of protein database search programs. Nucleic Acids Res *25*, 3389-3402.

Anderson, L.K., Offenberg, H.H., Verkuijlen, W.M., and Heyting, C. (1997). RecA-like proteins are components of early meiotic nodules in lily. Proc Natl Acad Sci U S A *94*, 6868-6873.

Armstrong, S.J., Caryl, A.P., Jones, G.H., and Franklin, F.C. (2002). Asy1, a protein required for meiotic chromosome synapsis, localizes to axis-associated chromatin in Arabidopsis and Brassica. J Cell Sci *115*, 3645-3655.

Armstrong, S.J., Franklin, F.C., and Jones, G.H. (2001). Nucleolus-associated telomere clustering and pairing precede meiotic chromosome synapsis in Arabidopsis thaliana. J Cell Sci *114*, 4207-4217.

Assenmacher, N., and Hopfner, K.P. (2004). MRE11/RAD50/NBS1: complex activities. Chromosoma *113*, 157-166.

Bai, X., Peirson, B.N., Dong, F., Xue, C., and Makaroff, C.A. (1999). Isolation and characterization of SYN1, a RAD21-like gene essential for meiosis in Arabidopsis. Plant Cell *11*, 417-430.

Baroni, E., Viscardi, V., Cartagena-Lirola, H., Lucchini, G., and Longhese, M.P. (2004). The functions of budding yeast Sae2 in the DNA damage response require Mec1- and Tel1-dependent phosphorylation. Mol Cell Biol *24*, 4151-4165.

Basile, F., Sandonato, L., Robulotta, S., Costa, N., Saglimbene, F., and Aurite, M. (1992a). [Diagnosis and treatment of pancreatic pseudocysts]. Minerva Chir *47*, 307-310.

Basile, G., Aker, M., and Mortimer, R.K. (1992b). Nucleotide sequence and transcriptional regulation of the yeast recombinational repair gene RAD51. Mol Cell Biol *12*, 3235-3246.

Bender, C.F., Sikes, M.L., Sullivan, R., Huye, L.E., Le Beau, M.M., Roth, D.B., Mirzoeva, O.K., Oltz, E.M., and Petrini, J.H. (2002). Cancer predisposition and hematopoietic failure in Rad50(S/S) mice. Genes Dev *16*, 2237-2251.

Bergerat, A., de Massy, B., Gadelle, D., Varoutas, P.C., Nicolas, A., and Forterre, P. (1997). An atypical topoisomerase II from Archaea with implications for meiotic recombination. Nature *386*, 414-417.

Bhaskara, V., Dupre, A., Lengsfeld, B., Hopkins, B.B., Chan, A., Lee, J.H., Zhang, X., Gautier, J., Zakian, V., and Paull, T.T. (2007). Rad50 adenylate kinase activity regulates DNA tethering by Mre11/Rad50 complexes. Mol Cell *25*, 647-661.

Bhatt, A.M., Lister, C., Page, T., Fransz, P., Findlay, K., Jones, G.H., Dickinson, H.G., and Dean, C. (1999). The DIF1 gene of Arabidopsis is required for meiotic chromosome segregation and belongs to the REC8/RAD21 cohesin gene family. Plant J *19*, 463-472.

Bianco, P.R., Tracy, R.B., and Kowalczykowski, S.C. (1998). DNA strand exchange proteins: a biochemical and physical comparison. Front Biosci *3*, D570-603.

Birrell, G.W., Brown, J.A., Wu, H.I., Giaever, G., Chu, A.M., Davis, R.W., and Brown, J.M. (2002). Transcriptional response of Saccharomyces cerevisiae to DNA-damaging agents does not identify the genes that protect against these agents. Proc Natl Acad Sci U S A *99*, 8778-8783.

Bishop, D.K. (1994). RecA homologs Dmc1 and Rad51 interact to form multiple nuclear complexes prior to meiotic chromosome synapsis. Cell *79*, 1081-1092.

Bishop, D.K., Ear, U., Bhattacharyya, A., Calderone, C., Beckett, M., Weichselbaum, R.R., and Shinohara, A. (1998). Xrcc3 is required for assembly of Rad51 complexes in vivo. J Biol Chem *273*, 21482-21488.

Bishop, D.K., Park, D., Xu, L., and Kleckner, N. (1992). DMC1: a meiosis-specific yeast homolog of E. coli recA required for recombination, synaptonemal complex formation, and cell cycle progression. Cell *69*, 439-456.

Blat, Y., Protacio, R.U., Hunter, N., and Kleckner, N. (2002). Physical and functional interactions among basic chromosome organizational features govern early steps of meiotic chiasma formation. Cell *111*, 791-802.

Bleuyard, J.Y., Gallego, M.E., Savigny, F., and White, C.I. (2005). Differing requirements for the Arabidopsis Rad51 paralogs in meiosis and DNA repair. Plant J *41*, 533-545.

Bleuyard, J.Y., Gallego, M.E., and White, C.I. (2004). The atspo11-1 mutation rescues atxrcc3 meiotic chromosome fragmentation. Plant Mol Biol *56*, 217-224.

Bleuyard, J.Y., Gallego, M.E., and White, C.I. (2006). Recent advances in understanding of the DNA double-strand break repair machinery of plants. DNA Repair (Amst) *5*, 1-12.

Bleuyard, J.Y., and White, C.I. (2004). The Arabidopsis homologue of Xrcc3 plays an essential role in meiosis. EMBO J *23*, 439-449.

Boisvert, F.M., van Koningsbruggen, S., Navascues, J., and Lamond, A.I. (2007). The multifunctional nucleolus. Nat Rev Mol Cell Biol *8*, 574-585.

Borde, V. (2007). The multiple roles of the Mre11 complex for meiotic recombination. Chromosome Res *15*, 551-563.

Brenneman, M.A., Wagener, B.M., Miller, C.A., Allen, C., and Nickoloff, J.A. (2002). XRCC3 controls the fidelity of homologous recombination: roles for XRCC3 in late stages of recombination. Mol Cell *10*, 387-395.

Bugreev, D.V., Golub, E.I., Stasiak, A.Z., Stasiak, A., and Mazin, A.V. (2005). Activation of human meiosis-specific recombinase Dmc1 by Ca2+. J Biol Chem *280*, 26886-26895.

Bundock, P., and Hooykaas, P. (2002). Severe developmental defects, hypersensitivity to DNA-damaging agents, and lengthened telomeres in Arabidopsis MRE11 mutants. Plant Cell *14*, 2451-2462.

Cai, X., Dong, F., Edelmann, R.E., and Makaroff, C.A. (2003). The Arabidopsis SYN1 cohesin protein is required for sister chromatid arm cohesion and homologous chromosome pairing. J Cell Sci *116*, 2999-3007.

Cartagena-Lirola, H., Guerini, I., Viscardi, V., Lucchini, G., and Longhese, M.P. (2006). Budding Yeast Sae2 is an In Vivo Target of the Mec1 and Tel1 Checkpoint Kinases During Meiosis. Cell Cycle *5*, 1549-1559.

Cary, R.B., Chen, F., Shen, Z., and Chen, D.J. (1998). A central region of Ku80 mediates interaction with Ku70 in vivo. Nucleic Acids Res *26*, 974-979.

Caryl, A.P., Armstrong, S.J., Jones, G.H., and Franklin, F.C. (2000). A homologue of the yeast HOP1 gene is inactivated in the Arabidopsis meiotic mutant asy1. Chromosoma *109*, 62-71.

Chelysheva, L., Diallo, S., Vezon, D., Gendrot, G., Vrielynck, N., Belcram, K., Rocques, N., Márquez-Lema, A., Bhatt, A.M., Horlow, C.*, et al.* (2005). AtREC8 and AtSCC3 are essential to the monopolar orientation of the kinetochores during meiosis. J Cell Sci *118*, 4621-4632.

Chen, P.L., Liu, F., Cai, S., Lin, X., Li, A., Chen, Y., Gu, B., Lee, E.Y., and Lee, W.H. (2005). Inactivation of CtIP leads to early embryonic lethality mediated by G1 restraint and to tumorigenesis by haploid insufficiency. Mol Cell Biol *25*, 3535-3542.

Chen, Y.K., Leng, C.H., Olivares, H., Lee, M.H., Chang, Y.C., Kung, W.M., Ti, S.C., Lo, Y.H., Wang, A.H., Chang, C.S.*, et al.* (2004). Heterodimeric complexes of Hop2 and Mnd1 function with Dmc1 to promote meiotic homolog juxtaposition and strand assimilation. Proc Natl Acad Sci U S A *101*, 10572-10577.

Chi, P., San Filippo, J., Sehorn, M.G., Petukhova, G.V., and Sung, P. (2007). Bipartite stimulatory action of the Hop2-Mnd1 complex on the Rad51 recombinase. Genes Dev *21*, 1747-1757.

Clerici, M., Mantiero, D., Lucchini, G., and Longhese, M.P. (2005). The Saccharomyces cerevisiae Sae2 protein promotes resection and bridging of double strand break ends. J Biol Chem *280*, 38631-38638.

Clerici, M., Mantiero, D., Lucchini, G., and Longhese, M.P. (2006). The Saccharomyces cerevisiae Sae2 protein negatively regulates DNA damage checkpoint signalling. EMBO Rep *7*, 212-218.

Connelly, J.C., and Leach, D.R. (2002). Tethering on the brink: the evolutionarily conserved Mre11-Rad50 complex. Trends Biochem Sci *27*, 410-418.

Costantini, S., Woodbine, L., Andreoli, L., Jeggo, P.A., and Vindigni, A. (2007). Interaction of the Ku heterodimer with the DNA ligase IV/Xrcc4 complex and its regulation by DNA-PK. DNA Repair (Amst) *6*, 712-722.

Couteau, F., Belzile, F., Horlow, C., Grandjean, O., Vezon, D., and Doutriaux, M.P. (1999). Random chromosome segregation without meiotic arrest in both male and female meiocytes of a dmc1 mutant of Arabidopsis. Plant Cell *11*, 1623-1634.

Critchlow, S.E., Bowater, R.P., and Jackson, S.P. (1997). Mammalian DNA double-strand break repair protein XRCC4 interacts with DNA ligase IV. Curr Biol *7*, 588-598.

D'Amours, D., and Jackson, S.P. (2002). The Mre11 complex: at the crossroads of dna repair and checkpoint signalling. Nat Rev Mol Cell Biol *3*, 317-327.

Dahm, K. (2007). Functions and regulation of human artemis in double strand break repair. J Cell Biochem *100*, 1346-1351.

de Jager, M., van Noort, J., van Gent, D.C., Dekker, C., Kanaar, R., and Wyman, C. (2001). Human Rad50/Mre11 is a flexible complex that can tether DNA ends. Mol Cell *8*, 1129-1135.

DeFazio, L.G., Stansel, R.M., Griffith, J.D., and Chu, G. (2002). Synapsis of DNA ends by DNA-dependent protein kinase. EMBO J *21*, 3192-3200.

Deng, C., Brown, J.A., You, D., and Brown, J.M. (2005). Multiple endonucleases function to repair covalent topoisomerase I complexes in Saccharomyces cerevisiae. Genetics *170*, 591-600.

Dernburg, A.F., McDonald, K., Moulder, G., Barstead, R., Dresser, M., and Villeneuve, A.M. (1998). Meiotic recombination in C. elegans initiates by a conserved mechanism and is dispensable for homologous chromosome synapsis. Cell *94*, 387-398.

Deveaux, Y., Alonso, B., Pierrugues, O., Godon, C., and Kazmaier, M. (2000). Molecular cloning and developmental expression of AtGR1, a new growth-related Arabidopsis gene strongly induced by ionizing radiation. Radiat Res *154*, 355-364.

Douglas, P., Gupta, S., Morrice, N., Meek, K., and Lees-Miller, S.P. (2005). DNA-PK-dependent phosphorylation of Ku70/80 is not required for non-homologous end joining. DNA Repair (Amst) *4*, 1006-1018.

Doutriaux, M.P., Couteau, F., Bergounioux, C., and White, C.I. (1998). Isolation and characterisation of the RAD51 and DMC1 homologs from Arabidopsis thaliana. Mol Gen Genet *257*, 283-291.

Dray, E., Siaud, N., Dubois, E., and Doutriaux, M.P. (2006). Interaction between Arabidopsis Brca2 and its partners Rad51, Dmc1, and Dss1. Plant Physiol *140*, 1059-1069.

Dresser, M.E., Ewing, D.J., Conrad, M.N., Dominguez, A.M., Barstead, R., Jiang, H., and Kodadek, T. (1997). DMC1 functions in a Saccharomyces cerevisiae meiotic pathway that is largely independent of the RAD51 pathway. Genetics *147*, 533-544.

Dubin, M.J., Stokes, P.H., Sum, E.Y., Williams, R.S., Valova, V.A., Robinson, P.J., Lindeman, G.J., Glover, J.N., Visvader, J.E., and Matthews, J.M. (2004). Dimerization of CtIP, a BRCA1- and CtBP-interacting protein, is mediated by an N-terminal coiled-coil motif. J Biol Chem *279*, 26932-26938.

Dudas, A., and Chovanec, M. (2004). DNA double-strand break repair by homologous recombination. Mutat Res *566*, 131-167.

Dumon-Jones, V., Frappart, P.O., Tong, W.M., Sajithlal, G., Hulla, W., Schmid, G., Herceg, Z., Digweed, M., and Wang, Z.Q. (2003). Nbn heterozygosity renders mice susceptible to tumor formation and ionizing radiation-induced tumorigenesis. Cancer Res *63*, 7263-7269.

Enomoto, R., Kinebuchi, T., Sato, M., Yagi, H., Kurumizaka, H., and Yokoyama, S. (2006). Stimulation of DNA strand exchange by the human TBPIP/Hop2-Mnd1 complex. J Biol Chem *281*, 5575-5581.

Enomoto, R., Kinebuchi, T., Sato, M., Yagi, H., Shibata, T., Kurumizaka, H., and Yokoyama, S. (2004). Positive role of the mammalian TBPIP/HOP2 protein in DMC1-mediated homologous pairing. J Biol Chem *279*, 35263-35272.

Fernandez-Capetillo, O., Lee, A., Nussenzweig, M., and Nussenzweig, A. (2004). H2AX: the histone guardian of the genome. DNA Repair (Amst) *3*, 959-967.

Foray, N., Marot, D., Gabriel, A., Randrianarison, V., Carr, A.M., Perricaudet, M., Ashworth, A., and Jeggo, P.A. (2003). A subset of ATM- and ATR-dependent phosphorylation events requires the BRCA1 protein. Embo J *22*, 2860-2871.

Forget, A.L., Bennett, B.T., and Knight, K.L. (2004). Xrcc3 is recruited to DNA double strand breaks early and independent of Rad51. J Cell Biochem *93*, 429-436.

Franklin, A.E., McElver, J., Sunjevaric, I., Rothstein, R., Bowen, B., and Cande, W.Z. (1999). Three-dimensional microscopy of the Rad51 recombination protein during meiotic prophase. Plant Cell *11*, 809-824.

Friesner, J., and Britt, A.B. (2003). Ku80- and DNA ligase IV-deficient plants are sensitive to ionizing radiation and defective in T-DNA integration. Plant J *34*, 427-440.

Friesner, J.D., Liu, B., Culligan, K., and Britt, A.B. (2005). Ionizing radiation-dependent gamma-H2AX focus formation requires ataxia telangiectasia mutated and ataxia telangiectasia mutated and Rad3-related. Mol Biol Cell *16*, 2566-2576.

Fusco, C., Reymond, A., and Zervos, A.S. (1998). Molecular cloning and characterization of a novel retinoblastoma-binding protein. Genomics *51*, 351-358.

Gallego, M.E., Bleuyard, J.Y., Daoudal-Cotterell, S., Jallut, N., and White, C.I. (2003). Ku80 plays a role in non-homologous recombination but is not required for T-DNA integration in Arabidopsis. Plant J *35*, 557-565.

Garcia, V., Bruchet, H., Camescasse, D., Granier, F., Bouchez, D., and Tissier, A. (2003). AtATM is essential for meiosis and the somatic response to DNA damage in plants. Plant Cell *15*, 119-132.

Gell, D., and Jackson, S.P. (1999). Mapping of protein-protein interactions within the DNA-dependent protein kinase complex. Nucleic Acids Res *27*, 3494-3502.

Gerton, J.L., and DeRisi, J.L. (2002). Mnd1p: an evolutionarily conserved protein required for meiotic recombination. Proc Natl Acad Sci U S A *99*, 6895-6900.

Gerton, J.L., and Hawley, R.S. (2005). Homologous chromosome interactions in meiosis: diversity amidst conservation. Nat Rev Genet *6*, 477-487.

Grawunder, U., Zimmer, D., and Leiber, M.R. (1998). DNA ligase IV binds to XRCC4 via a motif located between rather than within its BRCT domains. Curr Biol *8*, 873-876.

Greenberg, R.A., Sobhian, B., Pathania, S., Cantor, S.B., Nakatani, Y., and Livingston, D.M. (2006). Multifactorial contributions to an acute DNA damage response by BRCA1/BARD1-containing complexes. Genes Dev *20*, 34-46.

Grelon, M., Vezon, D., Gendrot, G., and Pelletier, G. (2001). AtSPO11-1 is necessary for efficient meiotic recombination in plants. Embo J *20*, 589-600.

Haber, J.E., and Leung, W.Y. (1996). Lack of chromosome territoriality in yeast: promiscuous rejoining of broken chromosome ends. Proc Natl Acad Sci U S A *93*, 13949-13954.

Habu, T., Taki, T., West, A., Nishimune, Y., and Morita, T. (1996). The mouse and human homologs of DMC1, the yeast meiosis-specific homologous recombination gene, have a common unique form of exon-skipped transcript in meiosis. Nucleic Acids Res *24*, 470-477.

Hartsuiker, E., Mizuno, K., Molnar, M., Kohli, J., Ohta, K., and Carr, A.M. (2009a). Ctp1CtIP and the Rad32Mre11 nuclease activity are required for Rec12Spo11 removal

but Rec12Spo11 removal is dispensable for other MRN-dependent meiotic functions. Mol Cell Biol.

Hartsuiker, E., Neale, M.J., and Carr, A.M. (2009b). Distinct requirements for the Rad32(Mre11) nuclease and Ctp1(CtIP) in the removal of covalently bound topoisomerase I and II from DNA. Mol Cell *33*, 117-123.

Hartung, F., Wurz-Wildersinn, R., Fuchs, J., Schubert, I., Suer, S., and Puchta, H. (2007). The catalytically active tyrosine residues of both SPO11-1 and SPO11-2 are required for meiotic double-strand break induction in Arabidopsis. Plant Cell *19*, 3090-3099.

Higgins, J.D., Sanchez-Moran, E., Armstrong, S.J., Jones, G.H., and Franklin, F.C. (2005). The Arabidopsis synaptonemal complex protein ZYP1 is required for chromosome synapsis and normal fidelity of crossing over. Genes Dev *19*, 2488-2500.

Hollingsworth, N.M., Ponte, L., and Halsey, C. (1995). MSH5, a novel MutS homolog, facilitates meiotic reciprocal recombination between homologs in Saccharomyces cerevisiae but not mismatch repair. Genes Dev *9*, 1728-1739.

Hopfner, K.P., Craig, L., Moncalian, G., Zinkel, R.A., Usui, T., Owen, B.A., Karcher, A., Henderson, B., Bodmer, J.L., McMurray, C.T.*, et al.* (2002). The Rad50 zinc-hook is a structure joining Mre11 complexes in DNA recombination and repair. Nature *418*, 562-566.

Hopfner, K.P., Karcher, A., Shin, D.S., Craig, L., Arthur, L.M., Carney, J.P., and Tainer, J.A. (2000). Structural biology of Rad50 ATPase: ATP-driven conformational control in DNA double-strand break repair and the ABC-ATPase superfamily. Cell *101*, 789-800.

Hsieh, P., Camerini-Otero, C.S., and Camerini-Otero, R.D. (1992). The synapsis event in the homologous pairing of DNAs: RecA recognizes and pairs less than one helical repeat of DNA. Proc Natl Acad Sci U S A *89*, 6492-6496.

Hunter, N., and Kleckner, N. (2001). The single-end invasion: an asymmetric intermediate at the double-strand break to double-holliday junction transition of meiotic recombination. Cell *106*, 59-70.

Huyton, T., Bates, P.A., Zhang, X., Sternberg, M.J., and Freemont, P.S. (2000). The BRCA1 C-terminal domain: structure and function. Mutat Res *460*, 319-332.

Ijichi, H., Tanaka, T., Nakamura, T., Yagi, H., Hakuba, A., and Sato, M. (2000). Molecular cloning and characterization of a human homologue of TBPIP, a BRCA1 locus-related gene. Gene *248*, 99-107.

Ishiguro, K., and Watanabe, Y. (2007). Chromosome cohesion in mitosis and meiosis. J Cell Sci *120*, 367-369.

Ivanov, E.L., Sugawara, N., Fishman-Lobell, J., and Haber, J.E. (1996). Genetic requirements for the single-strand annealing pathway of double-strand break repair in Saccharomyces cerevisiae. Genetics *142*, 693-704.

Jackson, N., Sanchez-Moran, E., Buckling, E., Armstrong, S.J., Jones, G.H., and Franklin, F.C. (2006). Reduced meiotic crossovers and delayed prophase I progression in AtMLH3-deficient Arabidopsis. EMBO J *25*, 1315-1323.

Jessberger, R. (2002). The many functions of SMC proteins in chromosome dynamics. Nat Rev Mol Cell Biol *3*, 767-778.

Johnson, R.D., and Jasin, M. (2001). Double-strand-break-induced homologous recombination in mammalian cells. Biochem Soc Trans *29*, 196-201.

Jones, J.M., Gellert, M., and Yang, W. (2001). A Ku bridge over broken DNA. Structure *9*, 881-884.

Junop, M.S., Modesti, M., Guarne, A., Ghirlando, R., Gellert, M., and Yang, W. (2000). Crystal structure of the Xrcc4 DNA repair protein and implications for end joining. EMBO J *19*, 5962-5970.

Kadyk, L.C., and Hartwell, L.H. (1992). Sister chromatids are preferred over homologs as substrates for recombinational repair in Saccharomyces cerevisiae. Genetics *132*, 387-402.

Keeney, S. (2001). Mechanism and control of meiotic recombination initiation. Curr Top Dev Biol *52*, 1-53.

Keeney, S., Giroux, C.N., and Kleckner, N. (1997). Meiosis-specific DNA double-strand breaks are catalyzed by Spo11, a member of a widely conserved protein family. Cell *88*, 375-384.

Kerzendorfer, C., Vignard, J., Pedrosa-Harand, A., Siwiec, T., Akimcheva, S., Jolivet, S., Sablowski, R., Armstrong, S., Schweizer, D., Mercier, R.*, et al.* (2006a). The Arabidopsis thaliana MND1 homologue plays a key role in meiotic homologous pairing, synapsis and recombination. J Cell Sci *119*, 2486-2496.

Kerzendorfer, C., Vignard, J., Pedrosa-Harand, A., Siwiec, T., Akimcheva, S., Jolivet, S., Sablowski, R., Armstrong, S., Schweizer, D., Mercier, R.*, et al.* (2006b). The Arabidopsis thaliana MND1 homologue plays a key role in meiotic homologous pairing, synapsis and recombination. J Cell Sci *119*, 2486-2496.

Klimyuk, V.I., and Jones, J.D. (1997). AtDMC1, the Arabidopsis homologue of the yeast DMC1 gene: characterization, transposon-induced allelic variation and meiosis-associated expression. Plant J *11*, 1-14.

Kobayashi, J., Antoccia, A., Tauchi, H., Matsuura, S., and Komatsu, K. (2004). NBS1 and its functional role in the DNA damage response. DNA Repair (Amst) *3*, 855-861.

Kobayashi, J., Tauchi, H., Sakamoto, S., Nakamura, A., Morishima, K., Matsuura, S., Kobayashi, T., Tamai, K., Tanimoto, K., and Komatsu, K. (2002). NBS1 localizes to gamma-H2AX foci through interaction with the FHA/BRCT domain. Curr Biol *12*, 1846-1851.

Kobayashi, T., Kobayashi, E., Sato, S., Hotta, Y., Miyajima, N., Tanaka, A., and Tabata, S. (1994). Characterization of cDNAs induced in meiotic prophase in lily microsporocytes. DNA Res *1*, 15-26.

Krogh, B.O., Llorente, B., Lam, A., and Symington, L.S. (2005). Mutations in Mre11 phosphoesterase motif I that impair Saccharomyces cerevisiae Mre11-Rad50-Xrs2 complex stability in addition to nuclease activity. Genetics *171*, 1561-1570.

Krogh, B.O., and Symington, L.S. (2004). Recombination proteins in yeast. Annu Rev Genet *38*, 233-271.

Kuznetsov, S., Pellegrini, M., Shuda, K., Fernandez-Capetillo, O., Liu, Y., Martin, B.K., Burkett, S., Southon, E., Pati, D., Tessarollo, L.*, et al.* (2007). RAD51C deficiency in mice results in early prophase I arrest in males and sister chromatid separation at metaphase II in females. J Cell Biol *176*, 581-592.

Leu, J.Y., Chua, P.R., and Roeder, G.S. (1998). The meiosis-specific Hop2 protein of S. cerevisiae ensures synapsis between homologous chromosomes. Cell *94*, 375-386.

Li, S., Ting, N.S., Zheng, L., Chen, P.L., Ziv, Y., Shiloh, Y., Lee, E.Y., and Lee, W.H. (2000). Functional link of BRCA1 and ataxia telangiectasia gene product in DNA damage response. Nature *406*, 210-215.

Li, W., Chen, C., Markmann-Mulisch, U., Timofejeva, L., Schmelzer, E., Ma, H., and Reiss, B. (2004). The Arabidopsis AtRAD51 gene is dispensable for vegetative development but required for meiosis. Proc Natl Acad Sci U S A *101*, 10596-10601.

Li, W., Yang, X., Lin, Z., Timofejeva, L., Xiao, R., Makaroff, C.A., and Ma, H. (2005). The AtRAD51C gene is required for normal meiotic chromosome synapsis and double-stranded break repair in Arabidopsis. Plant Physiol *138*, 965-976.

Liang, F., and Jasin, M. (1996). Ku80-deficient cells exhibit excess degradation of extrachromosomal DNA. J Biol Chem *271*, 14405-14411.

Lim, D.S., and Hasty, P. (1996). A mutation in mouse rad51 results in an early embryonic lethal that is suppressed by a mutation in p53. Mol Cell Biol *16*, 7133-7143.

Limbo, O., Chahwan, C., Yamada, Y., de Bruin, R.A., Wittenberg, C., and Russell, P. (2007). Ctp1 is a cell-cycle-regulated protein that functions with Mre11 complex to control double-strand break repair by homologous recombination. Mol Cell *28*, 134-146.

Lisby, M., Barlow, J.H., Burgess, R.C., and Rothstein, R. (2004). Choreography of the DNA damage response: spatiotemporal relationships among checkpoint and repair proteins. Cell *118*, 699-713.

Liu, N., Lamerdin, J.E., Tebbs, R.S., Schild, D., Tucker, J.D., Shen, M.R., Brookman, K.W., Siciliano, M.J., Walter, C.A., Fan, W.*, et al.* (1998). XRCC2 and XRCC3, new human Rad51-family members, promote chromosome stability and protect against DNA cross-links and other damages. Mol Cell *1*, 783-793.

Liu, N., Schild, D., Thelen, M.P., and Thompson, L.H. (2002). Involvement of Rad51C in two distinct protein complexes of Rad51 paralogs in human cells. Nucleic Acids Res *30*, 1009-1015.

Liu, Y., Masson, J.Y., Shah, R., O'Regan, P., and West, S.C. (2004). RAD51C is required for Holliday junction processing in mammalian cells. Science *303*, 243-246.

Liu, Y., Tarsounas, M., O'Regan, P., and West, S.C. (2007). Role of RAD51C and XRCC3 in genetic recombination and DNA repair. J Biol Chem *282*, 1973-1979.

Liu, Z., and Makaroff, C.A. (2006). Arabidopsis separase AESP is essential for embryo development and the release of cohesin during meiosis. Plant Cell *18*, 1213-1225.

Llorente, B., Smith, C.E., and Symington, L.S. (2008). Break-induced replication: what is it and what is it for? Cell Cycle *7*, 859-864.

Llorente, B., and Symington, L.S. (2004). The Mre11 nuclease is not required for 5' to 3' resection at multiple HO-induced double-strand breaks. Mol Cell Biol *24*, 9682-9694.

Lobachev, K.S., Gordenin, D.A., and Resnick, M.A. (2002). The Mre11 complex is required for repair of hairpin-capped double-strand breaks and prevention of chromosome rearrangements. Cell *108*, 183-193.

Luo, G., Yao, M.C., Bender, C.F., Mills, M., Bladl, A.R., Bradley, A., and Petrini, J.H. (1999). Disruption of mRad50 causes embryonic stem cell lethality, abnormal embryonic development, and sensitivity to ionizing radiation. Proc Natl Acad Sci U S A *96*, 7376-7381.

Lydeard, J.R., Jain, S., Yamaguchi, M., and Haber, J.E. (2007). Break-induced replication and telomerase-independent telomere maintenance require Pol32. Nature *448*, 820-823.

Ma, Y., Pannicke, U., Schwarz, K., and Lieber, M.R. (2002). Hairpin opening and overhang processing by an Artemis/DNA-dependent protein kinase complex in nonhomologous end joining and V(D)J recombination. Cell *108*, 781-794.

Malik, S.B., Ramesh, M.A., Hulstrand, A.M., and Logsdon, J.M. (2007). Protist Homologs of the Meiotic Spo11 Gene and Topoisomerase VI reveal an Evolutionary History of Gene Duplication and Lineage-Specific Loss. Mol Biol Evol *24*, 2827-2841.

Malkova, A., Naylor, M.L., Yamaguchi, M., Ira, G., and Haber, J.E. (2005). RAD51-dependent break-induced replication differs in kinetics and checkpoint responses from RAD51-mediated gene conversion. Mol Cell Biol *25*, 933-944.

Mansour, W.Y., Schumacher, S., Rosskopf, R., Rhein, T., Schmidt-Petersen, F., Gatzemeier, F., Haag, F., Borgmann, K., Willers, H., and Dahm-Daphi, J. (2008). Hierarchy of nonhomologous end-joining, single-strand annealing and gene conversion at site-directed DNA double-strand breaks. Nucleic Acids Res *36*, 4088-4098.

Marchler-Bauer, A., Panchenko, A.R., Ariel, N., and Bryant, S.H. (2002). Comparison of sequence and structure alignments for protein domains. Proteins *48*, 439-446.

Mari, P.O., Florea, B.I., Persengiev, S.P., Verkaik, N.S., Bruggenwirth, H.T., Modesti, M., Giglia-Mari, G., Bezstarosti, K., Demmers, J.A., Luider, T.M.*, et al.* (2006). Dynamic assembly of end-joining complexes requires interaction between Ku70/80 and XRCC4. Proc Natl Acad Sci U S A *103*, 18597-18602.

Markmann-Mulisch, U., Wendeler, E., Zobell, O., Schween, G., Steinbiss, H.H., and Reiss, B. (2007). Differential requirements for RAD51 in Physcomitrella patens and Arabidopsis thaliana development and DNA damage repair. Plant Cell *19*, 3080-3089.

Masson, J.Y., Tarsounas, M.C., Stasiak, A.Z., Stasiak, A., Shah, R., McIlwraith, M.J., Benson, F.E., and West, S.C. (2001). Identification and purification of two distinct complexes containing the five RAD51 paralogs. Genes Dev *15*, 3296-3307.

McEachern, M.J., and Haber, J.E. (2006). Break-induced replication and recombinational telomere elongation in yeast. Annu Rev Biochem *75*, 111-135.

McGill, C., Shafer, B., and Strathern, J. (1989). Coconversion of flanking sequences with homothallic switching. Cell *57*, 459-467.

McKee, A.H., and Kleckner, N. (1997). A general method for identifying recessive diploid-specific mutations in Saccharomyces cerevisiae, its application to the isolation

of mutants blocked at intermediate stages of meiotic prophase and characterization of a new gene SAE2. Genetics *146*, 797-816.

McKim, K.S., Jang, J.K., and Manheim, E.A. (2002). Meiotic recombination and chromosome segregation in Drosophila females. Annu Rev Genet *36*, 205-232.

Mercier, R., and Grelon, M. (2008). Meiosis in plants: ten years of gene discovery. Cytogenet Genome Res *120*, 281-290.

Mercier, R., Grelon, M., Vezon, D., Horlow, C., and Pelletier, G. (2001). How to characterize meiotic functions in plants? Biochimie *83*, 1023-1028.

Mimori, T., and Hardin, J.A. (1986). Mechanism of interaction between Ku protein and DNA. J Biol Chem *261*, 10375-10379.

Modesti, M., Junop, M.S., Ghirlando, R., van de Rakt, M., Gellert, M., Yang, W., and Kanaar, R. (2003). Tetramerization and DNA ligase IV interaction of the DNA double-strand break repair protein XRCC4 are mutually exclusive. J Mol Biol *334*, 215-228.

Molinier, J., Stamm, M.E., and Hohn, B. (2004). SNM-dependent recombinational repair of oxidatively induced DNA damage in Arabidopsis thaliana. EMBO Rep *5*, 994-999.

Nabeshima, K., Kakihara, Y., Hiraoka, Y., and Nojima, H. (2001). A novel meiosis-specific protein of fission yeast, Meu13p, promotes homologous pairing independently of homologous recombination. EMBO J *20*, 3871-3881.

Nairz, K., and Klein, F. (1997). mre11S--a yeast mutation that blocks double-strand-break processing and permits nonhomologous synapsis in meiosis. Genes Dev *11*, 2272-2290.

Nakada, D., Hirano, Y., and Sugimoto, K. (2004). Requirement of the Mre11 complex and exonuclease 1 for activation of the Mec1 signaling pathway. Mol Cell Biol *24*, 10016-10025.

Nasmyth, K.A. (1982). Molecular genetics of yeast mating type. Annu Rev Genet *16*, 439-500.

Neale, M.J., and Keeney, S. (2006). Clarifying the mechanics of DNA strand exchange in meiotic recombination. Nature *442*, 153-158.

Neale, M.J., Pan, J., and Keeney, S. (2005). Endonucleolytic processing of covalent protein-linked DNA double-strand breaks. Nature *436*, 1053-1057.

Nick McElhinny, S.A., Snowden, C.M., McCarville, J., and Ramsden, D.A. (2000). Ku recruits the XRCC4-ligase IV complex to DNA ends. Mol Cell Biol *20*, 2996-3003.

Ogawa, T., Yu, X., Shinohara, A., and Egelman, E.H. (1993). Similarity of the yeast RAD51 filament to the bacterial RecA filament. Science *259*, 1896-1899.

Osakabe, K., Yoshioka, T., Ichikawa, H., and Toki, S. (2002). Molecular cloning and characterization of RAD51-like genes from Arabidopsis thaliana. Plant Mol Biol *50*, 71-81.

Paques, F., and Haber, J.E. (1999). Multiple pathways of recombination induced by double-strand breaks in Saccharomyces cerevisiae. Microbiol Mol Biol Rev *63*, 349-404.

Paques, F., Leung, W.Y., and Haber, J.E. (1998). Expansions and contractions in a tandem repeat induced by double-strand break repair. Mol Cell Biol *18*, 2045-2054.

Passy, S.I., Yu, X., Li, Z., Radding, C.M., Masson, J.Y., West, S.C., and Egelman, E.H. (1999). Human Dmc1 protein binds DNA as an octameric ring. Proc Natl Acad Sci U S A *96*, 10684-10688.

Paull, T.T., and Gellert, M. (1999). Nbs1 potentiates ATP-driven DNA unwinding and endonuclease cleavage by the Mre11/Rad50 complex. Genes Dev *13*, 1276-1288.

Penkner, A., Portik-Dobos, Z., Tang, L., Schnabel, R., Novatchkova, M., Jantsch, V., and Loidl, J. (2007). A conserved function for a Caenorhabditis elegans Com1/Sae2/CtIP protein homolog in meiotic recombination. EMBO J *26*, 5071-5082.

Petukhova, G.V., Pezza, R.J., Vanevski, F., Ploquin, M., Masson, J.Y., and Camerini-Otero, R.D. (2005). The Hop2 and Mnd1 proteins act in concert with Rad51 and Dmc1 in meiotic recombination. Nat Struct Mol Biol *12*, 449-453.

Petukhova, G.V., Romanienko, P.J., and Camerini-Otero, R.D. (2003). The Hop2 protein has a direct role in promoting interhomolog interactions during mouse meiosis. Dev Cell *5*, 927-936.

Pezza, R.J., Petukhova, G.V., Ghirlando, R., and Camerini-Otero, R.D. (2006). Molecular activities of meiosis-specific proteins Hop2, Mnd1, and the Hop2-Mnd1 complex. J Biol Chem *281*, 18426-18434.

Pezza, R.J., Voloshin, O.N., Vanevski, F., and Camerini-Otero, R.D. (2007). Hop2/Mnd1 acts on two critical steps in Dmc1-promoted homologous pairing. Genes Dev *21*, 1758-1766.

Pittman, D.L., Cobb, J., Schimenti, K.J., Wilson, L.A., Cooper, D.M., Brignull, E., Handel, M.A., and Schimenti, J.C. (1998). Meiotic prophase arrest with failure of chromosome synapsis in mice deficient for Dmc1, a germline-specific RecA homolog. Mol Cell *1*, 697-705.

Ploquin, M., Petukhova, G.V., Morneau, D., Dery, U., Bransi, A., Stasiak, A., Camerini-Otero, R.D., and Masson, J.Y. (2007). Stimulation of fission yeast and mouse Hop2-Mnd1 of the Dmc1 and Rad51 recombinases. Nucleic Acids Res *35*, 2719-2733.

Prieler, S., Penkner, A., Borde, V., and Klein, F. (2005). The control of Spo11's interaction with meiotic recombination hotspots. Genes Dev *19*, 255-269.

Prinz, S., Amon, A., and Klein, F. (1997). Isolation of COM1, a new gene required to complete meiotic double-strand break-induced recombination in Saccharomyces cerevisiae. Genetics *146*, 781-795.

Puizina, J., Siroky, J., Mokros, P., Schweizer, D., and Riha, K. (2004). Mre11 deficiency in Arabidopsis is associated with chromosomal instability in somatic cells and Spo11-dependent genome fragmentation during meiosis. Plant Cell *16*, 1968-1978.

Rabitsch, K.P., Tóth, A., Gálová, M., Schleiffer, A., Schaffner, G., Aigner, E., Rupp, C., Penkner, A.M., Moreno-Borchart, A.C., Primig, M*., et al.* (2001). A screen for genes required for meiosis and spore formation based on whole-genome expression. Curr Biol *11*, 1001-1009.

Rao, B.J., Chiu, S.K., and Radding, C.M. (1993). Homologous recognition and triplex formation promoted by RecA protein between duplex oligonucleotides and single-stranded DNA. J Mol Biol *229*, 328-343.

Rattray, A.J., McGill, C.B., Shafer, B.K., and Strathern, J.N. (2001). Fidelity of mitotic double-strand-break repair in Saccharomyces cerevisiae: a role for SAE2/COM1. Genetics *158*, 109-122.

Rechsteiner, M., and Rogers, S.W. (1996). PEST sequences and regulation by proteolysis. Trends Biochem Sci *21*, 267-271.

Richardson, C., Horikoshi, N., and Pandita, T.K. (2004). The role of the DNA double-strand break response network in meiosis. DNA Repair (Amst) *3*, 1149-1164.

Ristic, D., Modesti, M., Kanaar, R., and Wyman, C. (2003). Rad52 and Ku bind to different DNA structures produced early in double-strand break repair. Nucleic Acids Res *31*, 5229-5237.

Ross, K.J., Fransz, P., Armstrong, S.J., Vizir, I., Mulligan, B., Franklin, F.C., and Jones, G.H. (1997). Cytological characterization of four meiotic mutants of Arabidopsis isolated from T-DNA-transformed lines. Chromosome Res *5*, 551-559.

Ross, K.J., Fransz, P., and Jones, G.H. (1996). A light microscopic atlas of meiosis in Arabidopsis thaliana. Chromosome Res *4*, 507-516.

Saito, T.T., Tougan, T., Kasama, T., Okuzaki, D., and Nojima, H. (2004). Mcp7, a meiosis-specific coiled-coil protein of fission yeast, associates with Meu13 and is required for meiotic recombination. Nucleic Acids Res *32*, 3325-3339.

Sanchez-Moran, E., Santos, J.L., Jones, G.H., and Franklin, F.C. (2007). ASY1 mediates AtDMC1-dependent interhomolog recombination during meiosis in Arabidopsis. Genes Dev *21*, 2220-2233.

Sauvageau, S., Stasiak, A.Z., Banville, I., Ploquin, M., Stasiak, A., and Masson, J.Y. (2005). Fission yeast rad51 and dmc1, two efficient DNA recombinases forming helical nucleoprotein filaments. Mol Cell Biol *25*, 4377-4387.

Schild, D., Lio, Y.C., Collins, D.W., Tsomondo, T., and Chen, D.J. (2000). Evidence for simultaneous protein interactions between human Rad51 paralogs. J Biol Chem *275*, 16443-16449.

Schommer, C., Beven, A., Lawrenson, T., Shaw, P., and Sablowski, R. (2003). AHP2 is required for bivalent formation and for segregation of homologous chromosomes in Arabidopsis meiosis. Plant J *36*, 1-11.

Schwacha, A., and Kleckner, N. (1997). Interhomolog bias during meiotic recombination: meiotic functions promote a highly differentiated interhomolog-only pathway. Cell *90*, 1123-1135.

Sehorn, M.G., Sigurdsson, S., Bussen, W., Unger, V.M., and Sung, P. (2004). Human meiotic recombinase Dmc1 promotes ATP-dependent homologous DNA strand exchange. Nature *429*, 433-437.

Sheridan, S.D., Yu, X., Roth, R., Heuser, J.E., Sehorn, M.G., Sung, P., Egelman, E.H., and Bishop, D.K. (2008). A comparative analysis of Dmc1 and Rad51 nucleoprotein filaments. Nucleic Acids Res *36*, 4057-4066.

Shiloh, Y. (1998). Ataxia-telangiectasia, ATM and genomic stability: maintaining a delicate balance. Two international workshops on ataxia-telangiectasia, related disorders and the ATM protein. Biochim Biophys Acta *1378*, R11-18.

Shin, D.S., Pellegrini, L., Daniels, D.S., Yelent, B., Craig, L., Bates, D., Yu, D.S., Shivji, M.K., Hitomi, C., Arvai, A.S*., et al.* (2003). Full-length archaeal Rad51 structure and mutants: mechanisms for RAD51 assembly and control by BRCA2. EMBO J *22*, 4566-4576.

Shinohara, A., Gasior, S., Ogawa, T., Kleckner, N., and Bishop, D.K. (1997). Saccharomyces cerevisiae recA homologues RAD51 and DMC1 have both distinct and overlapping roles in meiotic recombination. Genes Cells *2*, 615-629.

Shinohara, A., Ogawa, H., Matsuda, Y., Ushio, N., Ikeo, K., and Ogawa, T. (1993). Cloning of human, mouse and fission yeast recombination genes homologous to RAD51 and recA. Nat Genet *4*, 239-243.

Shinohara, A., and Shinohara, M. (2004). Roles of RecA homologues Rad51 and Dmc1 during meiotic recombination. Cytogenet Genome Res *107*, 201-207.

Siaud, N., Dray, E., Gy, I., Gerard, E., Takvorian, N., and Doutriaux, M.P. (2004a). Brca2 is involved in meiosis in Arabidopsis thaliana as suggested by its interaction with Dmc1. Embo J *23*, 1392-1401.

Siaud, N., Dray, E., Gy, I., Gérard, E., Takvorian, N., and Doutriaux, M.P. (2004b). Brca2 is involved in meiosis in Arabidopsis thaliana as suggested by its interaction with Dmc1. EMBO J *23*, 1392-1401.

Sibanda, B.L., Critchlow, S.E., Begun, J., Pei, X.Y., Jackson, S.P., Blundell, T.L., and Pellegrini, L. (2001). Crystal structure of an Xrcc4-DNA ligase IV complex. Nat Struct Biol *8*, 1015-1019.

Silberman, R., and Kupiec, M. (1994). Plasmid-mediated induction of recombination in yeast. Genetics *137*, 41-48.

Singleton, B.K., Torres-Arzayus, M.I., Rottinghaus, S.T., Taccioli, G.E., and Jeggo, P.A. (1999). The C terminus of Ku80 activates the DNA-dependent protein kinase catalytic subunit. Mol Cell Biol *19*, 3267-3277.

Smith, G.C., and Jackson, S.P. (1999). The DNA-dependent protein kinase. Genes Dev *13*, 916-934.

Smith, K., and Nicolas, A. (1998). Recombination at work for meiosis. Curr Opin Genet Dev *8*, 200-211.

Stacey, N.J., Kuromori, T., Azumi, Y., Roberts, G., Breuer, C., Wada, T., Maxwell, A., Roberts, K., and Sugimoto-Shirasu, K. (2006). Arabidopsis SPO11-2 functions with SPO11-1 in meiotic recombination. Plant J *48*, 206-216.

Strathern, J., Shafer, B., Hicks, J., and McGill, C. (1988). a/Alpha-specific repression by MAT alpha 2. Genetics *120*, 75-81.

Strathern, J.N., Klar, A.J., Hicks, J.B., Abraham, J.A., Ivy, J.M., Nasmyth, K.A., and McGill, C. (1982). Homothallic switching of yeast mating type cassettes is initiated by a double-stranded cut in the MAT locus. Cell *31*, 183-192.

Sugawara, N., Ira, G., and Haber, J.E. (2000). DNA length dependence of the single-strand annealing pathway and the role of Saccharomyces cerevisiae RAD59 in double-strand break repair. Mol Cell Biol *20*, 5300-5309.

Sung, P. (1997). Yeast Rad55 and Rad57 proteins form a heterodimer that functions with replication protein A to promote DNA strand exchange by Rad51 recombinase. Genes Dev *11*, 1111-1121.

Sung, P., Krejci, L., Van Komen, S., and Sehorn, M.G. (2003). Rad51 recombinase and recombination mediators. J Biol Chem *278*, 42729-42732.

Sung, P., and Robberson, D.L. (1995). DNA strand exchange mediated by a RAD51-ssDNA nucleoprotein filament with polarity opposite to that of RecA. Cell *82*, 453-461.

Symington, L.S. (2002). Role of RAD52 epistasis group genes in homologous recombination and double-strand break repair. Microbiol Mol Biol Rev *66*, 630-670, table of contents.

Symington, L.S., and Holloman, W.K. (2004). Molecular biology. New Year's resolution--resolving resolvases. Science *303*, 184-185.

Szostak, J.W., Orr-Weaver, T.L., Rothstein, R.J., and Stahl, F.W. (1983). The double-strand-break repair model for recombination. Cell *33*, 25-35.

Takanami, T., Sato, S., Ishihara, T., Katsura, I., Takahashi, H., and Higashitani, A. (1998). Characterization of a Caenorhabditis elegans recA-like gene Ce-rdh-1 involved in meiotic recombination. DNA Res *5*, 373-377.

Takata, M., Sasaki, M.S., Tachiiri, S., Fukushima, T., Sonoda, E., Schild, D., Thompson, L.H., and Takeda, S. (2001). Chromosome instability and defective recombinational repair in knockout mutants of the five Rad51 paralogs. Mol Cell Biol *21*, 2858-2866.

Tamura, K., Adachi, Y., Chiba, K., Oguchi, K., and Takahashi, H. (2002). Identification of Ku70 and Ku80 homologues in Arabidopsis thaliana: evidence for a role in the repair of DNA double-strand breaks. Plant J *29*, 771-781.

Tanaka, T., Nakamura, T., Takagi, H., and Sato, M. (1997). Molecular cloning and characterization of a novel TBP-1 interacting protein (TBPIP):enhancement of TBP-1 action on Tat by TBPIP. Biochem Biophys Res Commun *239*, 176-181.

Terasawa, M., Shinohara, A., Hotta, Y., Ogawa, H., and Ogawa, T. (1995). Localization of RecA-like recombination proteins on chromosomes of the lily at various meiotic stages. Genes Dev *9*, 925-934.

Theunissen, J.W., Kaplan, M.I., Hunt, P., Williams, B.R., Ferguson, D., Alt, F.W., and Petrini, J.H. (2003). Checkpoint failure and chromosomal instability without lymphomagenesis in Mre11(ATLD1/ATLD1) mice. Mol Cell *12*, 1511-1523.

Tomkinson, A.E., Vijayakumar, S., Pascal, J.M., and Ellenberger, T. (2006). DNA ligases: structure, reaction mechanism, and function. Chem Rev *106*, 687-699.

Tsubouchi, H., and Ogawa, H. (1998). A novel mre11 mutation impairs processing of double-strand breaks of DNA during both mitosis and meiosis. Mol Cell Biol *18*, 260-268.

Tsubouchi, H., and Roeder, G.S. (2002). The Mnd1 protein forms a complex with hop2 to promote homologous chromosome pairing and meiotic double-strand break repair. Mol Cell Biol *22*, 3078-3088.

Tsubouchi, H., and Roeder, G.S. (2003). The importance of genetic recombination for fidelity of chromosome pairing in meiosis. Dev Cell *5*, 915-925.

Tsukamoto, Y., Mitsuoka, C., Terasawa, M., Ogawa, H., and Ogawa, T. (2005). Xrs2p regulates Mre11p translocation to the nucleus and plays a role in telomere elongation and meiotic recombination. Mol Biol Cell *16*, 597-608.

Tsuzuki, T., Fujii, Y., Sakumi, K., Tominaga, Y., Nakao, K., Sekiguchi, M., Matsushiro, A., Yoshimura, Y., and MoritaT (1996). Targeted disruption of the Rad51 gene leads to lethality in embryonic mice. Proc Natl Acad Sci U S A *93*, 6236-6240.

Turner, J.M. (2007). Meiosis 2007--where have we got to and where are we going? Chromosome Res *15*, 517-521.

Uanschou, C., Siwiec, T., Pedrosa-Harand, A., Kerzendorfer, C., Sanchez-Moran, E., Novatchkova, M., Akimcheva, S., Woglar, A., Klein, F., and Schlögelhofer, P. (2007). A novel plant gene essential for meiosis is related to the human CtIP and the yeast COM1/SAE2 gene. EMBO J *26*, 5061-5070.

Usui, T., Ogawa, H., and Petrini, J.H. (2001). A DNA damage response pathway controlled by Tel1 and the Mre11 complex. Mol Cell *7*, 1255-1266.

Usui, T., Ohta, T., Oshiumi, H., Tomizawa, J., Ogawa, H., and Ogawa, T. (1998). Complex formation and functional versatility of Mre11 of budding yeast in recombination. Cell *95*, 705-716.

van Attikum, H., Bundock, P., Overmeer, R.M., Lee, L.Y., Gelvin, S.B., and Hooykaas, P.J. (2003). The Arabidopsis AtLIG4 gene is required for the repair of DNA damage, but not for the integration of Agrobacterium T-DNA. Nucleic Acids Res *31*, 4247-4255.

Van Dyck, E., Stasiak, A.Z., Stasiak, A., and West, S.C. (1999). Binding of double-strand breaks in DNA by human Rad52 protein. Nature *401*, 403.

Vignard, J., Siwiec, T., Chelysheva, L., Vrielynck, N., Gonord, F., Armstrong, S.J., Schlogelhofer, P., and Mercier, R. (2007a). The interplay of RecA-related proteins and

the MND1-HOP2 complex during meiosis in Arabidopsis thaliana. PLoS Genet *3*, 1894-1906.

Vignard, J., Siwiec, T., Chelysheva, L., Vrielynck, N., Gonord, F., Armstrong, S.J., Schlögelhofer, P., and Mercier, R. (2007b). The interplay of RecA-related proteins and the MND1-HOP2 complex during meiosis in Arabidopsis thaliana. PLoS Genet *3*, 1894-1906.

Walker, J.R., Corpina, R.A., and Goldberg, J. (2001). Structure of the Ku heterodimer bound to DNA and its implications for double-strand break repair. Nature *412*, 607-614.

Wang, X., Ira, G., Tercero, J.A., Holmes, A.M., Diffley, J.F., and Haber, J.E. (2004). Role of DNA replication proteins in double-strand break-induced recombination in Saccharomyces cerevisiae. Mol Cell Biol *24*, 6891-6899.

Watanabe, Y., and Kitajima, T.S. (2005). Shugoshin protects cohesin complexes at centromeres. Philos Trans R Soc Lond B Biol Sci *360*, 515-521, discussion 521.

Weinstock, D.M., Richardson, C.A., Elliott, B., and Jasin, M. (2006). Modeling oncogenic translocations: distinct roles for double-strand break repair pathways in translocation formation in mammalian cells. DNA Repair (Amst) *5*, 1065-1074.

West, C.E., Waterworth, W.M., Jiang, Q., and Bray, C.M. (2000). Arabidopsis DNA ligase IV is induced by gamma-irradiation and interacts with an Arabidopsis homologue of the double strand break repair protein XRCC4. Plant J *24*, 67-78.

West, C.E., Waterworth, W.M., Story, G.W., Sunderland, P.A., Jiang, Q., and Bray, C.M. (2002). Disruption of the Arabidopsis AtKu80 gene demonstrates an essential role for AtKu80 protein in efficient repair of DNA double-strand breaks in vivo. Plant J *31*, 517-528.

Weterings, E., and Chen, D.J. (2008). The endless tale of non-homologous end-joining. Cell Res *18*, 114-124.

Weterings, E., Verkaik, N.S., Keijzers, G., Florea, B.I., Wang, S.Y., Ortega, L.G., Uematsu, N., Chen, D.J., and van Gent, D.C. (2009). The Ku80 carboxy terminus stimulates joining and artemis-mediated processing of DNA ends. Mol Cell Biol *29*, 1134-1142.

Wiese, C., Collins, D.W., Albala, J.S., Thompson, L.H., Kronenberg, A., and Schild, D. (2002). Interactions involving the Rad51 paralogs Rad51C and XRCC3 in human cells. Nucleic Acids Res *30*, 1001-1008.

Yoshida, K., Kondoh, G., Matsuda, Y., Habu, T., Nishimune, Y., and Morita, T. (1998). The mouse RecA-like gene Dmc1 is required for homologous chromosome synapsis during meiosis. Mol Cell *1*, 707-718.

Yoshihara, T., Ishida, M., Kinomura, A., Katsura, M., Tsuruga, T., Tashiro, S., Asahara, T., and Miyagawa, K. (2004). XRCC3 deficiency results in a defect in recombination and increased endoreduplication in human cells. EMBO J *23*, 670-680.

Yoshimura, Y., Morita, T., Yamamoto, A., and Matsushiro, A. (1993). Cloning and sequence of the human RecA-like gene cDNA. Nucleic Acids Res *21*, 1665.

Yu, X., and Chen, J.J. (2004). DNA damage-induced cell cycle checkpoint control requires CtIP, a phosphorylation-dependent binding partner of BRCA1 C-terminal domains. Mol Cell Biol *24*, 9478-9486.

Yu, X., Fu, S., Lai, M., Baer, R., and Chen, J.J. (2006). BRCA1 ubiquitinates its phosphorylation-dependent binding partner CtIP. Genes Dev *20*, 1721-1726.

Yu, X., Wu, L., Bowcock, A.M., Aronheim, A., and Baer, R. (1998). The C-terminal (BRCT) domains of BRCA1 interact in vivo with CtIP, a protein implicated in the CtBP pathway of transcriptional repression. J Biol Chem *273*, 25388-25392.

Zickler, D., and Kleckner, N. (1998). The leptotene-zygotene transition of meiosis. Annu Rev Genet *32*, 619-697.

Zickler, D., and Kleckner, N. (1999). Meiotic chromosomes: integrating structure and function. Annu Rev Genet *33*, 603-754.

Zierhut, C., Berlinger, M., Rupp, C., Shinohara, A., and Klein, F. (2004). Mnd1 is required for meiotic interhomolog repair. Curr Biol *14*, 752-762.